Isotope geochemistry and denitrification processes in groundwaters

Wilson, George B.

Award date:
1986

Awarding institution:
University of Bath

ISOTOPE GEOCHEMISTRY AND DENITRIFICATION PROCESSES IN GROUNDWATERS

Submitted by George B. Wilson

for the degree of Ph.D. of the

University of Bath

1986

GB Wilson

ProQuest LLC
789 East Eisenhower Parkway
P.O. Box 1346
Ann Arbor, MI 48106-1346

MEMORANDUM

The work described in this thesis was conducted in the School of Chemistry of the University of Bath during the period October 1982 to September 1985 and has not been submitted for any other degree. All the work described in the original work of the author except where specially acknowledged.

Dedicated to my family and
especially to Elaine

ABSTRACT

The application of fertilisers to agricultural land in the recharge zone of aquifer systems may introduce nitrates into the underlying groundwaters. The groundwater quality downdip in the system will be dependent on the extent of nitrate reduction processes in the aquifer. This study assesses such processes in a Triassic sandstone aquifer in Nottinghamshire and a Jurassic limestone aquifer in Lincolnshire. Nitrogen geochemistry was investigated using dissolved N_2/Ar ratios as an index of denitrification and $^{15}N/^{14}N$ ratios to evaluate the origins of the nitrate.

Groundwater ages in the confined zone of the Triassic sandstone aquifer are such that in general only natural nitrate inputs can have occurred. The dissolved N_2/Ar ratios across the aquifer are not significantly above that from atmospheric inputs, and the nitrate concentrations are very low. There is no evidence for the denitrification of large quantities of nitrate in the confined zone of this aquifer. The outcrop sites contain higher nitrate concentrations with $^{15}N/^{14}N$ isotopic compositions which can be related to different nitrate sources.

In the Lincolnshire limestone, recent waters penetrate the confined zone of the aquifer. The nitrate concentrations in the confined zone are very low but the dissolved N_2/Ar ratios are high and this is attributed to denitrification processes in this aquifer. The $^{15}N/^{14}N$ ratios for the dissolved excess nitrogen gas from denitification vary according to the quantity of denitrified nitrogen.

It has been shown that denitrification processes in aquifers can be identified on the basis of quantitative N_2/Ar ratios and $^{15}N/^{14}N$ isotopic compositions on nitrates and nitrogen gas dissolved in the groundwaters.

ACKNOWLEDGEMENT

I would like to thank my two supervisors, Dr. J.N. Andrews (University of Bath) and Dr. A.H. Bath (BGS, Keyworth) for their guidance in all aspects of this thesis. Dr. A. Mariotti (University of Paris) kindly instructed me in the techniques of nitrogen-isotope analysis during a short visit to his laboratory. My thanks also go to M.J. Youngman (University of Bath) for assistance with the noble gas analyses, and A. Brunsden, A. Lardner, and W.G. Darling (BGS, Wallingford) for instruction in the use of isotope-ratio mass spectrometry.

The Anglian and Severn-Trent Water Authorities, the C.E.G.B., and the owners of private water supplies allowed access to the sampling sites and their cooperation is gratefully acknowledged. The text was typed by J. Emery.

I also wish to thank the Natural Environment Research Council for the award of a research studentship and the University of Bath for a research bursary.

LIST OF TABLES

LIST OF FIGURES

CONTENTS

CHAPTER I

INTRODUCTION

1.1. Aims and scope of the study

The element nitrogen is an essential constituent of protein and genes and is necessary for all life on earth. It is however, only available to most living things when it is incorporated in certain chemical compounds such as nitrates. Since the 1950's natural and synthetic nitrate fertilisers have been applied in excess to agricultural land areas in order to maximise crop yields. This may be correlated with a 50-400% increase in nitrate levels over the last 20 years in the underlying large aquifer groundwater systems (Tudge, 1984).

Approximately 30% of Britain's water supply comes from major underground aquifers, and this has raised concern with respect to nitrate pollution. Although necessary for all life, an excess of nitrates can be poisonous, producing blood disorders in the short term and cancer of the gut in the long term (Wild, 1977; Wolf, 1972). The particular concern is that the nitrate levels will increase, and that the presently observed nitrate excess percolating down through the soils and bedrock to the main groundwater aquifer bodies may result in maximum nitrate concentrations being reached in some 20-30 years time.

Virtually nothing is known about the processes affecting nitrates from the time they enter an aquifer. It is important to determine if the nitrates are subject to bacterial breakdown whilst in an aquifer, or whether they reflect an important long-term influx into the Nitrogen Cycle. This work is an attempt to answer some of these questions with particular emphasis on two major British aquifers; namely the Nottinghamshire Triassic Sandstone and the Lincolnshire Limestone (Fig. 1). The study basically concerns identifying in detail how the dissolved gas contents of these aquifers have evolved from the time of initial water input. This enables a potential component of dissolved nitrogen gas to be identified which could be due to bacterial degradation

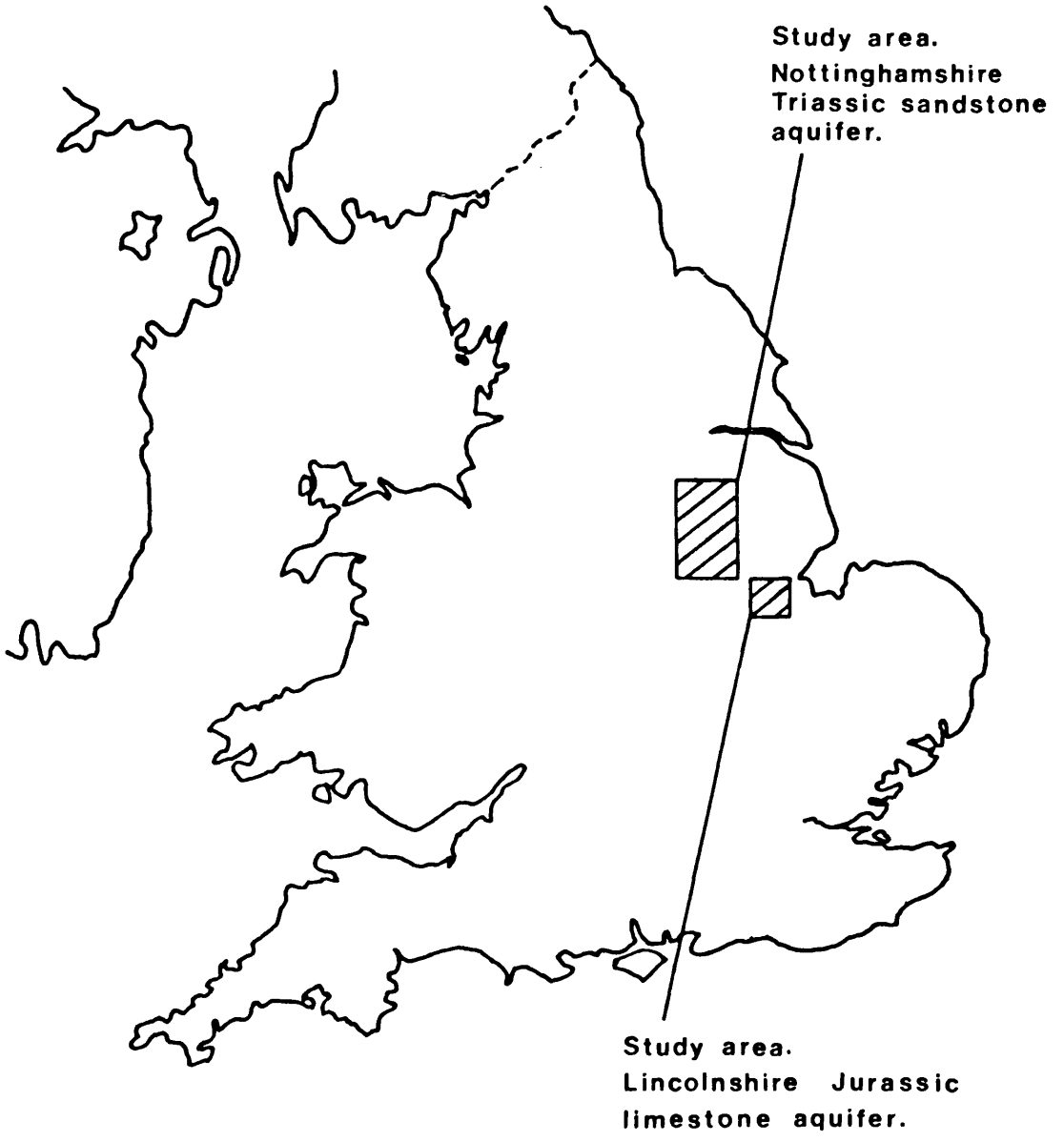

FIG.1 Location of studied aquifer regions in Great Britain.

of nitrates. The development of sampling methods and analytical techniques has been a necessary requirement of this work.

This introduction concerns a review of the relevant geochemistry of this subject. The project is essentially a bridge between the soil scientist/biochemist on the one hand and the geologist/geochemist on the other, and as such is interdisciplinary drawing on data from all the natural sciences.

1.2 The Nitrogen Cycle

Nitrogen's variety of oxidation states (from -3 to +5) explains its ability to combine with hydrogen, oxygen and other atoms to form a great variety of biological compounds. However almost all the nitrogen not contained in the Earth's interior is in the form of N_2, an unusable and therefore unavailable form for all but a few free-living or symbiotic organisms. Molecular N_2 does not readily undergo transformations to or from other nitrogen species firstly because of the low reactivity of N_2, and secondly because the transformations that do involve chemically pure N_2 are extremely slow.

In the biosphere the essential nitrogen species are: N_2, NH_4^+, NO_2^-, and NO_3^-, although minor components of NH_3 and oxides of N may be present in the atmosphere. The purely chemical transformations of the N-species are, in fact, all rather slow. What makes the system so reactionary and drives the Nitrogen Cycle is the role of microbiological enzymes, which are crucial to the conditioning of the natural environment in hastening the N-transformations (Fig. 2).

The process which makes the nitrogen of the atmosphere into combined nitrogen is fixation. In a six-electron transfer, using the enzyme nitrogenase, triple-bonded N_2 is thought to be directly converted to amino-nitrogen. Subsequent degradation will yield ammonia (NH_3) which

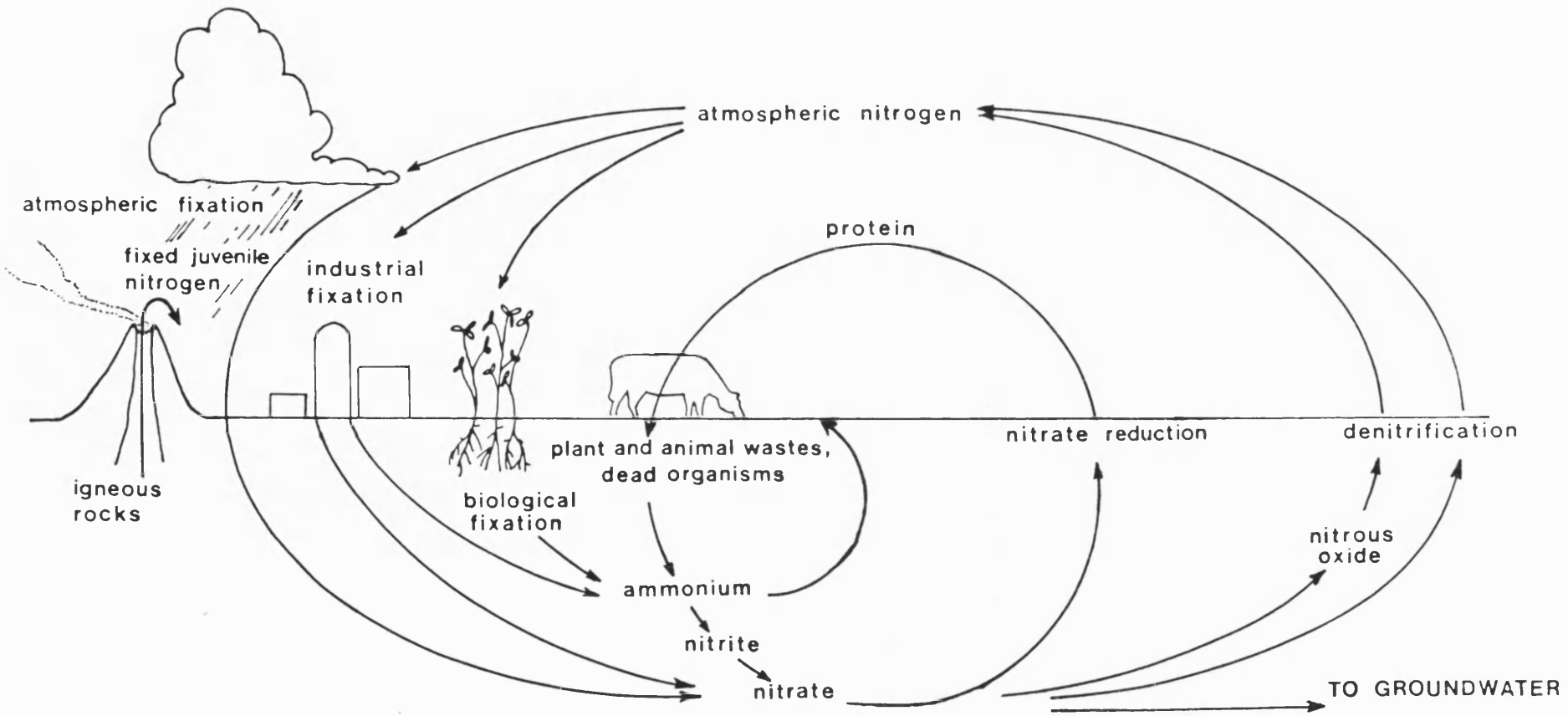

FIG.2 The Nitrogen Cycle.

can be utilised by the cell in biosynthesis. The oxidation of liberated NH_3 to nitrite (NO_2^-) and nitrate (NO_3^-) by bacteria is called nitrification, making the nitrogen available to higher plants and animals. Such transformations are not solely a one-way process otherwise atmospheric N_2 would have long since been depleted. Natural fixation processes are in theory closely balanced by the amount returned to the atmosphere by organisms that convert organic nitrates to gaseous nitrogen, a process called denitrification.

It is evident that some organisms find it profitable to oxidise nitrogen compounds whilst others owe their survival to their ability to reduce nitrogen compounds. Nitrogen can be cycled in this way because the reduced inorganic compounds of nitrogen can be oxidised by atmospheric oxygen to yield energy. Under anaerobic conditions the oxidised compounds of nitrogen can act as oxidising agents for the burning of organic compounds again with a yield of energy. Table 1 lists some examples of reactions characteristic of the Nitrogen Cycle.

The role of denitrification in returning nitrogen to the atmosphere should not be underestimated. Of all man's recent interventions in the cycles of nature the industrial fixation of nitrogen far exceeds all the others in magnitude. Since 1950 the amount of nitrogen annually fixed for the production of fertiliser has increased approximately fivefold, until it now equals the amount that was fixed by all terrestrial ecosystems before the advent of modern agriculture. In 1968, the world's annual output of industrially fixed nitrogen amounted to 30 million tonnes of nitrogen; by the year 2000 the industrial fixation of nitrogen may well exceed 100 million tonnes. Delwiche (1970) has calculated the global balance sheet for nitrogen, listed in Table 2. He suggests there is now a global deficit in the balance of the nitrogen cycle, with some 9 million tonnes of fixed nitrogen per year accumulating in the biosphere,

Table 1. Energy Yields of reactions in the Nitrogen Cycle.

Reaction	Energy yield (kilocalories)
Denitrification	
$C_6H_{12}O_6 + 6KNO_3 \rightarrow 6CO_2 + 3H_2O + 6KOH + 3N_2O$	545
$5C_6H_{12}O_6 + 24KNO_3 \rightarrow 30CO_2 + 18H_2O + 24KOH + 12N_2$	570
Respiration	
$C_6H_{12}O_6 + 6O_2 \rightarrow 6CO_2 + 6H_2O$	686
Nitrification	
$NH_3 + 1.5O_2 \rightarrow HNO_2 + H_2O$	66
$KNO_2 + 0.5O_2 \rightarrow KNO_3$	17.5
Nitrogen Fixation	
$N_2 \rightarrow 2N$ 'Activation of Nitrogen'	-160
$2N + 3H_2 \rightarrow 2NH_3$	12.8

Table 2. The balance sheet for the Nitrogen Cycle

	Million tonnes/year
Biological Fixation:	
Terrestrial (historic)	30
Legume crops	14
Marine	10
Industrial Fixation	30
Atmospheric Fixation	7.6
Juvenile Addition	0.2
Total Fixation	92.0
Denitrification:	
Terrestrial	43
Marine	40
Sediments	0.2
Total Loss	83

i.e. in the oceans, rivers and lakes, soils, and of course, in groundwater reservoirs. Such a study, if nothing else, exposes the huge uncertainties in man's knowledge of the global Nitrogen Cycle.

1.3 The biochemistry of denitrification

Denitrifying bacteria are structurally simple microorganisms, i.e. prokaryotic. They are distinct from eukaryotes in that genetic material is not confined within a nuclear membrane. The cytoplasm, cytoplasmic membrane, and cell wall are the three most structurally important divisions of prokaryotic cells. The cytoplasmic membrane is particularly important with respect to denitrification because many of the enzymes are contained within it.

The most common denitrifying bacteria found in soil are Thiobacillus denitrificans, Micrococcus denitrificans, Pseudomonas denitrificans, and Achromobacter. Nevertheless they are biochemically and taxonomically very diverse. Such bacteria are 0.5 - 10μ in diameter occuring in a variety of forms, usually rod-shaped or spherical, and occupying water-filled interstitial soil crumb voids or pore rock spaces.

Most denitrifying bacteria are facultatively anaerobic. This means that normally under oxidising conditions they respire by reduction of oxygen. Once however, oxygen availability diminishes to low levels, or is completely absent, the organism can still respire but by using nitrate (NO_3^-) as the electron acceptor instead of O_2. This is accomplished because at low oxygen levels an enzyme is manufactured in the cytoplasmic membrane known as Nicotinamide Adenine Dinucleatide (NADH). Respiration generates Adenosine Triphosphate (ATP), an energy rich compound which, by transferring its terminal phosphate group to another molecule such as glucose, will convert a relatively inert substance into a more reactive

one. ATP is therefore the immediate source of energy for many reactions needed for the maintainance of life. In order for ATP to be generated, the cell contains a special set of compounds capable of being reversibly oxidised and reduced, i.e. they can accept electrons from one compound and donate them to another, ultimately to the terminal electron acceptor, oxygen or nitrate. The generation of ATP by this electron transport chain is called oxidative phosporylation. For denitrification of nitrates to occur, NADH is a principle reductant enzyme in the electron transport chain.

Organic carbon is the principle electron donor for nitrate reduction, although reported electron donors include hydrogen, formate, succinate, lactate and glycerol phosphate. In some cases linear hydrocarbons and aromatic compounds can act as electron donors.

As with all bacteria, denitrifiers require a micronutrient supply of most common elements. Since a supply is required in trace concentrations their essentiality may be technically difficult to demonstate. A bacterial denitrifying population is most probably limited to the availability of organic carbon and nitrogen. For every 100 units of carbon incorporated into the cell, approximately 5-10 units of N are incorporated, producing a C/N ratio of about 7.

The microbiological nitrogen cycle is illustrated in Fig. 3. The dotted arrows represent the reductive assimilation and subsequent decomposition of organic nitrogen compounds. The dashed arrow indicates a short-cut via which NO_2^- is reduced to NH_3 thereby avoiding nitrogen fixation which is the rate-limiting step of the cycle. The degree of importance of this short-cut step should not be underestimated. Sorensen (1978) studied nitrate reduction in the sediments of the Limfjorden, Northern Denmark and concluded that NO_3^- dissimilation to NH_3 was equally important as denitrification ($NO_3^- \rightarrow N_2$) in the turnover of nitrate in

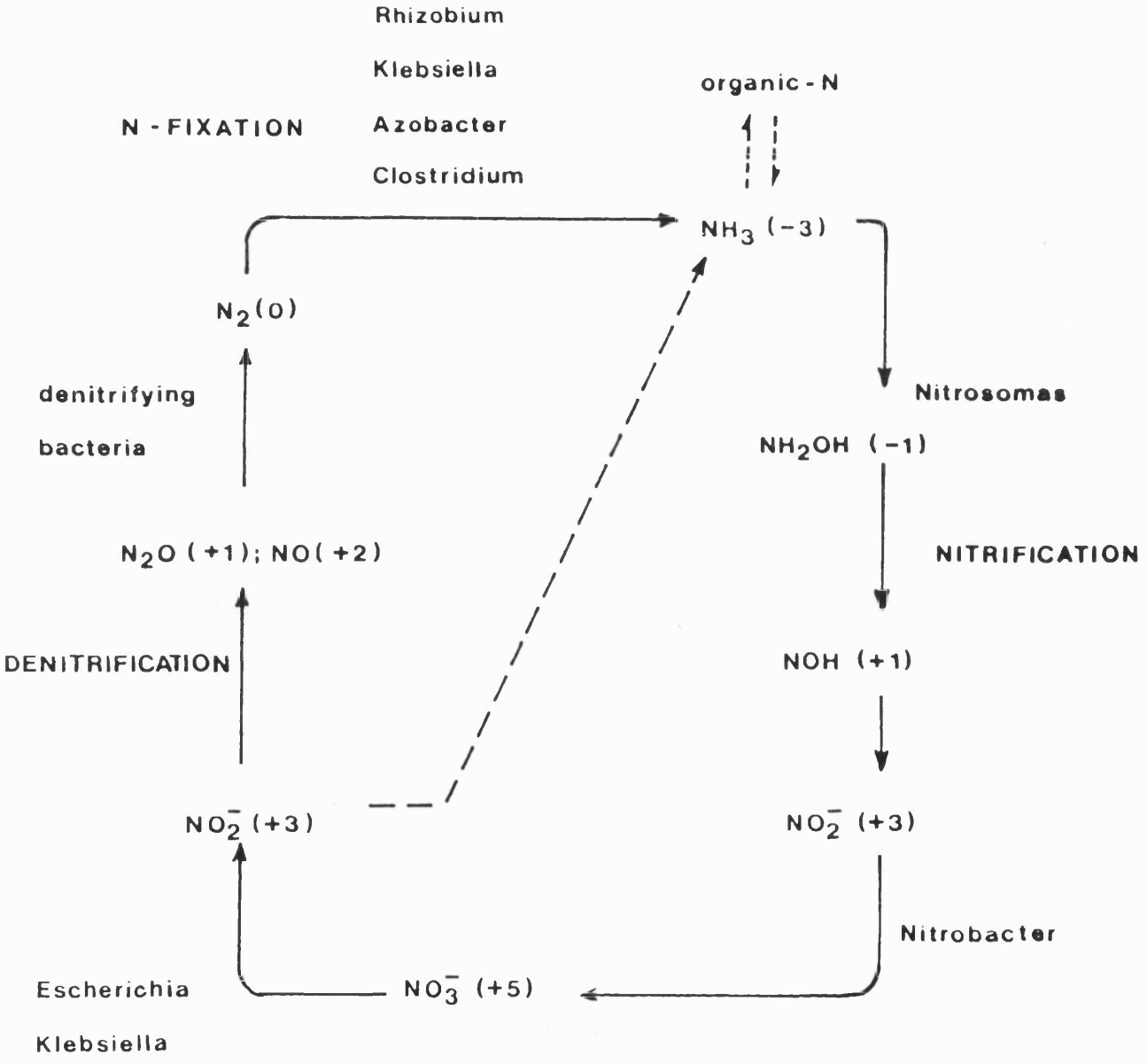

FIG. 3 The microbiological Nitrogen Cycle. Numbers in brackets refer to oxidation state of nitrogen.

marine sediments. Koike et al., (1978) have shown that between 20-67% of ^{15}N tracer NO_3^- is converted to NH_3 or particulate organic N in anaerobic coastal sediments. It seems that nitrate reduction to NH_3 and denitrification may proceed simultaneously within anaerobic marine sediments.

Since dentrification may be limited according to the availability of organic carbon (carbon-limiting) or limited to the availability of nitrate (nitrate-limiting), Herbert (1982) studied the effects of these two rate-limiting factors on the products of bacterial nitrate reduction. He noted that where the system was nitrate-limiting, NH_3 was preferentially excreted. Where the system was carbon-limiting, NO_2^- was preferentially excreted with the potential for further reduction to N_2. Mariotti et al., (1982) and Bowman et al., (1974) have studied the kinetics of the dentrification process. If the system is carbon-limiting, then the reaction rates are high and tend to follow zero-order kinetics, i.e.

$$[NO_3^-] = -Kt + [NO_3^-]o$$

where $[NO_3^-]$ and $[NO_3^-]o$ are the nitrate concentrations at some time t and t = o respectively. K is the rate constant expressed in concentration per unit time. At lower nitrate concentrations, i.e. nitrate-limiting, the reaction rates are lower and appear to be first order, i.e.

$$[NO_3^-] = [NO_3^-]o\, e^{-Kt}$$

The rate constant K in this case has the units of reciprocal time, because it is independant of the units used to measure concentration. Herbert (1982) has studied the influence of oxygen tension on the

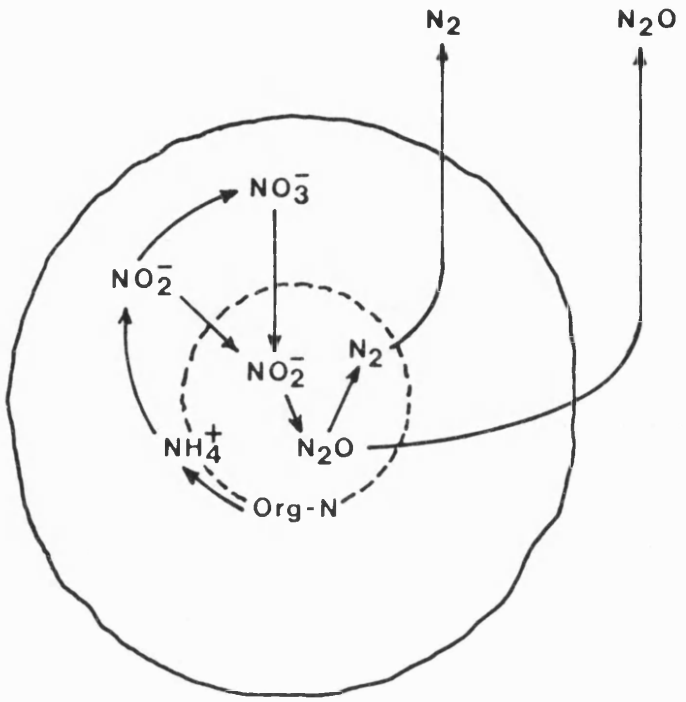

FIG.4 A schematic soil crumb with an aerobic outer sector in which nitrification can take place, and an inner anaerobic centre from which nitrogen may be lost through denitrification.

dentrification process. Denitrification was observed only to occur once the oxygen-level approached 10% air saturation. Evidently denitrification can occur before completely anaerobic conditions are reached, a conclusion which is supported by thermodynamic considerations (Berner, 1971).

The microniche concept of nitrogen cycling has recently received attention, due to the observation that nitrification and denitrification may occur side-by-side in the same environment (Knowles, 1978). The operation of such an internal cycle is clearly advantageous to both nitrifying and denitrifying bacteria, and it has been estimated that most soil crumbs with a diameter of more than 3mm have anaerobic centres, (Fig. 4). The extent to which the N-cycling is in a steady-state in such microniche environments is largely unknown, and it is not known if the microniche concept can be applied to all environments. For example, the general anaerobic dependance of dentrification suggests that in soils the process may occur in punctuated bursts. Only after heavy rainfall would the denitrifying bacteria be activated to reduce nitrate, due to the temporary onset of anaerobic conditions caused by waterlogging of the soil. A few hours after the rainfall anaerobic conditions would cease and so would denitrification.

1.4 Gas Solubilities

1.4.1 The atmospheric occurence of the Noble Gases

The noble gases are essentially chemically inert due to their filled outermost shells. This does not mean that they completely fail to interact with anything, but the interactions are of the van der Waals type and are much weaker than normal chemical reactions. Each of the noble gases has a number of different isotopic species; xenon for example, has no less than nine isotopes known.

A range of nuclear reactions and decay schemes are known to be responsible for the synthesis of each of the noble gases (Ozima et al., 1984). Table 3 lists the most common noble gas isotopes found in the atmosphere along with their principal source of nucleosynthesis.

The abundance of the noble gases in air is very small (< 1%). Although as a group the noble gases are rare in the terrestrial environment they are not actually rare in the cosmic sense. At some point in the evolution of the solar system, a stage was passed in which some of its constituent elements were mostly in solid phases, whilst others, including the most abundant, were in a gas phase. The outstanding chemical characteristic of the terrestrial planets (and meteorites) is that they are made from solids, to the virtual exclusion of the gases. Their chemical inertness resulted in the noble gases being overwhelmingly partitioned into the gas phase and so are depleted in the earth and its atmosphere.

The chemical inertness of the noble gases makes them ideal for deriving palaeoclimatic information from groundwaters. In principle their concentrations in solution will reflect the conditions of initial water input into an aquifer (recharge conditions) even though thousands of years may separate the time of recharge from the time of sampling. Bath et al., (1978) and Andrews et al., (1979) have determined recharge temperatures on waters from the Nottinghamshire Triassic Sandstone Aquifer and indicate a temperature difference of 5-6^{o}C between the older waters and the modern waters over the last 40,000 years. Such calculations require a detailed knowledge of gas solubilities and this topic will now be reviewed.

1.4.2 **Gas solubility laws**

A major contribution to the early work on the solubility of the

Table 3. Compositional data for most abundant isotope noble gas species in air.

Isotope	% abundance (atomic)	Principle Source
^{4}He	~100.0	α decay
^{20}Ne	89.4	$^{17}O(\alpha,n)$ ^{20}Ne (Primordial)
^{40}Ar	99.6	^{40}K decay
^{84}Kr	57.0	^{238}U fission
^{129}Xe	26.4	^{129}I decay (extinct)

noble gases in water was made by Morrison and Johnstone (1954) for pure water and Konig (1963) for seawater. Since then more accurate experimental data has led to a refinement of the solubility data. Complementary to this, important advances in mechanico-statistical treatments and the use of computational techniques have been developed which model the behaviour of gas solubilities in liquids. The "Scaled-Particle Theory" has in particular shown some success in describing the distinct behaviour observed at room temperature for simple aqueous solutions as opposed to those in non-polar solvents (e.g. Shoor and Gubbins, 1968). The predictions of this theory are based essentially upon the values of the molecular size parameters for both solute and solvent, the solvent density, and its temperature dependence.

There are a number of conventions used to report naturally occuring gas concentrations in solution. Here it is defined as the number of cm^3 gas at STP dissolved in 1 cm^3 water. For example, a gas concentration of 0.02 cm^3 STP/cm^3 H_2O means that if the dissolved gas in 1 cm^3 of water was totally extracted, it would occupy a volume of 0.02 cm^3 at STP.

The dissolved gas concentration, c, is proportional to the partial pressure of the gas above the solution, p (atm) by:

$$c = p.K$$

where K is the Henry's Law Constant. Since gas concentrations in this work are expressed in volumetric units, the Henry's Law Constant must also be expressed in comparable units of volume. It is common, for instance, to quote values of K in moles/l atm^{-1}, or moles gas/mole solvent atm^{-1}, which would obviously require conversion to the volumetric equivalents.

In order to remove the effect of pressure and hence make comparisons between the gases, solubility data is commonly reported under 1 atm pressure for the respective gas in question. This value is known as the

Bunsen Coefficient, identical to the Henry's Law Constant expressed in volumetric units.

1.4.3 The Noble Gases, Nitrogen and Oxygen

The most recent and comprehensive work for the solubility of the noble gases in pure water is the data given by Benson and Krause (1976) for He, Ne, Ar, Kr, Xe, N_2 and O_2. Their high precision solubility data were fitted in terms of the Henry's Law Constant K in:

$$f = Kx$$

where f is the gas fugacity above a solution in which the mole fraction of the gas is x. They fitted their data to the functional form:

$$\ln (1/K) = A_3(T_1/T-1) + A_2(T_1/T-1)^2$$

with T the absolute temperature. A_2 is a dimensionless constant = 36.855. The T_1 and A_3 coefficients for this equation for each respective gas are listed in Table 4a. The Benson and Krause equation enables values of the Henry's Law Constant, K, to be determined in units of solute mole fraction per atmosphere. This is related to the Bunsen coefficient by:

$$\beta = \frac{1244.142P}{K}$$

where P is the partial pressure at 1 atm. Inserting any chosen partial pressure value in p will give the corresponding solubility. The partial pressures for each of seven gases used in atmospherically equilibrated gas solubilities in water are listed in Table 4b. The variation of the Bunsen coefficient with temperature for each of the gases is illustrated in fig. 5. It is clear qualitatively that the solubility for each gas depends strongly on temperature, and that both the solubilities and their temperature gradients increase with the molecular weight of the gas.

1.4.4 The solubility of Carbon Dioxide and Methane

Table 4a. Gas solubility parameters from Benson and Krause data.

Gas	T_1	A_3
He	131.42	41.824
Ne	142.5	41.667
Ar	168.87	40.404
Kr	179.21	39.781
Xe	188.78	39.273
N_2	162.02	41.712
O_2	168.85	40.622

Table 4b. Partial pressures of atmospheric gasses in air.

Gas	P (atm)
He	5.239×10^{-6}
Ne	1.818×10^{-5}
Ar	9.34×10^{-3}
Kr	1.139×10^{-6}
Xe	8.6×10^{-8}
N_2	0.7803
O_2	0.2099

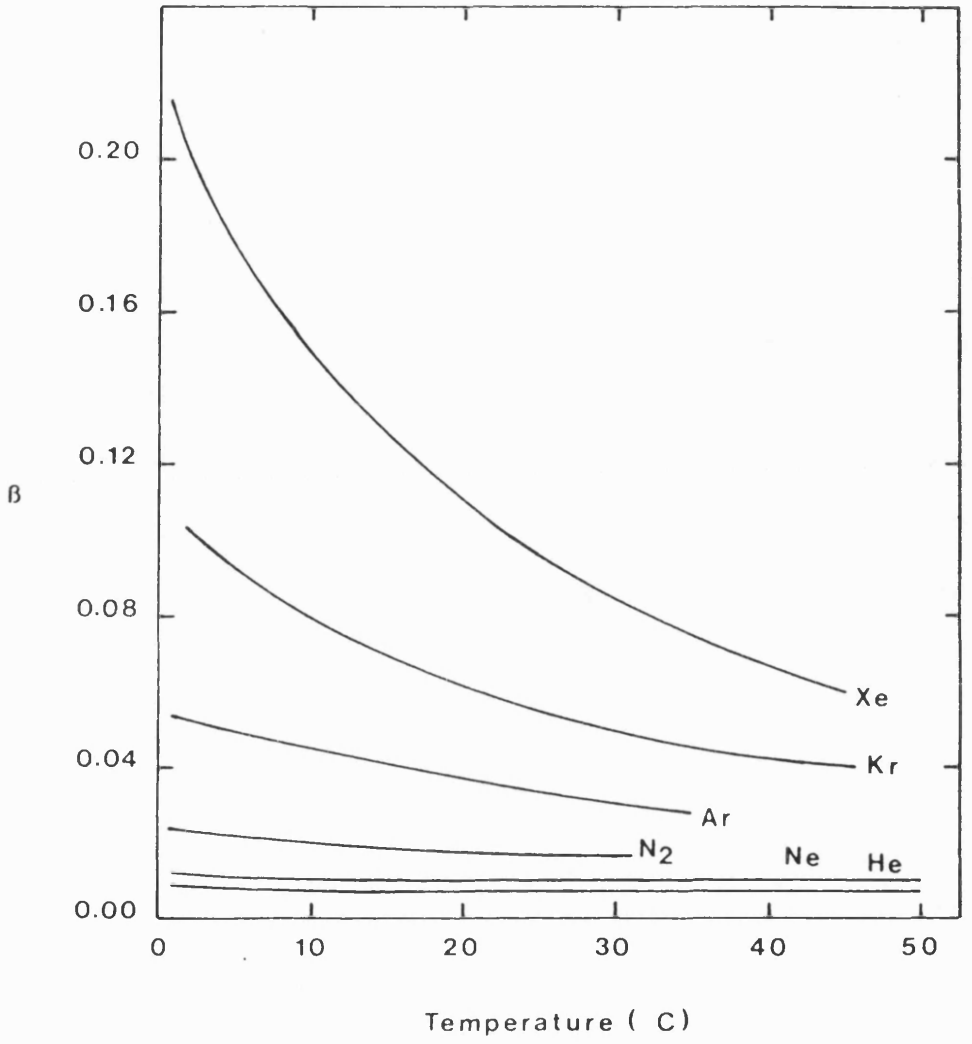

FIG.5 Graphs of the Bunsen Coefficent vs. temperature for He, Ne, Ar, Kr, Xe and N_2 in pure water.
ß = Bunsen Coefficient ($cm^3/cm^3\ H_2O\ atm^{-1}$)

The solubilities of these two gases are included here although they are not concerned with the estimation of recharge temperatures. Stumm and Morgan (1970) and the International Critical Tables respectively list Henry's Law Constants in pure water for CO_2 and CH_4 over a range of temperatures. (Table 5a). The temperature-solubility dependence of the Bunsen Coefficients was then fitted in each case to a polynomial cubic equation of the form:

$$\beta \ (cm^3/cm^3 \ atm^{-1}) = AZ^3 + BZ^2 + CZ + D$$

where Z = T(K)/100. The parameter for these constants are also listed in Table 5b.

1.4.5 The effect of salinity on solubility

The gas solubilities in seawater or any saline aqueous solution encounter the additional problem of the 'salting-out' effect; that is, the more saline the solution, the less soluble the gases become. This effect is not directly applicable to this study since the salinities of the groundwaters involved are all very low. Nevertheless, the modification of the solubility data to account for varying salinities is discussed here, since the ongoing programme of groundwater studies may involve its use at some later date.

The salting-out effect can be modelled by the Setchenow equation, which states that at constant temperature the logarithm of the solubility coefficient is a linear function of salt-concentration, i.e.

$$\text{Ln } (Bo/B) = M.Ks$$

where Bo is the freshwater Bunsen coefficient at the temperature of interest, and M the alkali-halide molarity. The salting coefficient, Ks, can be either positive or negative, according to whether the non-electrolyte in solution is being salted-out or salted-in. Ks varies with temperature but is independent of M.

Table 5a. Henry's Law Constants for CO_2 and CH_4 from 0-80°C in pure water. (moles/l atm^{-1}).

T	CO_2	$CH_4 \times 10^{-3}$
0	0.0776	2.484
10	0.0537	1.870
20	0.0389	1.480
30	0.0295	1.239
40	0.0229	1.070
50	0.0191	0.963
60	0.0166	0.888
70	0.0145	0.834
80	0.0133	0.815

Table 5b. Parameters for calculation of CO_2 and CH_4 Bunsen Coefficients in pure water.

Gas	A	B	C	D
CO_2	-6.5455	63.6611	-207.2720	226.3128
CH_4	-0.1229	1.2416	-4.1919	4.7509

The approach used here was to first obtain solubility data at a specific temperature for each gas at the salinity of seawater. This data, coupled with the Benson and Krause freshwater solubilities at the same temperature allow the corresponding Ks values to be obtained using the above equation. Repeating this procedure for a range of temperatures enables the Ks temperature dependence to be listed. Seawater solubilities were obtained from data by Weiss (1970), (N_2, O_2, Ar); Weiss (1971), (He, Ne); Smith and Kennedy (1982), (Kr, Xe); Broecker (1974), (CO_2); and Shoor and Gubbins (1968), (CH_4).

Calculation of the saline water solubility requires determination of the alkali-halide molarity, M. In seawater the salinity (S) in per mill is related to the chlorinity (Cl) by:

$$S\ {}^{o}/_{oo} = 1.806\ Cl\ {}^{o}/_{oo}$$

(Brownlow, 1979). The molecular weight of the seawater solutes is therefore 1.806 multiplied by the atomic weight of chlorine (35.5) = 64.113. The molarity of a saline fluid is therefore:

$$M = \frac{S^{o}/oo}{64.113}$$

This approach is of course only strictly applicable to waters of a seawater composition. In groundwaters an analysis of the total ions in solution would be necessary to obtain a true value for M. In many cases this is not possible, but since chlorinity is a commonly measured variable, the above relationships could be used as an approximation to obtaining M.

Each of the calculated Ks-temperature lists for each gas were then fitted to a polynomial cubic equation, using the temperature variable

$Z = T(K)/100$

$$Ks = AZ^3 + BZ^2 + CZ + D$$

The parameters A, B, C and D used in calculating Ks for each gas are listed in Table 6. Fig. 6 illustrates the temperature dependence of Ks

Table 6. Parameters for use in estimation of salting coefficients for curve-fitted data.

Gas	A	B	C	D
He	-0.2304	2.2951	-7.7154	9.0060
Ne	-0.3022	3.6278	-13.6641	16.8309
Ar	-0.4050	3.8471	-12.3389	13.6921
Kr	-0.1124	1.3282	-5.1432	6.8403
Xe	-0.1611	1.9007	-7.3019	9.5072
N_2	-0.2427	2.1504	-6.6100	7.4294
O_2	-0.3616	3.3454	-10.5501	11.6687
CH_4	-0.0210	0.2089	-0.7894	1.5653
CO_2	-0.0964	1.0183	-3.5065	4.0378

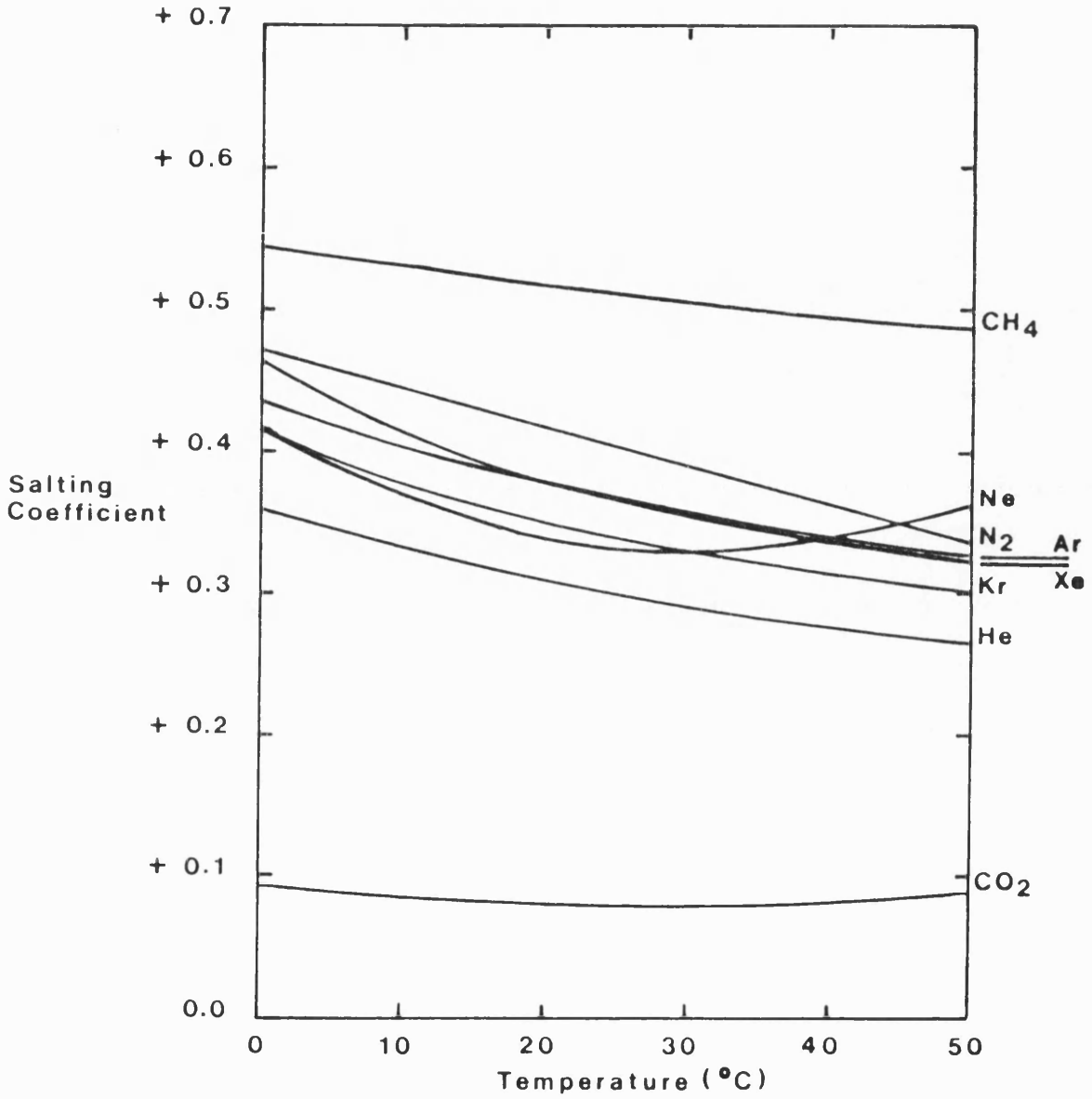

FIG.6 Salting coefficients for the noble gases, nitrogen, methane, and carbon dioxide.

on each gas as calculated in this work. Table 7 lists the solubilities for some of the gases for a salinity of 0 $^{o}/_{oo}$ and 35.5 $^{o}/_{oo}$ respectively when equilibrated under air. At higher temperatures and salinities, the data probably becomes more uncertain. However at low temperatures and salinities (i.e. T = 0 - 40^{o}C, S $^{o}/_{oo}$ = 0 - 40) the data is very accurate since this is the region from which the salting-coefficient and pure water data was initially derived.

1.5 N_2/Ar ratios in the environment

Argon is the most abundant of the noble gases in air and its concentration will remain constant after aquifer recharge providing no additional inputs occur particularly from the ratioactive decay of ^{40}K. The N_2/Ar ratio will therefore provide an index with respect to elevated N_2 concentrations. Denitrification would cause an enhancement in this ratio in aquifer groundwaters.

Measurement of N_2/Ar ratios have primarily been applied to marine environments (Benson et al., 1961), or soil atmospheres (Focht, 1978), and volcanic gases (Matsuo et al., 1978). Often the environments are complex with major problems in sampling and subsequent caution in interpretation, so the trends are more important than the actual figures. In particular it is interesting to note that the N_2/Ar ratio in a soil atmosphere may be quite variable. If a reducing environment is present Rightmire (1979) has noted that N_2/Ar ratios in the unsaturated zone of an aquifer decrease from the atmospheric value of 83.54 due to N_2 reduction to NH_4^+ which is then absorbed onto clays. However a depressed N_2/Ar ratio below atmospheric is one important criteria by which mining companies may prospect in soil atmospheres for mineral deposits, due to enhanced argon gas released from the orebody. Nevertheless Focht (1978) points out that for a N_2/Ar ratio in the soil atmosphere above the

Table 7. Comparison of atmospherically equilibrated gas concentrations at 0.0 °/oo salinity and 35.5°/oo salinity (cm^3/cm^3 H_2O)

Salinity = 0‰

	x 10^{-7}	x 10^{-4}	x 10^{-8}	x 10^{-8}	x 10^{-2}
T	Ne	Ar	Kr	Xe	N_2
0	2.295	4.997	12.659	1.939	1.845
10	2.065	3.891	9.244	1.325	1.467
20	1.914	3.182	7.146	0.967	1.220
30	1.819	2.710	5.796	0.746	1.053
40	1.764	2.389	4.896	0.602	0.938

Salinity = 35.5°/oo

T	Ne	Ar	Kr	Xe	N_2
0	1.823	3.921	10.070	1.503	1.421
10	1.686	3.111	7.503	1.054	1.147
20	1.588	2.580	5.893	0.785	0.968
30	1.516	2.222	4.839	0.614	0.848
40	1.464	1.977	4.123	0.501	0.767

atmospheric ratio, denitrification can be the only explanation. These soil atmosphere studies are important when one considers that such atmospheres may affect the N_2/Ar ratio subsequently dissolved into an aquifer.

A number of workers (e.g. Heaton et al., 1981) have noted the presence of extra air saturation in groundwaters; this seems to be a normal occurence rather than the exception. Such extra air components can be related to pockets of trapped air/soil atmosphere being drawn down with the percolating water and being forced into solution by the increasing pressure as depth increases.

A denitrified N_2 component has been potentially recognised by Vogel et al., (1981) in their study of the Auob Sandstone aquifer of the Western Kalahari desert. Here N_2/Ar ratios were measured up to values as high as 73. When the N_2 and Ar concentrations are corrected for extra air, a definite N_2 excess is present which they attribute to in-situ aquifer denitrification of nitrates.

There is generally little data on N_2/Ar ratios in different environments. With respect to groundwaters, it is important to determine whether the ratio is controlled by N_2 enhancement/depletion, or Ar enhancement/depletion. Absolute concentrations of these gases should therefore always be borne in mind when interpreting N_2/Ar ratios.

1.6 Nitrogen Isotope Ratios in the Environment.

The element N occurs in nature as a mixture of two stable isotopes, ^{14}N and ^{15}N. The percentage of the heavy isotope in atmospheric N_2 is 0.3663% (Sweeney et al., 1976) and is constant within analytical precision (Mariotti, 1983). Atmospheric N_2 is therefore used as a standard for nitrogen isotope analysis. Several radioactive isotopes of N are also known to exist, the longest 1/2-life being 10 mins for ^{13}N. Such short 1/2-lives limit the usefulness of the radioactive nitrogen isotopes in environmental studies.

Small variations in the natural abundance of ^{15}N can be determined by comparison of the sample $^{15}N/^{14}N$ ratio with a standard $^{15}N/^{14}N$ ratio; this being atmospheric N_2. Although the absolute abundances cannot be measured with accuracy, expressing the results as a change against a standard allows very small isotopic variation to be identified. For this reason results are expressed in the delta-notation and multiplied by 1000 to give convenient handling figures in per mille.

$$\delta^{15}N\ {}^{o}/_{oo} = \left[\frac{(^{15}N/^{14}N)_{SPL} - (^{15}N/^{14}N)_{AIR}}{(^{15}N/^{14}N)_{AIR}}\right] x\ 1000$$

Positive values indicate ^{15}N enrichment in the sample, negative values indicate ^{15}N depletion (with respect to the standard). The $\delta^{15}N$ of air has by definition a value of $0.0^{o}/_{oo}$.

The small natural variations in the relative abundances of stable isotope pairs result from the difference in mass between molecules containing the heavy vs the light isotope. Such differences arise as a result of quantum mechanical effects. The vibrational frequency of a molecule depends inversely on the masses of the atoms in the molecule, and since vibrational frequency is proportional to energy, bonds formed by the light isotope are weaker than bonds involving the heavy isotope

(Hoefs, 1980). Thus, during a chemical reaction, molecules bearing the light isotope will in general react slightly more readily than those with the heavy isotope.

Nitrogen compounds are widely distributed in terrestrial substances, but their concentrations are rather low and their isotopic compositions are, at least for the upper lithosphere, essentially controlled by biological rather than inorganic thermodynamic processes (Fig. 7). The main application of nitrogen isotopes has been in identifying nitrate sources in aqueous environments based on their isotopic signature (Kreitler et al., 1978); in medicine and biology (Macko, 1983); and in biochemistry with respect to nitrification and denitrification (Mariotti et al., 1981). $\delta^{15}N$ variations in petroleum may prove more useful than carbon or oxygen isotopes in delineating oil fields (Macko et al., 1983), and data for variations in igneous rocks and meteorites is accumulating (Frick et al., 1981).

If the denitrification step is considered to be a first-order, unidirectional single step process, then:

substrate product

$$NO_3^- \longrightarrow N_2$$

The isotope fractionation can be described by the alpha fractionation factor, α, i.e.

$$\alpha = \frac{Rp}{Rs}$$

where Rp is the isotopic ratio of the product increment which appears in an infinitely short time at some time t, and Rs the isotope ratio of the substrate at the same time. The α-fractionation factor expressed in terms of the δ-notation is:

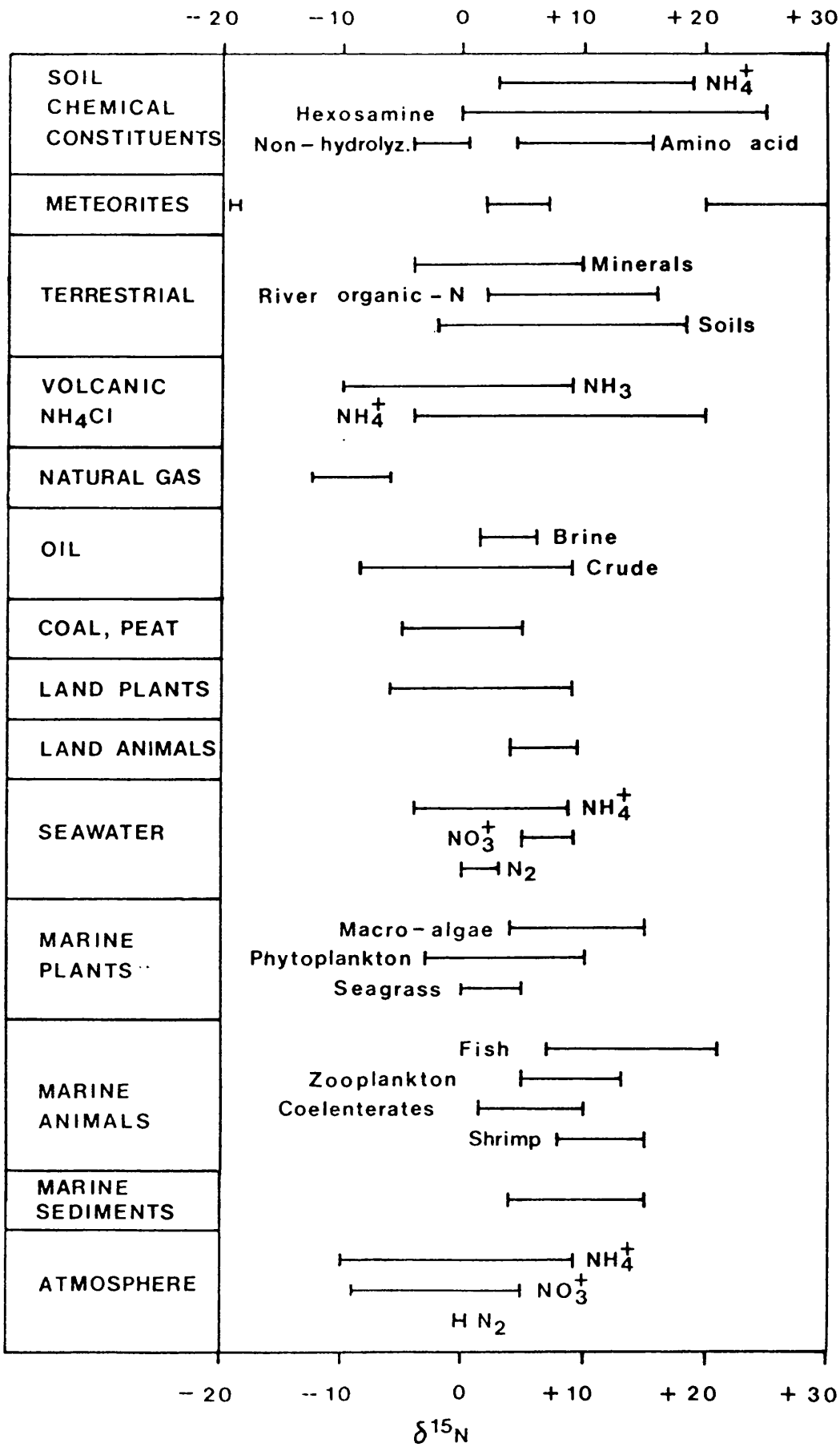

FIG. 7 Global nitrogen isotope abundances.

$$\alpha = \frac{1000 + \delta p}{1000 + \delta s}$$

Determination of the α-fractionation factor in natural systems is an important quantifiable aim in nitrogen isotope studies. A value <1 indicates the product is depleted in ^{15}N with respect to the substrate.

There are two types of fractionation effects. Firstly there are kinetic isotope effects which are a function of the differences in reaction rates of isotopic species, independent of the reaction order. This is the type controlling the denitrification process, essentially unidirectional and biologically mediated, i.e.

$$\begin{array}{lcl} ^{15}N \text{ reactant} & \xrightarrow{K_{15}} & ^{15}N \text{ products} \\ + \text{ other reactants} & & + \text{ other products} \end{array}$$

$$\begin{array}{lcl} ^{14}N \text{ reactant} & \xrightarrow{K_{14}} & ^{14}N \text{ products} \\ + \text{ other reactants} & & + \text{ other products} \end{array}$$

and $\alpha = \frac{K_{15}}{K_{14}}$

The second type of fractionation effect is produced by isotopic equilibrium, i.e. the isotopes distribute themselves between two phases governed by the laws of thermodynamics, i.e.

$$\alpha = K^{1/n}$$

where K is the equilibrium constant for the reaction and n is the number of atoms exchanged. This type of fractionation controls the dissolution of molecular nitrogen in water and the evaporation of volatile nitrogen compounds. Table 8 lists some α values characteristic of the more important processes occuring in the Nitrogen Cycle, from Schidlovski et al., (1983). Although only one typical value is given for each process, the α value, particularly for kinetic processes such as denitrification,

Table 8. Observed isotope fractionation factors for the major nitrogen-involving processes occuring in nature.

Isotope Effect	Observed fractionation factors
Kinetic Isotope Effects	
Nitrogen Fixation: Atm $N_2 \rightarrow$ fixed nitrogen	$\alpha = 0.998$
Nitrification: $NH_4^+ \rightarrow NO_2^-$	$\alpha = 0.98$
Denitrification: $NO_3^- \rightarrow N_2$	$\alpha = 0.98$
Equilibrium Isotope Effects	
Ammonia Volatilisation: $NH_4^+(aq) \rightleftharpoons NH_3(g), 25^oC$	$\alpha = 0.967$
Solution of Nitrogen Gas: $N_2(soln) \rightleftharpoons N_2(g), 0^oC$	$\alpha = 0.99915$

is probably unique to any one particular system and dependent on such variables as temperature, bacterial species, and availability of oxidant and reductant to name but a few.

An alternative way of expressing the fractionation effect between the products and the substrate (with respect to denitrification) is the enrichment factor, ε, expressed in per mille:

$$\varepsilon = (\alpha - 1) \times 1000 \text{ ‰}$$

The ε value has the advantage of immediately indicating the isotopic 'gap' between the products and the substrate. Its value can be positive or negative, indicating enrichment or depletion of ^{15}N in the products.

The continuous removal of the reaction products involved in denitrification can be compared with a Rayleigh Fractionation process, whereby the isotopic composition of the nitrate changes as a function of residual nitrate left and of the α fractionation factor, i.e.

$$Rs = Rs,o \; f^{(\alpha - 1)}$$

where Rs and Rs,o are the isotopic ratios of the substrate at time t and time t = 0 respectively. f refers to the fraction of substrate remaining. This can be expressed in the δ-notation as:

$$(\alpha - 1) \ln f = \ln \left[\frac{10^{-3} \, \delta s + 1}{10^{-3} \, \delta s,o + 1} \right]$$

expressing α as ε subsequently gives:

$$\varepsilon \ln f = 1000 \ln \left[\frac{10^{-3} \, \delta s + 1}{10^{-3} \, \delta s,o + 1} \right] \qquad (1)$$

Providing ε values are < $+20^{o}/oo$, and the δ s,o values are not too different from $0^{o}/oo$, the following simplified relation holds. (Mariotti, 1981).

$$\varepsilon_{lnf} = \delta s - \delta s,o$$

A schematic example is illustrated in Fig. 8 using this equation to plot the change in δ s, where δ s,o = $0^{o}/oo$.

Modelling the isotopic change of the product is dependant upon the subsequent fate of the nitrogen gas. If the products are continuously removed, then the increments of denitrified N_2 gas will vary according to:

$$\delta pi = \delta s \left(1 + \frac{\varepsilon}{1000}\right) + \varepsilon$$

If ε is small relative to 1000, the following approximation can be used:

$$\delta pi = \delta s + \varepsilon$$

So the curve for δ pi in Fig. 8 as a function of f is derived by the translation of ε on the delta-coordinate from the δ s curve. α and hence ε will be constant during the reaction (f $\rightarrow$ o).

Alternatively, the 'instantaneous products' may accumulate, forming a reservoir of accumulated products. In such a closed system, the products and substrate must together equal the initial isotopic substrate composition. This allows an isotope mass balance equation to be written.

$$f.Rs + (1 - f)Rp^{*} = Rs,o$$

where Rp* is the isotopic ratio of the accumulated product. This may be written in the delta-notation as:

$$f.\delta s + (1 - f)\,\delta p^{*} = \delta s,o$$

combining this equation with equation (1) gives

$$\delta p^* = \delta s,o - \frac{\varepsilon f \ln f}{1 - f}$$

In this case, Fig. 8 shows that δp^* evolves along a curve in which the final isotopic composition of the accumulated reservoir is equal to the starting composition of the substrate.

Satisfactory laboratory studies of these relationships have been carried out by Mariotti et al., (1981) and Mariotti et al., (1982), usually limiting the study to one particular step of the dentrification process, eg. $NO_2^- \rightarrow N_2O$. In particular, it was noted that the isotope enrichment factor, ε, decreases as temperature and hence reaction rate increases. Observed ε values varied between $-11^o/oo$ and $-33^o/oo$.

There is less information concerning the isotope effects of denitrification in natural systems. Vogel et al., (1981) describe a system in the Aoub sandstone aquifer of the Kalahari desert of Africa where dissolved N_2 components in excess of that derived from recharge have isotope values indicative of an accumulated product curve. The f values approach 0 with increasing groundwater age, and an ε value of $-30^o/oo$ is suggested.

All too often it has been noted that the predicted relationships according to theory are not observed in practice. For example, laboratory studies by Cook et al., (1970) suggest that in some cases the denitrifying bacteria may discriminate against the $^{15}NO_3$, preferring to reduce only the $^{14}NO_3$. Only at the later stages when most of the nitrate has been denitrified is $^{15}NO_3$ consumed, producing a pulse of very heavy $\delta^{15}N$ nitrogen gas. This effect has been called the 'Last Gasp Effect', and illustrates the difficulties of applying classical thermodynamic principles to biologically mediated systems.

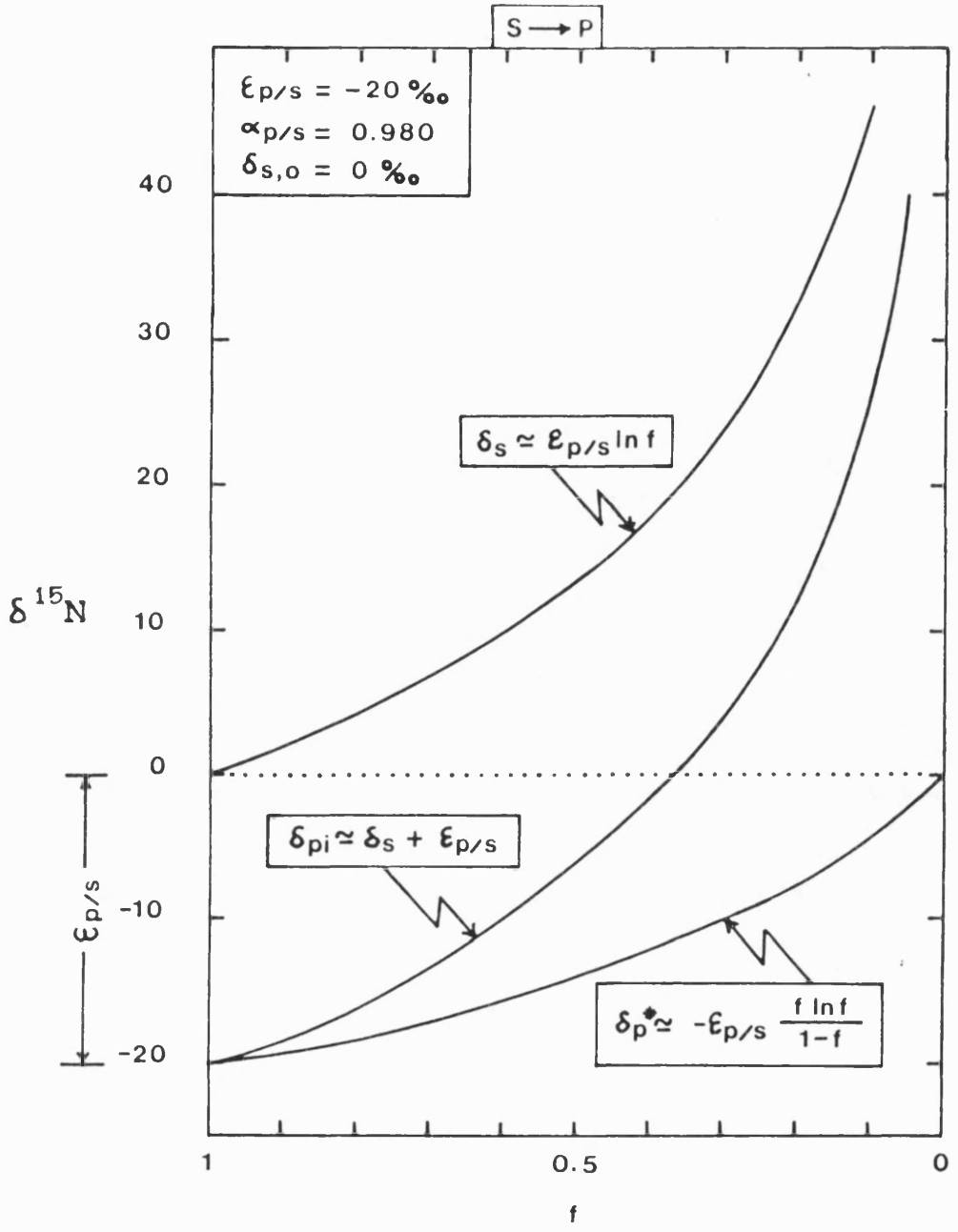

FIG.8 Theoretical change in substrate and product isotopic composition in a single step unidirectional reaction.

The late 1960's and early 70's saw a marked increase in the measurement of nitrogen isotopes particularly in nitrate compounds. This was largely because it was believed that the isotope signature of the nitrogen compounds would characterise their source, especially with respect to nitrate fertiliser pollution, i.e. natural vs. artificial nitrate sources (eg. Kreitler, et al., 1978; Kreitler, 1979; Kreitler 1983).

Animal matter is usually enriched in ^{15}N if compared to vegetal matter. This is due to the catabolic pathways which favour the elimination of small nitrogen molecules depleted in ^{15}N (Letolle, 1980). This is illustrated in Fig. 9. On the otherhand, vegetal organic matter is normally slightly depleted in ^{15}N with respect to the nitrogen source. Artificial fertiliser $\delta^{15}N$ values lie close to $0^{o}/oo$ because they are industrially fixed from atmospheric N_2 which has itself a $\delta^{15}N$ of $0^{o}/oo$. Table 9 summarises the typical range of nitrates with isotopic values attributed to specific sources. What is interesting to note is the degree of overlap between the supposedly different sources. Both fertilised anbd unfertilised cultivated fields may have nitrates with similar isotopic compositions irrespective of whether artificial or natural fertilisers are used. This is because although artificial fertiliser NO_3 may have a $\delta^{15}N$ close to $0^{o}/oo$, ammonia volatilisation or denitrification may enrich the NO_3 to $\delta^{15}N$ values comparable to a natural fertiliser source. To what extent is an observed $\delta^{15}N(NO_3)$ value a function of its discrete source or to subsequent modification? When one considers the complexities of the dentrification process alone in modifying the isotopic composition of nitrates it seems clear that a very detailed knowledge of all the ecological parameters of a system is necessary to correctly interpret observed $\delta^{15}N$ values in nitrates.

Such a detailed study has been undertaken by Mariotti et al. (1977)

Table 9. **$\delta^{15}N$ nitrate contents of selected environments.**

$\delta^{15}N(NO_3)$ ‰	Source
~0 ‰	artificial fertiliser
+ 5	soil mitrate/natural fertiliser
+ 2 → + 8	unfertilised cultivated fields
+ 3 → + 9	fertilised cultivated fields
-10 → + 8	vegetal organic matter
+10 → +22	animal waste

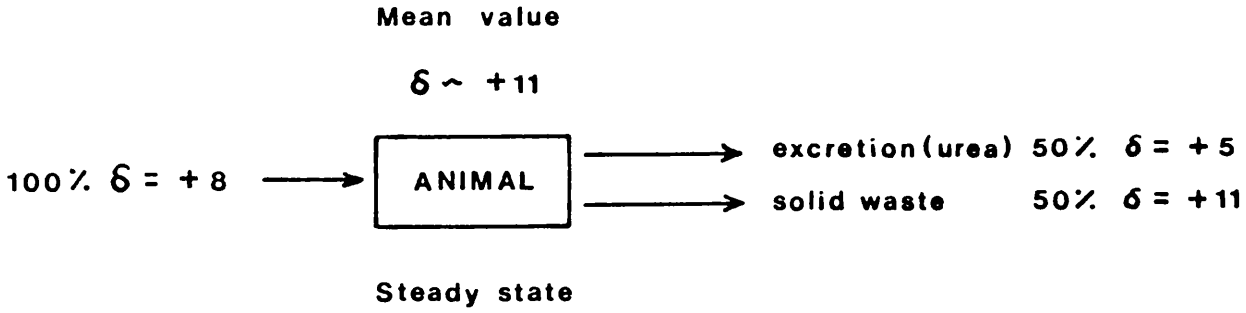

FIG.9 A possible model to explain how animal organic matter is enriched in ^{15}N due to the elimination of low ^{15}N urea.

in their study of the $\delta^{15}N$ of nitrates in the Melarchez basin east of Paris. A complex interaction is present between the $\delta^{15}N(NO_3)$ of rainfall, season, recharge rivers, biological activity of the soil, and the underlying limestone aquifer.

1.7 The stable isotope composition of water

Information concerning an aquifer's recharge conditions can be obtained from studying the stable isotopes of hydrogen and oxygen which are bound up in the water molecule. Oxygen is the most abundant chemical element in the crust of the Earth and is combined with hydrogen to form water (H_2O). Oxygen has three stable isotopes whose approximate abundances are: ^{16}O = 99.756%; ^{17}O = 0.039%; ^{18}O = 0.205%. Hydrogen has two stable isotopes whose abundances are: ^{1}H = 99.985% and ^{2}H = 0.015% (^{2}H = Deuterium, D). Hydrogen also has a naturally occuring radioactive isotope ^{3}H (Tritium, T), which has a 1/2-life of 12.3 years.

Differences in the isotopic composition of H_2O reflect mass fractionation effects caused by evaporation and subsequent cloud condensation, (Dansgaard, 1964). This precipitation may recharge an aquifer. Providing no water-rock interaction has taken place and no substantial mixing with other water sources has occured, the isotopic signature of the water molecule should be retained indefinitely since the time of recharge.

Isotopic compositions of oxygen and hydrogen are reported in terms of differences of $^{18}O/^{16}O$ and $^{2}H/^{1}H$ ratios relative to a standard called SMOW (Standard Mean Ocean Water) i.e.

$$\delta^{18}O = \left[\frac{(^{18}O/^{16}O)SPL - (^{18}O/^{16}O)STD}{(^{18}O/^{16}O)STD} \right] \times 1000$$

$$\delta^{2}H = \left[\frac{(^{2}H/^{1}H)SPL - (^{2}H/^{1}H)STD}{(^{2}H/^{1}H)STD} \right] \times 1000$$

The delta values are multipled by 1000 to express the data in $^{o}/_{oo}$. Positive values of $\delta^{18}O$ and $\delta^{2}H$ indicate enrichment of a sample in ^{18}O and ^{2}H compared to SMOW, while negative values imply depletion of these isotopes in the sample relative to the standard.

Dansgaard (1964) has been mainly responsible for deducing how hydrological and climatological information can be derived from plotting $\delta^{18}O$ against $\delta^{2}H$. The processes of condensation and evaporation of oceanic water produce precipitation compositions which, taking worldwide data, follow the relationship:

$$\delta^{2}H = 8\ \delta^{18}O + 10$$

The precipitation process occurs by equilibrium condensation, and its subsequent removal from a cloud can be described by Rayleigh Fractionation. Increments of rain derived from an air mass undergoing equilibrium condensation would plot along a line towards progressively lighter compositions as the fractionation proceeds. This line would be characterised by a slope of 8. The equation for the worldwide precipitation line described above does indeed have a slope of 8, but it is also displaced $+10^{o}/_{oo}$ $\delta^{2}H$ relative to SMOW. If equilibrium evaporation and condensation were the only processes operating, then the line should intersect SMOW since all meteoric freshwater is initially derived from the oceans. This deviation can be explained by a non-equilibrium (kinetic) evaporation process. The air masses which produce higher latitude precipitation originate down in the Tropics, where extensive evaporation of ocean water occurs. Here the kinetic evaporation produces water vapour which is enriched in $H_2{}^{16}O$ molecules relative to its equilibrium composition. This shift to a lighter composition is reflected in the subsequent equilibrium condensation as the air mass tracks polewards.

In regions where kinetic evaporation is dominant the local rainfall may plot with a slope <8 due to differing evaporation rates producing corresponding shifts in the compositions of the first rains. In a similar way, regions of excessive condensation may produce kinetic effects which would give rise to a slope >8. The local climate of a particular region will therefore be indicated by the slope of the precipitation data, reflecting the balance between equilibrium and non-equilibrium processes; such data is ususally plotted against the Worldwide Precipitation line for reference.

The driving force behind condensation is a lowering of temperature. There is therefore an altitude effect as well as a latitudinal effect. In fact a relationship between the $\delta^{18}O$ values of average annual precipitation and the average annual air temperature is present:

$$\delta^{18}O = 0.69t - 13.6$$

where t = temperature (^{o}C). This relationship reflects the fact that isotopic fractionation increases with decreasing temperature. If the main surface temperature varies in parallel to the mean condensation temperature then:

$$\frac{\Delta\delta^{18}O}{\Delta t} = 0.7\ {}^{0}/_{00}\ {}^{0}C^{-1}$$

The range of $\delta^{18}O$ values of meteoric waters is from about 0 to $-60^{o}/oo$, whilst $\delta^{2}H$ varies from about 0 to $-400^{o}/oo$. The lowest values occur in snow precipitated at high latitude and/or high elevations with low temperatures.

There has been essentially no latitudinal variation in the position of Britain over the timescale of the Pleistocene. Therefore any

variations in $\delta^{18}O$ and $\delta^{2}H$ from aquifer groundwaters must reflect climatological changes in the recharge conditions, with a colder environment reflected in more negative delta values. For example, Bath et al., (1978) have studied $\delta^{18}O$ and $\delta^{2}H$ values of waters from the Nottinghamshire Triassic sandstone aquifer in the U.K. They recognised a bimodal grouping of data which lies approximately on Dansgaard's World Wide Precipitation line and the $\Delta\ \delta^{18}O$ suggests a change in cloud precipitation temperature of some 1 - 2°C since the Late Devensian.

1.8 Hydrogeochemistry of the Nottinghamshire Triassic Sandstone Aquifer.

1.8.1 Hydrogeology

The Triassic sandstone aquifer of Nottinghamshire outcrops in the East Midlands where it has a uniform easterly dip of 1 in 50 over the studied region (Fig. 10). The sandstone (the Bunter Sandstone) varies in thick ness from 120 m in the south to 300 m in the north, and reflects deposition in a fluviatile environment during Triassic times under a semi-arid climate.

Above and below the Bunter Sandstone are transitional non-marine lithologies. The upper unit to the sandstone is the Keuper marl mainly comprising mudstones and argillaceous sequences. This unit unconformably overlies the sandstone forming a confining horizon to the aquifer. At the base of the sandstone a mixed sequence of Permian mudstones, marls and dolomite limestones forms a generally impermeable layer except where local faulting occurs. The sandstone is therefore effectively sealed above and below by the transitional non-marine lithologies, limiting the area of groundwater recharge to the area of outcrop.

The sandstone itself is yellow or red-brown in colour and is poorly cemented, especially in the middle of the formation (Land, 1966). The

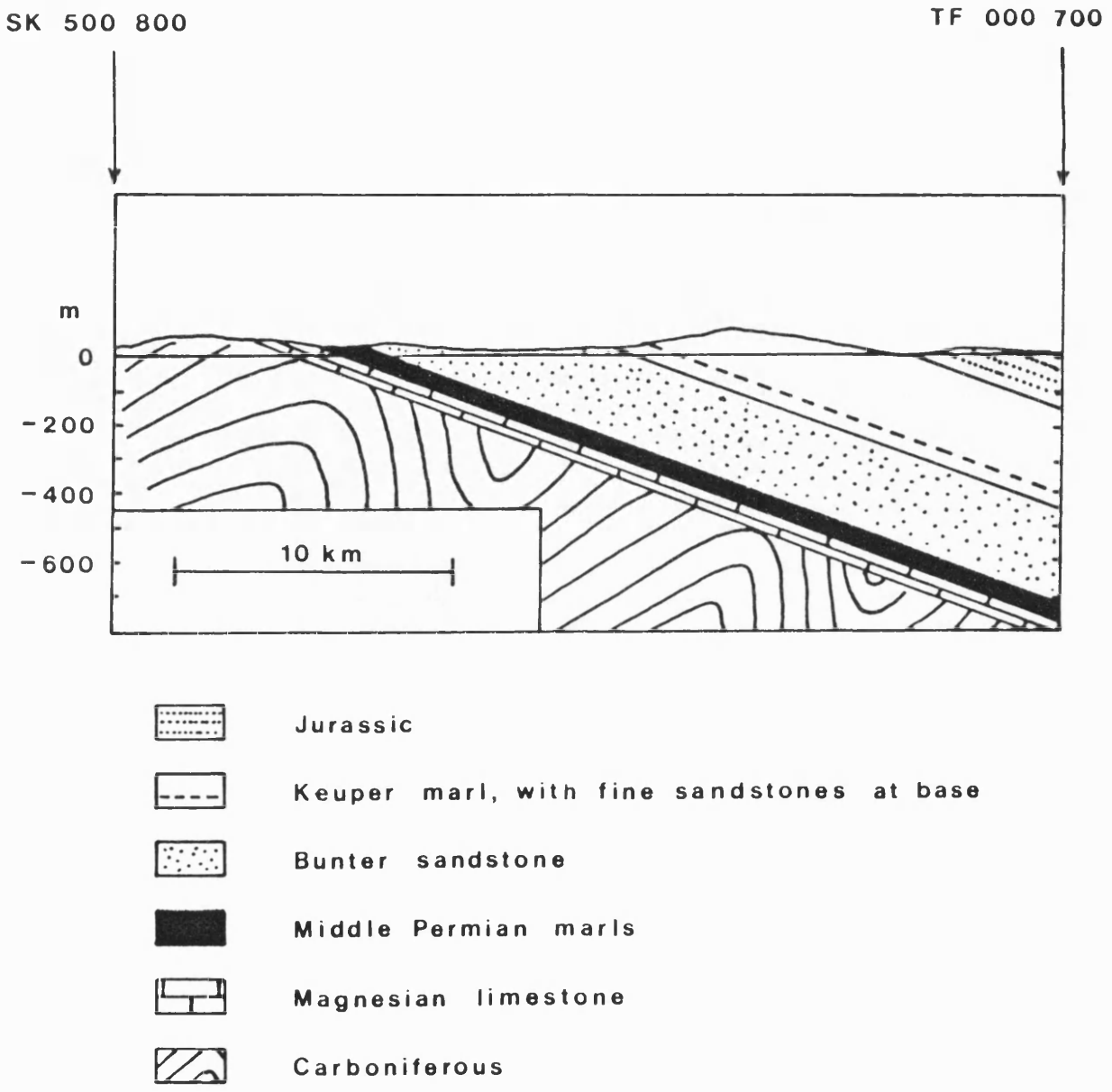

FIG.10 Cross-section of the North Nottinghamshire area, showing major lithological units.

mean intergranular porosity is 30%, although the overall permeability is increased by the local presence of fissures. The mineralogy predominantly consists of quartz grains, but feldspars are also present both as detrital minerals and as late overgrowths. Muscovite, biotite and illite are common detrital micas near the top of the sandstone. Occasional grey-green horizons of microcrystalline iron sulphide are found in the basal sandstones of the aquifer. These horizons are thought to have formed from the incomplete oxidation of fine-grained sediments by migrating groundwaters. The red colouration of the sandstone is due to the iron mineralogy predominantly consisting of a mixture of haematite (forming pellicles around individual sand grains) and amorphous interstitial iron oxides. The carbonate phases of the sandstone (calcite and dolomite) constitute 1-5% of the unit, with dolomite >50% the total carbonate. Calcite occurs as fine grained clasts intergrown with clay minerals and dolomite. Both calcite and dolomite are sometimes evidently derived from the recrystallisation of prior carbonate phases.

Aquifer recharge at outcrop occurs mainly via direct infiltration of rainwaters (mean rainfall = 650 mm/yr; mean recharge = 150 mm/yr) which percolate through the soil zone. However local rivers such as Rainworth Water and Vicor Water may also directly recharge the aquifer when high water velocities cause flow to occur out of bank or to strip away the sealing sediment on the river bed. The groundwater flow is mainly by fissure flow although intergranular flow is locally important. Typical water velocities lie between 9 m/yr in the north to 3 m/yr in the south, and are undoubtedly some function of the present day pumping regime.

1.8.2 Hydrochemistry

Most of the information given here is a summary of the work by Edmunds et al., (1982) and Bath et al., (1979). In any redox

environment, three factors are the major controls on the Eh-pH (definitions of Eh and pH are given in the relevant sections in the Experimental Techniques chapter). Firstly, the organic processes of photosynthesis, respiration and decay; secondly, oxidation - reduction reactions involving primarily iron, sulphur and carbon; and finally the balance between dissolved carbon dioxide and calcium carbonate ($CaCO_3$) in natural waters.

In surface water environments characterised by biological activity, organic processes control the pH. Photosynthesis converts light energy ($+ H_2O + CO_2$) to chemical energy in the form of organic compounds ($+ O_2$). The organic compounds have a high Gibbs Function and are therefore rather unstable. Respiratory and decay processes reduce the Gibbs Function, use up O_2 and produce CO_2. The oxidation of organic matter thus removes oxygen and lowers the Eh. The production of CO_2 by oxidation of organic matter also lowers the pH, since CO_2 combines with H_2O to form a slightly ionised acid, H_2CO_3, ie.

$$H_2O + CO_2 \rightarrow H_2CO_3 \rightarrow H^+ + HCO_3^-$$

A lowering of both the Eh and pH is indeed observed in the Nottinghamshire Triassic groundwaters (Eh: +300 to -50 approx; pH: 8.5 to 7.5). This lowering in both the Eh and pH cannot be explained by organic processes because the levels of organic carbon to act as an energy source, and for growth of heterotrophic bacteria, are negligible (levels <0.1 mg/l organic carbon). This is consistent with the persistence of dissolved O_2 in the aquifer for at least 30 years from recharge, according to levels of tritium in the modern outcrop waters.

Inorganic processes must therefore explain the decline in Eh and pH. The abundance of H_2CO_3 is virtually constant over the temperature range of interest ($\sim 10^oC$). Since $CaCO_3$ is slightly soluble in H_2CO_3, any reactions involving the solution of carbonate phases would raise the pH,

because H_2CO_3 would be removed from the water. This is certainly possible because dolomite and calcite together constitute 1-4 wt % of the sandstone. The carbonate minerals could go into solution by the following mechanisms:

1. $CaCO_3 + H_2CO_3 \rightarrow Ca^{2+} + 2HCO_3^-$
2. $CaMg(CO_3)_2 + 2H_2CO_3 \rightarrow Ca^{2+} + Mg^{2+} + 4HCO_3^-$
3. $CaMg(CO_3)_2 + H_2CO_3 \rightarrow CaCO_3 + Mg^{2+} + 2HCO_3^-$

If the groundwaters are in equilibrium with the carbonate minerals, then the molal ratios of the measured concentrations of Ca^{2+}, Mg^{2+} and HCO_3^- should reflect the stoichiometry of the above reactions. This is indeed the case, with congruent dissolution of dolomite (reaction 2), and some calcite occuring in outcrop waters. Deeper in the aquifer however, the molal ratios reflect reaction 3, the incongruent dissolution of dolomite, from which the precipitation of calcite can be inferred. Since reaction 3 favours half as much H_2CO_3 as reaction 2, more H_2CO_3 is available for ionisation, and hence the pH is lowered from its value at outcrop.

The dissolution of dolomite can be related to a mechanism for the lowering of the Eh. The oxidation of organic matter alone cannot account for the depletion in oxygen content because the organic matter content is so low. Indeed the persistence of dissolved oxygen is notable until the groundwaters enter the confined aquifer, where O_2 levels drop close to zero and Eh values markedly decrease indicating a redox boundary. A sequential order of redox reactions is present in any environment according to the availability of the reducing agent. The most energetically stable reaction involves reduction of oxygen. Should oxygen be lacking, then the next most favourable reaction is the reduction of nitrates, and finally the reduction of sulphates. In this red-bed lithology, the O_2 would be most easily removed by oxidation of

Fe^{2+} released during the dissolution of iron-bearing carbonate. This oxidation does not precipitate crystalline iron minerals (eg haematite Fe_2O_3) but ferric oxyhydroxides, deduced from the petrology of the sandstone.

In the deeper confined aquifer, the correlation between the carbonate dissolution reactions and the dissolved ionic species becomes less obvious. SO_4^{2-} levels tend to increase, suggesting dissolution of gypsum ($CaSO_4$) is occuring. The influx of $CaSO_4$ derived Ca^{2+} is probably balanced by the precipitation of calcite to maintain equilibrium, but the Ca^{2+}/HCO_3^- carbonate-dissolution stoichiometry is no longer quite so predictable. As the SO_4^{2-} increases, the $FeSO_4^o$ complex becomes a significant contribution to the total dissolved iron. Reduced sulphur is also present, but this is unlikely to have been derived via SO_4^{2-} reduction because the measured Eh values are too high for the SO_4^{2-}/HS^- couple to have a dominant control on the redox potential. SO_4^{2-} reduction via oxidation of organic carbon is also not feasible because of the low quantities of organic matter. It is likely that the dissolved iron and sulphur concentrations in the reducing zone reflect some form of metastable equilibrium with iron mineral phases in the aquifer, such as pyrite and siderite.

The Eh-pH of this aquifer is therefore primarily controlled by carbonate equilibria and the oxidation of Fe^{2+}. The question as to whether dentrification is occuring lies primarily on the observation that outcrop nitrate levels may approach 50 mg/l, but waters in the confined aquifer are much lower, usually <2 mg/l. When one considers that fertiliser nitrates are continuously being applied to outcrop agricultural land the ultimate fate of these nitrates is brought into question.

The Nottinghamshire Triassic groundwaters, especially in the

confined aquifer, are essentially very old. Bath et al., (1979) have estimated on the basis of ^{14}C activity in the water that the outcrop sites contain modern waters but in the deeper confined aquifer are probably older than 30,000 years. BP. These ages may well be minimum ages due to the probable degree of mixing of waters of different ages in the aquifer, although for the most part the waters tend to retain their input characteristics from outcrop. Any interpretation of these waters must be done in the context of the timescales involved.

1.9 Hydrogeochemistry of the Lincolnshire Limestone Aquifer

1.9.1 Hydrogeology

The lincolnshire Limestone (Inferior Oolite) is a cemented oolitic limestone of Middle Jurassic age. The outcrop region extends for some 120 km across England in a NE-SW direction, and regionally dips $1^{o}E$. The land use is intensly agricultural, particularly in the Fenland area of south Lincolnshire, where the maximum outcrop elevation is only 120 m.

The limestone has a thickness of over 30 m at outcrop but thins to less than 20 m in the east, where it is confined beneath clays, shales and marls of the Upper Estuarine Series. The Lower Estuarine Series confines the limestone below with sequences of sands with silts, clays and shales (Fig. 11).

Two lithological classes of rock can be recognised in the limestone (Downing et al., 1969). The lower half is generally more highly fractured with locally sandy facies near the base, whilst the upper half has a more massive limestone facies. The unaltered rock at depth is grey-green in colour, but diagenesis by migrating groundwaters on both a recent and geological timescale has progressively oxidised the rock to a light-brown colour in the upgradient aquifer.

Groundwater flow in the limestone is predominantly by fissure flow,

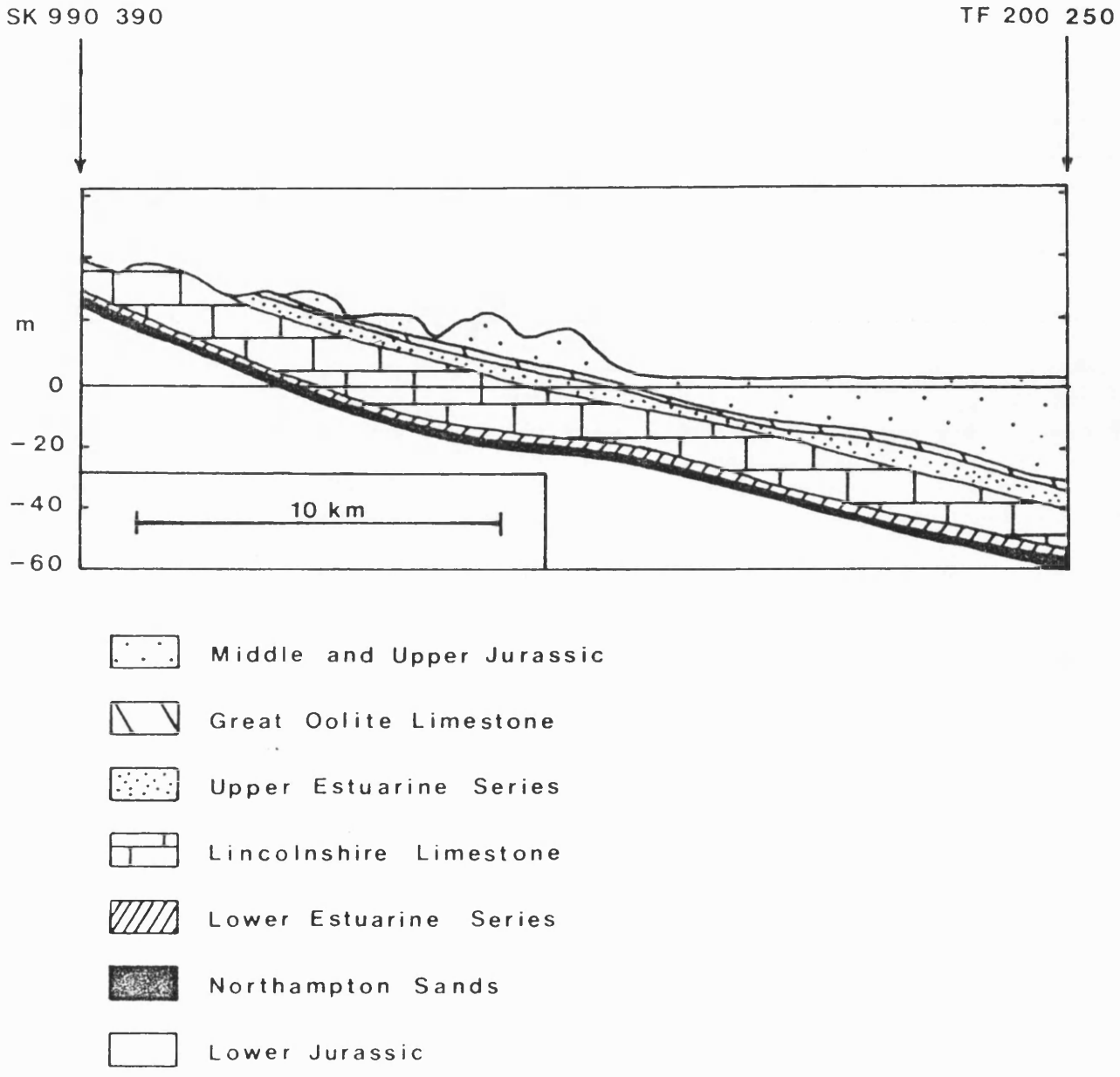

FIG.11 Cross-section of the Lincolnshire area, showing major lithological units.

with velocities as high as 30 m/day. The fracture porosity of the limestone is however only 0.25 - 0.8% in comparison to the primary porosity of the rock which is 25%. This means that the fissure storage capacity is only a few per cent of the total interstitial storage of the aquifer, and that a very large quantity of much older water is present in the aquifer which undergoes limited exchange with the rapidly moving modern fissure waters. The permeability of the limestone is slightly higher in the oxidised limestone allowing increased intergranular flow in the upgradient aquifer. If no mixing with the interstitial storage occured, the fissure system would be completely flushed in 1-3 years (Andrews et al., 1982). In the developed artesian area, most of the wells are cased to the top of the limestone, and penetrate it for at least a further few metres. The limestone is totally penetrated in the case of the Water Authority pumping stations. At the present rates of abstraction, and depending on the rate of fissure/interstitial exchange, it is probable that the entire storage would be completely flushed in 100-200 years.

Recharge to the aquifer is limited to the outcrop area of the Lincolnshire limestone and occurs via direct precipitation, recharge through swallow holes, and through the beds of rivers (mean annual rainfall = 500 mm/yr.; annual recharge = 110 mm). Like the Nottinghamshire Trias, the hydrological flow regime is largely controlled by pumping, and the vertical stratification of the groundwater is complex rather than simple. The abstracted waters (mainly fissure-waters) may only be a few years old, although the small component derived from the interstitial sources is considerably older.

1.9.2 Hydrochemistry

Most of the information given here is derived from Edmunds (1973) and Edmunds et al., (1981). Unlike the Nottinghamshire Trias, rock sections of the Lincolnshire limestone contain notable amounts of organic carbon. This implies that organic reactions as well as inorganic reactions could influence the hydrochemistry of the aquifer.

At outcrop, the Eh is around +400 mV, but gradually decreases in the confined part of the aquifer down to +150 mV. At this point, some 10-12 km from outcrop, a redox boundary is present where the Eh drops down to -100 mV. In contrast, the pH gradually increases from 7.2 at outcrop to 8.3 in the east, and this can be correlated with an increase in the HCO_3^- content.

In the oxidising groundwaters at or near outcrop, the light-brown colour of the limestone, including alteration zones adjacent to joints and fractures, reflects the oxidation of Fe^{2+} to Fe^{3+} in finely disseminated pyrite and other ferrous minerals in the limestone. The organic carbon in the rock (up to 0.23% in the reduced section) is also readily oxidised to CO_2 (organic carbon = 0.03% oxidised section) and this accounts for the rapid depletion in dissolved oxygen within a short distance into the confined aquifer.

The evolved CO_2 reacts with H_2O to form H_2CO_3. This slightly ionises to bicarbonate in the following manner:

$$H_2O + CO_2 \rightarrow H_2CO_3 \rightarrow H^+ + HCO_3^-$$

The greater the amount of H_2CO_3, the greater the potential for an increase in the bicarbonate content and a decrease in the pH. Although an increase in HCO_3^- is certainly observed, the pH is also raised. This suggests that H_2CO_3 is being removed from the system, and that some other factor is increasing the HCO_3^- content. The most likely explanation is that carbonate dissolution is occuring, i.e.

$$H_2CO_3 + CaCO_3 \rightarrow Ca^{2+} + 2HCO_3^-$$

This reaction releases Ca^{2+} ions into the groundwaters, and accounts for observed high Ca^{2+} concentrations in the oxidising waters. Carbonate dissolution therefore removes H_2CO_3, hence raises the pH, whilst liberating HCO_3^- ions and increasing the bicarbonate content. The bicarbonate concentrations of the oxidising groundwaters are typically elevated at around 180 mg/l.

The gradual decline in the Eh eastwards into the confined aquifer does not exactly correlate with the dissapearance of dissolved oxygen, which occurs close to outcrop and is rather abrupt. It is likely that the production of CO_2 is at least in part bacterially controlled. Such reactions tend to mimic what would occur anyway via inorganic reactions, but the bacterially controlled reactions are substantially more rapid. The less rapid lowering of the Eh may reflect the slow attainment of water equilibria in the aquifer in response to the rapid removal of dissolved O_2. The persistence of the positive Eh values for some distance into the anaerobic part of the confined aquifer may imply that oxidation of Fe^{2+} and/or especially organic carbon is occuring via reduction of species other than oxygen.

As the waters become more reducing, both the pH and the HCO_3^- contents continue to increase. This can presumably only be explained by further inputs of CO_2, even through the waters are anaerobic. This CO_2 could be derived from sulphate reduction, since SO_4^{2-} concentrations are observed to decline into the aquifer and HS^- becomes detectable below an Eh of +100 mV. This is very likely to be bacterially controlled, i.e.

$$SO_4^{2-} + 2CH_2O + H^+ \rightarrow HS^- + 2CO_2 + 2H_2O$$

Since the reduction of SO_4^{2-} is thermodynamically less preferable than the reduction of NO_3^-, it can be inferred that NO_3^- might be reduced under bacterial control via the oxidation of organic matter i.e.:

$$4NO_3^- + 2CH_2O \rightarrow 4NO_2^- + 2CO_2 + 2H_2O$$

The decline in nitrate levels from high levels at outcrop to <1 mg/l in the confined aquifer is quite consistent with this model. Downing et al., (1977) have identified nitrate-reducing bacteria in 12 sites across the limestone, with population numbers increasing from 10 near outcrop to 900 near the redox boundary (per 500 ml water). A small number of SO_4^{2-} reducers were also found in six of the sites. Towler (1982) also identified denitrifying bacteria from groundwaters in this limestone, including chromobacterium violateum, pseudomonas indinium and bacillus cereus v. mycoides. These are facultative anaerobic denitrifiers, typical of the soil zone.

The dominant control on the calcium concentration in the oxidising groundwaters is carbonate dissolution, with the waters being saturated with respect to calcite. The dissolution of dolomite can also be inferred due to the continuous increase in Mg^{2+} and Sr^{2+} ions from the oxidising waters through the redox barrier into the reducing waters. At the redox boundary however, the Na^+ concentration increases at the expense of the Ca^{2+} concentration whilst maintaining calcite saturation. This reflects a growing importance of cation exchange reactions with clay minerals in the limestone. A solution containing clay minerals with Na^+ filled exchange sites would preferentially exchange Sr^{2+} ions, Ca^{2+} ions, and finally Mg^{2+} ions if they occured in equal dilute concentrations. This order is reversed in more concentrated solutions of these ions. In the limestone, Ca^{2+} is selectively exchanged with Na^+ in preference

to Sr^{2+} and Mg^{2+} because the Ca concentration is high whereas the Sr and Mg concentrations are low. Any removal of Sr^{2+} or Mg^{2+} by ion exchange is so small that it does not compensate for the release of these ions by carbonate dissolution. Beyond the redox barrier, the Ca concentration therefore declines, whilst the Mg and Sr continue to increase. As this occurs, the preference for Na^{+} exchange with Sr^{2+} and Mg^{2+} also increases. Eventually a theshold point is reached, some 25 kms from outcrop, when ion exchange causes the Mg^{2+} and Sr^{2+} concentrations to peak and then to decline to low levels, as the water is scavenged of Sr^{2+}, Mg^{2+} and Ca^{2+}. Some 20 kms from outcrop, saline formation waters are encountered with Na^{+} and Cl^{-} the dominant ions in solution.

The precipitation of calcite in the deeper reducing waters of the aquifer has also been identified. This is according to $\delta^{13}C$ measurements on the system which suggests that exchange of carbon between the groundwater and the matrix by a continuous process of precipitation and further solution of calcite is occuring. Calcite precipitation would also explain the distribution of U-234/U-238 activity ratios in the groundwaters. Andrews et al., (1982) show that the ratios unexpectedly decline from initially enhanced values just beyond the redox boundary. This suggests that Th-234 is prevented from recoiling into the groundwater from the precipitated reduced uranium. The precipitation of calcite around the rock grains may provide a coating of sufficient thickness to prevent ejection of the Th-234 particles into the water.

CHAPTER TWO

EXPERIMENTAL METHODS

2.1 Field Measurements

2.1.1 Groundwater Temperature

At each wellhead site the groundwater temperature was measured using a mercury-in-glass thermometer. The temperature is a reliable guide to the depth of abstraction, the deeper wells correlating with the higher temperatures. Since the studied aquifer systems are characterised by uniformly dipping stata, the temperature can also be used as an index of the distance from outcrop.

2.1.2 Conductivity

The conductivity of a water sample refers to its ability to conduct an electric current. Concentrations of charged ions in groundwaters are low enough for them to behave independently allowing conductivity to have a linear relationship with concentration. The conductivity measurements were made using a PTI-10 conductivity meter, the values expressed in $\mu S \ cm^{-1}$ using a conductivity cell supplied with the meter. Measurements of a standard conductivity solution were then taken (0.01 M KCl), and from this a calibration correction to the standard value was obtained. All field measurements would subsequently be corrected by this factor. The temperature dependent standard conductivity values (in $\mu S \ cm^{-1}$) for different KCl concentrations are listed in Table 10.

In the field, the meter was standardised against the conductivity cell immediately prior to use, and the subsequent measurement then corrected by the standard solution correction factor.

2.1.3 pH

The pH of a solution is a measure of the hydrogen ion concentration. Since a hydrogen ion is nothing more than a proton, the pH reflects the

abundance of protons. In simple, dilute solutions there is essentially no difference between hydrogen ion activity and hydrogen ion concentration. The pH is defined as

$$pH = - \log_{10}[H^+]$$

where $[H^+]$ is the hydrogen ion activity. Measurement of the pH in the field is essentially similar to that of Eh, with two electrodes immersed in the solution creating an electrochemical cell and allowing measurement of the EMF of the solution. The electrodes are designed so that the voltage of the cell is a function specifically of the hydrogen ion activity. Any solution with a pH of 7 is by definition neutral, having a hydrogen ion concentration of 10^{-7} moles/l. A pH >7 is alkaline, whilst a pH <7 is acidic.

2.1.4 Eh

A water solution that contains ions can serve as an electrical conductor. Two electrodes placed in the solution produces an electrochemical cell in which oxidation occurs at the anode and reduction occurs at the cathode. Oxidation and reduction may be represented as a loss or gain of electrons respectively; for example:

$$\text{reduced species} \longrightarrow \text{oxidised species} + ne^-$$

where n is the number of electrons involved per atoms. The Standard Oxidation Potential for this half-reaction, E^o, is the potential that would occur if both the reduced and oxidised species are present at unit activity at 25°C and 1 atmosphere. When the species are present at other activities the equilibrium potential is referred to as the Redox Potential, Eh. This is related to E^o by the Nernst Equation:

$$Eh = E^o + \frac{0.0257}{n} \cdot \ln \frac{[\text{oxidised state}]}{[\text{reduced state}]}$$

The relative oxidising and reducing powers of various reactions can be compared against a standard reference half-reaction. This is the hydrogen half-reaction:

$$H_2 \rightarrow 2H^+ + 2e^-$$

This is assigned a standard potential of 0.000 volts. The redox potential of a solution may be determined by measuring the EMF of a cell formed by a Pt-electrode placed in the solution and a reference electrode. The reference electrode is chemically maintained at a known voltage relative to the hydrogen half-reaction.

In natural solutions, the Eh is rarely dependent upon one redox couple but rather is dependent on a number of oxidation/reduction reactions. Eh measurements were taken in the field using a PTl-ll digital Eh meter, using a Ag/AgCl reference electrode. The pole reaction in this case is

$$AgCl + e^- \rightarrow Ag + Cl^-$$

The cell EMF is given by:

$$E\ cell = E\ Pt - E\ ref$$

so for Eh measurements, the potential of the Pt electrode is given by:

$$E\ Pt = Eh = E\ cell + E\ Ag/AgCl$$

The Ag/AgCl reference potential varies slightly with temperature. The measured E cell value is thus added to the corresponding E Ag/AgCl value for the water temperature in question, as listed in Table ll. The Eh meter was calibrated prior to each field excursion using a Zobell I Eh reference solution, the preparation of which is given in Appendix l.

In an oxidising environment, more electrons are donated to the external circuit producing a greater cell EMF and a high Eh measurement. In a reducing environment, less electrons are donated to the circuit and hence a lower Eh value will be measured.

Table 10. Standard Conductivity values for different KCl concentrations (in $\mu S\ cm^{-1}$)

Concentration:		1M	0.1M	0.01M
T°C	5	74,140	8,220	896
	10	83,190	9,330	1,020
	15	92,520	10,480	1,147
	20	102,070	11,670	1,278
	25	111,800	12,880	1,413

Table 11. Ag/AgCl reference potentials and Zobell I Eh reference values (in millivolts).

T°C	Ag/AgCl	Zobell I, Eh
10	232	461
15	229	450
20	225	439
25	222	428

2.1.5 Dissolved Oxygen

In waters which contain dissolved oxygen greater than 1% saturation, the Eh values tend to be lowered from that calculated from the ionic composition of the water. In such cases the dissolved oxygen measurement is more useful than the Eh. An E.I.L. 1520 portable oxygen meter was used for determination of % saturation dissolved oxygen content in the field. The meter uses an electrode containing a lead anode. The anode is surrounded by a silver cathode which is permeable only to gaseous diffusion. The electrode core is filled with an electrolyte solution of potassium bicarbonate and sodium carbonate, and when oxygen passes through the gas-permeable membrane it is reduced at the cathode to give a current proportional to the oxygen potential pressure. A temperature effect is present, but is compensated for by means of a thermistor in the electrode. The meter was standardised at 0% oxygen saturation with a saturated solution of sodium sulphite, and at 100% oxygen saturation with aerated water.

2.1.6 Bicarbonate content

The alkalinity of a solution is defined as the capacity of a solution to neutralise acid. Any ion in the solution that could react with acid added to the water is part of the total alkalinity. For natural waters the most important ions are the carbonate and bicarbonate ions, the alkalinity usually being reported in terms of concentrations of these two ions. The amount of dissolved CO_2 in the form of CO_3^{2-}, HCO_3^- and H_2CO_3 varies with pH. For waters with a pH between 7.8 and 8.5 more than 90% of the dissolved CO_2 is in the form of HCO_3^-. Below a pH of 8 the remaining CO_2 is in the form of H_2CO_3, and above a pH of 8 the

remaining CO_2 is as CO_3^{2-}. Most of the studied waters have a pH between 7.0 and 9.0, and therefore the alkalinity is best expressed as a bicarbonate content.

Bircarbonate determinations were measured on site by titration using a Hach digital titrator with a 0.08 M H_2SO_4 cartridge. The indicator solution was 3 parts 0.1% bromocresol green solution mixed with 2 parts 0.1% mythyl red solution (both 50% ethanol/water). This gives a red (acid)/green (alkaline) pronounced colour change.

2.1.7 Calculation of PCO_2

The field measurements of pH, groundwater temperature, and HCO_3^- allow calculation of the carbonate species in natural waters (Stumm and Morgan, 1981). CO_2 dissolves in water partly as dispersed CO_2, aq and partly as undissociated H_2CO_3. The total CO_2 in solution, $[H_2CO_3^*]$ is related to the concentrations of CO_2, aq and undissociated H_2CO_3 by the equation:

$$[H_2CO_3^*] = [CO_2,aq] + [H_2CO_3]$$

The equilibrium constant reflecting the relative proportions of these two species in solution is very large, so in fact only 0.2% of dissolved CO_2 is in the form of H_2CO_3. Therefore the $[CO_2,aq]$ is nearly identical to the analytical concentration $[H_2CO_3^*]$.

Ionic carboante species are present. HCO_3^- ions form according to the equilibrium reaction:

$$[H_2CO_3^*] = [H^+] + [HCO_3^-]$$

for which the equilibrium constant is:

$$K_1 = \frac{[H^+][HCO_3^-]}{[H_2CO^{3*}]} = 5.01 \times 10^{-7}$$

Doubly charged ions also form:

$$[HCO_3^-] = [H^+] + [CO_3^{2-}]$$

for which the equilibrium constant is:

$$K_2 = \frac{[H^+][CO_3^{2-}]}{[HCO_3^-]} = 5.62 \times 10^{-11}$$

The total concentration of CO_2 and carbonate ion species in solution (CT), is defined as:

$$CT = [H_2CO_3^*] + [HCO_3^-] + [CO_3^{2-}]$$

Three ionisation fractions can be recognised; a fraction with 0 charge, designated α_0; with a single charge (α_1); and with a double charge (α_2). The main contribution to α_0 is from the dissolved CO_2,aq and H_2CO_3, whilst HCO_3^- contributes mostly to α_1, and CO_3^{2-} to α_2. These fractions are related to the pH and the equilibrium constants in the following manner:

$$\alpha_0 = [H_2CO_3^*]/CT = (1+K_1/[H^+] + K_1K_2/[H^+]^2)^{-1}$$

$$\alpha_1 = [HCO_3^-]/CT = ([H^+]/K_1 + 1 + K_2/[H^+])^{-1}$$

$$\alpha_2 = [CO_3^{2-}]/CT = ([H^+]^2/K_1.K_2 + [H^+]/K_2 + 1)^{-1}$$

In order to calculate the partial pressure of CO_2 that would theoretically be in equilibrium with the water (PCO_2), the Henry's Law Constant for CO_2 is required (KH) i.e.

$$[H_2CO_3^*] = KH.\ PCO_2$$

From the above equations this gives:

$$PCO_2 = \frac{\alpha_0.\ [HCO_3^-]}{\alpha_1.\ KH}$$

The Henry's Law Constant can be obtained from tabulated data as in Table 5a for the groundwater temperature in question. The pH and equilibrium constants allow α_0 and α_1 to be calculated. Since $[HCO_3^-]$ is measured in the field, PCO_2 values can be obtained. $[CO_3^{2-}]$ and CT can also be calculated if desired.

2.2 Sample Collection

2.2.1 Noble Gases

The method of collection involves the trapping of a quantity of sample water before it comes into contact with the atmosphere. The sample container comprises a length of hollow copper tubing, 9mm in diameter and approximately 35cms long. In principle a section of water flowing through the copper tube is sealed off.

The trapping of the water sample is done using two clamps held in position 11cms apart by an aluminium bracket (Fig. 12). The copper tube is fitted between the clamps before the sample is taken. A gentle preliminary tightening of the clamps ensures the tube is solidly in place. Plastic or rubber tubing from the wellhead carrying the flowing water is then fitted over one end of the tube. At this stage the flow is not restricted but flows through the copper tube. The outermost clamp is then tightened first. Providing the jaws of this clamp are as tight as possible, the flow will be halted. The second inner clamp is then closed, and the whole apparatus removed. The aluminium bracket supporting the two clamps is then detached.

A copper tube sample collected in this way contains approximately 5.5 cm^3 of water, typically containing 0.1 cm^3 of gas at STP and providing some 2.5×10^{-3} cm^3 of noble gases (STP) for analysis.

2.2.2 Nitrogen isotopes and N_2/Ar ratios.

Groundwater dissolved gas samples for N_2/Ar ratio measurements and nitrogen isotope measurements on the N_2 gas were collected in 50 cm^3 glass ampoule bulbs. The gas samples were obtained at the wellhead site by degassing a fraction of emergent water in an evacuated sampling apparatus, illustrated in Fig. 13.

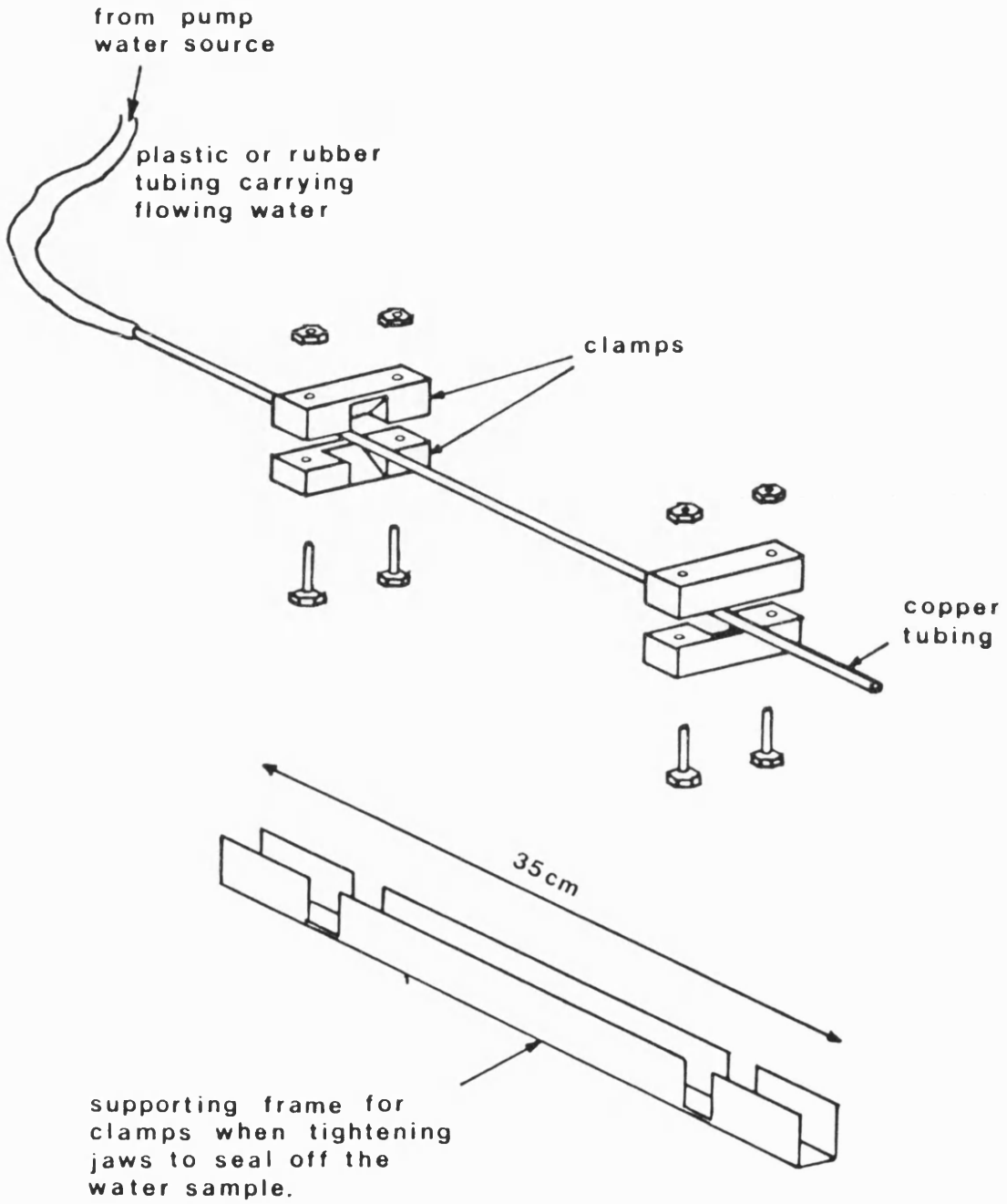

FIG. 12 Copper tube sampling apparatus.

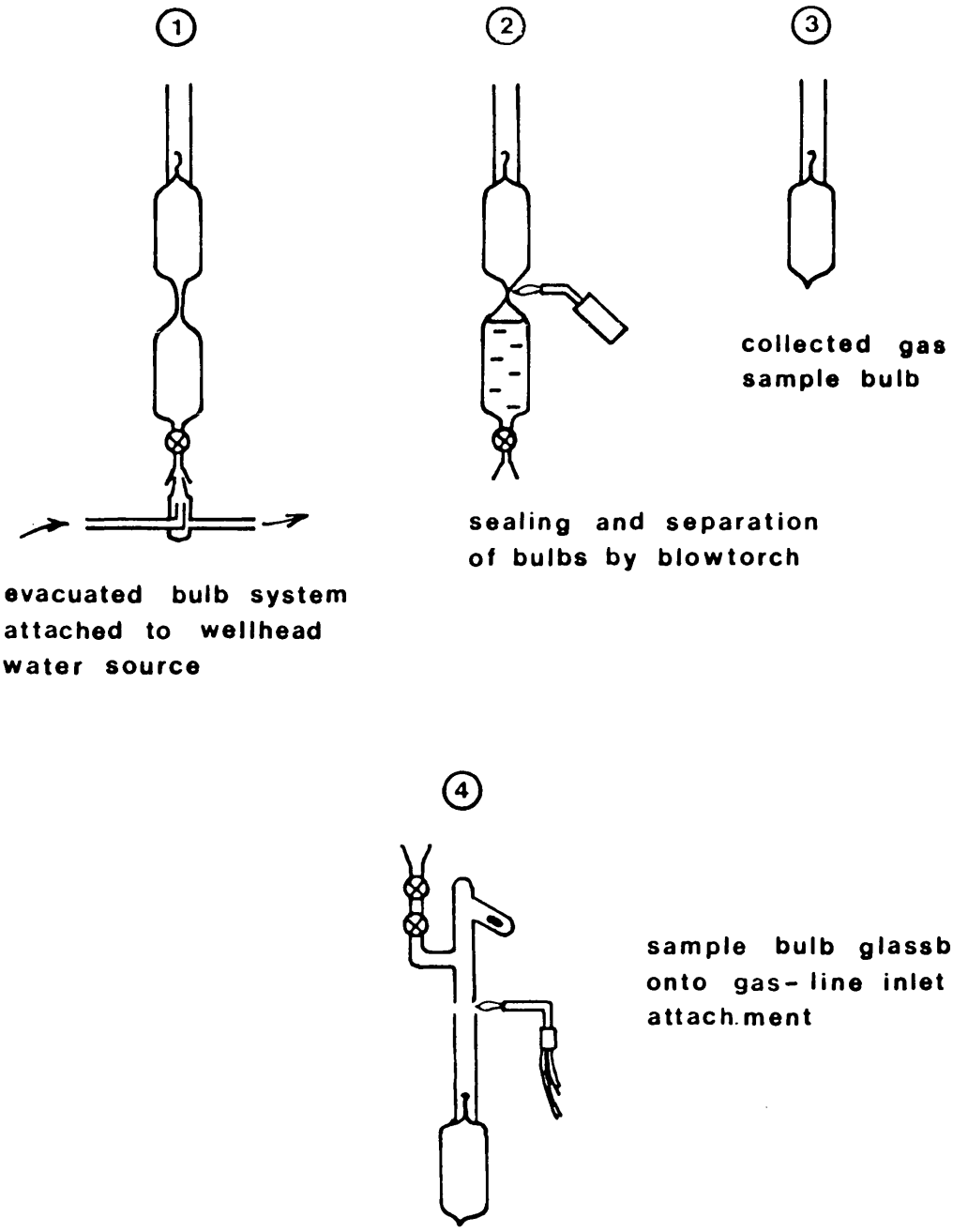

FIG.13 N_2/Ar gas sample collection procedure.

The sampling apparatus was evacuated on site immediately prior to collection by a portable Edwards two-stage rotary pump to $<5 \times 10^{-3}$ mbars. Tubing from the wellhead outlet was directed via the socket of the sampling apparatus by means of an adapted cone ensuring circulation of water in the vicinity of the connecting socket. The flow was usually branched to reduce water pressure, enabling field measurements to be simultaneously taken on an additional reservoir.

When the flow of water in the vicinity of the connecting socket is clear of bubbles, the tap on the sampling apparatus is slowly opened to allow a flow of water into the lower bulb. When the lower bulb is nearly full, the tap is closed off, and the sampling apparatus detatched from the tubing. Any dissolved gases vesiculate out into the upper bulb above the water. The thin glass tubing between the two bulbs is then immediately sealed and separated by heating over a flame. The advantage of this collection method is that the bulbs can be stored indefinitely without loss of sample gas. The size of the lower bulb determines the quantity of gas collected. N_2/Ar gas samples were drawn from 50 mls of water providing about 1 cm^3 of gas at STP for analysis. 250 mls of water were required to obtain sufficient gas (about 5 cm^3 STP) for the nitrogen isotope measurements.

2.2.3 **Additional water samples**

250 ml samples were collected from selected sites in plastic bottles for subsequent Cl^- and NO_3^- analyses. Large quantities of water were collected from those sites where analyses of the nitrogen isotopes in nitrates was required. Such samples were collected in 1, 5, or 25 litre plastic containers. In addition, 20 ml samples were collected in glass bottles for oxygen and hydrogen isotope analyses.

2.3 Nitrogen - Argon Ratios

2.3.1 Sample preparation

When required for analysis, each sample bulb is glass-blown into a gasline inlet for attachment to the gas frame (Fig. 14). The sample is immersed in a dry ice/ethanol cold trap (-80°C) to freeze out water vapour, and the line pumped down. Aliquot taps X and Y are shut, and the sample broken by dropping a weight onto the breakseal, using a magnet to manipulate the weight recessed in the glassware. An aliquot of this gas is then expanded into the main line of the gas frame. Sample aliquots can then be metered into the spectrometer as required. Most samples required trapping off and further expanding of the gas before this was done in order to reduce the pressure to a level acceptable for measurements.

2.3.2 Mass spectrometric analysis

All N_2/Ar ratio determinations were carried out on a AEI MS10 mass spectrometer at Bath University Chemistry Department. This machine is a single inlet/single collector system.

Aliquots of gas from the gas line can be directly admitted into the spectrometer. Once the gas enters the ion cage the constituent molecules are bombarded by electrons from a hot rhenium filament. The molecules are ionised and positive ions are accellerated in circular orbit and separated by a magnetic field on the basis of their mass-to-charge ratio (m/e ratio). Increasing the accelerating voltage decreases the radius of any particular flight path and in this way specific species are focussed into the single fixed 0.01" collector slit.

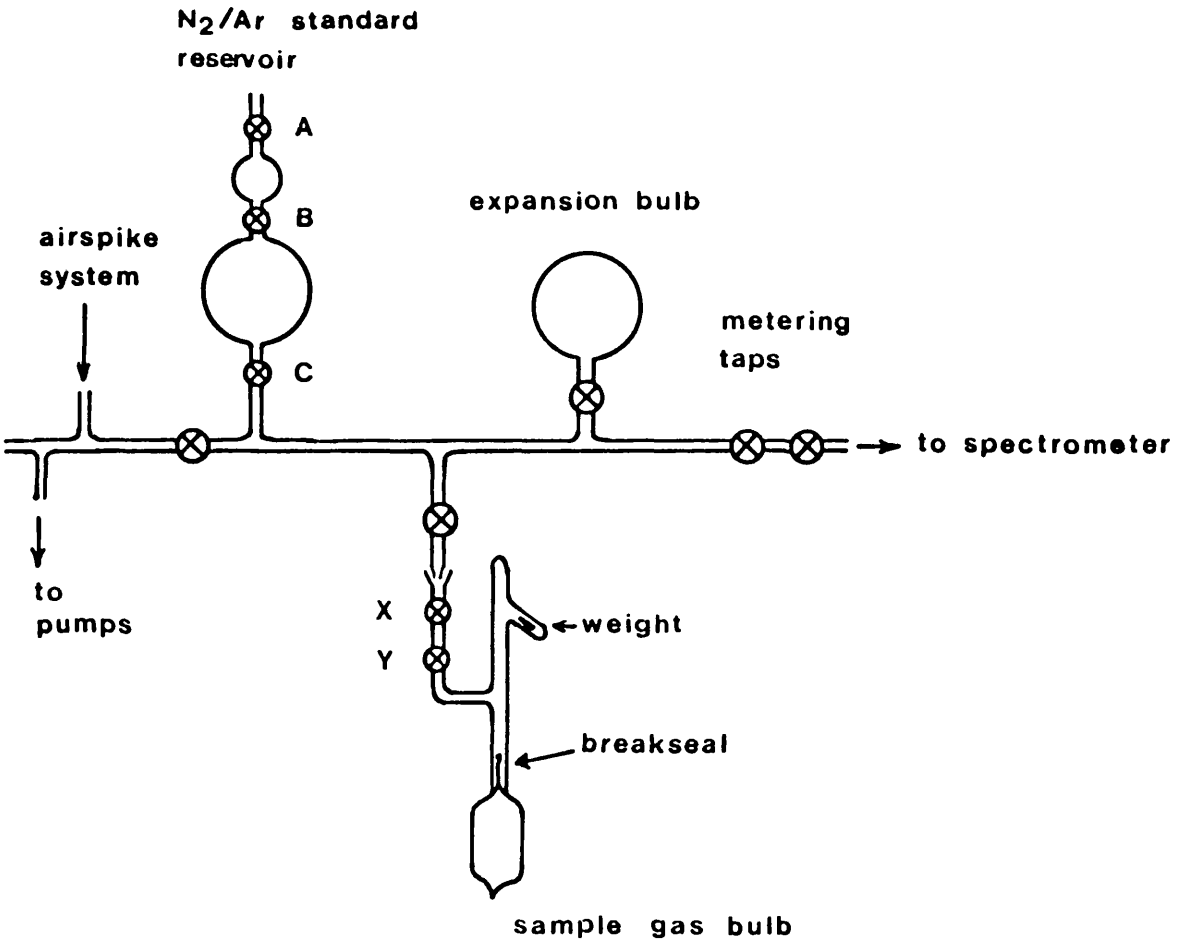

FIG. 14 N_2/Ar gas - preparation line.

The quantities of gas collected from groundwaters are typically very small, so the system is basically static. This means that an aliquot of gas, once metered into the ion cage, is ionised, can be measured, and will essentially stay there until opened to a Triode Ion Pump. This is not a pump in the physical sense of the word, but involves the permanent transference of the gas to the structure of the system. This is done by further ionising the gas, attracting the ions to anode and cathode surfaces, and then burying the gas molecules in sputtered titanium.

The N_2/Ar ratio is determined by measuring the 28 and 40 m/e ion currents. The m/e 28/40 ratio is then corrected for the relative sensitivities of N_2 and Ar as discriminated by the spectrometer, based on the measurement of a standard known N_2/Ar mixture. The source parameter settings are as follows:

Ion Repeller voltage	+ 1v
Electron volts	70v
Trap current	50 μA

Although the sample gas is basically static when not opened to the ion pump, absorption of N_2 gas onto the walls of the ion cage occurs. This produces a change in the ion current as a function of the length of time since sample admission. This effect was observed to be most pronounced with O_2, secondly with CO_2, and then with N_2. A negligible effect was observed for the noble gases. The rate of ion current change with time is linear, and so the effect can be corrected by extrapolation. Two readings of each ion current peak were taken on any one aliquot. This was separated by a noted time interval so as to obtain the rate of change, and hence extrapolate the ion current peak back to its value at the time of sample admission, i.e.

$$I_o = I_1 + T_1 \times \left(\frac{I_1 - I_2}{T_2 - T_1} \right)$$

where I_1, I_2 are the first and second ion current readings of one peak, taken at times T_1 and T_2. I_o is the extrapolated ion current value at T = 0. Four or five aliquots were measured in this way on any one sample, and the average m/e 28/40 ion current ratio noted.

The main peak for nitrogen lies at m/e = 28, but there is also a subsidiary peak at m/e = 14 due to the formation of doubly charged N_2 ions, $(^{14}N^{14}N)^{++}$. The m/e 28/14 cracking ratio of pure nitrogen (BOC 99.998% N_2) is quantitatively constant, with the m/e 14 peak having a relative sensitivity of 7% the m/e 28 peak. This is useful because if the gas contains significant quantities of CO_2, CO^+ ions form which contribute to the m/e 28 peak. The 28/14 ratio can therefore be used as a check or subsequent correction for the formation of CO^+ ions. However in the case of the analysed samples from the Nottinghamshire Triassic and Lincolnshire Limestone groundwaters, interference from CO^+ was insignificant.

The calibration of the sample against the standard is necessary due to the markedly different sensitivities of N_2 and Ar in the spectrometer. The correction to obtain the N_2/Ar ratio of the sample is applied as follows:

$$N_2/Ar \text{ spl} = 28/40 \text{ spl} \times \frac{N_2/Ar \text{ std}}{28/40 \text{ std}}$$

Earlier samples were calibrated against the N_2/Ar ratio in air (83.54), but later samples use a prepared volumetrically calibrated gas mixture of N_2 and Ar. This mixture is without interference from other gases giving better reproducibility and its value (N_2/Ar = 32.043) is closer to the naturally occuring values found in low-temperature groundwaters.

2.3.3 Water-gas equilibration correction

The collection method for N_2/Ar ratios necessitates a subsequent correction to be made to the measured N_2/Ar ratio because of water/gas equilibration in the evacuated glassware apparatus. Although most of the dissolved gases move into the evacuated space, the extracted gases exert a small but not negligible partial pressure in this volume. As a result of this, some gases remain in solution. The experimentally measured N_2/Ar ratio must therefore be corrected for the incomplete extraction of the gases using the following equations:

$$XN = KN.R$$

$$XA = KA.R$$

$$N_2/Ar = NM. \frac{(1 - XA - XA^2 + XA^3)}{(1 - XN - XN^2 + XN^3)}$$

where R = ratio of the water bulb volume to the gas bulb volume.

KN and KA = Bunsen Coeffients for nitrogen and argon at 10^oC.

i.e. 1.884×10^{-2} and 4.121×10^{-2} cm^3 $STP(cm^3H^2O)^{-1}$ respectively.

NM = experimentally measured N_2/Ar ratio.

The exact mathematical derivation of this correction method is given in Appendix 2. Small errors in determining R and the assumption of 10^oC equilibration will for low temperature groundwaters have little effect on the correction. For N_2/Ar samples collected in 50 cm^3 bulbs from 50 cm^3 of water the correction to the $\overset{a}{\lambda}$nalysed ratio is only 0.979. This value decreases as R increases.

2.3.4 Preparation of standard gas mixtures

In order to provide a N_2/Ar mixture of known composition for

routine sample analysis a glassware system was constructed comprising two bulbs and three taps, A, B and C (Fig. 14). Tap C is a one-way aliquot tap. The large and small bulbs, connecting tap B, and the aliquot tap C, were all volumetrically calibrated with mercury. The bulbs were filled at atmospheric pressure by first inserting a thin length of glass tubing down into the larger bulb and flushing out with cylinder nitrogen. The gas flow is reduced, and the tube slowly withdrawn, immediately closing tap B when possible. The smaller bulb is filled with argon in a similar way. Tap B can then be opened to allow the gases to mix, and left for at least 24 hours before use. Successive extraction of aliquots from this reservoir produces a continuous depletion of gas, but the N_2/Ar ratio remains constant.

The volumetrically calibrated N_2/Ar ratio of this mixture is 32.043. To check this value, the standard mixture itself was measured several times as a sample, calibrating against air. Successive results are listed in Table 12. The mean value is slightly lower than the calibrated value (1.4%, but the calibrated value is within one standard deviation of this mean.

2.3.5 Calibration correction to standard

In practice, aliquots of the standard mixture were measured between each sample analysis. An average of the calibration before correction, before and after the sample was used, i.e.

$$\text{calibration correction} = \frac{N_2/Ar \text{ std}}{m/e\ 28/40 \text{ std}}$$

The correction is always close to 1.5, but such calibrations had to be done so often because the relative sensitivities of the nitrogen and argon ion currents could vary not only from day to day but also

Table 12. **N_2/Ar measurements on prepared mixture = 32.043, calibrated to air N_2/Ar ratio.**

1	31.96	
2	30.96	
3	30.64	
4	31.90	
5	31.60	
6	32.20	
7	32.01	
8	32.08	
9	30.45	
10	32.00	
X	31.58	σ = 0.62

during any one day as well. This is illustrated in Table 13, where such variations are listed for three typical days.

2.3.6 Methane - nitrogen ratios

In addition to N_2/Ar ratios it is also possible to determine CH_4/N_2 ratios on samples using the MS10.

Ionisation of the CH_4 molecule produces $(CH_4)^+$ with a major m/e peak at 16. However substantial interference on this peak is usually present from the cracking products of other gaseous species, including oxygen, carbon dioxide, and water vapour. The cracking of the CH_4 molecule produces a subsidiary peak at m/e 15, $(CH_3)^+$. This peak has no interference from other species and therefore may be quantitatively used to determine CH_4 presence in the sample. Measurements on the proportion of m/e 15 to m/e 16 in pure cylinder CH_4 show that the subsidiary peak is always 84.3% of the m/e 16 peak.

In a similar way that sample m/e 28/40 ratios are calibrated against a N_2/Ar standard, 15/28 ratios can be calibrated against a known mixture of CH_4/N_2. No methane, however, was detected in any of the samples from the Nottinghamshire Trias or Lincolnshire Limestone aquifers.

Table 13. Variations in N_2/Ar calibration corrections.

10th May, 1985

1.518
1.524
1.505
1.516

15th May, 1985

1.491
1.489
1.494
1.502
1.502

20th May, 1985

1.509
1.537
1.536
1.530

2.4 Noble Gases

2.4.1 Principle

All noble gas analyses were determined using a AEI MS10 mass spectrometer at Bath University Chemistry Department. Details of this machine are given in the section for N_2/Ar ratio measurements. Absolute measurements on the noble gases is made by isotope dilution using a tracer gas mixture of known composition. The analyses can then be used to determine recharge temperatures using solubility data. Concentrations of the dissolved noble gases in the water are obtained because the sample volume of water is measured.

2.4.2 Gas separation and mass spectrometric analysis

The gas-line shown in Fig. 15 was used to prepare the samples prior to their analysis in the mass spectrometer. Aliquots of gas from the main line of the frame could be directly admitted to the spectrometer, via aliquot taps as shown in the diagram.

Prior to analysis, the copper tube water sample is weighed. It is weighed again after analysis so as to determine the volume of water by difference. The samples are attatched to the gas frame by means of a greased 'O'-ring seal recessed in a length of flexible tubing (Fig. 15). When the frame is pumped down the lower clamp sealing the copper tube is opened. This admits the water sample into trap A where vesiculation of the gases occurs. These gases must pass through B, a dry-ice/ethanol trap ($-80^{o}C$) before entering the main line of the gas frame, so freezing out water vapour. To ensure total extraction of gases from the water, the water is heated and totally evaporated, so that all the sample water is ultimately transferred to the cold trap. The gases can then be admitted to the main line of the gas frame, and an aliquot of tracer gas

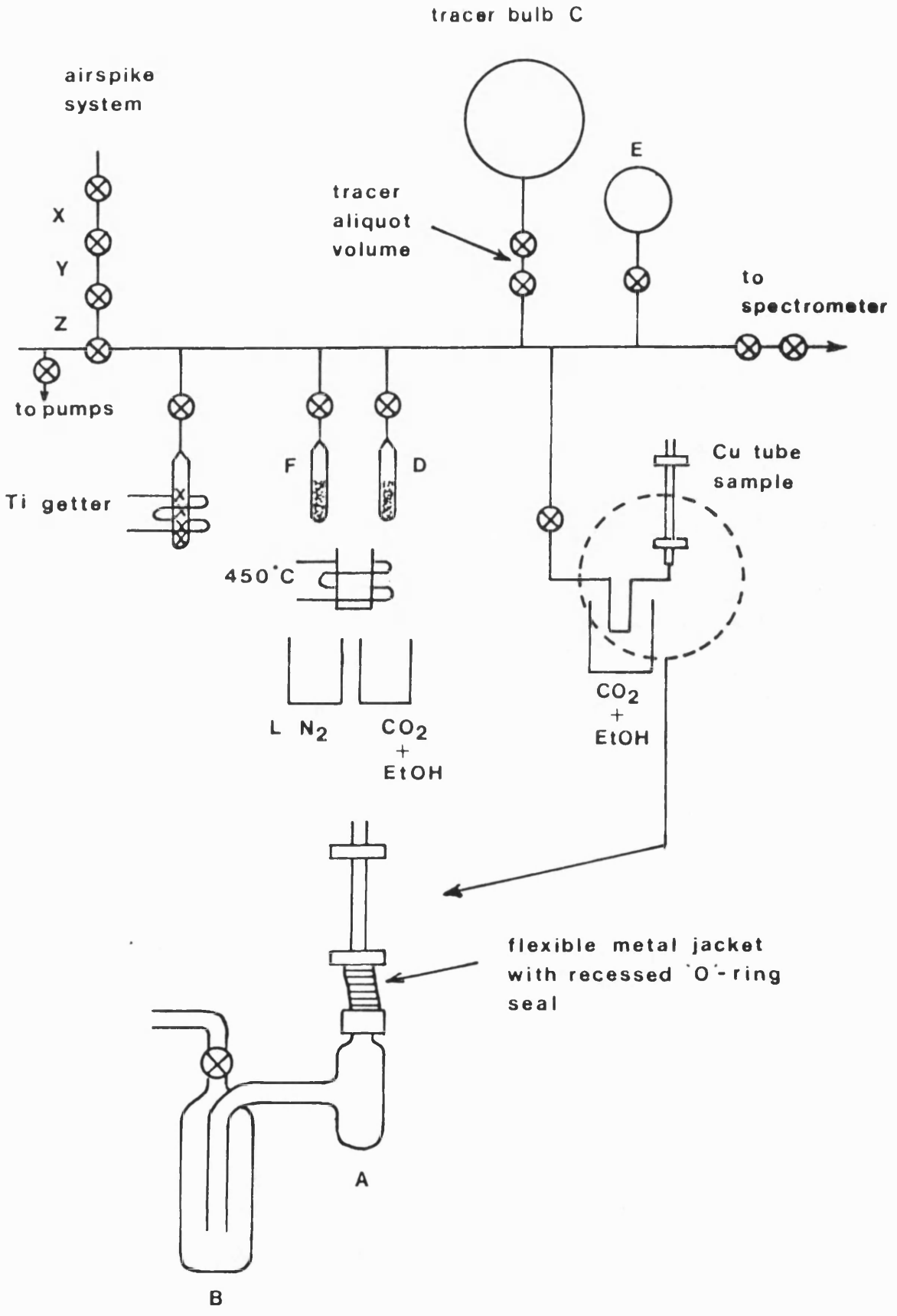

FIG. 15 Gas preparation line for noble gas analyses.

is mixed with the sample from tracer bulb C.

Nitrogen is first removed by titanium getter, and krypton and xenon taken up on charcoal trap D by cooling in a dry-ice/ethanol mix for 10 minutes. A volume of the spiked sample is then isolated for subsequent argon measurement (bulb E). The remaining argon in the line is removed by absorption onto charcoal trap F by cooling in liquid N_2 for 10 minutes. Aliquots of gas in the main line are then admitted into the MS10 and analysed for the two remaining major gas constituents, helium and neon. After pumping down, gas from the argon bulb (E) is then used for analysis of argon in the spectrometer. Krypton and xenon, released from the charcoal trap by prior heating to 450^{o}C, is then admitted to the main line when the frame is again evacuated. Gettering removes any excess N_2 still in the gas, after which the kyrpton and xenon can be analysed. Before and after each copper tube sample analysis, the getter is cleaned and the charcoal traps heated.

The mass spectrometric source settings are the same as those listed for N_2/Ar measurement, with the exception that neon is analysed with a source electron voltage of 40V instead of 70V. This is to prevent the creation of Ar^{++} ions with an m/e of 20 interfering with the neon measurement.

2.4.3 **Noble gas isotope dilution**

The volume of noble gas of natural isotopic composition may be determined by Isotope Dilution. This requires mixing the sample gas with a known volume of the same but isotopically-enriched noble gas. The measured isotopic ratios of the 'tracer' and sample mixture allow calculation of the sample gas volume. The advantage of this technique is that it enables very accurate measurements to be made on very small

sample quantities. For example, the parameters for a mixture of naturally occuring atmospheric Ar and tracer Ar may be symbolised as follows:

$Vat\ (Ar)$ = volume of atmospheric Ar at STP

$Vt\ (Ar)$ = volume of tracer Ar at STP

$^{\infty}Xat$ = mole fraction of isotope $^{\infty}Ar$ in atmospheric Ar

$^{\infty}Xt$ = mole fraction of isotope $^{\infty}Ar$ in tracer Ar

For the tracer and sample mixture, then:

$$R = \frac{^{36}Ar}{^{40}Ar} = \frac{^{36}Xat.Vat(Ar) + {}^{36}Xt.Vt(Ar)}{^{40}Xat.Vat(Ar) + {}^{40}Xt.Vt(Ar)}$$

If Vt(Ar) and the isotopic compositions of the tracer and atmospheric Ar are known, Vat(Ar) may be calculated once the ratio, R, is determined experimentally by mass spectrometry. Rearrangement of the above equation for Vat(Ar) gives:

$$Vat(Ar) = Vt(Ar).\frac{[^{36}Xt - {}^{40}Xt.R]}{[^{40}Xat.R - {}^{36}Xat]}$$

In practice the tracer spike volume, Vt(Ar) is determined first by mixing with a known volume of atmospheric Ar from an airspike. The BASIC computer program "AIRCAL-TWO", calculates the Vt values for the noble gases from which subsequent samples can be analysed (Appendix 3). The sample volume calculations are determined using the BASIC computer program "GASAN-TWO", derived from the measurements of the light/heavy isotopic rates of the inert gases (Appendix 4). These quantities are then divided by the volume of sample water, edited for each new sample into line 40 of the "GASAN-TWO" program, so as to express the

concentrations in unit cm^3 of gas per unit cm^3 of water.

2.4.4 Preparation of Tracer

Naturally occuring gas samples predominantly contain ^{4}He, ^{20}Ne, ^{40}Ar, ^{84}Kr and ^{129}Xe. The tracer isotope for each gas must be some corresponding isotope of the same element that is low in natural abundance. The tracer isotopes chosen in this case are ^{3}He, ^{22}Ne, ^{36}Ar, ^{78}Kr and ^{136}Xe. Tracer ampoule standards of the respective gases are obtainable in which the mole fractions of the isotopes are known. Table 14 compares the differing isotopic composition of the noble gases between natural samples and the tracer.

The tracer spike mixture was prepared by expanding volumes of the respective tracer ampoules into a larger confined glass storage bulb, isolated from the remaining glassware by two aliquot keys. The storage bulb and aliquot keys were then separated from the tracer preparatory glassware and glassblown onto the gas frame illustrated in Fig. 15.

The volume of the tracer storage bulb and aliquot were respectively calibrated with Hg prior to filling with the tracer. These two volumes must be accurately known in order to subsequently correct the tracer gas volume for the successive depletion of the tracer in the storage bulb. Futhermore, some approximate consideration of the aliquot volume is necessary so as to ensure that when the tracer and sample are mixed, comparable ion current measurements are possible between the light and heavy isotopes of the respective noble gases.

2.4.5 Air calibration

In order to determine the respective tracer spike volumes at STP in one tracer aliquot, an aliquot of tracer is mixed with a known volume of

Table 14. Isotopic mole fractions of tracer gas in comparison with atmospheric values.

Element		Atmosphere X light	Atmosphere X heavy	Tracer X light	Tracer X heavy
He	3, 4	1.3×10^{-6}	0.999999	0.9958	0.0042
Ne	20, 22	0.9105	0.0894	0.0012	0.9988
Ar	36, 40	0.0033	0.996	0.9947	0.0053
Kr	78, 84	0.0035	0.57	0.9999	0.0001
Xe	129, 136	0.2644	0.0887	0.0001	0.9999

atmospheric gas from the airspike shown in Fig. 15. Three volumes, X, Y and Z were used in the expansion and trapping off of an air sample, in order to bring the pressure down to that comparable for mixing with an aliquot of tracer. Each of the volumes were calibrated with Hg so as to know exactly what spike volume of air is present at STP prior to mixing with the tracer aliquot.

Since the mole fractions of the isotopes for each gas in both the airspike and the tracer are known, and the volume of each respective gas in the airspike is known, then Vt for each gas can be calculated once R has been measured, e.g.

$$Vt(Ar) = Vat(Ar).\frac{[^{40}Xat.R - {}^{36}Xat]}{[^{36}Xt - {}^{40}Xt.R]}$$

The "AIRCAL-TWO" program calculates the Vt values for all the noble gases in the tracer aliquot. In practice this is done three or four times and the average Vt values taken. These calculated Vt values are then edited into line 1190 in the "GASAN-TWO" program.

2.4.6 Correction for successive aliquot extraction from tracer

Once the tracer has been calibrated, samples can then be analysed by comparison of the isotope ratios. However each successive tracer aliquot used since the last calibration will contain a slightly smaller quantity of tracer gas. This is because of the reduction in pressure of the reservoir gas each time it is expanded into the tracer aliquot volume. A correction can be applied as follows; where V is the volume of the storage bulb, v is the volume of tracer aliquot, Vt,ac is the volume of tracer aliquot gas at the time of air calibration (the 1st aliquot), and Vt is the volume of tracer aliquot gas at a particular

n'th aliquot extraction:

$$Vt = Vt,ac \times \left(\frac{V}{V + v}\right)^{n-1}$$

The V/(V+v) term in this case was measured to be 0.998708, and so:

$$Vt = Vt,ac \times 0.998708^{n-1}$$

Since the volume of the storage bulb, V, is large in comparison with the tracer aliquot volume, v, then a large number of aliquots are required before any noticable change in tracer volume occurs. After 50 aliquots, the reduction in tracer aliquot gas volume would be only 6%. The exact derivation of the correction equation is given in Appendix 5. An air calibration is carried out every 10-15 weeks or every 30-40 aliquots used.

2.4.7 Estimation of Recharge Temperatures

The concentrations of the dissolved noble gases are originally fixed by equilibration with the atmosphere at the time of aquifer recharge. Each analysed concentration for neon, argon, krypton and xenon from one sample should therefore correspond to four temperaure estimates which are identical. When incorporated bubbles of trapped air go into solution due to the increasing hydrostatic pressure as the waters migrate downwards, the estimated recharge temperatures for each gas concentration will no longer reflect atmospheric equilibrium. Each estimated recharge temperature will therefore be different due to the unaccounted for extra air component.

Although most groundwaters contain variable amounts of dissolved air in excess of that characterising the recharge temperature, it is still possible to estimate the recharge temperature by correcting for

the extra air content in the measured noble gas analysis. The computer program "RCH.BASIC" (Appendix 6) calculates the solubilities of the noble gases in atmospherically equilibrated water for a temperature range between $-10^{o}C$ and $20^{o}C$. For each of the four noble gases, Ne, Ar, Kr, Xe, the program compares the actual sample concentration with the solubility data to determine a set of potential recharge temperatures. Theoretical increments of air are then subtracted from the noble gas concentrations, the increment being determined by subtracting $0.0625 \times 10^{-8} cm^3/cm^3 H_2O$ from the neon concentration, and corresponding fixed amounts from the other noble gas concentrations according to their abundance relative to neon in the atmosphere. Each time an increment is subtracted, a potential set of recharge temperatures, one for each gas, is calculated. This is done until either the calculated recharge temperature for neon exceeds $15^{o}C$, or until the number of subtracted increments reaches 200. The closest set of matching temperatures in the determined sets of temperatures indicates the vicinity of the recharge temperature. This is identified by recognising the temperature array with the smallest standard deviation on the mean for that particular array - the mean being taken as the recharge temperature. An example output from the program for a sample is shown in Table 15.

Since the estimation of the recharge temperature involves the subtraction of a fixed quantity of dissolved air, the amount of extra air above that due to atmospheric equilibration is determined. A guide to the degree of extra air entrainment can be given by dividing the measured sample Ne concentration by the Ne concentration at recharge; a value which we will call the Contamination Index, (C.I.). A value of 1 would indicate no atmospheric entrainment, whilst values >1 indicate the degree of air entrainment.

Table 15. Recharge Temperature output data for Rampton.

Recharge temperature from Benson and Krause data 01/24/83

Sample name: Rampton

Reference number: NT01 A

He	Ne	Ar	Kr	Xe	CI	T	SD
82.57	2.87	5.14	11.66	1.77			
	-10.00	-1.00	2.50	2.30			
80.85	2.27	4.84	11.28	1.74			
	0.80	1.20	3.50	2.70	1.26	2.05	1.10
80.84	2.27	4.83	11.28	1.74			
	1.00	1.30	3.50	2.70	1.27	2.12	1.02
80.82	2.26	4.83	11.28	1.74			
	1.20	1.30	3.50	2.70	1.27	2.17	0.97
80.80	2.26	4.83	11.27	1.74			
	1.50	1.30	3.50	2.70	1.27	2.25	0.90
80.78	2.25	4.82	11.27	1.74			
	1.70	1.30	3.50	2.70	1.28	2.30	0.86
80.76	2.24	4.82	11.26	1.74			
	1.90	1.40	3.50	2.80	1.28	2.40	0.81
80.75	2.24	4.82	11.26	1.74			
	2.20	1.40	3.50	2.80	1.28	2.47	0.77
80.73	2.23	4.82	11.26	1.74			
	2.40	1.40	3.60	2.80	1.29	2.55	0.79
80.71	2.22	4.81	11.25	1.74			
	2.70	1.40	3.60	2.80	1.29	2.62	0.79
80.68	2.22	4.81	11.25	1.74			
	2.90	1.50	3.60	2.80	1.29	2.70	0.76
80.67	2.21	4.81	11.24	1.74			
	3.20	1.50	3.60	2.80	1.30	2.77	0.79
80.66	2.21	4.80	11.24	1.74			
	3.40	1.50	3.60	2.80	1.30	2.82	0.82
80.64	2.20	4.80	11.24	1.74			
	3.70	1.50	3.60	2.80	1.31	2.90	0.88
80.62	2.19	4.80	11.23	1.73			
	4.00	1.60	3.60	2.80	1.31	3.00	0.92
80.60	2.19	4.79	11.23	1.73			
	4.20	1.60	3.60	2.80	1.31	3.05	0.97
80.58	2.18	4.79	11.22	1.73			
	4.50	1.60	3.60	2.80	1.32	3.12	1.07
80.57	2.17	4.79	11.22	1.73			
	4.80	1.60	3.70	2.80	1.32	3.22	1.18
80.55	2.17	4.78	11.22	1.73			
	5.00	1.70	3.70	2.80	1.32	3.30	1.21
80.53	2.16	4.78	11.21	1.73			
	5.30	1.70	3.70	2.80	1.33	3.37	1.32

The emphasis on using Ne for solubility calculations is because its concentration is unlikely to be affected by additional inputs other than extra air entrainment. Ar concentrations, for example, seem to be rather high in some cases possibly due to the preferential dissolution of radiogenic Ar from K-bearing minerals. Helium is not used at all in the estimation of the recharge temperatures. This is because groundwaters are usually enriched to a greater or lesser extent by ^{4}He accumulation from alpha particles derived from the radioative decay of U and Th (and their daughter products). A contamination index based on Kr and Xe would be difficult to apply with the same accuracy due to their lower natural abundance.

The analyses of noble gases are totally orientated towards derivation of recharge temperatures. For this reason precision and accuracy are expressed as errors on the estimation of the recharge temperature, rather than errors on the actual analytical noble gas measurements. The precision on each sample recharge temperature is usually to within +/- 0.5^{o}C (1 standard deviation). Analytical reproducability between replicate samples is +/- 1.0^{o}C.

2.5 Nitrogen Isotopes

2.5.1 Principle of analysis

All nitrogen isotopes were analysed on a V.G. Micromass 602E at B.G.S., Wallingford. This machine is a double inlet/double collector mass spectrometer designed specifically for the determination of oxygen and hydrogen isotopes, but can be readily adapted for measurements of nitrogen isotopes.

The mass spectrometric analysis of nitrogen isotopes involves admitting molecular dinitrogen, N_2, into the machine. The isotope ratio is determined by measuring the m/e 29 and m/e 28 ion currents. This ratio is compared with a reference gas and the isotopic composition of the sample expressed as the difference from this reference. All results are expressed in the delta notation, where:

$$\delta^{15}N\ ‰ = \left[\frac{m/e(29/28)SPL - m/e(29/28)STD}{m/e(29/28)STD} - 1\right] \times 1000$$

The advantage of such a notation is that even though naturally occuring absolute abundances of nitrogen isotopes cannot be precisely determined, differences from a universal standard allow very small isotopic changes in the environment to be measured. Sample delta values are by convention expressed as changes against atmospheric nitrogen, with intermediate working standards, such as bottled N_2, often being used as was done here.

In order to prevent interference on the m/e 28 and m/e 29 peaks from CO^+, some gas sample purification is necessary principally to remove O_2 and CO_2. For dissolved gas samples and air standards, the gas is first deoxygenated by reaction with reduced copper at 700°C, and then dried in a liquid N_2 trap. The purified N_2 gas is then absorped onto

activated silica Gel in sample flasks prior to mass spectrometric analysis. In the case of nitrogen isotopes in nitrates, the N_2 gas is liberated via oxidation of ammonium sulphate samples. This gas is then also dried and absorped onto silica gel.

For such sample preparation, a gas line was built as shown in Fig. 16. Essentially this system provides two means of preparing samples. The upper limb is used for the oxidation and purification of ammonium sulphate samples, and the lower limb for purifying gas and air samples.

2.5.2 Silica Gel

Uptake of N_2 gas onto activated silica gel is essentially complete, and so no isotope fractionation can occur (Mariotti, 1983). The silica gel is in the form of granules and prior to use must be ground and sieved to a mesh size of 1-2 mm diameter. 0.3g of silica gel (about 12 grains) were added to each sample flask, and the flasks then placed in a heating block at 200°C. The flasks were evacuated and heated under constant vacuum for 48 hours, after which time the flasks should never be opened to atmospheric air. The gel becomes active to gas absorption when cooled in liquid N_2, and completely desorbs at room temperature.

Successive use of a Si-gel collection flask can be made for many samples. Only when the grains take on a universal dark brown colouration should the gel grains be replaced.

2.5.3 Silver Coated Copper

Gas samples were deoxygenated by heating the gas at 700°C in a quartz trap containing copper metal. At this temperature the copper combusts with oxygen in the gas, a reaction which is essentially irreversible. The specific product used was a quantity of

'silver-coated copper' supplied by Erba Science (UK) Ltd. As the copper becomes progressively more oxidised with repetitive use, it takes on a distinctive blackened appearance. When completely oxidised, the copper should be replaced, or, less conveniently, reduced by heating under an atmosphere of pure hydrogen.

2.5.4 Procedure for gas sample preparation

A total quantity of $5cm^3$ N_2 STP was required for the analytical procedure described here. Gas samples were collected in 50 ml glass bulbs. A glass socket was glassblown to each sample bulb complete with a recess in which to rest a small breakseal weight. The samples could then be connected to the gas line at Y, as illustrated in Fig. 16. For standard air preparation, a small air-sample container was used.

Referring to Fig. 16, once the air or gas sample is fitted to the inlet at Y, the line is pumped down. The 'nitrate-arm' of the gas line is not used here, so E is shut whilst A, B, C, D and the collection flask are open. Both the Si-gel and copper are respectively heated at $200^{o}C$ and $700^{o}C$ for 10 minutes during this line preparation. If the copper is being used for the first time, it should be heated under vacuum for about 1 hour.

Once a good vacuum is achieved, ($<10^{-3}$ mbar), taps A, B and C are closed. The breakseal to the sample is broken (or alternatively the air sample container is opened) and tap B also opened. The copper trap, already hot is heated for a further 15 minutes to take out O_2 before being removed. Tap D is then closed, and a liquid N_2 Dewar placed under the vapour trap before opening tap C. After 5 minutes, the Si-gel heater is replaced by a liquid N_2 Dewar and tap D opened. After 5 minutes both tap D and the collection flask are sealed, and the

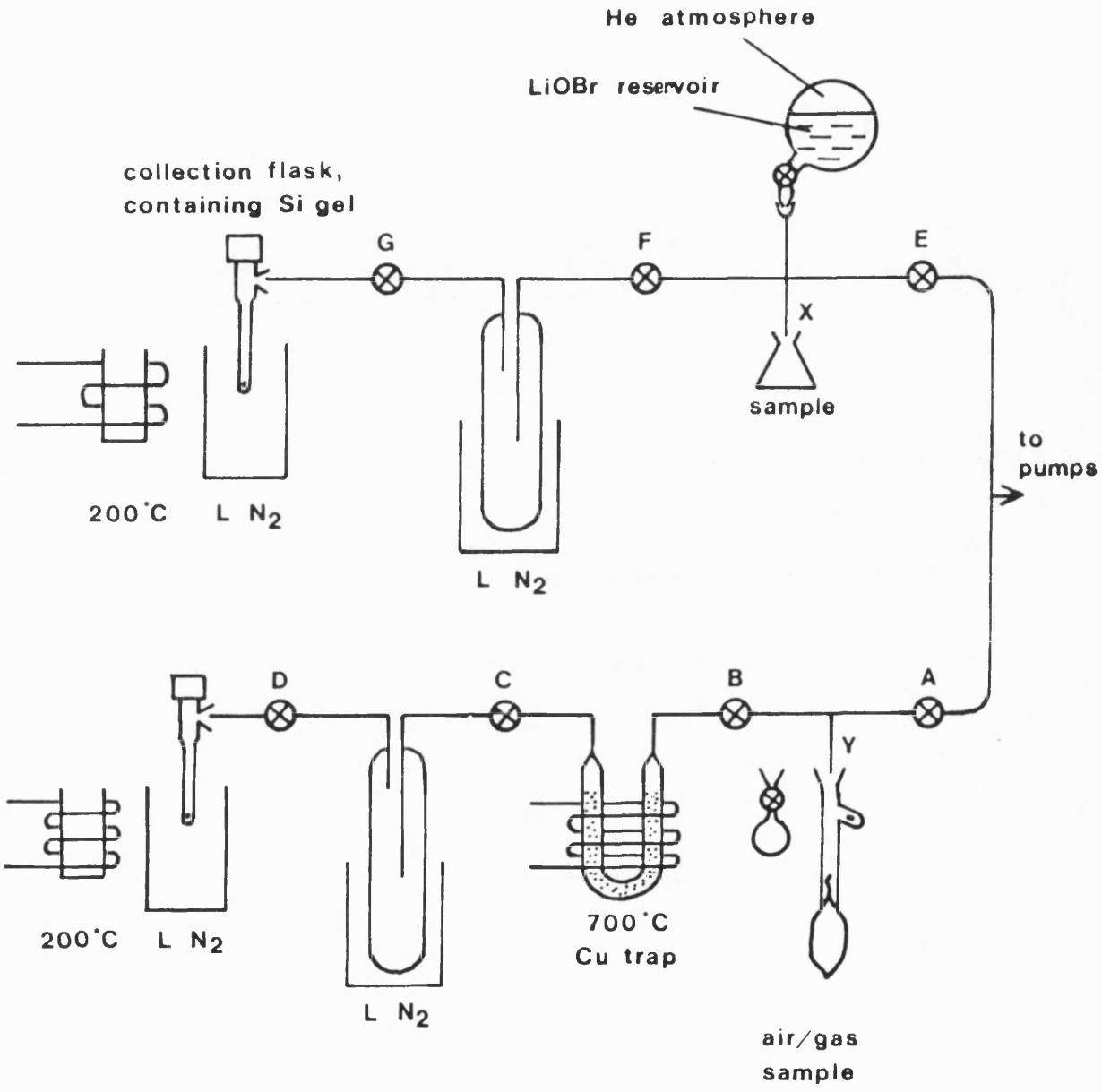

FIG.16 Gas-line apparatus for gas and ammonium sulphate sample preparation for nitrogen-isotope analyses.

collection flask can be removed. Once this flask has warmed up to room temperature, the gas sample is ready for analysis on the mass spectrometer. The vapour traps were cleaned every 12 samples to prevent the possibility of any isotopic memory affect occuring using 50% HCl.

In the procedure outlined above, all the sample gas is taken up onto the Si-gel after deoxygenation and drying. No volumetric expansion followed by trapping off of gas was necessary with the currently analysed samples or air standards. Such expansions, if followed by trapping of the gas, should always be made in the absence of a temperature gradient to prevent any isotopic fractionation occuring.

2.5.5 Procedure for nitrate reduction

Isotopic measurement of N_2 derived from NO_3^- requires preconcentration of the water sample followed by reduction to ammonium sulphate. The ammonium sulphate samples are then attached to the gas line at X in Fig. 16 for oxidation to N_2 gas.

The volume of sample water initially collected from a site is dependent on the concentration of NO_3^- in the water. An optimum quantity of 20 mg NO_3^- was required for the method and gas line apparatus used here, although a minimum quantity of 10 mg can be used. Consequently, the collected volume of water varied from less than 1 litre to several litres in those cases where the NO_3^- concentration was low.

After collection, each sample was evaporated down quite rapidly to about 100 mls on a hot plate, but never allowed to boil. The remaining 100 mls was then transferred to a suitable beaker and evaporated to dryness under a hotlamp. The dry residue samples could then be stored indefinitely in a dry atmosphere.

The reduction of NO_3^- to ammonium sulphate, $(NH_4)_2SO_4$, was undertaken using Devardas Alloy which contains aluminium metal, i.e.

$$3NO_3^- + 8Al + 5OH^- + 2H_2O \rightarrow 8AlO_2 + 3NH_3 \uparrow$$

This reaction is pushed to the right in alkaline conditions, so MgO is added. The evolved ammonia gas is recovered by distillation into a collection flask containing H_2SO_4. This reacts with the NH_3 producing stable $(NH_4)_2\ SO_4$, i.e.

$$2NH_3 + H_2SO_4 \rightarrow (NH_4)_2\ SO_4$$

The apparatus used for this nitrate reaction (i.e. a Kjeldahl distillation) is shown in Fig. 17.

a) Method

Each evaporated sample is re-hydrated by the addition of 100 mls distilled H_2O. The suspension is thoroughly stirred to break up the precipitated solids. 10 mls 0.05M H_2SO_4 added to collection flask and placed in position (see Fig. 17). Usually a 200 ml flask with 10 mls H_2SO_4 is sufficient, but this varies from sample to sample. If a lot of NH_3 is produced, more H_2SO_4 should be added to keep the collection distillate acidic. In practice the alkalinity and acidity of the distillate and distillate + H_2SO_4 can be monitored by universal litmus paper as the reaction proceeds.

3 g MgO is added to the distillation flask, followed by 3 g Devqrdas Alloy, and then the 100 ml re-hydrated sample and precipitated solids not in solution. The reaction is started by

500ml reaction vessel :

3g MgO
3g Devardas Alloy
100 mls sample

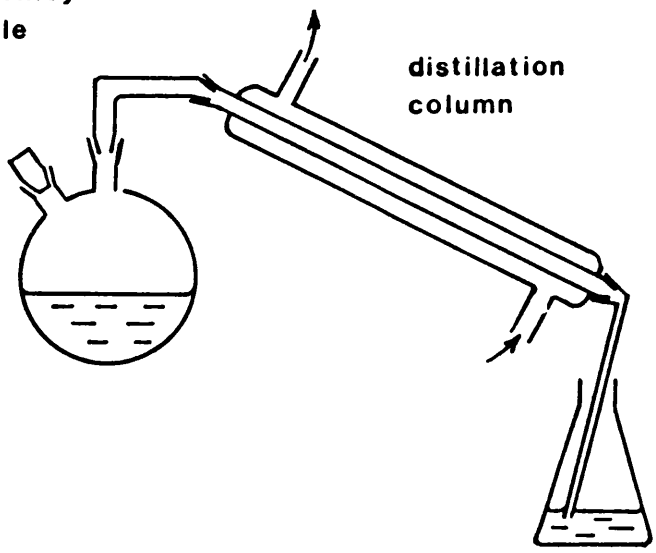

FIG. 17 Kjeldahl distillation method for reduction of nitrate to ammonium sulphate.

warming the solution. Particular care should be taken especially in the initial stages because the reaction may become quite vigorous. Normally a continuous stable bubbling is maintained. The exit drops of the distillate should be alkaline, the H_2SO_4 reservoir always acidic. When the exit drops become neutral, the reaction is complete. This may be any length of time between 10 minutes to over one hour, depending on the quantity of nitrate and on the quantity of precipitated solids in the sample. The reservoir H_2SO_4 should have further H_2SO_4 added if the litmus paper indicates the solution is approaching neutrality. Once the reaction is complete, 2 aliquots of ethyl alcohol is added to the reaction vessel and the procedure continued for a further 2 minutes. This ensures all the NH_3 is recovered and cleans the system.

The sample solution is now set to a pH of 3-4 by adding 0.1M NaOH to the distillate. This is crucial because although the solution must be acidic in order to keep the $(NH_4)_2\ SO_4$ stable, the pH must not be less than 3 because otherwise the sample will not subsequently evaporate to dryness, but rather forms an oleum.

After setting the pH, the samples are evaporated down into flat-bottomed Quickfit 50 ml conical flasks. A white precipitate eventually forms, the $(NH_4)_2\ SO_4$. This sample can now be stored indefinitely prior to gas-line treatment for the oxidation step.

b) Titration

To prevent any isotopic fractionation, the chemical efficiency of the distillation step should be >95%. This is tested at the start of the sample batch run and then after every twelve samples.

A known quantity of KNO_3 is used to produce NH_3, and $(NH_4)_2\ SO_4$ produced by reaction with a known quantity of H_2SO_4. The excess H_2SO_4 can then be titrated with NaOH to determine the % recovery.

1 mole $NO_3^- \rightarrow$ 1 mole NH_3

2 moles NH_3 reacts with 1 mole H_2SO_4

2 moles NaOH reacts with 1 mole H_2SO_4.

In practice 20 mg KNO_3 was used, reacting with standardised 0.05M H_2SO_4, and the excess titrated with standardised 0.1M NaOH using Phenol Red.

2.5.6 Preparation of Lithium Hypobromite solution

Mass spectrometric measurement of the m/e 29/28 ratio requires the oxidation of the previously prepared $(NH_4)_2\ SO_4$ samples to nitrogen gas. The upper limb of the gas line illustrated in Fig.16 is used for this procedure. The $(NH_4)_2\ SO_4$ sample is attached to the line at X immediately under a flask containing a reservoir of oxidising reagent, lithium hypobromite solution (LiOBr). The LiOBr is contained under a helium atmosphere, firstly to ensure a rapid expulsion of a quantity of the reagent when reacting the sample, and secondly to prevent back-contamination of evolved N_2 from the reacted samples. The oxidation reaction is:

$$3LiOBr + (NH_4)_2SO_4 \rightarrow N_2\uparrow + 3LiBr + H_2SO_4 + 3H_2O$$

The evolved N_2 is then dried to remove H_2O and CO_2 and taken up on activated Si-gel. The sample flask is then ready for analysis when warmed to room temperature.

The LiOBr reagent was first prepared by dissolving 60g of

Analytical Reagent lithium hydroxide ($LiOH.H_2O$) in 600 mls distilled water, giving a 10% w/v concentration. The dissolution is a slow process and was aided by gentle heating. The solution was then transferred to a 1-litre volumetric flask and stored overnight in a refrigerator at 0-5°C. 20 mls of bromine (Br_2) was then added to the cold solution in 2 ml aliquots, vigorously swirling the volumetric flask until each increment of Br_2 added was dissolved. The final solution has a clear, deep yellow appearance, and was permantly stored at 0-5°C in order to prevent decomposition of the reagent.

2.5.7 Preparation of Lithium Hypobromite reservoir

The reservior flask attached to the gas line as illustrated in Fig. 16 contains about 70 mls of lithium hypobromite under an atmosphere of helium. This was prepared in the following manner. About 100 mls of the LiOBr was first added to a beaker from the cold stock solution. A 100 ml flask with a single greased tap was used as the LiOBr reservoir flask. This flask was first evacuated and then its tap immersed into the quantity of LiOBr. About 70 mls of the reagent can therefore be drawn up into the flask in this manner.

The reservoir flask was then reattached to a gas line (not shown) and opened directly to the pumps for 1 hour to throughly degas the solution. This method optimises the fact that in a vertical position, fluid within the partially-filled vessel will overlie the tap, but in a horizontal position the tap would be in contact with the volume overlying the solution. After 1 hour, the gas line and reservoir flask were then flooded with helium to a pressure of 400 mbar. The reservoir flask could then be removed, inverted, and attached to the ammonium-sulphate oxidation line shown in Fig. 16. The quantity of

reagent in the reservoir is enough for about 7 sample reactions.

2.5.8 Procedure for Ammonium Sulphate Oxidation

With the $(NH_4)_2\ SO_4$ sample and LiOBr reservoir in place, the line is pumped down to $<10^{-3}$ mbar. The 'lower' limb illustrated in Fig. 16 for gas sample preparation is not used in this procedure, so tap A is closed and taps E, F and G are opened, along with the collection flask, and Si-gel heated at 200°C. Taps F and E are then shut, and the LiOBr reservoir opened to allow a aliquot of reagent to shoot down into the sample ammonium sulphate. The reservoir tap is only opened for a second and then immediately closed. Tap G is then closed, and tap F opened to expand the gas through into the vapour trap. At this stage, no liquid N_2 Dewar is in place to ensure no temperature gradient is present between the sample and the vapour trap. The gas is left for 5 minutes to throughly equilibrate and to ensure the oxidation reaction proceeds to completion. Tap F is then closed, and a liquid N_2 Dewar then placed in position around the vapour trap. After a further five minutes, the collection flask heater is removed and replaced by a liquid N_2 Dewar to activate the Si-gel, and tap G opened for 5 minutes. The collection flask can then be sealed, tap G closed, and the sample is ready for analysis when the Si-gel is warmed up to room temperature.

It is important to note that in this case expansion and trapping off of the gas is necessary. The procedure therefore avoids any temperature gradient which could produce isotopic fractionation by ensuring that the liquid N_2 bath is only placed in position after the expansion and trapping off has occured. Testing of this procedure on laboratory ammonium sulphate requires an optimum quantity of 40 mg $(NH_4)_2\ SO_4$, and a minimum quantity of 20 mg.

2.5.9 Mass Spectrometric Analysis

The V.G. Micromass 602E at B.G.S., Wallingford is a double inlet/double collector system. The double inlet system comprises two gas reservoirs, one filled with the sample and the other with the reference. The double collector system comprises a major and a minor collector which allows the simultaneous measurement of two ion current beams, particularly on a gaseous chemical compound containing two isotopic species in differing abundancies.

The gas pressure is independently adjustable in the two reservoirs to produce the same ion current across the major collector. The two reservoirs are independently connected with the ion source through viscous leaks and a system of valves. This allows increments of gas from each reservoir to be alternately leaked to the ion source of the mass spectrometer, which is maintained under a high vacuum. The N_2 molecules in the ion source are bombarded by electrons from a filament, and some molecules acquire a single positive charge. A large potential at the front of the ion source accellerates these positive ions into the flight tube where they pass through a high-intensity magnetic field. The ions containing the lighter isotope $(^{14}N^{14}N)^+$, of mass 28 are deflected more than the ions containing the heavier isotope $(^{14}N^{15}N)^+$ mass 29, and $(^{15}N^{15}N)^+$, mass 30. The magnetic separation permits the two major ions $(^{28}N_2)^+$ and $(^{29}N_2)^+$ to be distinguished on the basis of their momentum, and hence on the basis of the mass difference between them.

The minor collector slit was used to focus the resolution of the $(^{29}N_2)^+$ ion current beam. The major beam was run at 2.5×10^{-9}A on both reference and sample sides, with the major beam scale setting on

5×10^{-9} FSD and the minor on 10^{-10} FSD (Full Scale Deflection). The source parameters are listed below:

Accellerating voltage:		4210 eV approx.
Trap current	:	200 μA
Ion Repeller Voltage	:	+ 7.1 v
Electron volts	:	94% (of 100 v)
Half-plate voltage	:	1010 v
Half-plate ΔV	:	max
Response	:	0.3 secs.

Deoxygenation of the sample is important to prevent the formation of CO^+ ions through possible combination with carbon from the filament. Drying of the gas to take out CO_2 is necessary because cracking of the CO_2 molecule also produces CO^+ ions. These CO^+ ions have m/e of 28 and 29 and would superimpose on the corresponding N_2 m/e peaks, giving inaccurate results and poor precision.

2.5.10 Correction for atmospheric contamination of $\delta^{15}N(NO_3)$ analysis

A correction to the measured δ-value on samples from nitrates can be made to account for atmospheric contamination. This correction is based on the presence of an argon peak and therefore is not applicable to other gas samples which would contain atmospheric argon. The atmospheric contribution to the major m/e 28 peak is calculated from:

$$\text{N-28 p} = \text{Ar-40 p} \times \frac{\text{N-28 air}}{\text{Ar-40 air}}$$

and $\frac{\text{N-28 p} \times 100}{\text{N-28 m}}$ = % atmospheric contribution to N-28 ion current. = α

All values refer to the m/e ion current measurements. N-28 p is the atmospheric pollution component of the total measured m/e 28 (N-28 m) of the sample. Ar-40 refers to the m/e ion current peak for argon which reflects the atmospheric contamination. A prior determination of the ion current m/e 28/40 ratio in air is necessary and the 602E measures this value to lie between 41.9 and 38.1. A value of 40.0 was therefore assumed for all calculations. Before each sample run, the argon ion current peak (m/e 40 at about 3 KeV) is noted as well as the major beam ion current under the conditions of the run. This enables the % atmospheric contribution to the N-28 ion current to be calculated (α). After the sample run is over, the measured delta-value (δm) can be corrected to the real sample delta-value (δr) using the equation:

$$\delta r = \frac{(\delta m \times 100)}{(100 - \alpha)}$$

The correction is ususally very small but in some cases may be of the order of $1.0^{o}/oo$.

2.5.11 Measurements on I.A.E.A. standards

The precision on each analysed sample delta value is based on twice the Standard Error on the mean (Appendix 8), calculated from ten instrumental measurements on any one sample. All samples were measured to a precision better than $2\sigma_{10} = 0.03^{o}/oo$.

Unlike SMOW for oxygen and hydrogen isotopes in water, or PDB for carbon isotopes in carbonates, an international standard for nitrogen isotopes has not yet been defined. Mariotti (1983) has however measured air samples from worldwide localities and showed that the $\delta^{15}N$ value of atmospheric N_2 may, for all practical purposes, be considered as

universally constant.

It is not however, particularly easy to prepare samples of air as a working standard every time a batch of samples is analysed. This is because it is both time consuming and wasteful of the finite quantity of reduced copper necessary for deoxygenation. A cylinder of oxygen free nitrogen gas (BOC 99.998% N_2) was therefore used as the working standard. The measured delta value of the sample against the working standard can then be expressed against air by calculation using the procedure given in Appendix 8. The corrections necessary to a 'raw' sample delta value measured against cylinder N_2 are summarised as follows:

1) correction for atmospheric contamination.

2) correction for depletion of bottled N_2 during sample batch run.

3) calculation to obtain $\delta^{15}N$ vs. air.

Step 1 is not used in samples other than those from nitrates, and steps 2 and 3 use the same formulae as listed in Appendix 8. Mariotti (1984) has noted an 'Argon effect' whereby the apparent delta-value becomes more negative with increasing argon content in the sample. This appears to be an instrumental effect unique to any particular insturment. This effect, if present at all on the 602E will be insignificant because the sample N_2/Ar ratios are too high (about 45:1).

All quoted delta values in any listed results are expressed against air. The working standard N_2 cylinder gas was measured several times against air and found to be slightly depleted in ^{15}N, having a $\delta^{15}N$ value of $-2.1^{o}/oo$ with a reproducibility to $+/- 0.2^{o}/oo$. Two ammonium sulphate standards, N-1 and N-2, and a KNO_3 standard are currently available from the International Atomic Energy Authority (Vienna) for use in isotope laboratories. As yet there is no internationally

accepted value for these standards to allow inter-laboratory calibrations. $\delta^{15}N$ measurements on these compounds are listed in Table 16. The N-1 and N-2 values are here respectively measured to be 1.31 and 0.85 $^{o}/oo$ lighter than the same standards as the mean measurements collated by Gonfiantini, (1983). The reproducibility on gas samples is to within +/- 0.2$^{o}/oo$, but the reproducibility on $\delta^{15}N(NO_3)$ samples is no better than +/- 1.0$^{o}/oo$ due to the greater scope for errors because of the more involved sample preparation.

Table 16 $\delta^{15}N$ measurements on I.A.E.A. Standards

(‰)

	N-1 Vienna	N-2 Vienna	KNO_3 Vienna
1	- 0.90	+ 19.28	+ 3.24
2	- 0.84	+ 19.32	+ 3.44
3	-	+ 19.33	+ 3.55
4	-	+ 19.40	+ 3.51
$\bar{X}$	- 0.87	+ 19.33	+ 3.44

2.6 Oxygen and Hydrogen Isotopes

2.6.1 Principle of Analysis

Oxygen and hydrogen isotope measurements on the water molecule of water samples collected from aquifer sites were determined on a VG Micromass 602E mass spectrometer at Wallingford. H_2 was prepared by reduction of water over zinc shot at 450°C, and hydrogen gas is the species analysed in the spectrometer, expressed using the delta notation:

$$\delta^2H = \left[\frac{(^3H_2/^2H_2)spl - (^3H_2/^2H_2)STD}{(^3H_2/^2H_2)STD}\right] \times 1000$$

The results given in °/oo. For oxygen isotopes, the sample water is equilibrated with CO_2 and the CO_2 is the medium used to determine $\delta^{18}0$, i.e.

$$\delta^{18}0 = \left[\frac{(^{46}CO_2/^{44}CO_2)SPL - (^{46}CO_2/^{44}CO_2)STD}{(^{46}CO_2/^{44}CO_2)STD}\right] \times 1000\ °/oo$$

Results are expressed against Standard Mean Ocean Water (SMOW). Only a brief description of the analytical procedure will be given here. A more detailed account is given by Darling, et al., 1982.

2.6.2 Hydrogen Isotope Sample Preparation

The reduction of water to H_2 takes place in the sample flask, which can then be directly attached to the inlet of the spectrometer. 0.25g Zn shot are first placed in each sample flask followed by 10 µl sample water. The flasks are then attached to a gas line, immersed in liquid N_2 to freeze the water, and the flasks opened to the pumps to evacuate the flasks. The sample flasks are then closed and removed from the gas line. Each flask is then placed in a heating block at 450°C for 1 hour. The following reaction occurs at this temperature:

$$Zn + H_2O \rightarrow ZnO + H_2$$

Each sample flask is then ready for analysis.

2.6.3 Oxygen Isotope Sample Preparation

The preparation involves two stages:

a) CO_2 equilibration procedure.

10 μl 50% HNO_3 are added to each equilibration flask followed by 5mls sample water. The HNO_3 aids the water-gas equilibration. The flasks are sealed and placed on a gas line, as shown in Figure 18, and the water sample frozen out with liquid N_2. The flasks are then opened to the pumps to evacuate these containers, re-sealed, and removed from the gas line. Once the ice in each flask has melted, they are re-attached to the gas line and the line flooded with CO_2. Each equilibration flask is then opened, flooding the flasks with cylinder CO_2 to a pressure of 300 mbar. After 30 seconds the equilibration flasks are re-sealed, removed, and placed in a water bath at 25°C for 24 hours.

b) CO_2 sample flask collection

Each equilibration flask is attatched to the gas line (Fig. 18) with a corresponding collection flask in place. The line, including the collection flasks, is evacuated, and then a -80°C bath is placed in position around the U-tube vapour trap. Gas from the equilibration flask is then expanded through into the line to B, and tap A and the collection flask shut after 20 seconds. Any H_2O in this central portion freezes out. After 3 minutes the line is shut off to the pumps and B is opened, expanding through the dried sample gas into the collection flasks. A liquid N_2 bath is raised around these collection flasks for a further 2 minutes.

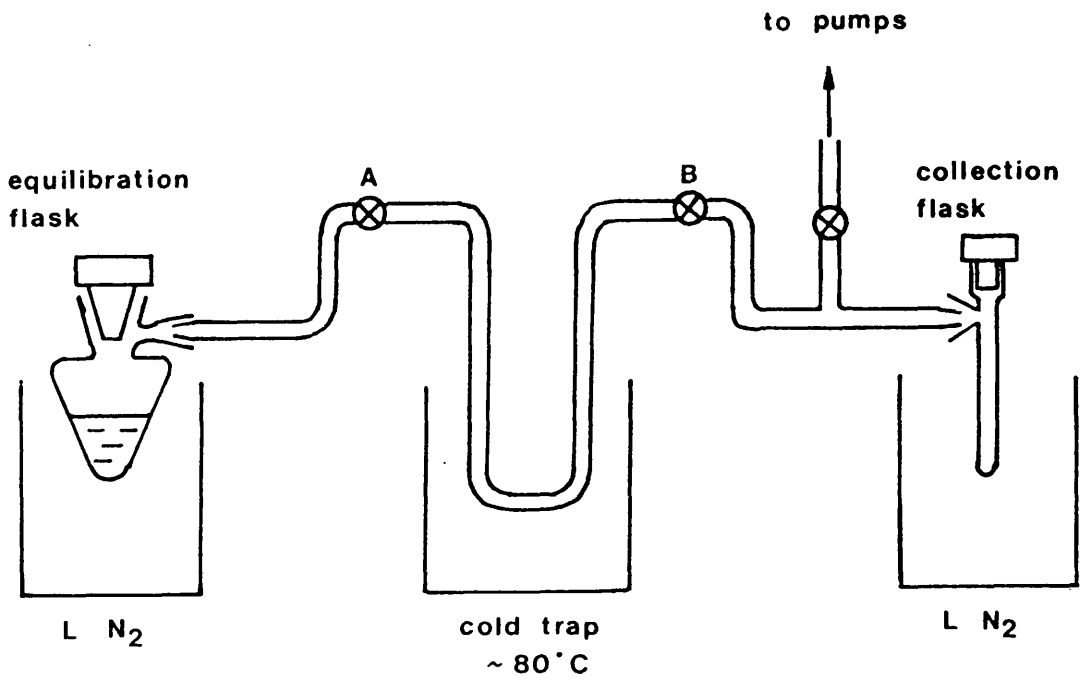

FIG. 18 Carbon dioxide sample collection line for oxygen isotope analyses.

This freezes down all the CO_2 into the flasks. The flasks are then sealed, removed, and ready for mass spectrometric analysis.

2.6.4 Mass Spectrometric Analysis

Both $\delta^{18}O$ and $\delta^{2}H$ values were measured on a major beam of 5.0×10^{-9} Amps, (10^{-8}FSD), and the minor on 10^{-10}FSD. The same source parameter settings are used as listed for $\delta^{15}N$ analysis.

In all cases delta values were measured against the local working standard, Wallingford Tap Water (WTW). A number of minor corrections have to be applied to these raw delta values.

For $\delta^{2}H$, a correction for the formation of $(H_3)^+$ ions is necessary, because of its superimposition on the m/e peak for the $(^{2}H^{1}H)^+$ ion. For $\delta^{18}O$, a correction is first made for the isotopic equilibration between the aqueous water sample and the gaseous CO_2 at $25^{o}C$. The fractionation factor is 1.0412. The correction is made quantitative from knowing the molar volume ratio of H_2O:CO_2 in the equilibration flask. The equilibration flask volume, water sample volume, and CO_2 pressure at the time of equilibration are always noted so this calculation can be made. A second correction to the $\delta^{18}O$ value is made in order to account for the presence of $(^{46}CO_2)^+$ and $(^{44}CO_2)^+$ ions which do not contain ^{18}O or ^{16}O in the molecule. This correction is very small.

2.6.5 Standard

All measured sample delta-values vs WTW are expressed against the international SMOW standard by manipulation of the data using the equations in Appendix 8. WTW is measured every few months against SMOW, its value being lighter than SMOW (e.g. $\delta^{18}O = -7.2^{o}/oo$;

$\delta^2H = -48.9^o/oo$).

A calibration correction to Standard Light Antarctic Precipitation (SLAP) is also applied. This standard has by international concensus a δ^2H value of $-428^o/oo$ and a $\delta^{18}O$ value of -55.5. The respective instrumental bias of any one spectrometer as determined by its measurement of SLAP can therefore be eliminated. The correction applied is:

$$\text{correction} = \frac{\text{'true' SLAP}}{\text{measured SLAP}}$$

Quoted sample results are therefore expressed against SMOW with a SLAP calibration. The precision on each analysis is better than +/- 0.03‰ ($2\sigma_{10}$). Reproducability for $\delta^{18}O$ is +/- $0.1^o/oo$, and reproducibility for δ^2H is +/- $1^o/oo$.

CHAPTER THREE

RESULTS

3.1 Presentation of Results

The analytical results are presented separately for the Nottinghamshire Trias and the Lincolnshire Limestone respectively. Some sites were sampled in replicate, and in such cases each individual analysis is given as well as their means. Those instances in which an analysis was not determined is marked by dash in the appropriate space.

3.1.1 Results from the Nottinghamshire Triassic groundwaters

Table 17 and Fig. 19 list the grid references, name sites, and geographical locations of each of the sampled sites in the aquifer. All field measurements, N_2/Ar ratios, noble gas and recharge temperatures, nitrogen isotope data, oxygen and hydrogen isotope data, and nitrate/chlorinity determinations are listed in Tables 18 to 23 respectively.

3.1.2 Results from the Lincolnshire Limestone groundwaters

Table 24 and Fig. 20 list the grid references, name sites, and geographical locations of each of the sampled sites. All results are listed in Tables 25 to 30 respectively in a similar format to that of the Nottinghamshire Trias.

Table 17. Location of groundwater sites from the Nottinghamshire Triassic Sandstone Aquifer

Sample Number	Site	SK Grid Reference
NT01	Rampton	776 776
NT02	Markham Clinton No.3	711 727
NT03	Ompton No.3	678 648
NT04	Halam No.3	670 537
NT05	Far Baulker No.2	612 543
NT06	Newark, Clay Lane	800 540
NT07	Gainsborough, Lea Rd., No.3	816 889
NT08	Grove No.1	740 803
NT09	Newton No.1	826 742
NT10	South Scarle	856 650
NT11	High Marnham	808 713
NT12	Cottam	815 792
NT13	Everton No.1	694 901
NT14	Elkesley No.3	664 760
NT15	Budby No.3	604 702
NT16	Boughton No.4	669 697
NT17	Amen Corner No.3	642 655
NT18	Clipstone No.1	603 643
NT19	Rufford No.2	632 610
NT20	Caunton	739 600
NT21	Rainworth No.3	587 586
NT22	Farnsfield	656 568
NT23	Fishpool	576 553
NT24	Papplewick	582 521
NT25	Bestwood	579 482
NT27	Lumbley	626 450
NT27	Burton Joyce No.3	654 443
NT28	West Burton	790 855

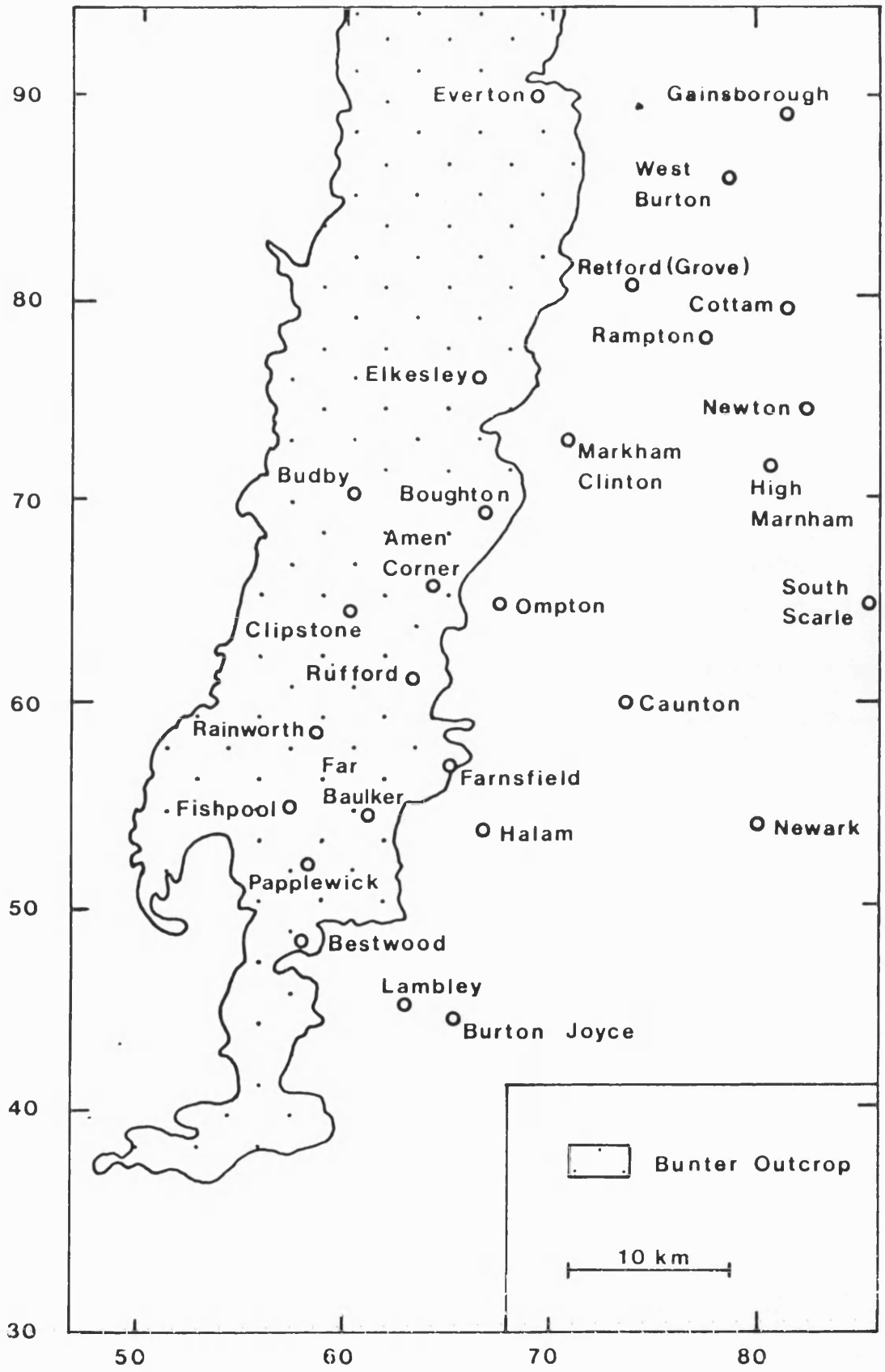

FIG.19 Map of sampled sites within the Nottinghamshire area.

Table 18. Field Measurements on the Nottinghamshire Triassic Groundwaters.

Sample Number	Borehole Data Depth m	lined to m	T°C	pH	Eh mV	1 %O_2	2 K μScm^{-1}	HCO_3 mg/l	3 pCO_2 x 10^3
NT01	306	183	14.2	7.05	+133	0	377	-	-
NT02	230	60	12.2	7.80	+386	52	-	-	-
NT03	176	50	11.4	7.70	+451	90	210	-	-
NT04	171	76	10.9	7.75	+377	92	258	-	-
NT05	137	55	9.7	7.45	+379	93	415	-	-
NT06	366	63	17.4	7.40	+125	0	539	-	-
NT07	498	290	18.1	7.45	+161	0	583	-	-
NT08	335	168	12.6	7.35	+175	0	387	-	-
NT09	381	246	17.5	7.45	+151	0	458	-	-
NT10	354	292	19.8	7.35	+133	0	520	-	-
NT11	420	220	16.5	7.60	+ 80	0	378	-	-
NT12	410	208	-	6.45	+ 84	5	494	-	-
NT13	-	-	11.2	7.66	+321	29	449	166	2.48
NT14	-	-	11.2	8.13	+443	92	373	86	0.44
NT15	76	33	11.2	7.62	+546	80	533	90	1.47
NT16	76	46	10.4	7.69	+?78	80	514	114	1.59
NT17	130	26	10.8	8.13	+437	95	412	66	0.33
NT18	91	13	9.6	7.50	+293	78	1509	114	2.20
NT19	122	14	10.0	7.56	+314	58	626	99	1.66
NT20	256	26	13.8	7.60	+441	2	524	229	3.93
NT21	86	24	9.8	8.03	+383	76	495	101	0.57
NT22	32	18	10.0	7.92	+391	85	400	81	0.59
NT23	59	24	10.4	8.07	+399	90	417	58	0.34
NT24	62	-	9.6	8.20	+371	100	363	53	0.20
NT25	53	-	10.0	7.84	+?98	92	476	96	0.85
NT26	155	68	11.8	7.96	+437	78	265	133	1.00
NT27	147	57	11.9	7.34	+385	10	723	241	7.52
NT28	No field measurements taken.								

1. Dissolved O_2 % saturation.
2. Conductivity.
3. Partial Pressure CO_2. (atms)

Table 19. **N_2/Ar ratios for dissolved gases in groundwaters from the Nottinghamshire Triassic Sandstone.**

Sample No.		N_2/Ar	Mean	+/- range
NT01	a	41.6	41.4	0.3
	b	41.1		
NT02		42.3	42.1	0.2
		41.9		
NT03		41.7	42.8	1.1
		43.8		
NT04		42.0	41.4	0.6
		40.8		
NT05		40.6	40.8	0.2
		40.9		
NT06		43.3	43.3	0.1
		43.1		
NT07		42.6	42.6	0.1
		42.6		
NT08		41.6	42.3	0.7
		42.9		
NT09		41.9	42.1	0.2
		42.3		
NT10		41.6	42.2	0.6
		42.7		
NT11		42.0	42.2	0.2
		42.4		
NT12		41.5	41.5	0.8*
		-		
NT13		47.3	46.4	0.9
		45.5		
NT14		41.8	41.8	0.1
		41.7		
NT15		42.6	41.6	1.0
		40.6		
NT16		41.3	41.0	0.3
		40.7		
NT17		39.5	40.5	1.0
		41.5		

Sample No.		N_2/Ar	Mean	+/- range
NT18	a	41.6	42.2	0.6
	b	42.7		
NT19		45.6	46.7	1.0
		47.5		
NT20		46.4	45.2	1.3
		43.9		
NT21		42.3	40.9	1.4
		39.5		
NT22		41.9	42.0	0.1
		42.1		
NT23		40.9	43.6	2.7
		46.2		
NT24		42.3	42.5	0.2
		42.6		
NT25		43.0	42.5	0.5
		42.0		
NT26		42.6	42.4	0.2
		42.2		
NT27		44.2	43.8	0.4
		43.4		
NT28		41.6	41.6	0.8*
		-		

* error based on +/- 2%of single measurement.

a,b = replicate samples

Table 20. Noble gas contents and derived recharge temperatures for groundwaters from the Nottinghamshire Triassic Sandstone.

Sample Number		$^4He.10^8$	$Ne.10^7$	$Ar.10^4$	$Kr.10^8$	$Xe.10^8$	C.I.	Average R.T.	S.D. +/-
NT01-A	a	82.57	2.87	5.14	11.66	1.77			
	b	80.67	2.22	4.81	11.25	1.74	1.30	2.6	0.8
	c	-	2.9	1.5	3.6	2.8			
NT01-B	a	84.63	2.94	5.25	11.85	1.76			
	b	82.58	2.22	4.89	11.41	1.72			
	c	-	2.7	0.9	3.1	3.0			
NT02-A	a	14.59	2.54	4.35	9.61	1.41			
	b	13.29	2.09	4.12	9.33	1.38	1.21	8.3	0.8
	c	-	8.6	7.6	9.7	8.8			
NT02-B	a	12.39	2.54	4.42	9.86	1.46			
	b	11.15	2.11	4.20	9.59	1.44			
	c	-	7.9	6.8	8.8	7.8			
NT03-A	a	14.28	2.44	4.48	9.74	1.40			
	b	13.30	2.10	4.30	9.53	1.38	1.18	8.1	1.2
	c	-	8.2	5.8	9.0	8.9			
NT03-B	a	16.56	2.53	4.47	9.77	1.39			
	b	15.32	2.10	4.25	9.50	1.37			
	c	-	8.2	6.3	9.1	9.0			
NT04-A	a	13.90	2.35	4.33	9.49	1.37			
	b	13.12	2.08	4.19	9.32	1.36	1.14	8.9	1.2
	c	-	9.2	6.9	9.8	9.4			
NT04-B	a	10.19	2.38	4.31	9.35	1.35			
	b	9.34	2.09	4.16	9.17	1.34			
	c	-	8.9	7.2	10.3	9.7			
NT05-A	a	12.45	2.32	4.24	9.33	1.36			
	b	11.77	2.08	4.12	9.19	1.35	1.09	8.9	1.0
	c	-	9.2	7.6	10.3	9.4			
NT05-B	a	8.82	2.23	4.25	9.39	1.37			
	b	8.42	2.09	4.18	9.30	1.37			
	c	-	8.7	7.0	9.8	9.2			
NT06-A	a	183.02	3.21	5.66	11.93	1.68			
	b	180.18	2.23	5.15	11.31	1.63	1.46	2.3	2.1
	c	-	2.4	-1.0	3.4	4.4			
NT06-B	a	178.24	3.28	5.69	12.04	1.66			
	b	175.22	2.23	5.15	11.38	1.61			
	c	-	2.4	-1.0	3.2	4.8			

Sample Number		$^4He.10^8$	$Ne.10^7$	$Ar.10^4$	$Kr.10^8$	$Xe.10^8$	C.I.	Average R.T.	S.D. +/-
NT07-A	a	201.91	2.92	5.33	11.35	1.58			
	b	199.82	2.20	4.96	10.89	1.55	1.36	3.8	1.8
	c	-	3.7	0.4	4.6	5.7			
NT07-B	a	200.79	3.02	5.26	11.33	1.59			
	b	198.38	2.18	4.83	10.80	1.55			
	c	-	4.5	1.3	4.8	5.7			
NT08-A	a	32.54	2.61	4.62	10.00	1.42			
	b	31.10	2.11	4.37	9.69	1.39	1.23	7.4	1.4
	c	-	7.6	5.2	8.4	8.6			
NT08-B	a	31.05	2.59	4.62	10.11	1.40			
	b	29.69	2.11	4.38	9.82	1.28			
	c	-	7.6	5.1	8.0	9.0			
NT09-A	a	104.15	2.63	5.03	11.13	1.58			
	b	102.89	2.19	4.80	10.86	1.56	1.21	4.1	1.5
	c	-	4.0	1.5	4.7	5.5			
NT09-B	a	103.97	2.67	5.03	10.98	1.58			
	b	102.56	2.18	4.78	10.67	1.55			
	c	-	4.5	1.7	5.2	5.6			
NT10-A	a	135.48	2.75	5.04	11.07	1.62			
	b	133.83	2.18	4.74	10.71	1.60	1.24	4.0	1.4
	c	-	4.8	2.0	5.1	4.9			
NT10-B	a	134.85	2.67	5.08	11.24	1.58			
	b	133.49	2.19	4.83	10.95	1.55			
	c	-	4.0	1.3	4.4	5.6			
NT11-A	a	103.81	2.74	5.03	11.27	1.58			
	b	102.22	2.19	4.74	10.93	1.55	1.24	4.3	1.3
	c	-	4.0	2.0	4.5	5.7			
NT11-B	a	96.49	2.65	4.92	11.02	1.57			
	b	95.13	2.17	4.68	10.72	1.55			
	c	-	4.8	2.5	5.1	5.8			
NT12-A	a	120.83	2.70	5.02	11.07	1.54			
	b	119.33	2.18	4.76	10.75	1.52	1.24	5.2	1.6
	c	-	4.5	1.9	5.0	6.3			
NT12-B	a	117.60	2.66	4.77	10.61	1.47			
	b	116.12	2.15	4.51	10.29	1.45			
	c	-	5.9	3.9	6.4	7.5			
NT13	a	12.41	2.27	4.01	9.82	1.28			
	b	11.86	2.08	3.91	9.70	1.27	1.09	9.7	1.0
	c	-	9.4	9.8	8.4	11.3			

Sample Number		$^4He.10^8$	$Ne.10^7$	$Ar.10^4$	$Kr.10^8$	$Xe.10^8$	C.I.	Average R.T.	S.D. +/-
NT14	a	18.42	2.91	4.45	10.10	1.39			
	b	16.03	2.08	4.03	9.58	1.35	1.40	9.1	0.4
	c	-	9.2	8.6	8.8	9.6			
NT15	a	12.81	2.48	4.34	10.05	1.41			
	b	11.72	2.11	4.15	9.81	1.39	1.18	8.0	0.5
	c	-	7.9	7.3	8.0	8.7			
NT16	a	9.45	2.41	4.26	9.99	1.36			
	b	8.51	2.09	4.09	9.78	1.34	1.16	8.7	0.7
	c	-	8.9	7.9	8.1	9.7			
NT17	a	9.55	2.31	4.09	9.86	1.29			
	b	8.88	2.07	3.97	9.72	1.28	1.11	9.5	1.0
	c	-	9.5	9.1	8.3	11.0			
NT18	a	10.98	2.33	4.15	9.59	1.40			
	b	10.28	2.09	4.02	9.44	1.39	1.12	8.9	0.3
	c	-	9.8	8.6	9.3	8.7			
NT19	a	11.87	2.52	4.13	9.45	1.45			
	b	10.59	2.07	3.90	9.17	1.43	1.21	9.4	0.9
	c	-	9.5	9.9	10.3	7.9			
NT20	a	24.46	2.68	4.49	10.29	1.44			
	b	22.81	2.11	4.20	9.93	1.41	1.27	7.7	0.6
	c	-	7.9	6.8	7.6	8.3			
NT21	a	19.20	2.64	4.22	10.43	1.36			
	b	17.62	2.09	3.94	10.09	1.33	1.26	8.9	1.1
	c	-	8.9	9.5	7.1	9.9			
NT22	a	12.31	2.38	4.27	10.36	1.28			
	b	11.46	2.08	4.12	10.18	1.27	1.14	8.7	1.7
	c	-	9.2	7.6	6.8	11.3			
NT23-A	a	13.60	2.63	4.32	10.01	1.42			
	b	12.07	2.09	4.05	9.67	1.40	1.17	8.5	0.3
	c	-	8.6	8.3	8.5	8.6			
NT23-B	a	11.47	2.27	4.14	9.91	1.38			
	b	10.95	2.09	4.05	9.79	1.37			
	c	-	8.6	8.3	8.1	9.1			
NT24-A	a	15.74	2.75	4.36	7.99	1.34			
	b	13.64	2.02	3.98	7.54	1.30	1.38	9.4	1.4
	c	-	12.7	9.1	17.8	10.6			

Sample Number		$^4He.10^8$	$Ne.10^7$	$Ar.10^4$	$Kr.10^8$	$Xe.10^8$	C.I.	Average R.T.	S.D. +/-
NT24-B	a	24.75	2.92	4.30	10.20	1.30			
	b	22.30	2.07	3.87	9.69	1.26			
	c	-	9.9	10.3	8.4	11.5			
NT25-A	a	16.89	2.84	4.37	10.43	1.36			
	b	14.72	2.09	3.99	9.96	1.32	1.34	9.0	0.9
	c	-	8.9	9.0	7.5	10.1			
NT25-B	a	16.41	2.72	4.38	9.99	1.34			
	b	14.58	2.08	4.05	9.59	1.31			
	c	-	9.2	8.3	8.8	10.3			
NT26-A	a	20.45	2.63	4.34	10.37	1.33			
	b	18.89	2.09	4.06	10.03	1.31	1.26	8.9	1.1
	c	-	8.6	8.2	7.3	10.5			
NT26-B	a	21.14	2.61	4.22	10.19	1.34			
	b	19.63	2.09	3.95	9.86	1.32			
	c	-	8.9	9.3	7.8	10.2			
NT27-A	a	18.76	2.60	4.22	10.24	1.37			
	b	17.31	2.09	3.96	9.92	1.35	1.24	8.8	1.0
	c	-	8.6	9.2	7.6	9.6			
NT27-B	a	18.69	2.58	4.21	10.39	1.34			
	b	17.26	2.09	3.96	10.08	1.31			
	c	-	8.9	9.3	7.1	10.3			
NT28-A	a	112.9	2.90	5.00	11.27	1.65			
	b	110.8	2.18	4.63	10.82	1.62	1.34	4.6	0.9
	c	-	4.8	2.9	4.8	4.6			
NT28-B	a	121.5	2.92	4.99	10.99	1.63			
	b	119.3	2.16	4.60	10.51	1.59			
	c	-	5.3	3.1	5.7	5.0			

a. Original analysis; b. Analysis corrected for excess air; c. Recharge Temperature, ^oC.; C.I. Contamination Index; Average R.T. Average Recharge Temperature; S.D. Standard deviation for recharge temperature, ^oC.

Table 21. Nitrogen isotope composition for dissolved nitrates and nitrogen gas in groundwaters from the Nottinghamshire Triassic Sandstone

Sample Number	$\delta^{15}N(NO_3)$ ‰	$\delta^{15}N(N_2)$ ‰
NT01	- 5.8	-0.7
NT02	+ 9.3	-0.3
NT03	-13.1	-
NT04	-15.7	-
NT05	+ 5.4	+1.1
NT06	- 9.5	-0.6
NT07	-	-0.5
NT08	-	+0.5
NT09	-	+0.1
NT10	-	-
NT11	-	-
NT12	-14.8	-1.5
NT13	+ 4.0	+0.4
NT14	+ 4.5	-
NT15	- 0.4	+0.2
NT16	+ 1.0	+0.6
NT17	+ 1.3	+0.5
NT18	+31.1	-
NT19	- 1.3	+2.5
NT20	-	-1.0
NT21	+28.3	-
NT22	+22.7	-
NT23	-12.1	+1.0
NT24	-10.8	-
NT25	-12.9	-
NT26	+ 2.5	-
NT27	+14.9	-1.6
NT28	-	0.0

Table 22. Isotopic composition (oxygen and hydrogen) of groundwaters from the Nottinghamshire Triassic Sandstone

Sample Number	$\delta^{18}O$ °/oo	$\delta^{2}H$ °/oo
NT01	-9.2	-64
NT02	-8.0	-51
NT03	-8.1	-54
NT04	-8.0	-55
NT05	-8.2	-56
NT06	-9.1	-63
NT07	-9.1	-63
NT08	-8.1	-55
NT09	-8.8	-59
NT10	-9.1	-62
NT11	-9.3	-63
NT12	-9.0	-59
NT13	-8.2	-54
NT14	-8.2	-57
NT15	-8.2	-55
NT16	-8.1	-60
NT17	-8.3	-56
NT18	-8.2	-56
NT19	-8.2	-56
NT20	-7.9	-53
NT21	-8.2	-57
NT22	-8.2	-57
NT23	-8.3	-53
NT24	-8.2	-58
NT25	-8.0	-55
NT26	-8.1	-53
NT27	-7.8	-53

Table 23. Nitrate and chloride contents of groundwaters from the Nottinghamshire Triassic Sandstone

Sample Number	Cl mg/l	NO_3 mg/l	NO_3 mean	range
NT01	8.0	a < 2.0 b < 2.0	< 2.0	
NT02	12.1	5.8 < 2.0	2.9	2.9
NT03	12.8	6.6 6.4	6.5	0.1
NT04	11.2	20.0 17.8	18.9	1.1
NT05	20.8	32.0 28.0	30.0	2.0
NT06	17.3	a < 2.0 b < 2.0	< 2.0	
NT07	18.9	< 2.0 -	< 2.0	
NT08	6.3	< 2.0 -	< 2.0	
NT09	10.1	< 2.0 -	< 2.0	
NT10	-	< 2.0 -	< 2.0	
NT11	-	a - b < 2.0	< 2.0	
NT12	-	- < 2.0	< 2.0	
NT13	23.0	26.6 23.3	25.0	1.7
NT14	24.2	30.1 22.7	26.4	3.7
NT15	57.7	24.4 45.9	35.2	10.8
NT16	49.8	33.2 30.2	31.7	1.5

Sample Number	Cl mg/l		NO_3 mg/l	NO_3 mean	range
NT17	27.4	a	47.8	42.7	5.2
		b	37.5		
NT18	303.0		41.6	39.7	2.0
			37.7		
NT19	88.0		13.7	10.9	2.9
			8.0		
NT20	7.4		< 2.0	< 2.0	
			-		
NT21	35.1	a	31.5	28.7	2.8
		b	25.9		
NT22	23.5		46.5	45.8	0.8
			45.0		
NT23	24.5		39.4	39.3	0.2
			39.1		
NT24	24.4		32.3	32.4	0.1
			32.5		
NT25	29.3		45.2	43.3	2.0
			41.3		
NT26	7.4	a	7.1	6.9	0.2
		b	6.7		
NT27	12.0		2.2	1.1	1.1
			< 2.0		
NT28	-		-	< 2.0	
			< 2.0		

a,b = replicate samples.

Table 24. Location of groundwater sites in the Lincolnshire Limestone.

Sample Number	Site	T.F. Grid Reference	
LL01	Bourne	100	200
LL02	Northorpe	114	182
LL03	Ryhall South	039	101
LL04	Wilsthorpe	080	150
LL05	Baston Common	140	160
LL06	Block House Farm	133	190
LL07	Deeping St. James	183	112
LL08	Orchard Villa	213	159
LL09	Deeping St. Nicholas	222	180
LL10	Cuckoo Bridge	201	198

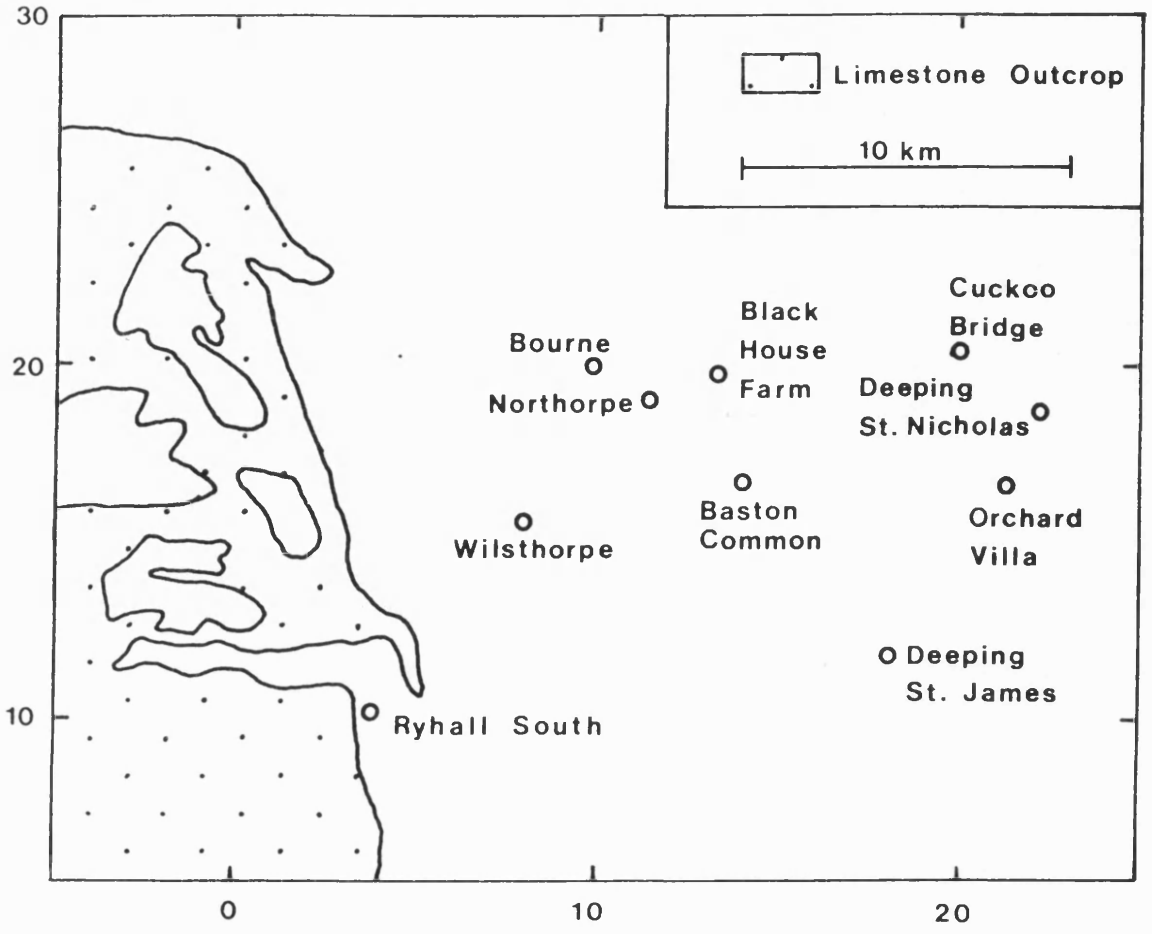

FIG.20 Map of sampled sites within the Lincolnshire area.

Table 25. Field measurements on groundwaters from the Lincolnshire Limestone.

Number	Well Type	T°C.	pH	Eh mV	Diss. O_2% saturation	C $\mu S\ cm^{-1}$	HCO_3 mg/l	pCO_2 atm.x10^3
LL01	P.S.	10.2	7.12	+188	2	783	190	9.84
LL02	O/W	12.2	7.20	+ 55	0	784	192	8.27
LL03	O/W	13.0	7.95	+226	55	886	186	1.43
LL04	P.S.	10.4	7.10	-	-	809	182	9.87
LL05	Private	11.0	7.43	+ 27	0	828	264	6.70
LL06	Private	11.4	7.20	+ 41	0	728	210	9.05
LL07	Private	12.2	7.95	- 1	0	1258	377	2.89
LL08	Private	13.8	8.39	-135	0	3365	479	1.33
LL09	O/W	11.8	8.51	- 95	0	4079	560	1.18
LL10	O/W	12.2	8.22	- 63	0	1358	406	1.67

P.S. = Pumping Station

O/W = Observation Well

Table 26. N_2/Ar ratios for dissolved gases in groundwaters from the Lincolnshire Limestone

Sample No.		N_2/Ar	mean +/- range
LL01	a	54.3	54.2 0.2
	b	54.0	
LL02	a	55.6	55.4 0.2
	b	55.2	
LL03	a	38.2	38.3 0.1
	b	38.4	
LL04	a	51.0	50.9 0.1
	b	50.8	
LL05	a	43.5	42.9 0.6
	b	42.3	
LL06	a	51.8	51.7 0.1
	b	51.6	
LL07	a	45.9	45.6 0.3
	b	45.3	
LL08	a	44.2	44.3 0.1
	b	44.3	
LL09	a	46.8	47.2 0.4
	b	47.6	
LL10	a	43.6	43.4 0.2
	b	43.2	

a,b replicate samples.

Table 27. Noble gas contents (cm^3STP/cm^3H_2O) and derived recharge temperatures for groundwaters from the Lincolnshire Limestone.

Sample Number		$^4He.10^8$	$Ne.10^7$	$Ar.10^4$	$Kr.10^8$	$Xe.10^8$	C.I.	Average R.T.	S.D. +/-
LL01-A	a	9.68	2.90	4.64	9.98	1.47			
	b	7.40	2.11	4.23	9.48	1.43	1.36	7.8	0.9
	c	-	7.8	6.4	9.2	7.9			
LL01-B	a	18.08	2.85	4.50	9.99	1.53			
	b	15.90	2.11	4.12	9.52	1.50			
	c	-	7.6	7.6	9.0	6.6			
LL02-A	a	14.97	2.96	4.62	10.12	1.44			
	b	12.50	2.09	4.18	9.58	1.40	1.40	7.9	0.9
	c	-	8.6	7.0	8.8	8.5			
LL02-B	a	12.57	2.94	4.61	10.11	1.54			
	b	10.20	2.11	4.19	9.59	1.50			
	c	-	7.6	6.9	8.8	6.6			
LL03-A	a	13.83	2.26	3.77	8.96	1.18			
	b	13.1	2.02	3.64	8.80	1.17	1.18	13.0	0.5
	c	-	12.9	13.1	11.8	13.8			
LL03-B	a	11.60	2.50	3.91	8.73	1.21			
	b	10.2	2.01	3.67	8.43	1.19			
	c	-	13.1	12.8	13.4	13.3			
LL04-A	a	16.84	2.63	4.36	9.79	1.34			
	b	15.3	2.08	4.07	9.44	1.31	1.27	9.1	0.8
	c	-	9.2	8.1	9.3	10.3			
LL04-B	a	11.32	2.63	4.35	9.57	1.40			
	b	9.7	2.09	4.07	9.23	1.38			
	c	-	8.9	8.1	10.1	9.0			
LL05-A	a	143.45	3.23	4.59	9.85	1.35			
	b	140.1	2.06	3.99	9.12	1.30	1.50	8.0	2.2
	c	-	10.2	9.0	10.5	10.7			
LL05-B	a	138.89	3.06	4.92	10.54	1.58			
	b	136.3	2.15	4.45	9.97	1.54			
	c	-	5.9	4.4	7.4	5.9			
LL06-A	a	20.70	3.12	4.79	10.26	1.47			
	b	17.8	2.11	4.27	9.63	1.42	1.50	7.9	0.8
	c	-	7.6	6.1	8.6	8.0			
LL06-B	a	27.12	3.20	4.65	10.44	1.47			
	b	23.9	2.1	4.08	9.75	1.42			
	c	-	8.2	8.0	8.2	8.1			

Sample Number		$^4He.10^8$	$Ne.10^7$	$Ar.10^4$	$Kr.10^8$	$Xe.10^8$	C.I.	Average R.T.	S.D. +/-
LL07	a	547.08	3.05	4.78	10.20	1.44			
	b	544.4	2.11	4.29	9.61	1.40	1.45	7.8	1.1
	c	-	7.9	5.9	8.7	8.5			
LL08	a	1492.9	3.00	4.72	10.08	1.20			
	b	1490.0	2.08	4.25	9.51	1.16	1.44	9.7	2.8
	c	-	9.2	6.3	9.1	14.1			
LL09-A	a	2174.1	2.89	4.57	9.16	0.89			
	b	2172.0	2.07	4.15	8.64	0.85	1.42	10.0	2.8
	c	-	9.9	7.3	12.5	[24.6]*			
LL09-B	a	2274.2	2.99	4.57	9.23	0.97			
	b	2271.0	2.07	4.10	8.65	0.92			
	c	-	9.9	7.8	12.4	[21.8]*			
LL10-A	a	469.0	3.08	4.79	10.40	1.50			
	b	466.0	2.13	4.31	9.81	1.45	1.56	7.7	1.0
	c	-	6.7	5.7	8.0	7.5			
LL10-B	a	500.8	3.58	4.80	10.49	1.51			
	b	497.0	2.09	4.03	9.56	1.44			
	c	-	8.6	8.5	8.9	7.7			

* Error in analysis.

a. Original analysis; b. Analysis corrected for excess air; c. Recharge Temperature, °C.; C.I. Contamination Index; Average R.T. Average Recharge Temperature; S.D. Standard deviation for recharge temperature, °C.

Table 28. **Nitrogen isotope composition for dissolved nitrates and nitrogen gas in groundwaters from the Lincolnshire Limestone**

Sample Number	$\delta^{15}N(NO_3)$ ‰		$\delta^{15}N(N_2)$ ‰	mean
LL01	-3.4	a	-0.21	-0.2
		b	-0.09	
LL02	-		+0.48	+0.4
			+0.39	
LL03	-9.7		+1.66	+1.1
			+1.47	
LL04	-0.3		+0.43	+0.3
			+0.22	
LL05	-		-1.00	-1.1
			-1.28	
LL06	-		-0.23	0.0
			+0.17	
LL07	-		-0.63	-0.9
			-1.13	
LL08	-		-1.04	-1.1
			-1.09	
LL09	-		-0.30	-0.6
			-0.85	
LL10	-		-0.63	-0.9
			-1.16	

a,b, = replicate samples

Table 29. Isotopic composition (oxygen and hydrogen) of groundwaters from the Lincolnshire Limestone.

Sample Number	$\delta^{18}O$ °/oo	$\delta^{2}H$ °/oo
LL01	-7.8	-53
LL02	-7.8	-55
LL03	-7.0	-46
LL04	-7.9	-53
LL05	-8.1	-57
LL06	-7.9	-54
LL07	-8.3	-56
LL08	-8.8	-57
LL09	-8.3	-54
LL10	-8.4	-57

Table 30. Nitrate contents of groundwaters from the Lincolnshire Limestone.

Sample Number	NO_3- mg/l
LL01	6.2
LL03	19.7
LL04	15.2

CHAPTER FOUR

DISCUSSION

4.1 Groundwater degassing processes

Groundwaters which circulate to sufficient depths to become heated as a consequence of the geothermal gradient, can also become supersaturated with respect to their atmospheric gases. The in-situ generation of other gases including nitrogen or methane would also enhance this supersaturation. Under such conditions, degassing could occur. With respect to the sample collection in particular, depressurisation of the groundwater to 1 bar at the wellhead could produce vesiculation and a potential loss of gas whilst sampling.

The computer program "OUTGAS" (Appendix 9) was written in order to investigate the influence of various parameters on the exsolution of gases from groundwaters. The program calculates the volume of a gas bubble exsolved from one litre of water under a given set of conditions which would produce vesiculation. The partial pressures of each of the gases in the bubble are calculated, and information concerning the fractionation of each gas species between the gaseous and liquid phases are subsequently derived based on their thermodynamic properties.

4.1.1 Mathematical procedure

The derivation of the gas bubble volume and its composition is based on a mass balance calculation, i.e.

$$S_i = S_i' + V_i \qquad (1)$$

where S_i is the in-situ volume of gas i in solution, S_i' is the volume of gas i remaining in solution after degassing and V_i is the volume of gas i in the gas phase. All gas volumes are normalised to STP and relative to

1 litre of groundwater. The equilibrium between the gas phase and dissolved gas is determined by Henry's Law, thus:

$$S_i' = P_i H_i \qquad (2)$$

where P_i is the partial pressure of gas i in the gas phase and H_i is the Henry's Law constant expressed in volumetric terms (Bunsen Coefficient) at the equilibration temperature. The volume of gas i in the gas phase is related to the total gas volume, V, evolved at the equilibrium pressure and temperature, T, by:

$$V_i = P_i V \qquad (3)$$

from which, on converting to STP:

$$V_i = P_i.V.273/T$$

substituting for S_i' and V_i in equation (1) and solving for P_i gives:

$$P_i = \frac{S_i}{H_i + (273.V/T)} \qquad (4)$$

The outgassing model involves inputting a known recharge temperature, contamination index, excess helium content, $^{40}Ar/^{36}Ar$ ratio, and a recharge salinity. From these parameters the respective S_i concentrations are calculated using the solubility data. Oxygen is not included at all in the model on the grounds that dissolved oxygen is usually removed by oxidation processes before the conditions favouring degassing are reached.

A chosen degassing temperature and pressure are input. This enables the Henry's Law constants expressed as Bunsen coefficients to be calculated at the degassing temperature of interest. The values may be modified according to an input final salinity in order to quantify the salting-out effect.

At this point, the gas bubble volume, V, still has to be derived before each of the partial pressures in the bubble can be calculated using equation (4). Carbon dioxide and water vapour are exceptions to this necessity, because their partial pressures can be independently calculated. The final pH and bicarbonate content determines the partial pressure of CO_2 using carbonate equilibria. The water vapour partial pressure is calculated using the Theisen equation where:

$$Ln(P) = 2.303 \times \left[\frac{5.409(t-100) - 0.508 \times 10^{-8}\,[(365-t)^4 - 265^4]}{t + 273.18}\right]$$

where $t = {}^{o}C$.

In order to estimate the gas bubble volume, V, an initial guess at the volume is made which is subsequently modified to the correct value by an iterative method. The major contributions to the gas partial pressures in an evolved gas bubble are those of nitrogen, P_{N_2}, water vapour PH_2O, and possibly hydrocarbons such as methane, PCH_4. The sum of these partial pressures must approximately equal the degassing pressure, P, thus:

$$P \simeq P_{N_2} + PH_2O + PCH_4$$

A guess at the partial pressure of nitrogen, P'_{N_2}, will be given by:

$$P'_{N_2} = \frac{P - PH_2O}{1 + HN}$$

where HN is the ratio of the hydrocarbon to nitrogen partial pressures in the gas phase. This ratio must be included in the data input, but a ratio of 0 still allows $P'N_2$ to be estimated. If the volume of gas evolved from solution is V, and since mass balance requires that $V_i = P_i.V$, then from equations (1), (2) and (3):

$$V' = \frac{S_{N_2} - H_{N_2} \cdot P''_{N_2}}{P'_{N_2}} \qquad (5)$$

This first approximation of the volume V' is used to decide whether or not outgassing can occur. If this estimate is less than 0.0005 cm^3 from 1 litre of water, then degassing is considered not to have occured under the chosen environmental parameters. If degassing is possible, then the partial pressures of each of the gas species (except CO_2 and H_2O) are calculated from the estimated V' using equation (5). If V has been correctly estimated then the sum of all the respective partial pressures for each gas should equal the degassing pressure, i.e.

$$P = \sum P_i$$

Any difference between the actual degassing pressure and the calculated bubble pressure can be used as the basis for correcting V', and the partial pressures can be recalculated. If $\sum P_i < P$, the V' is too large and must be reduced. Similarly, if $\sum P_i > P$, V' is too small and must be increased. In either case the correction applied is:

$$V = V' \cdot \frac{\sum P_i}{P}$$

where V' is the previous value of the gas bubble volume. Successive approximation in this manner is made until good agreement is obtained between the actual and calculated pressure. In practice the summed partial pressures are approximated to within 0.0005 atms of the degassing pressure.

The S_{CH_4} and S_{CO_2} concentrations are back-calculated from knowing V and the respective partial pressures in the bubble by combining equation (1) with (2) to give:

$$S_i = P_i.H_i + V_i$$

The outgassing model essentially calculates the initial gas concentrations, the final gas concentrations, and the composition of an exsolved gas bubble according to input environmental parameters. Respective gas ratios for each phase are consequently readily obtainable.

4.1.2 The OUTGAS computer program

The tabulated chart in Table 31 briefly outlines the procedures involved in the program. The OUTGAS program is listed in Appendix 9. Table 32 illustrates a typical output data from a program run.

Many runs of the program, essentially obtained by placing the input variables in a loop and tabulating selected output data allow construction of graphs such as Fig. 21 and Fig. 22. Fig. 21 shows how, for example, an in-situ N_2/Ar ratio of about 40 will degas to initially produce a small bubble with a N_2/Ar ratio close to air (> 70). As the temperature increases and more degassing occurs the N_2/Ar ratio in the gas phase is markedly depressed. Fig. 22 on the other hand, shows the wellhead pressure required to keep the gases in solution for variable N_2/Ar and CH_4/N_2 compositions dissolved in the groundwater.

Table 31. Summary of OUTGAS program.

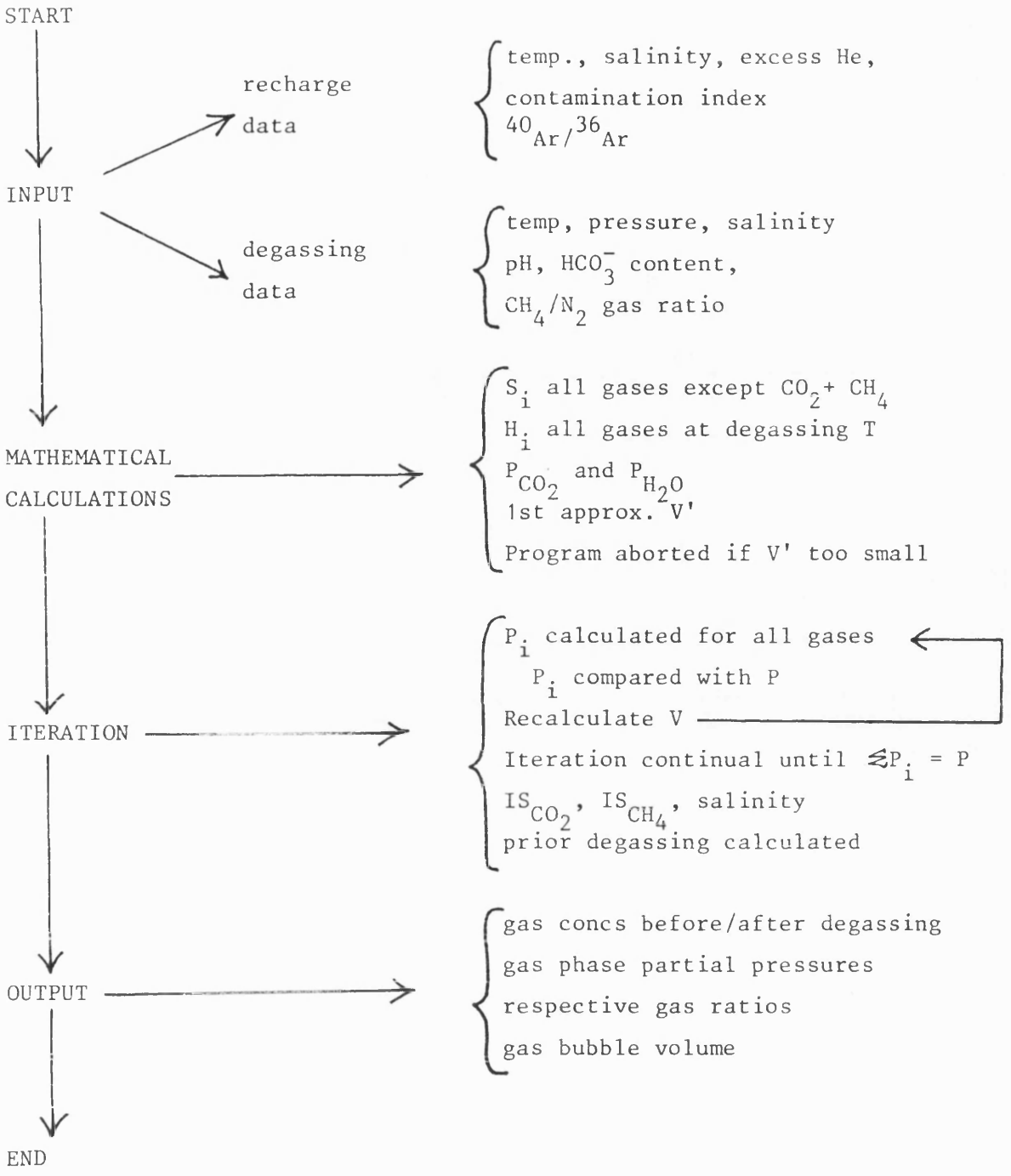

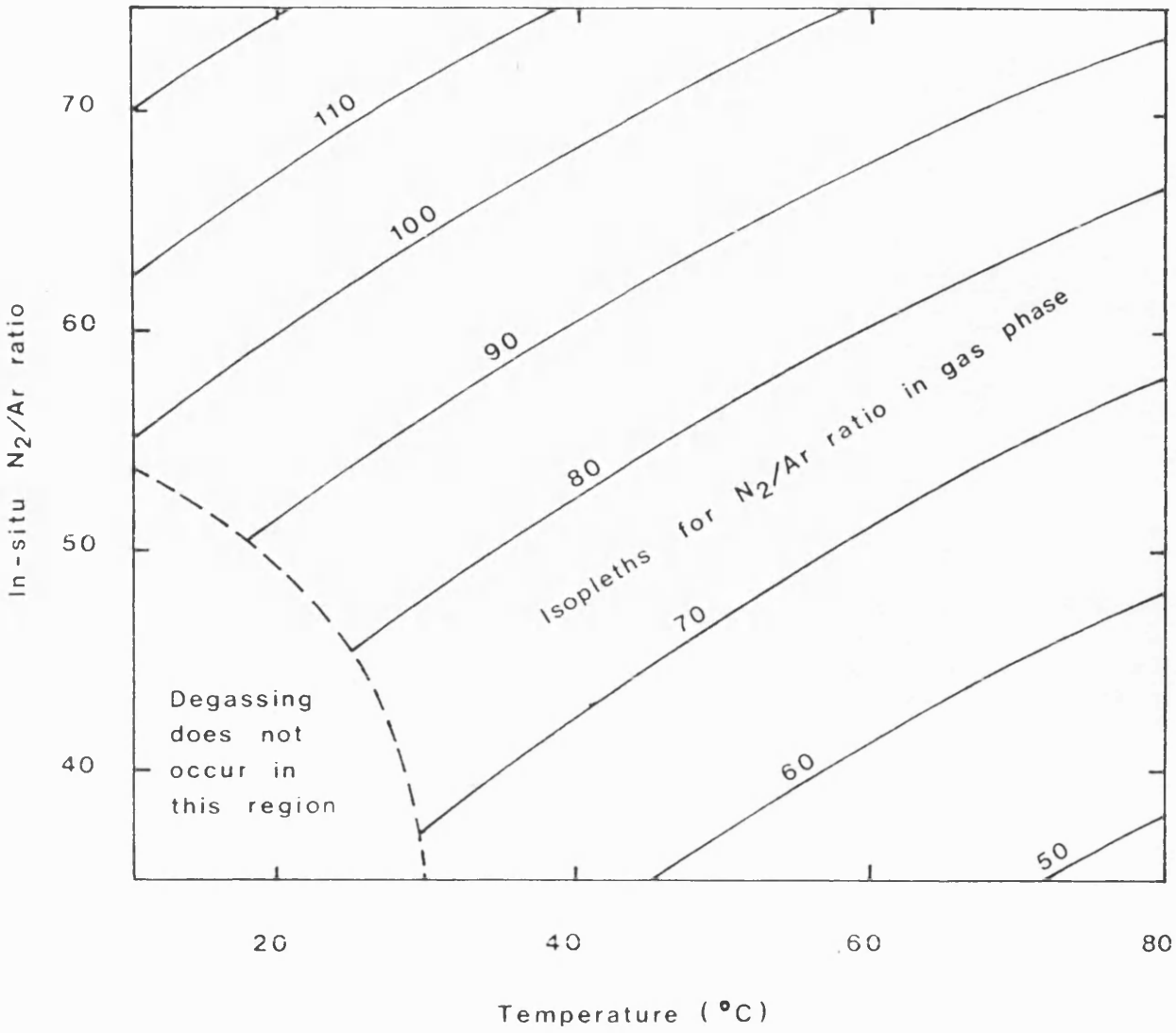

FIG.21 The N_2/Ar ratios in the gas phase and in solution for groundwater degassing at 1bar as a function of temperature. The in-situ gas content of the groundwater was that due to air-equilibration for recharge at 5 °C with excess air equivalent to 10% of the Ne content and a radiogenic He content of 10^{-5} cm^3 STP/cm^3 H_2O. Oxygen which was dissolved at recharge is assumed to have been removed by oxidation processes during groundwater migration. The groundwater HCO_3^- content was 100 mg/l.

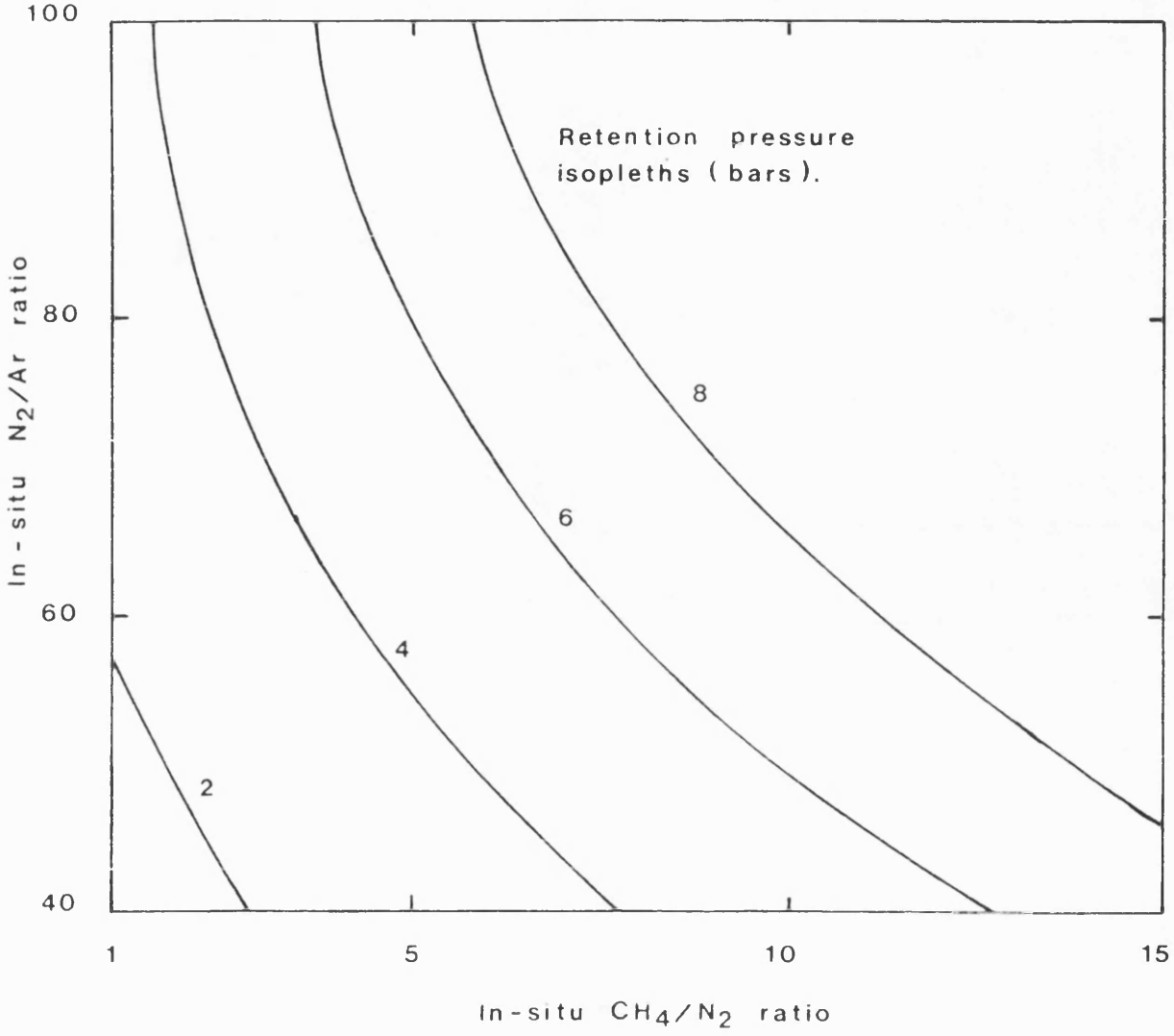

FIG. 22 The hydrostatic pressure necessary to retain gases in solution at 10°C for in-situ N_2/Ar and CH_4/N_2 ratios due to thermogenic production of N_2 and CH_4. Other recharge constraints as for FIG. 21.

Table 32. Example output from the OUTGAS computer program

EXSOLUTION OF GASES

```
RECHARGE TEMP, DEGREE C      :  3
DEGASSING TEMP, DEGREE C     :  20
DEGASSING PRESSURE (ATM)     :  .5
EXTRA AIR CONT. INDEX (NE)   :  1.3
RADIOGENIC HE (*1E8)         :  150
HYDROCARBON/NITROGEN RATIO   :  0
BICARBONATE CONTENT, MG/L    :  200
FLUID PH                     :  7.5
AR-40/AR-36 RATIO = 295.5
```

GAS	GAS PHASE PP.ATM		INITIAL SOLN CM3 STP/CM3		DEGASSED SOLN CM3 STP/CM3	
HE	+ .00004323	+	156.8231	+	38.1383	*1E-8
NE	+ .00000758	+	2.8804	+	.7985	*1E-7
AR	+ .00804818	+	4.9511	+	2.7415	*1E-4
KR	+ .00000131	+	11.8598	+	8.2498	*1E-8
XE	+ .00000012	+	1.7483	+	1.4052	*1E-8
N2	+ .46390835	+	1.9988	+	.7252	*1E-2
CH4	+ .00000000	+	.0000	+	.0000	*1E-2
CO2	+ .00526403	+	.4772	+	.4638	*1E-2
H2O	+ .02310616					

```
1ST. GAS VOL. APPROXIMATION (CM3)          :  26.2810098

VOL. GAS EVOLVED FROM 1L WATER (CM3)       :  29.4641739
VOL. GAS AT STP (CM3)                      :  13.7271011
VOL. GAS CORRECTED FOR VP (STP CM3)        :  13.0927398

GAS CONC. PRIOR DEGASSING (STP CM3/L)      :  25.258049
GAS CONC. AFTER DEGASSING (STP CM3/L)      :  12.1653092

WATER/GAS VOL. RATIO (DEGASSING T + P)     :  33.9395228
```

	N2/AR	HE/NE	KR/XE	CH4/N2
INITIAL SOLN.	40.372	5.444	6.783	.000
DEGASSED SOLN.	26.453	4.776	5.870	.000
GAS PHASE	57.641	5.700	10.520	.000

4.2 The Nottinghamshire Triassic Sandstone aquifer

4.2.1 Hydrochemical characteristics of the groundwaters

The distribution of field measurements including % dissolved O_2, Eh, pH and also the measured NO_3 concentrations across the aquifer are shown in Fig. 23. This data is plotted against groundwater temperature since this is an effective measurement of distance from the recharge source at outcrop. A detailed analysis of the distribution of these values is given in chapter 1 and elsewhere (e.g. Edmunds et al., 1982). this data will therefore only be discussed with reference to the potential for nitrate denitrification in this aquifer.

The nitrate, dissolved O_2 and Eh measurements all show an abrupt drop at apparently the same point in the aquifer. This could be interpreted as indicating that beyond the redox boundary the reduction of NO_3 is occuring. There are a number of arguments against this. Firstly, denitrification requires an organic carbon source necessary to support an active population of denitrifying bacteria. However measurements on the amount of total dissolved organic carbon within the groundwaters show that the waters are basically devoid of any organic carbon. Secondly, the drop in nitrate concentration at the redox boundary may only be coincidental, because the eastern older groundwaters reflect pre-modern recharge when nitrate inputs to the aquifer would have been very small. (Bath et al., 1978).

One possibility is that the nitrate 'disappearance' reflects the inorganic reduction of nitrate at the redox boundary. For example, the critical Eh for the NO_3^-/NO_2^- couple (i.e. where they are present in equivalent activities) is +421mV under ideal conditions at pH 7 and 25°C (Focht, 1978). So reduced species of nitrogen could well be present. The Eh for reduction of N_2O to N_2 appears to be about +250 mV at pH 7, so

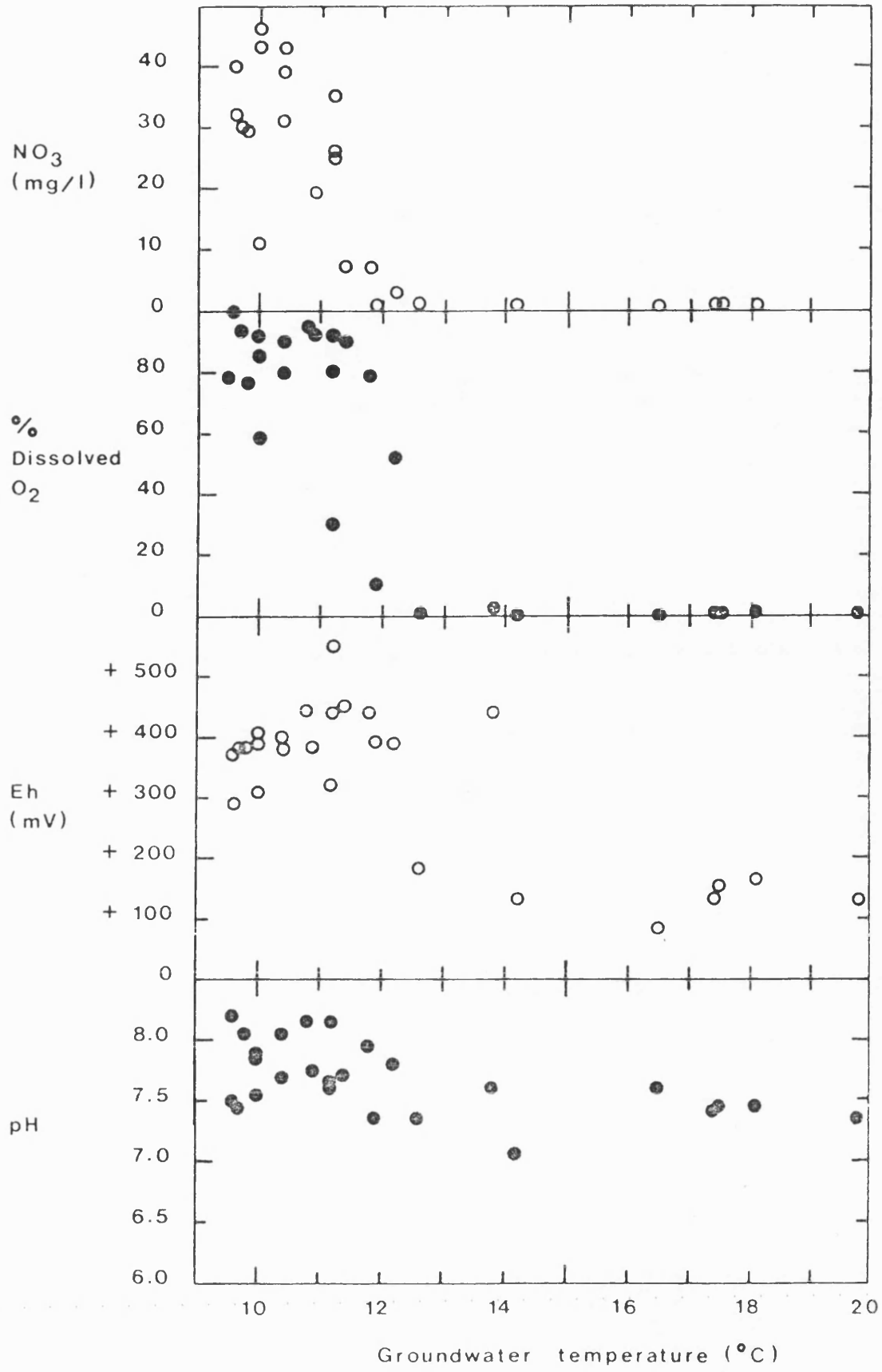

FIG.23 Downgradient variation in chemical measurements from the Nottinghamshire Triassic groundwaters.

those groundwaters with an Eh less than +250 mV could contain some N_2. The theoretical considerations do not however, match with practice. These groundwaters contain very little nitrogen species other than nitrates, probably because such equilibrium reactions involving nitrogen are so sluggish as to be almost inapplicable in practice.

From these considerations, an 'in-situ' denitrification process within the Nottinghamshire Triassic groundwaters would seem unlikely, principally because of the lack of an available organic carbon source. The outcrop sites however, being much younger waters with more variable pollutants present, could produce conditions amicable to denitrification. The presence of dissolved O_2 does not preclude this possibility, providing O_2 levels do not exceed some 10% of the saturation capacity.

4.2.2 Palaeoclimatic conditions for groundwater recharge.

The δ^2H and $\delta^{18}O$ values for groundwaters from the Nottinghamshire sites are plotted on a conventional δ-diagram in Fig. 24. The data clusters into two groups, verifying the work of Bath et al., (1978) who explained the grouping as reflecting a climatic change as Britain emerged from the last Ice Age. The older, more isotopically depleted groundwaters condensed as rain under colder climatic conditions than the younger groundwater samples. They explain the two-fold grouping as reflecting inhibited recharge during discontinuous permafrost cover.

The data differs from Dansgaard's Worldwide Precipitation Line ($\delta^2H = 8\,\delta^{18}O + 10$) in having a regression defined by:

$$\delta^2H = 7.1\,\delta^{18}O + 2.3$$

with a correlation coefficient of +0.89. Evans et al. (1978) have studied

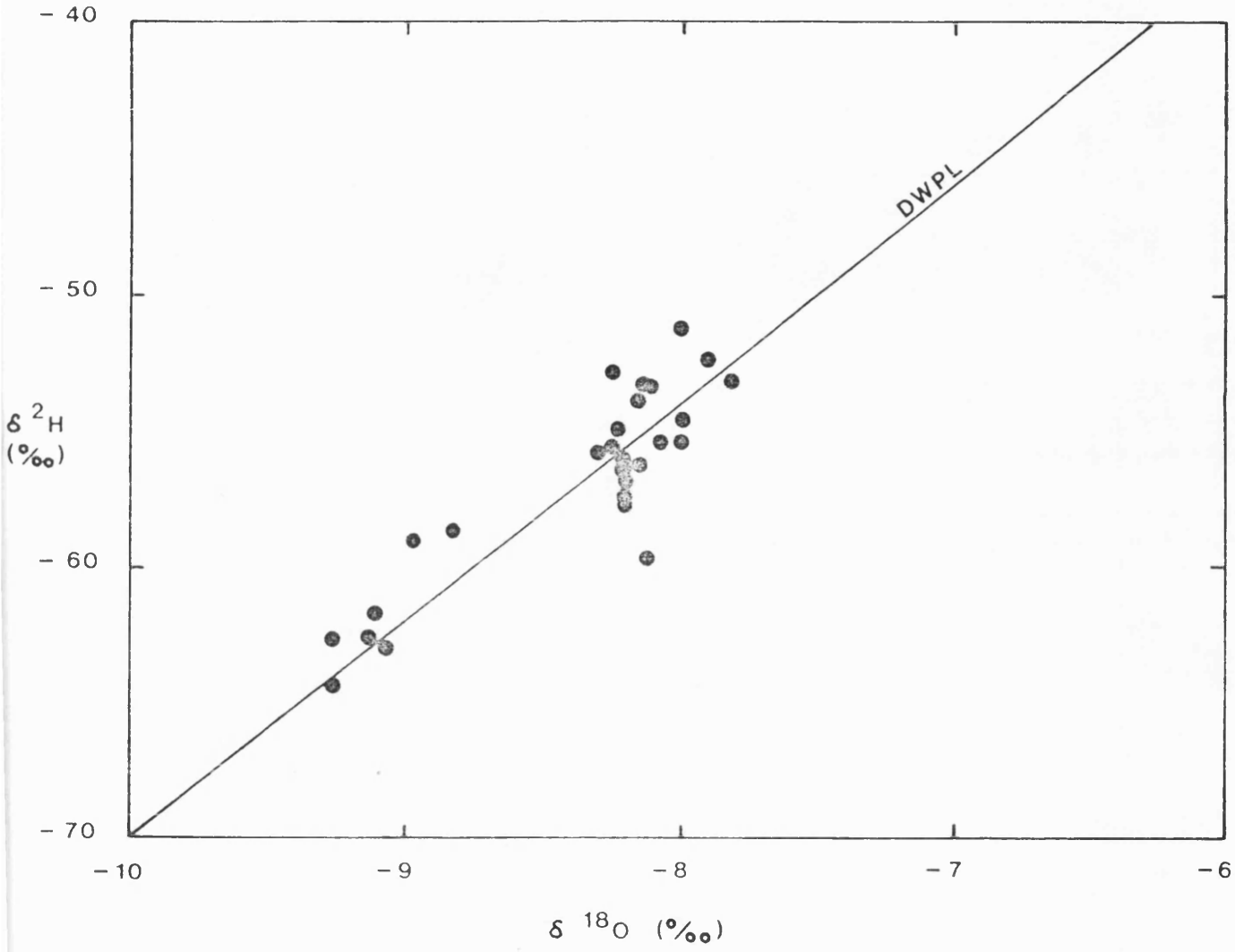

FIG. 24 Correlation of Oxygen and Hydrogen isotope measurements on the Nottinghamshire Triassic Sandstone groundwaters.
D WPL = Dansgaard's Worldwide Precipitation Line.

the isotopic composition of precipitation collected from Maritime European Stations. Their data suggests that the best representation for recent rainfall over Britain is given by the equation:

$\delta^2H = 6.9\ \delta^{18}O - 0.3$, and the data in this work is very close to this line.

Bath et al. (1978), have determined the carbon-14 ages of selected sites in the aquifer and the isotopically lightest waters correlate with the oldest sites. Table 33 lists the C-14 ages for selected sites within the aquifer. The fact that the oldest waters correlate with the lightest precipitations is to be expected since this reflects the colder climate of the Late Devensian.

The isotopic 'gap' in $\delta^{18}O$ between the two groups is of the order of $1^o/oo$. Taking Dansgaard's relationship:

$$\frac{\Delta\ \delta^{18}O}{\Delta\ T} = 0.7^o/oo\ {}^oC^{-1}$$

a temperature change in cloud condensation (Δ T) of $1\text{-}2^oC$ is indicated over the time scale involved.

It is interesting at this point to compare the noble gas recharge temperature information for the Nottinghamshire Triassic. Fig. 25 shows a plot of recharge temperature vs. $\delta^{18}O$ for the sites and it is immediately noticeable that a temperature difference of some $5 - 6^oC$ is implied. Only the most recent grouping of data falls on Dansgaard's temperature - dependence line $\delta^{18}O = 0.69T - 13.6^o/oo$.

The apparent discrepancy between recharge temperature and $\delta^{18}O$ data probably arises because the data may reflect two different types of temperature change. Noble gas concentrations are fixed according to the surface air temperature and atmospheric pressure, and it is not

Table 33. Carbon-14 ages for groundwaters from the Nottinghamshire Triassic Sandstone.

Site No.	Site	Age (yrs B.P.)	+/-
NT01	Rampton	34,550	1550
NT02	Markham Clinton	5,150	1650
NT03	Ompton	850	1350
NT04	Halam	2,900	1400
NT05	Far Baulker	-1,250	1350
NT06	Newark	26,400	1500
NT07	Gainsborough	31,750	1950
NT08	Grove	8,950	1650
NT09	Newton	26,850	1150
NT13	Everton	1,250	1450
NT14	Eklesley	-1,575	1625
NT16	Boughton	-100	1500
NT17	Amen Corner	-100	1700
NT19	Rufford	1,550	1350
NT20	Caunton	7,350	1550
NT22	Farnsfield	750	1350

Data from Bath et al. (1979).

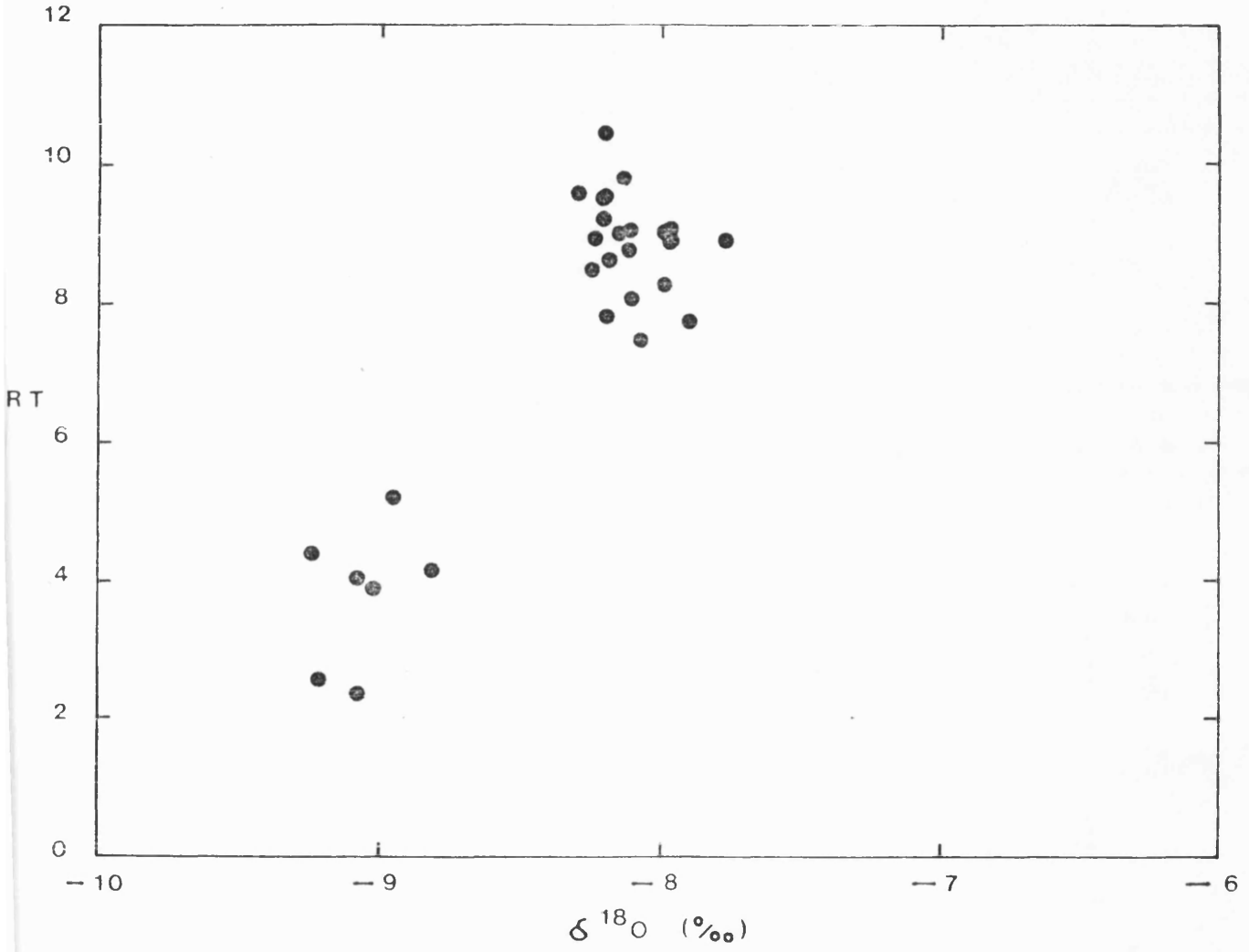

FIG. 25 Correlation between oxygen isotope and recharge temperature measurements on groundwaters from the Nottinghamshire Triassic Sandstone.

RT = Recharge Temperature.

inconceivable that over the time scale involved annual mean air surface temperatures warmed by some 5 - 6°C whilst the temperature of cloud condensation only warmed some 1 - 2°C. This is possible because surface air and cloud air can be regarded as independent systems with different sources.

All the sites contain some extra air dissolved in the water due to entrainment of bubbles trapped in the interstices of the soil or rock as the water percolated downwards. Fig. 26 plots the contamination indices of those sites against the corresponding available C-14 ages of the water.

It is apparent that there is a crude inverse correlation between the amount of extra air dissolved in the water and the recharge temperature. In other words, the older waters apparently contain more extra air. This might be due to an increase in the viscosity of water at lower temperatures, hence enabling the recharging water to entrain larger bubbles and prevent smaller ones escaping surfacewards quite so easily.

Alternatively the trend may reflect the mode of recharge. The soil and rock structure including respective pore and fracture porosities, grain shape and size may be important. For example, the melting of permafrost might result in an initial release of fracture-filled ice, and only later would interstitial pore ice melt and release their waters. Any fractionation effects during initial trapping of the waters could be expressed in the subsequent melting.

4.2.3 Nitrogen isotope data on the nitrates dissolved in the groundwaters.

A wide variation in $\delta^{15}N$ (NO_3) values is recorded from the sampled sites with values as high as +31.1°/oo at Clipstone and -15.7°/oo at

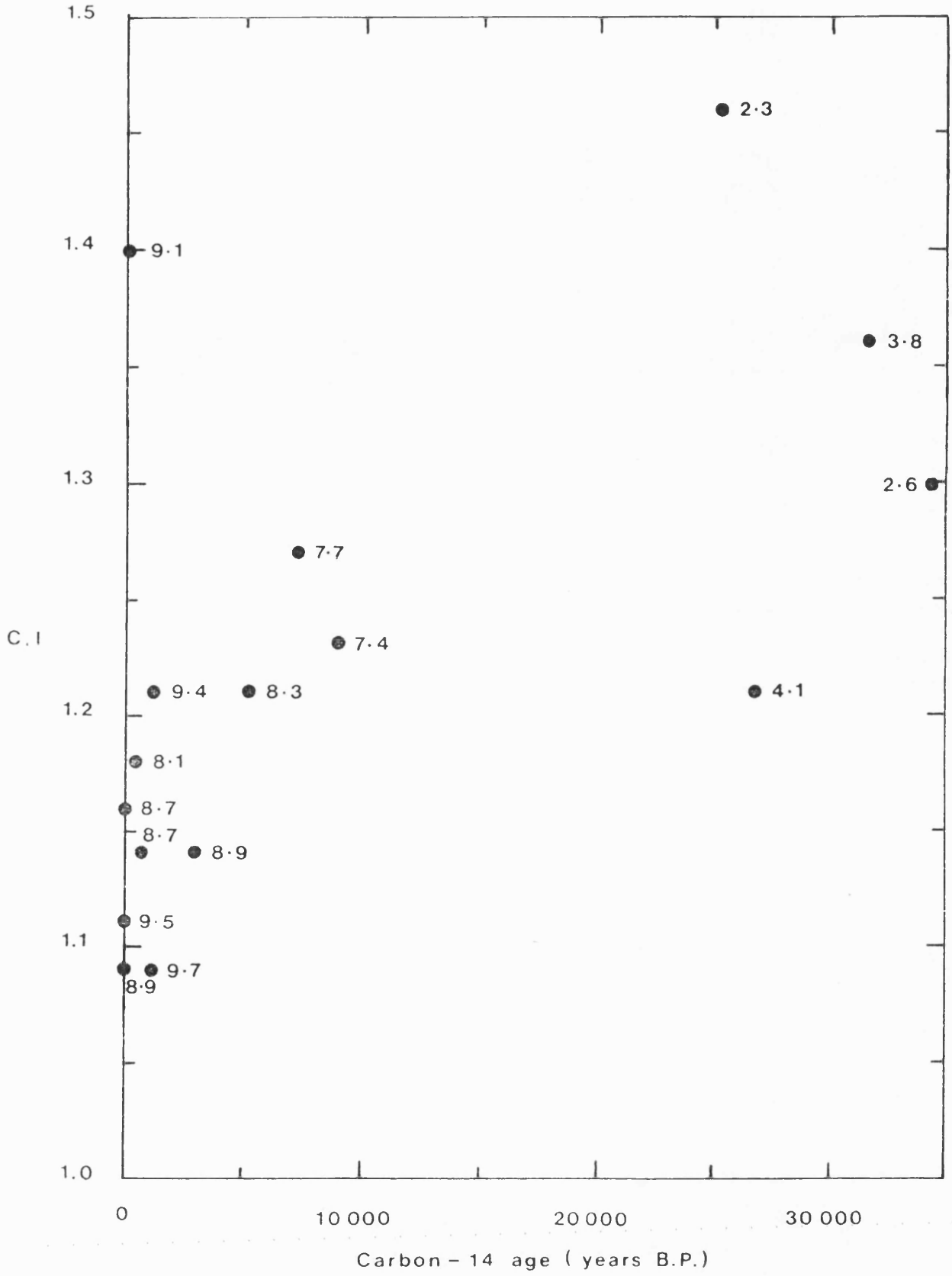

FIG. 26 Age vs. Extra Air component in groundwaters from the Nottinghamshire Triassic sandstone.

C.I. = Contamination Index.
Numbers by sample points refer to recharge temperature (°C).

Halam. The important consideration in any interpretation of these values is to determine to what extent they are a function of different source compositions, and to what extent they have been subsequently modified by other processes such as denitrification.

Fig. 27 illustrates the geographical distribution of the data in relation to land use, namely urban, forest, and agricultural use. Fig. 28 shows the same data plotted against the NO_3 concentration. This particular type of graph can be useful in determining the problem of different source composition vs. source modification. If a nitrate source is isotopically homogeneous with a constant input supply, samples would plot as a point-cluster on the graph. If the source is isotopically homogenous but the input concentration varies, a horizontal plot of data would result. Should nitrates of isotopically different sources but having a constant input concentration be plotted, a vertical line would result. A process such as denitrification would alter both the isotopic composition and the input concentration, producing some sort of trend line on the graph.

It is immediately apparent that three sites in particular are isotopically very heavy: Clipstone (NT18), Rainworth (NT21), and Farnsfield (NT22). These sites correlate with high nitrate concentrations and are geographically located in urban areas. These urban districts include New Clipstone (a suburb of Mansfield) and the townships of Rainworth and Farnsfield respectively. The $\delta^{15}N$ (NO_3) values are +31.1, +28.3 and +22.7 $^{o}/_{oo}$ for each of these sites, with nitrate concentrations of 39.7, 28.7 and 45.8 mg/l respectively. The most probable interpretation of these values is that the nitrates reflect human pollution via leakage of waste from old urban sewer systems. The enrichment in ^{15}N and the correlation of $\delta^{15}N$ with urban areas is

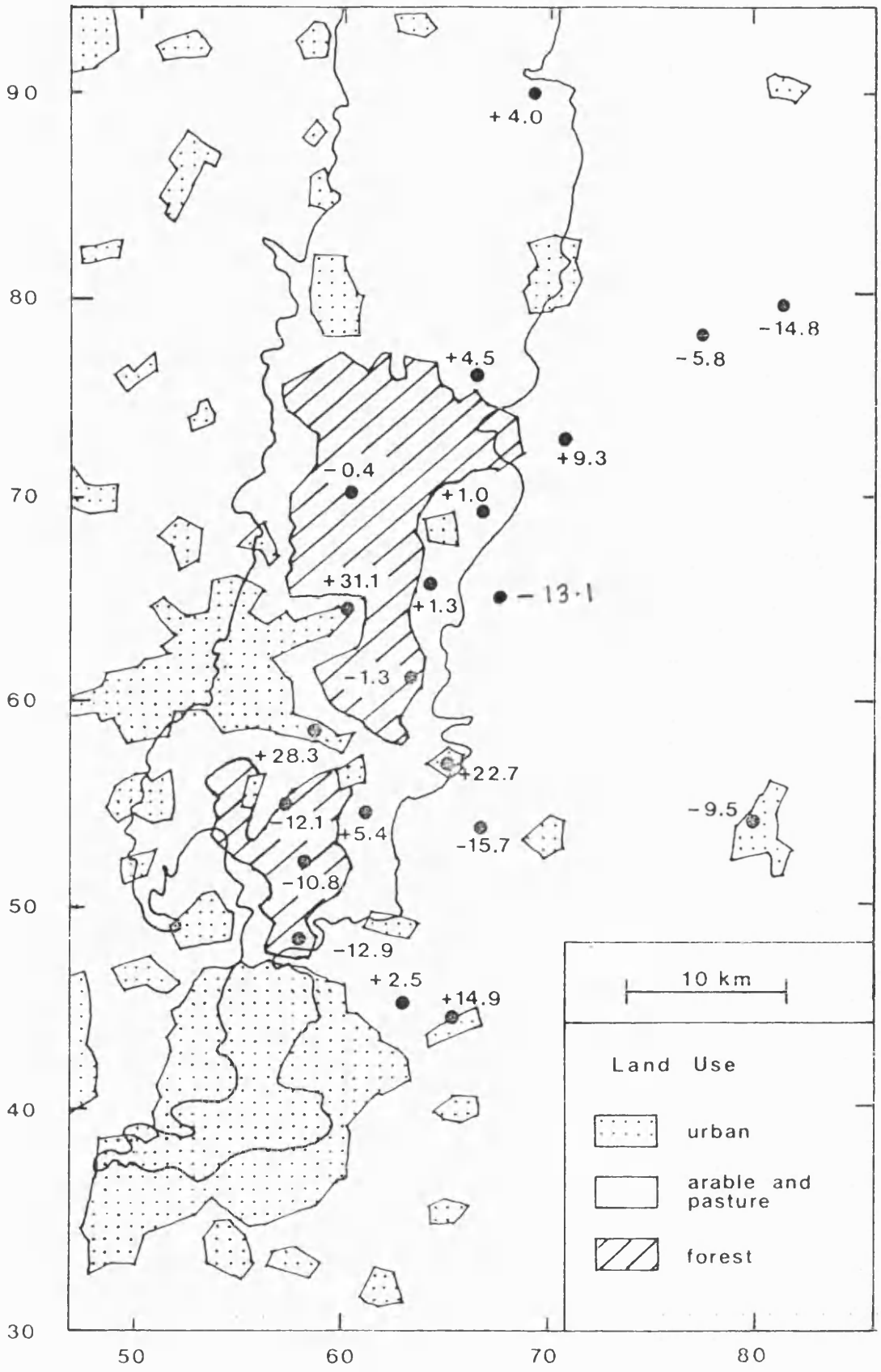

FIG. 27 Geographical distribution of $\delta^{15}N\ (NO_3^-)$ Nottinghamshire Triassic data and land use.

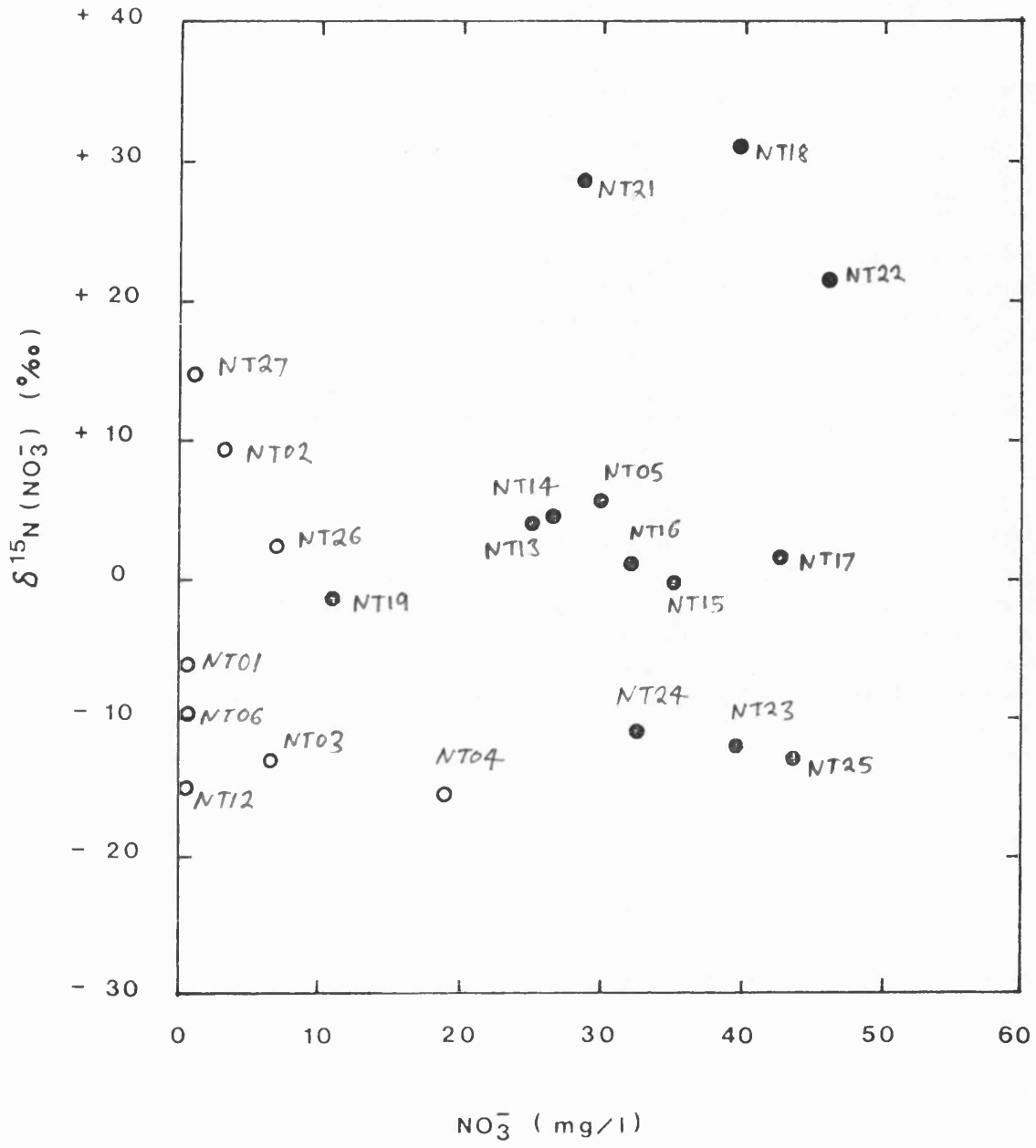

FIG.28 Isotopic composition vs. concentration of dissolved nitrates in groundwaters from the Nottinghamshire Triassic sandstone.

- ○ Confined sites.
- ◉ Unconfined (outcrop) sites.

typical evidence for this. As an approximation, the outcrop urban sites reflect human pollution producing point-source nitrate inputs of about 38 mg/l, $\delta^{15}N\ (NO_3) = +27^{o}/oo$.

Two other sites, Burton Joyce (NT27) and Newark (NT06) also lie on urban areas. They have lower $\delta^{15}N\ (NO_3)$ values (+14.9 and -9.5 $^{o}/oo$ respectively), and much lower nitrate concentrations (< 2 mg/l respectively). The difference between these two sites and the other urban sites probably arises because these sites lie within the confined part of the aquifer, hence drawing water from a much deeper source. Burton Joyce is lined to 57m and Newark to 63m, and it is unlikely that any sewage leaks (if present) near these two sites would percolate down through the impermeable cover. The river Trent, which drains the area, is probably the local destination of any polluting sewage nitrates rather than the underlying aquifer. The nitrate sources of Burton Joyce and Newark are therefore probably quite different from the urban outcrop sources.

An apparent grouping of six values is observed between 0 and $+5^{o}/oo$ $\delta^{15}N\ (NO_3)$ (Fig. 28). These sites are Far Baulker (NT05), Everton (NT13), Elkesley (NT14), Budby (NT15), Boughton (NT16), and Amen Corner (NT17). All these sites are outcrop sites and lie down the eastern side of the outcrop recharge region. They have varying nitrate concentrations between 25 and 45 mg/l suggesting variable nitrate inputs from a single homogenous isotopic source (within $5^{o}/oo$, mean = $+2.3^{o}/oo$). Such $\delta^{15}N(NO_3)$ values are typical of cultivated agricultural land and soil nitrates. Such values, coupled with the relatively high nitrate concentrations suggests these nitrates reflect fertiliser inputs from agricultural farming practice. The application of fertilisers will be variable and this may explain the horizontal spread of this grouped data

in Fig. 28.

If a process such as denitrification is occuring in a number of sites across the aquifer, then both the isotopic composition and the input concentration of the nitrate will be altered. The change in the residual nitrate should obey a Rayleigh fractionation relationship, i.e.:

$$\varepsilon \text{Lnf} = 10^3 . \text{Ln}\left[\frac{10^{-3}\,\delta s + 1}{10^{-3}\,\delta s,o + 1}\right] \qquad (6)$$

where $\delta s,o$ is the original nitrogen isotope composition of the nitrate, and δs is the subsequent composition of the fraction of nitrate remaining, f. ε is the isotope enrichment factor, in per mille. Using the approximation:

$$\delta s = \delta s,o + \varepsilon \text{Lnf} \qquad (7)$$

curves are plotted for different initial isotopic compositions of NO_3 for different $\delta s,o$ values.(Fig. 29). It can be seen that the more negative the enrichment factor, the greater the displacement of the residual nitrate to heavier compositions.

Referring again to Fig. 28, seven sites are consistent with such a trend. Burton Joyce (NT27), Markham Clinton (NT02), Lambley (NT26), and Rufford (NT19) have $\delta^{15}N\ (NO_3)$ values which could have been derived via denitrification from the high NO_3 sites of Papplewick (NT24), Fishpool (NT23) and Bestwood (NT25). This data indicates that at high nitrate concentrations in outcrop waters, the NO_3 is isotopically light (Bestwood, NO_3 = 44 mg/l, $\delta^{15}N\ (NO_3) = -12.9^{o}/oo$). As the groundwater passes into the confined part of the aquifer, the nitrate concentration falls and the $\delta^{15}N\ (NO_3)$ becomes more positive (Burton Joyce, NO_3 = 1.1

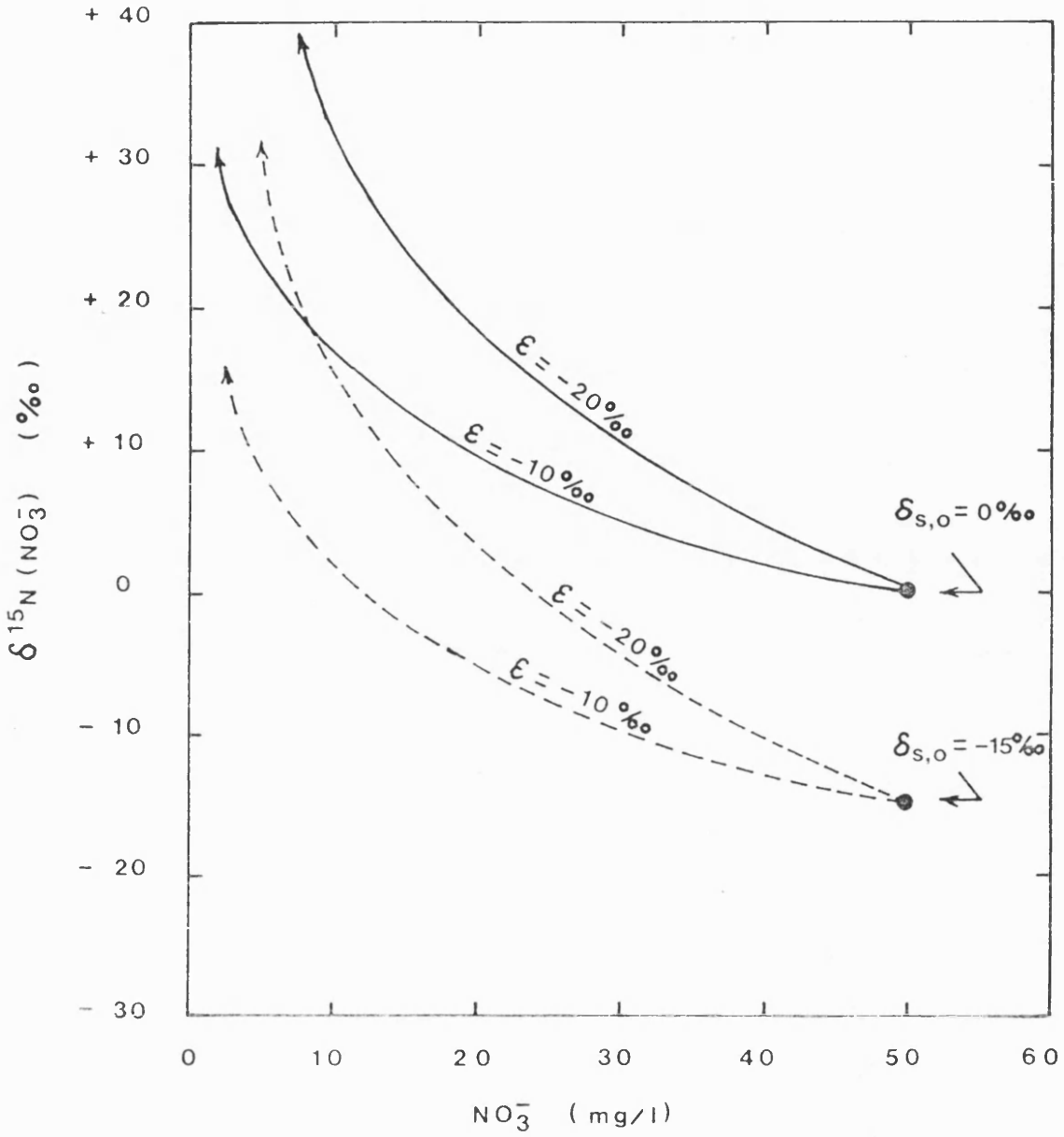

FIG. 29 Theoretical changes in nitrate composition and concentration from the denitrification of 50 mg/l NO_3^- at two $\delta^{15}N$ starting compositions, $\delta_{s,o}$. The trends are dependent on the enrichment factors (ε), shown at −20‰ and −10‰ for each example.

mg/l; $\delta^{15}N\ (NO_3) = +14.9^{o}/oo$). If this is a denitrification trend, an initial nitrate source which is isotopically very light is implied.

The enrichment factor, ε, of the seven sites can be derived by plotting Lnf against the right-hand side of equation (6). This should produce a straight line, the slope of which is equal to ε. $\delta s,o$ must be lighter or as light as the most negative $\delta^{15}N\ (NO_3)$ value observed in the group, so a value of $12.9^{o}/oo$ (Bestwood) will be used. Values of f cannot be known with certainty because the original nitrate concentration of these sites is not known. However, the original concentration must be greater than or equal to the highest observed NO_3 concentration, and so the value for the Bestwood site will again be used (NO_3 = 43.3 mg/l). The f value for each site is then subsequently the observed nitrate concentration as a fraction of this assumed starting concentration. These assumptions ensure that Bestwood will plot at the origin of the graph. If $\delta s,o$ and the estimated initial nitrate input are in error, then this in fact makes no difference to the slope of the graph and therefore no difference to the estimate of ε. Such errors would only displace the position of the line vertically or horizontally.

Table 34 lists the calculated paramters which have been used to plot Fig. 30. Table 34 also lists the ε values estimated for each site, which gives a mean ε of -8.0 +/- $0.5^{o}/oo$ (+/- standard deviation). The fitted regression line to the data (least squares method) is a more accurate approach, giving an ε value of $-7.8^{o}/oo$ +/- $0.5^{o}/oo$ (estimated standard error). The correlation coefficient for this line is -0.998, the equation being y = -7.8 Lnf + 0.3. The constant term in the equation (0.3) has an estimated standard error of +/- 0.2, and so the line can be assumed to pass through the origin.

The inversely correlated $\delta^{15}N\ (NO_3)$ vs NO_3 concentration data

Table 34. Denitrification enrichment factors from the nitrate-nitrogen isotope data, Nottinghamshire Triassic groundwaters.

Site No.	$10^3.\mathrm{Ln}\left[\frac{10^{-3}\ s + 1}{10^{-3}\ s,o + 1}\right]$	f	Lnf	ϵ
NT02	+22.2	0.07	-2.70	-8.2
NT19	+11.7	0.25	-1.38	-8.5
NT23	+ 0.8	0.91	-0.10	-8.0
NT24	+ 2.1	0.75	-0.29	-7.2
NT25	0.0	1.00	0.0	-
NT26	+15.5	0.16	-1.84	-8.4
NT27	+27.8	0.03	-3.67	-7.6

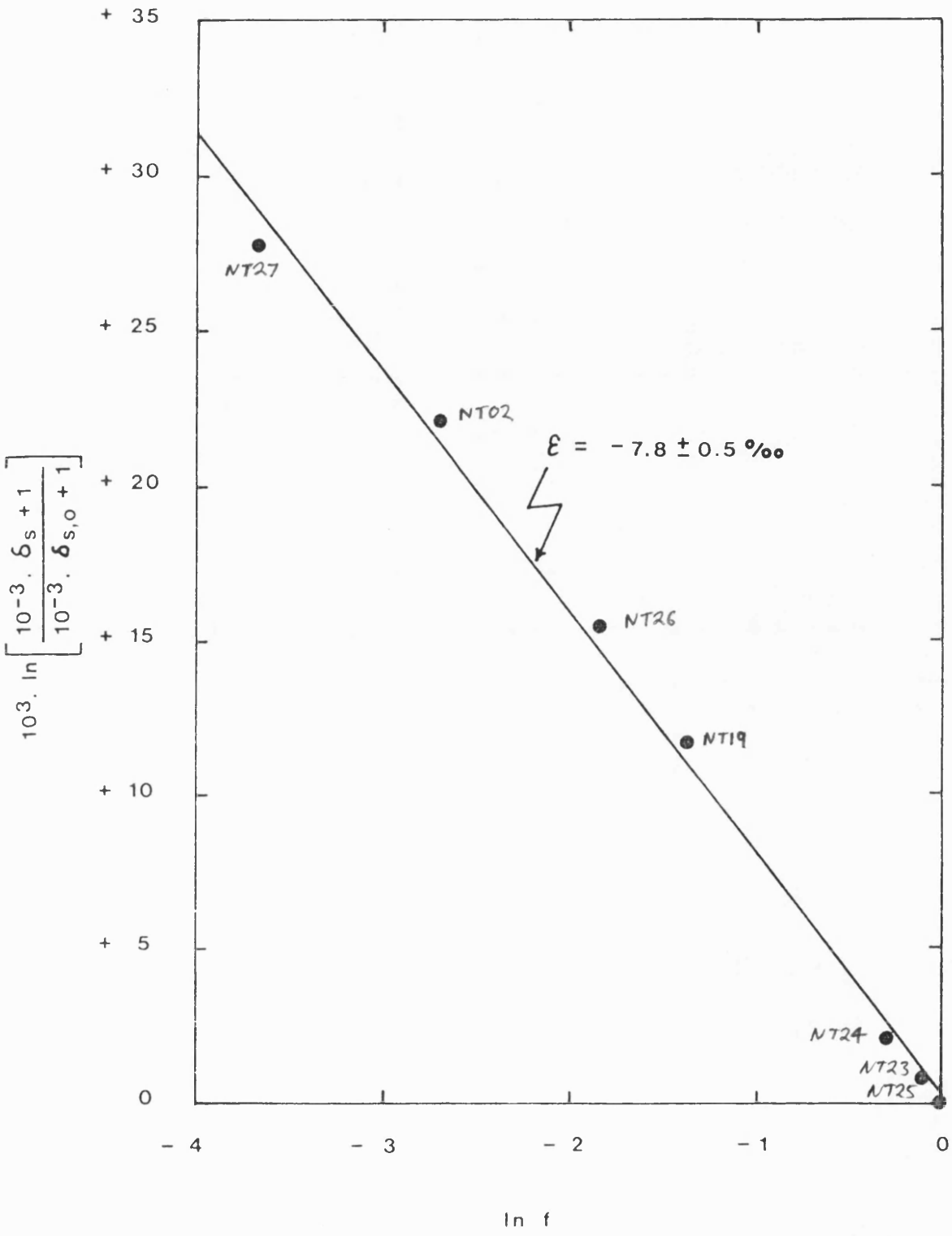

FIG. 30 Enrichment factor estimation on groundwater nitrates from the Nottinghamshire Triassic sandstone, using the $\delta^{15}N(NO_3^-)$ data listed in Table 34.

ε enrichment factor
f fraction of nitrate remaining
δ_s observed $\delta^{15}N(NO_3^-)$
$\delta_{s,o}$ initial $\delta^{15}N(NO_3^-)$ before denitrification

which reflect a dentrification trend give an ε value which is rather lower than most other literature quoted values which commonly lie between -20 and -40^{o}/oo. These sites together lie in a line across the unconfined/confined aquifer to the south of the sampled area just north of Nottingham, with the exception of Markham Clinton.

It is not possible at this stage to identify an 'in-situ' denitrification process in the aquifer because these values may be some sort of inherited isotopic distribution from dentrification in the soil zone. The quantity and isotopic composition of the dissolved nitrogen gas in these waters may aid such interpretation, the discussion of which is given in the next section.

It is however, interesting to speculate why these sites might reflect a dentrification trend whilst the other sites do not. Fig. 27 shows the three outcrop sites in question to lie in densely wooded land areas. It may be that forested land and its associated soil ecosystem is more conducive to denitrification of nitrate and its subsequent release to groundwater. The apparent increasing trend of denitrification into the aquifer suggested by these sites may be coincidental if soil denitrification is responsible.

The rather low ε value, -7.8^{o}/oo, is not inconsistent with any of these ideas, since ε is a function of the reaction rates of the denitrification process. Mariotti, et al. (1982) studied the effects of temperature on the denitrification reaction rates and observed that the greatest enrichment was obtained at lower temperatures and hence lower reaction rate. Conversely, for high rates of dentrification at higher temperatures inducing greater reaction rates, the ε value is smaller. In the particular experiment by Mariotti et al. (1982) ε values as low as -11^{o}/oo were observed. If these observations are applied to the

present data then it would imply a fairly rapid denitrification process.

Since the regression line passes essentially through the origin of the graph in Fig. 30 the estimation of the initial nitrate concentration and its isotopic composition using the data for Bestwood suggests that these values are indeed very close to the actual initial nitrate and $\delta s,o$ compositions. This implies that of the total fertiliser applied to agricultural land in the Nottinghamshire area, the unutilised nitrate excess produces a nitrate concentration in the immediate vicinity of the underlying groundwater of some 45 mg/l NO_3. This initial excess NO_3 is isotopically light, having a $\delta^{15}N(NO_3)$ value of about -13°/oo. By implication, the conditions beneath forested land would have to favour production of these high nitrate quantities which are isotopically light.

Since the necessary precurser to nitrate is ammonia from natural fixation processes, the subsequent nitrification of NH_4^+ could well produce isotopically light nitrates. Although a high initial nitrate production is necessary in this concept, the extent to which it is denitrified in the soil zone will control the observed NO_3 concentration subsequently admitted to the groundwater. This may make interpretation of observed NO_3 concentrations from the unsaturated/saturated zone interface in the soil difficult to interpret, since the actual levels of NO_3 could be high or low. This emphasises the importance of gaining additional information from the natural occurence of NO_3 and $\delta^{15}N$ (NO_3) from the environment, not least the dissolved N_2 gas components in the groundwaters.

The remaining sites have very low nitrate concentrations and are isotopically light. Rampton (NT01), Newark (NT06), Cottam (NT12), Halam (NT04) and Ompton (NT03) all have $\delta^{15}N$ (NO_3) values < -5.0°/oo. The nitrate concentrations are close to zero in these sites except for Halam

and Ompton (18.9 and 6.5 mg/l respectively). These sites are essentially old waters. Halam and Ompton which lie within the confined zone have C-14 ages of about 2900 and 850 yrs B.P. respectively. These two sites, although pre-agricultural revolution, are not apparently 'pre-modern' to the same extent as, say, Rampton is. The nitrate content of Halam and Ompton may be a relic of an ancient agricultural land practice in the recharge area. Of course the possibility of mixing of different age sources of groundwaters makes such postulations difficult to verify. The data however, clearly shows that the old groundwaters which contain nitrates are isotopically light ($\delta^{15}N\ (NO_3)$ = -5.8 to -15.7°/oo).

4.2.4 The Nitrogen-gas dissolved in the groundwaters

Of the total dissolved nitrogen gas in a groundwater, three components can be recognised. Firstly, there is a component due to water equilibration with the atmosphere (WEA), and is temperature dependant with a N_2/Ar ratio in freshwater of about 37:1. The second component is the extra air source (EA). Since air is characterised by a N_2/Ar ratio of about 84, the effect of extra air entrainment is to increase the dissolved N_2/Ar ratio. The third component contributing to the dissolved N_2 is an excess component potentially due to denitrification, (D). This will be dependent upon the quantity of nitrate available for denitrification, and involves no further atmospheric inputs, so further increasing the N_2/Ar ratio as well as the absolute concentration of N_2.

It is possible to calculate the concentrations of the N_2 components in detail for each sample. An example calculation is given in Appendix 10. This information is obtained from the noble gas data and the measured N_2/Ar ratios. Since the recharge temperature for each site is known, the corresponding WEA concentration is readily available from

the solubility data. The contamination index, based on neon, gives the amount of extra neon dissolved in the water above that from atmospheric equilibration. Multiplying this extra neon component by the proportion to which neon occurs with nitrogen in air (42920.8) provides an estimate of the extra air nitrogen dissolved in the water. The component potentially due to denitrification is obtained by the difference between the sum of the WEA and EA calculated N_2 concentrations and the measured N_2 concentration. The measured N_2 concentration is obtained by multiplying the calculated Ar concentration by the analytically determined N_2/Ar ratio. The results of such calculations are listed in Table 35. For comparison, the measured N_2/Ar ratios are listed alongside the predicted N_2/Ar ratio based on recharge and extra air inputs. Any difference between the two is potentially due to denitrification. The error on the % denitrified component is a function of the error range on the N_2/Ar ratio and the standard deviation on the recharge temperature.

The calculation of these N_2 components allows an estimate of the isotopic composition of the dentrified excess to be derived. The $\delta^{15}N$ measurement of the dissolved N_2 gas is a function of the delta value of the three N_2 components and their relative proportions. The measured $\delta^{15}N$ is thus a mixed product of these components, i.e.

$$\delta^{15}N_{MIX} = \delta^{15}N_{WEA}.f_{WEA}. + \delta^{15}N_{EA}.f_{EA} + \delta^{15}N_{D}.f_{D}$$

where $\delta^{15}N_{MIX}$ is the measured sample value and $\delta^{15}N_{WEA}$, $\delta^{15}N_{EA}$ and $\delta^{15}N_{D}$ are the respective $\delta^{15}N$ values of the three dissolved N_2 components. f_{WEA}, f_{EA} and f_{D} are their respective fractions. Nitrogen gas dissolved in atmospherically equilibrated water produces a small isotope fractionation effect with the dissolved N_2 being slightly

Table 35. Derived N_2 components for groundwaters from the Nottinghamshire Triassic Sandstone

Sample Number	1. N_2/Ar	2. N_2/Ar	Total N_2 (cm^3/cm^3 $H_2O \times 10^{-2}$)	%N_2 WEA	EA	D	error
NT01	41.5	40.4	2.075	83	14	3	2
NT02	42.1	40.0	1.798	84	11	5	1
NT03	42.8	39.7	1.822	84	9	7	3
NT04	41.4	39.3	1.713	88	7	5	2
NT05	40.8	38.7	1.667	90	5	5	1
NT06	43.3	41.8	2.261	77	20	3	1
NT07	42.6	41.1	2.096	80	16	4	1
NT08	42.3	40.1	1.853	84	11	5	2
NT09	42.1	39.6	1.985	84	10	6	1
NT10	42.2	39.9	2.009	83	11	6	2
NT11	42.2	39.9	1.995	83	11	6	1
NT12	41.5	40.0	1.919	85	12	3	2
NT13	46.5	38.8	1.862	79	4	17	2
NT14	41.8	42.1	1.838	81	19	0	1
NT15	41.6	39.7	1.775	86	9	5	2
NT16	41.0	39.5	1.713	88	8	4	1
NT17	40.5	39.0	1.641	90	6	4	3
NT18	42.2	39.1	1.737	86	6	8	1
NT19	46.7	40.1	1.946	76	10	14	2
NT20	45.2	40.6	1.986	78	12	10	3
NT21	40.9	40.6	1.745	86	13	0	0
NT22	42.0	39.3	1.746	86	7	7	1
NT23	43.6	39.6	1.835	83	8	9	6
NT24	42.5	41.9	1.848	81	18	1	0
NT25	42.5	41.5	1.846	81	17	2	1
NT26	42.4	40.6	1.809	83	13	4	1
NT27	43.8	40.4	1.864	81	11	8	1
NT28	41.6	40.9	2.003	82	16	2	1

1. Measured N_2/Ar ratio.
2. Calculated N_2/Ar ratio if no denitrification.
WEA Water equilibrated with the atmosphere.
EA Extra air component.
D Excess component potentially due to denitrification.

enriched in ^{15}N ($\delta^{15}N_{WEA}$ = +0.9 +/- 0.1°/oo). The extra air nitrogen component must have a $\delta^{15}N_{EA}$ value of 0.0°/oo because atmospheric N_2 by definition is the standard against which all samples are measured. f_{WEA}, f_{EA} and f_D are all known from the calculation of the N_2 components, so the only unknown in the equation is $\delta^{15}N_D$, which can therefore be derived. Since the $\delta^{15}N_{EA}$ value is 0.0°/oo the $\delta^{15}N_{EA}.f_{EA}$ term cancels out, and rearranging for $\delta^{15}N_D$ gives:

$$\delta^{15}N_D = \frac{\delta^{15}N_{MIX} - \delta^{15}N_{WEA}.f_{WEA}}{f_D}$$

However, $\delta^{15}N_D$ will have an error due to the propagation of errors in $\delta^{15}N_{MIX}$ and f_D in particular. The approach used here is to calculate the lightest and heaviest $\delta^{15}N_D$ values permissible by these errors and take $\delta^{15}N_D$ to be represented by the mean of these two extremes. The results for these calculations are listed in Table 36. An example calculation is listed in Appendix 10.

4.2.5 The dissolved nitrogen-gas components and their respective isotopic compositions.

Fig. 31 shows the distribution of the measured N_2/Ar ratio, excess N_2 expressed as equivalent nitrate concentration, $\delta^{15}N(N_2)$ and recharge temperatures for each site across the aquifer. These variables are plotted against the groundwater temperature as this is indicative of the distance from recharge.

The N_2/Ar ratios generally cluster around 42:1 and there is no apparent trend other than a greater spread of values in the outcrop sites. The consistency of the N_2/Ar ratio is perhaps initially surprising when one considers that there is a known recharge temperature

Table 36. $\delta^{15}N$ composition of dissolved excess nitrogen gas in the Nottinghamshire Triassic groundwaters.

Sample number	$\delta^{15}N_D$ ‰	+/- error
NT01	-95.1	69.9
NT02	-22.9	8.4
NT05	+ 6.8	5.3
NT06	-51.0	23.1
NT07	-33.9	13.1
NT08	- 8.2	7.2
NT09	-11.9	5.1
NT12	-144.3	102.7
NT13	- 2.0	1.4
NT15	-15.8	10.2
NT16	- 6.5	6.5
NT17	-27.4	25.6
NT19	+13.4	3.2
NT20	-19.5	7.8
NT23	+ 7.3	7.2
NT27	-29.9	6.1

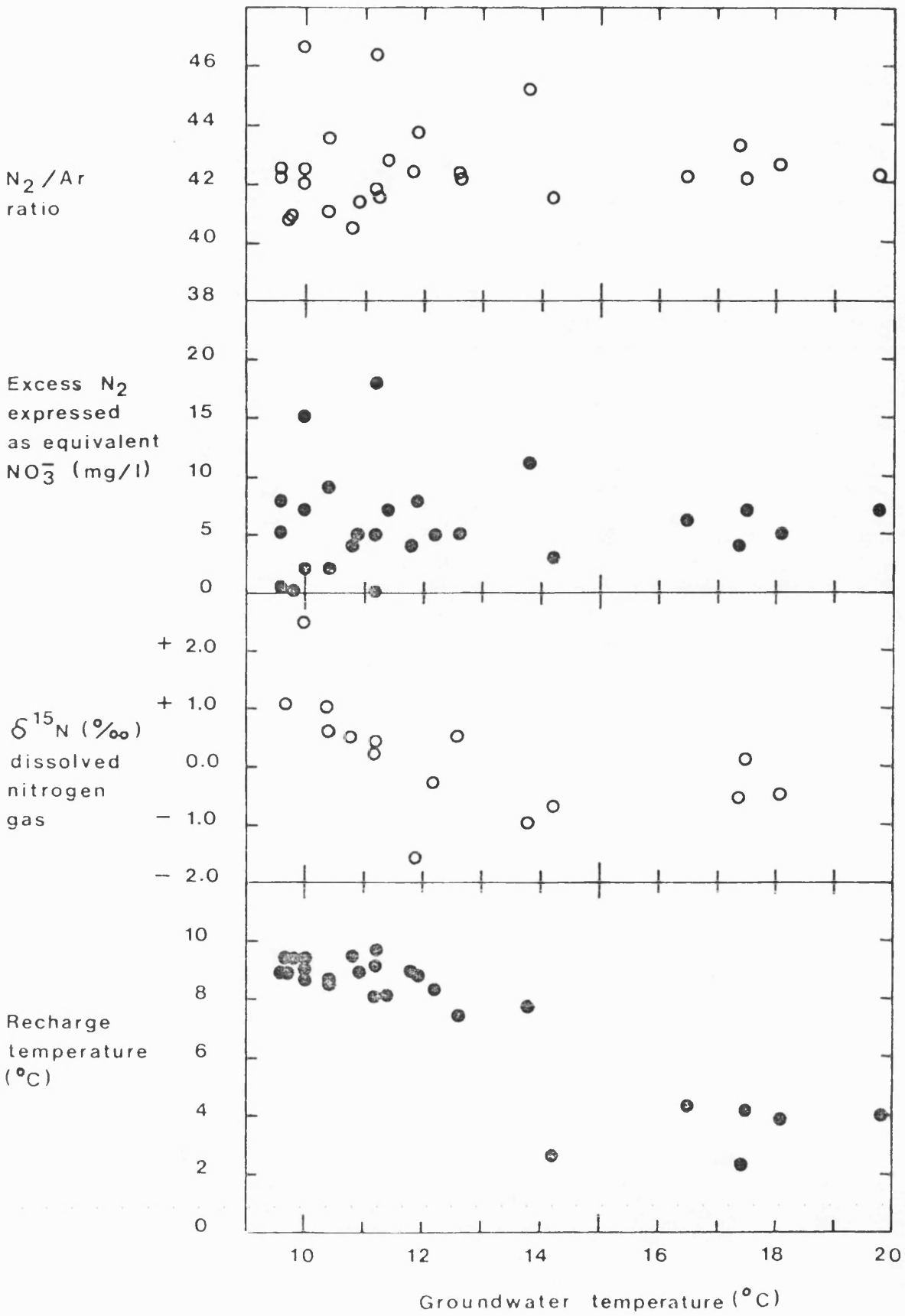

FIG. 31 Downgradient variation of dissolved gas data in groundwaters from the Nottinghamshire Triassic sandstone.

difference of some 5-6°C which would normally be associated with a detectable N_2/Ar decrease into the aquifer. The excess N_2/Ar components are generally quite small and so denitrification cannot account for the buffering of the ratio to 42:1. Any expected decline in the N_2/Ar ratio must be offset by N_2 additions other than a denitrification component. This is undoubtedly the N_2 from the extra air component, which increases as the groundwaters get older (Fig. 26).

The data on the dissolved N_2 components indicate that in general, some 80% of the dissolved N_2 is derived from water equilibration with the atmosphere. Some 15% is from extra air entrainment, and a small excess, about 5%, is usually present, (Table 35). There are exceptions to these observations. Two outcrop sites in particular, Everton (NT13) and Rufford (NT19) have N_2 excesses equivalent to dentrification of 17.5 and 15 mg/l NO_3 respectively (Table 37).

The three sites which have very high $\delta^{15}N$ (NO_3) data, possibly derived from leakage from local sewer systems/septic tanks (NT18, NT21, NT22) only contain very small increments of excess N_2. No $\delta^{15}N_D$ values are available for these sites. The small N_2 excesses however suggest the isotopically heavy nitrates are not a residual function of in-situ denitrification.

The outcrop sites with $\delta^{15}N$ (NO_3) values between 0 and 5°/oo and associated with agricultural land all have very small quantities of excess N_2 present, except for Everton which contains a moderately high excess dissolved N_2 equivalent to 17.5 mg/l NO_3. The $\delta^{15}N_D$ for these sites are all isotopically light and taking into account their common regions of error have $\delta^{15}N_D$ values of approximately 0 to -10°/oo. The small N_2 excess in these sites are therefore all lighter than their associated nitrate concentrations. This may once again be due to an

Table 37. **Excess N_2 concentrations and equivalent nitrate concentrations from the Nottinghamshire groundwaters.**

Sample number	N_2 excess (cm^3/cm^3 $H_2O \times 10^{-4}$)	Equivalent NO_3 mg/l
NT01	6.225	3.4
NT02	8.990	5.0
NT03	12.754	7.1
NT04	8.565	4.7
NT05	8.335	4.6
NT06	6.783	3.8
NT07	8.384	4.6
NT08	9.265	5.1
NT09	11.910	6.6
NT10	12.054	6.7
NT11	11.970	6.6
NT12	5.757	3.2
NT13	31.654	17.5
NT14	-	-
NT15	8.875	4.9
NT16	6.852	3.8
NT17	6.564	3.6
NT18	13.896	7.7
NT19	27.244	15.1
NT20	19.860	11.0
NT21	-	-
NT22	12.222	6.8
NT23	16.513	9.1
NT24	1.848	1.0
NT25	3.692	2.0
NT26	7.236	4.0
NT27	14.912	8.3
NT28	4.006	2.2

excess N_2 component derived incrementaly from denitrification in the soil at recharge.

The remaining sites are the old sites, Rampton (NT01), Newark (NT06), Cottam (NT12), Halam (NT04) and Ompton (NT03). They contain very little NO_3, very little excess N_2, and the $\delta^{15}N_D$ for Rampton and Newark have such large errors that no interpretation can be made other than the N_2 is isotopically light (less than $-25^{o}/oo$). This must be regarded with some caution since these $\delta^{15}N_D$ values are based on such small quantities of excess N_2 that the recognition of an excess component may not be valid.

4.2.6 A comparison of $\delta^{15}N$ (NO_3) and $\delta^{15}N$ (N_2) data.

The observed measurements of $\delta^{15}N$ (NO_3) and the calculated $\delta^{15}N_D$ (potentially denitrified component) enables the question of the source of the dissolved N_2 excess to be further considered.

There are twelve sites from the Nottinghamshire groundwaters for which both the $\delta^{15}N$ (NO_3) and $\delta^{15}N(N_2)$ data is available. If the denitrified N_2 component follows a Rayleigh Fractionation pathway the observed $\delta^{15}N$ (NO_3) values should be heavier than the corresponding $\delta^{15}N_D$ values. This is irrespective of whether the products accumulate or are removed incrementaly. Table 38 lists the available data for the Nottinghamshire sites including the isotopic difference, $\Delta^{15}N$, between the products and substrate, where

$$\Delta^{15}N = \delta^{15}N\ (NO_3) - \delta^{15}N_D$$

Of these sites, even taking into account the extent of errors on $\delta^{15}N_D$, two sites exhibit an inverse nitrogen isotope effect with the

Table 38. Isotopic separation between the dissolved nitrate and nitrogen gas $\delta^{15}N$ data from the Nottinghamshire Triassic groundwaters.

Site Number	$\delta^{15}N$ (NO_3)	$\delta^{15}N$ (‰)	*
	NO_3	$\delta^{15}N_D$ N_2 from denitrification	$\Delta^{15}N$
NT01	- 5.8	- 95.1	+ 89.3
NT02	+ 9.3	- 22.9	+ 32.2
NT05	+ 5.4	+ 6.8	- 1.4
NT06	- 9.5	- 51.0	+ 41.5
NT12	-14.8	-144.3	+129.5
NT13	+ 4.0	- 2.0	+ 6.0
NT15	- 0.4	- 15.8	+ 15.4
NT16	+ 1.0	- 6.5	+ 7.5
NT17	+ 1.3	- 27.4	+ 28.7
NT19	- 1.3	+ 13.4	- 14.7
NT23	-12.1	+ 7.3	- 19.4
NT27	+14.9	- 29.9	+ 44.8

* error on $\Delta^{15}N$ values equal to error on $\delta^{15}N_D$.

product N_2 gas apparently heavier than the residual nitrate; sites Rufford (NT19) and Fishpool (NT23). This really emphasises the problems of assuming the denitrification process is a single-step, unidirectional reaction modelled by Rayleigh Fractionation. Smejkal et al. (1971) have studied sulphur isotope fractionation by microorganisms from springs in Western Canada, which reduced SO_4^{2-} to H_2S. One species was noted to produce increasingly lighter $\delta^{34}S$ values as the reduction proceeded. This is quite contrary to the theoretical trend and in fact if such complexities are present with respect to denitrifying bacteria, a natural system such as the Nottinghamshire Triassic groundwaters may invalidate conventional modelling by Rayleigh Fractionation - at least for the evolution of the product N_2 gas. Furthermore, Rees (1972), has studied the bacterial reduction of sulphate and has produced mathematical treatments of the isotope effects. The isotopic behaviour of the product may not be consistent with that of the dissappearing reactant because of the formation of intermediate nitrogen compounds in the conversion.

Of the seven sites which could reflect a denitrification trend from the NO_3 data, only $\delta^{15}N$ (NO_3) and $\delta^{15}N_D$ data for four of the sites is available for each, (NT02, NT19, NT23 and NT27). Two of these sites exhibit the inverse isotopic effect, whilst the remaining two sites, Markham Clinton and Burton Joyce (NT02 and NT27) have $\Delta^{15}N$ values of +32.2 and +44.8‰ respectively. If the source of the excess N_2 component is inherited from soil zone denitrification, then the quantity of excess N_2 will be small and isotopically may be a function of denitrification by removal of incremental products. The complexities already outlined show that this cannot occur at every site, and bearing these reservations in mind, ϵ can be estimated from these two sites. For Burton Joyce and Markham Clinton, which both contain low excess N_2, ϵ

will be equal to $-\Delta^{15}N$, because of the approximation:

$$\varepsilon = \delta^{15}N_D - \delta^{15}N\ (NO_3)$$

If the N_2 excess in the two sites in question reflect instantaneous product removal by Rayleigh Fractionation, then ε for Markham Clinton is -32.2 +/- 8.4 and ε for Burton Joyce is -44.8 +/- 6.1. the mean of these two values, -38.5, is somewhat larger than the -7.8 value for ε obtained from the nitrate data. This however is not necessarily incompatible because if the following reaction occurs:

$$NO_3 \xrightarrow{K_1} \underset{\text{nitrogen species}}{NO_2 \text{ or intermediate}} \xrightarrow{K_2} N_2$$

where K_1 and K_2 are the respective reaction rates and $K_1 > K_2$ then the isotopic effects of K_2 will control the N_2 composition. Since the higher reaction rate is associated with smaller fractionations the association of $\varepsilon = -7.8$ derived from nitrate data and $\varepsilon = -38.5$ from N_2 data is an acceptable possibility.

The excess N_2 components and $\delta^{15}N_D$ values for the outcrop sites associated with agricultural land may reflect incremental excess N_2 additions from soil denitrification. If this is the case, then the $-\Delta^{15}N$ values should equal ε. However, the variable values for $\Delta^{15}N$ for these sites defies any detailed modelling because the ε value may be specific to each site. From the data here the ε value would vary from $0^{o}/oo$ to $-30^{o}/oo$.

4.3 The Lincolnshire Jurassic Limestone Aquifer

4.3.1 Hydrochemical characteristics of the groundwaters.

As with the Nottinghamshire Trias, a detailed discussion of the distribution of physical measurements and chemistry is included in Chapter 1, and has also been discussed elsewhere (e.g. Downing et al., 1969). Therefore only that information of concern with the potential for denitrification will be discussed here. Fig. 32 shows the distribution of % dissolved O_2, Eh and pH across the Lincolnshire Limestone aquifer.

Perhaps the most notable observation from the data in Fig. 32 is that the dissapearance of O_2 does not correlate with the redox boundary. Evidently once the recharge waters enter the confined aquifer the O_2 is stripped out of the water in a very short space of time, literally within a few hundred metres or less from outcrop. In contrast, the Eh remains predominantly high until some 12 km from outcrop, where it decreases from around +100 to -100mV. The inorganic reduction of nitrate is an unlikely possibility for these groundwaters for the same reasons as mentioned with respect to the Nottinghamshire groundwaters. Nevertheless the very low nitrate concentrations of all these waters is a real problem to explain because the residence time of waters flowing from modern recharge to well abstraction may be very rapid at around 2 years.

Unlike the Nottinghamshire Trias., the Lincolnshire Limestone does contain noticeable amounts of organic carbon (0.16 - 0.23%) (Edmunds et al., 1973), and so the denitrifying bacteria would have an organic carbon source. More interestingly, the zone between outcrop and the redox boundary, some 12 kms., is oxidising but yet anaerobic. Denitrification involves the reduction of NO_3 and the oxidation of organic carbon. In an oxidising environment, and in the absence of O_2, the oxidation of organic carbon via nitrate reduction must be energetically a favourable reaction.

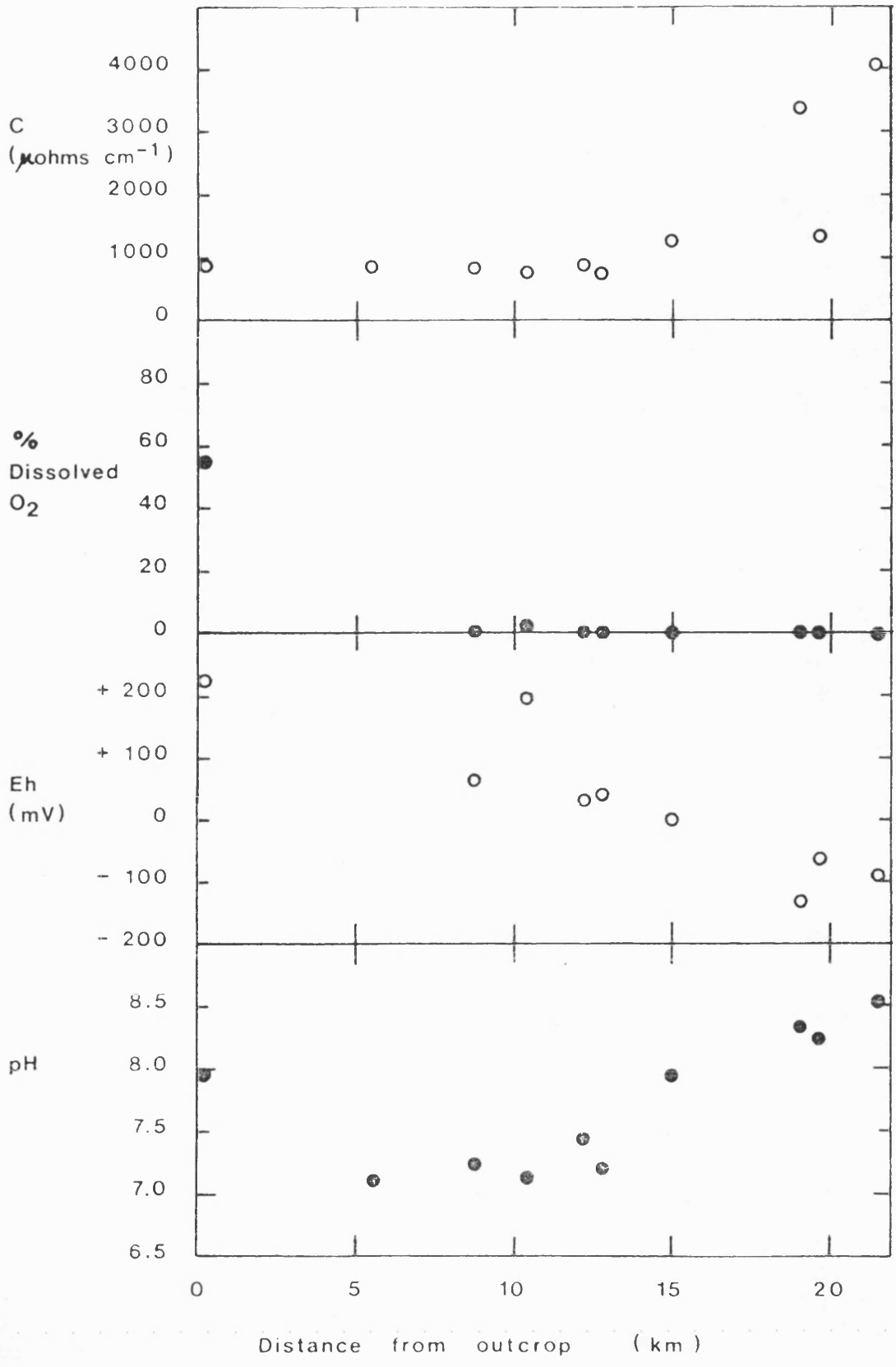

FIG. 32 Downgradient variation in chemical measurements from the Lincolnshire Jurassic limestone.

C = Conductivity

The broad chemical characteristics of the Lincolnshire Limestone groundwaters would therefore appear more conducive to supporting an active denitrifying population than would the Nottinghamshire Trias.

4.3.2 Palaeoclimatic conditions for groundwater recharge.

The δ^2H and $\delta^{18}O$ values for groundwaters from the Lincolnshire Limestone are plotted on a conventional δ-diagram in Fig. 33. The data falls on the Worldwide Meteoric line clustering about a point with $\delta^2H = -55$ and $\delta^{18}O = -8.2$ °/oo, with a regression line of $\delta^2H = 6\,\delta^{18}O - 5.8$ °/oo; correlation coefficient of +0.88. The data regression line is however, somewhat biased by Ryhall South, (LL03) which lies out of the cluster at $\delta^2H = -46$,$\delta^{18}O = -7.0$ °/oo. In fact Ryhall South is not a groundwater sample at all, but comprises an observation well in which the water level was a few feet from the surface and literally a few yards from one of the irrigation dykes which network the Fens. This sample is therefore a truly 'modern' analysis, and is reflected in the recharge temperature calculation for this site which gives a high temperature of 13.0°C.

The other sites comprise groundwaters which contain an older component. It is known that in the deeper sites diffusion between the connate waters and the fissure flow waters occur increasing the Cl^- and conductivity values, but for the sites sampled here it is probably not a major problem. Nevertheless, the flow mechanisms of the aquifer are complex, particularly with respect to a vertical stratification of the groundwaters. The hydraulic regime of the aquifer is further modified by the abstraction rates of pumping stations such as Bourne deeper into the aquifer. The net result is that it becomes difficult to 'date' the waters. On the basis of measured flow rates of 2m/yr the waters are very

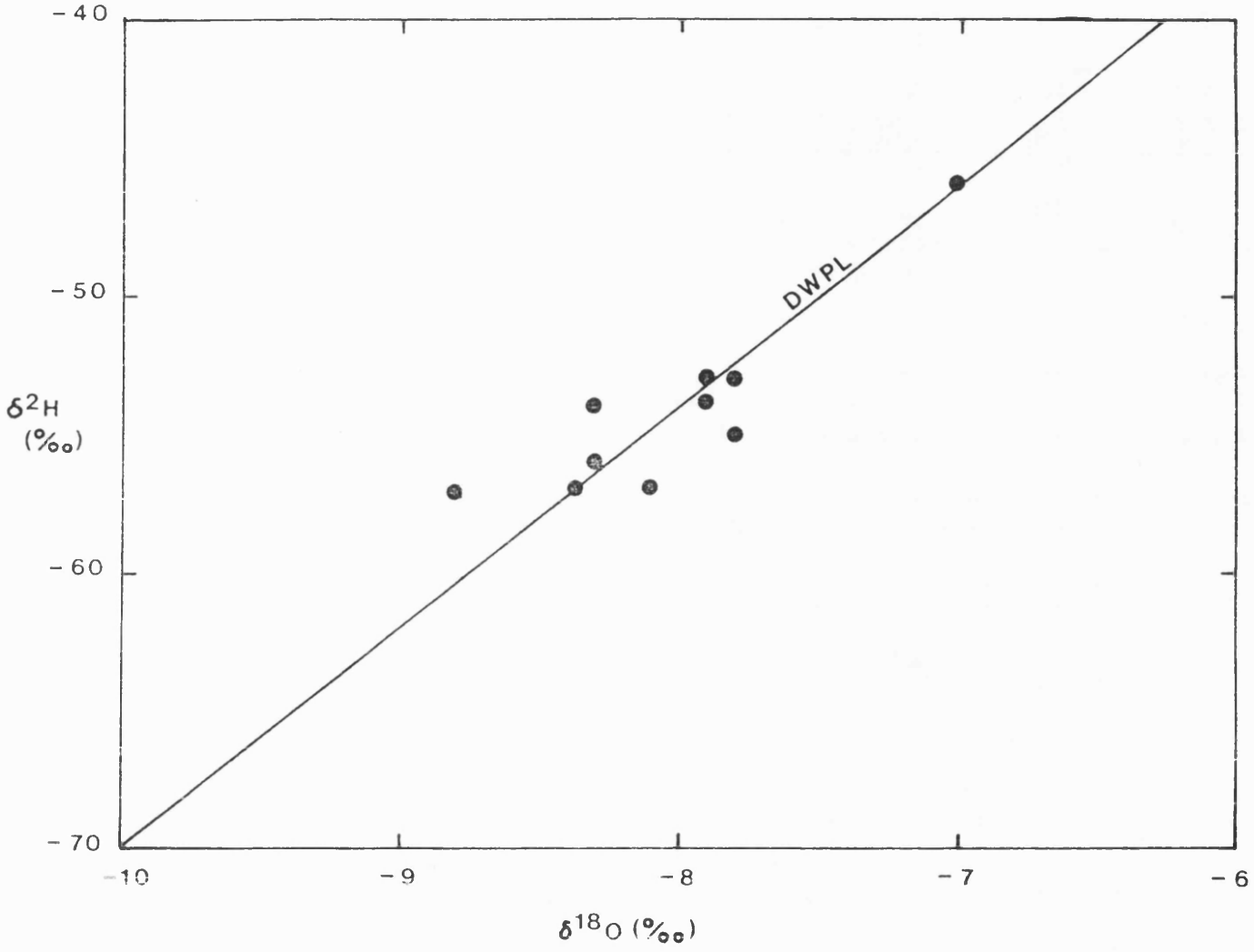

FIG.33 Correlation of Oxygen and Hydrogen isotope measurements on the Lincolnshire Jurassic Limestone groundwaters.
DWPL = Dansgaard's Worldwide Precipitation Line.

recent, but the variability of the $\delta^{18}O$ and $\delta^{2}H$ suggests that they are mixed with older waters probably from deeper in the aquifer. Disregarding the very old component from connate sources, the freshwater groundwaters are probably comparable with the outcrop and marginally confined sites of the Nottinghamshire Trias., since the $\delta^{2}H$ and $\delta^{18}O$ of these respective aquifer groupings are similar.

The contamination index for each site is plotted against recharge temperature (t_λ) in Fig. 34, to determine if a similar trend is observed as with the Nottinghamshire Trias - that is, the older groundwaters/low recharge temperature waters correlate with a higher contamination index. There is only a crude inverse correlation. This is not surprising in view of the small variation in recharge temperature ($2^{o}C$, excluding Ryhall South).

What however, is noticeable is that the contamination indices are all rather high in comparison with the Nottinghamshire waters. This must in some way reflect the nature of outcrop recharge. It may be, for example, that recharge via fissures and microfissures to the limestone may in some way favour air entrainment, or it may be a function of the rapidity of recharge - that is, recharge waters percolate down so quickly that more air bubbles become entrained with the migrating waters.

4.3.3 Nitrogen isotope data and dissolved nitrogen gas components.

Due to the low NO_3^- concentrations in the Lincolnshire Limestone groundwaters, only $\delta^{15}N\ (NO_3)$ data from three sites were obtained, (Bourne, LL01, $\delta^{15}N\ (NO_3) = -3.4^{o}/oo$; Ryhall South, LL03, $\delta^{15}N\ (NO_3) = -9.7^{o}/oo$ and Wilsthorpe, LL04, $\delta^{15}N\ (NO_3) = -0.3^{o}/oo$). This data will therefore be considered in conjunction with the $\delta^{15}N\ (N_2)$ data.

Fig. 35 shows the distribution of N_2/Ar ratios across the sampled

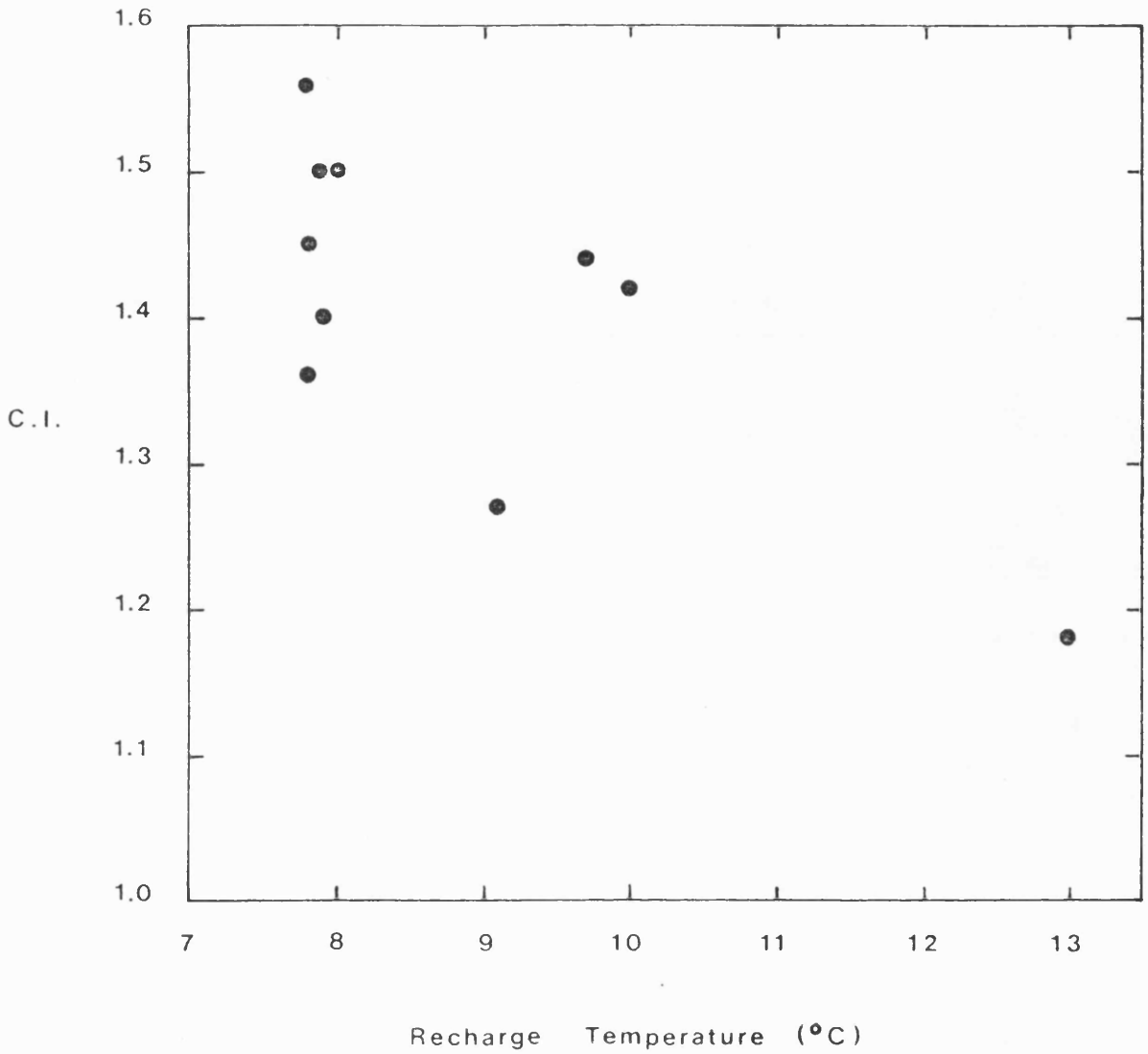

FIG. 34 Extra Air component vs. Recharge Temperature in groundwaters from the Lincolnshire Limestone.

C.I. = Contamination Index.

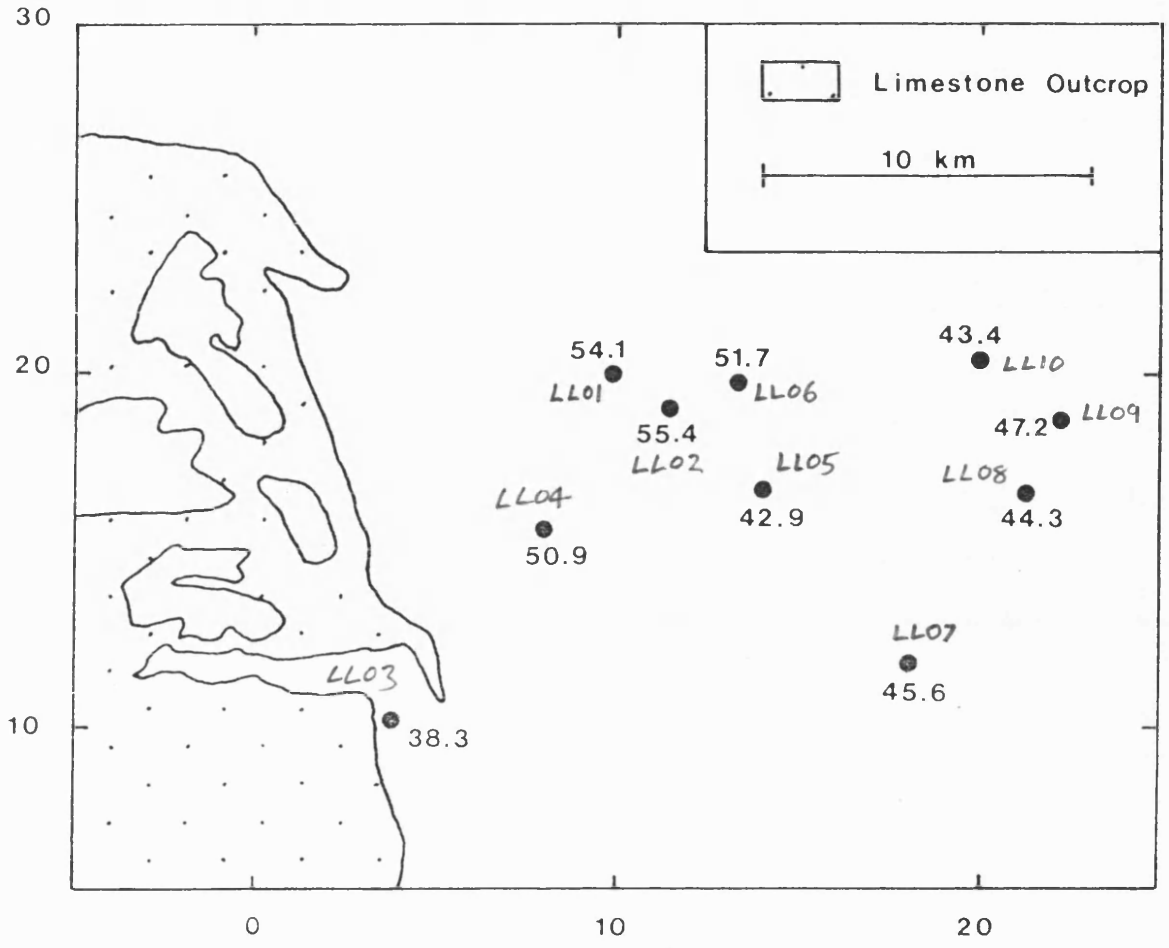

FIG. 35 Distribution of N_2/Ar ratios across the Lincolnshire Limestone aquifer.

region. High N_2/Ar ratios in excess of 50:1 are present at four sites apparently grouped around Northorpe (LL02) which itself has the highest N_2/Ar ratio observed at 55.9. It may be that the high ratios merely reflect the greater extra air entrainment since the neon contamination indices for these sites are rather high. Alternatively these N_2/Ar ratios could reflect a large excess N_2 component dissolved in the water above that from recharge, and potentially due to denitrification. A similar treatment to the data as outlined in the previous section for the derivation of N_2 components should clarify this issue.

Table 39 lists the N_2 components calculated for the Lincolnshire Limestone groundwaters. The data clearly shows that despite the high extra air contamination indices known for these sites, the four sites in question show a large discrepancy between the observed N_2/Ar ratio and the predicted ratio if atmospheric recharge was the only source of N_2. The N_2 components suggest that almost a quarter of the total dissolved N_2 at Northorpe is excessive. This excess is particularly clear in Table 40 which lists the N_2 excess and the corresponding equivalent NO_3 concentration for each of the sites. Bourne (LL01) , Northorpe (LL02), Wilsthorpe (LL04) and Black House Farm (LL06) have notably high excess N_2 concentrations.

Fig. 36 illustrates the relationship between the N_2/Ar ratios, excess N_2 equivalent nitrate concentrations, $\delta^{15}N\ (N_2)$ and recharge temperatures as a function of distance from recharge. The high equivalent nitrate concentrations clearly correlate with the high N_2/Ar ratios.

Table 41 lists the calculated $\delta^{15}N_D$ components for these groundwaters using the method described in the last section and outlined in detail in Appendix 10. The $\delta^{15}N_D$ values for Baston Common (LL05) and

Table 39. Derived N_2 components for groundwaters from the Lincolnshire Limestone.

Sample Number	1. N_2/Ar	2. N_2/Ar	Total N_2 (cm^3/cm^3 $H_2O \times 10^{-2}$)	% N_2 WEA	EA	D	Error
LL01	54.1	41.5	2.425	63	14	23	1
LL02	55.4	42.0	2.501	61	15	24	1
LL03	38.3	40.1	1.467	94	6	0	0
LL04	50.9	40.7	2.168	69	11	20	1
LL05	42.9	42.9	1.979	77	22	1	0
LL06	51.7	42.9	2.390	64	19	15	1
LL07	45.6	42.4	2.088	74	19	7	1
LL08	44.3	42.6	1.942	76	20	4	1
LL09	47.2	42.4	2.046	72	18	10	2
LL10	43.4	43.5	2.043	75	24	1	0

1. Measured N_2/Ar ratio.
2. Calculated N_2/Ar if no denitrification.
WEA Water equilibrated with the atmosphere.
EA Extra air component.
D Excess component potentially due to denitrification.

Table 40. **Excess N_2 concentrations and equivalent nitrate concentrations from the Lincolnshire Limestone groundwaters**

Sample Number	N_2 Excess (cm^3/cm^3 H_2Ox10^{-4})	Equivalent NO_3 mg/l
LL01	55.775	30.9
LL02	60.024	33.2
LL03	0.000	0.0
LL04	43.360	24.0
LL05	1.979	1.1
LL06	35.850	19.8
LL07	14.614	8.1
LL08	7.768	4.3
LL09	20.460	11.3
LL10	2.043	1.1

Table 41. **$\delta^{15}N$ composition of dissolved excess nitrogen gas in Lincolnshire Limestone groundwaters.**

Sample Number	$\delta^{15}N_D$ °/oo	+/- error
LL01	- 3.4	0.9
LL02	- 0.7	0.7
LL03	-	-
LL04	- 1.7	1.0
LL05	-251.4	143.6
LL06	- 4.0	1.4
LL07	- 23.3	5.9
LL08	- 48.9	16.8
LL09	- 13.5	4.5
LL10	-222.2	128.8

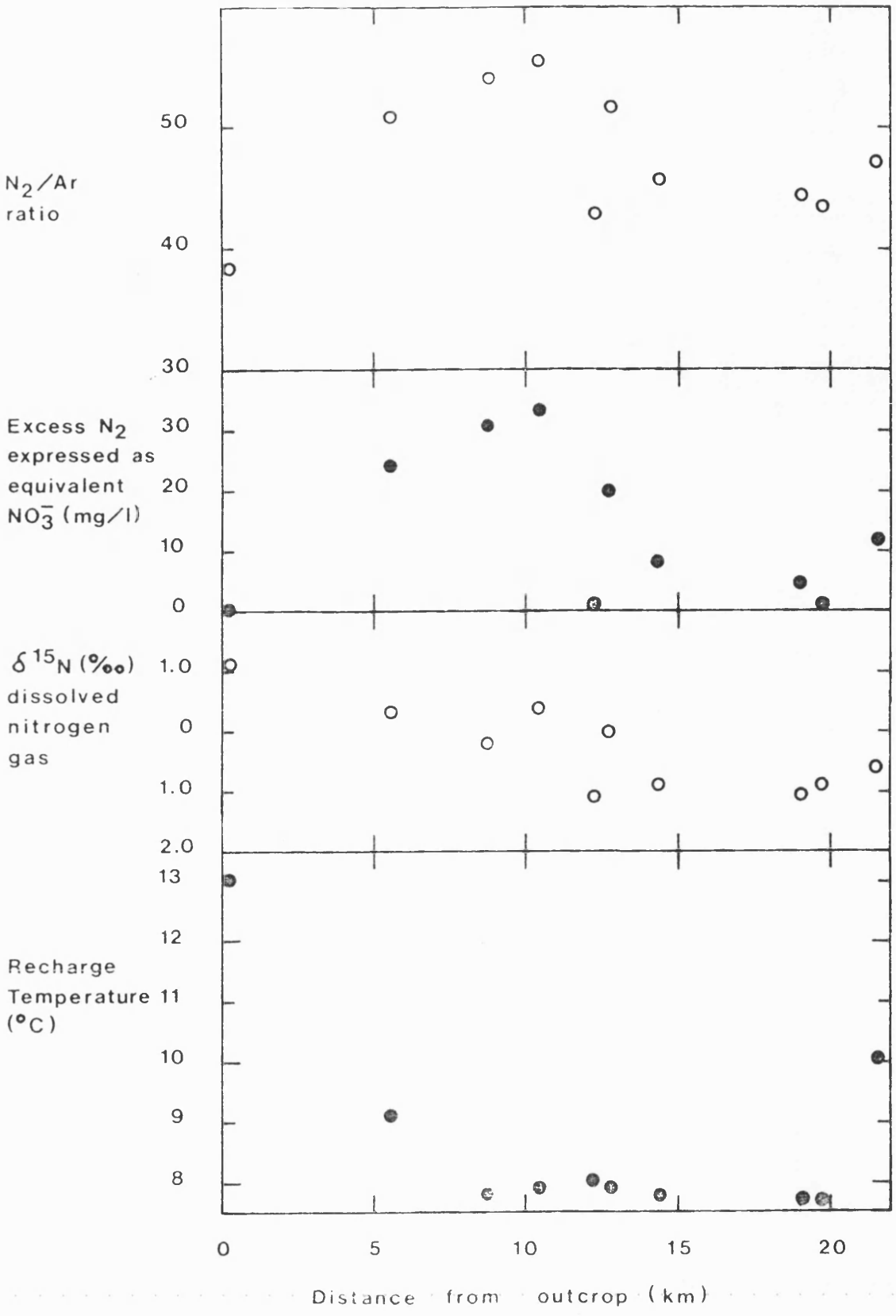

FIG. 36 Downgradient variation of dissolved gas data in groundwaters from the Lincolnshire Jurassic limestone.

Cuckoo Bridge (LL10) are very negative with very large errors in the values, mainly due to the small excess concentration of N_2 present (< 2mg/l equivalent NO_3). This data will be disregarded with respect to subsequent interpretation of the data.

The presence of a high excess N_2 component would immediately suggest the possibility of in-situ denitrification in this aquifer. The equation relating the $\delta^{15}N_D$ value to ε and the initial composition of the nitrate is:

$$\delta p = \delta s,o - \frac{\varepsilon \, flnf}{1-f}$$

where δp is the $\delta^{15}N$ of the excess N_2 gas ($\delta^{15}N_D$), $\delta s,o$ is the initial $\delta^{15}N$ (NO_3), and f is the fraction of nitrate remaining. A plot of $\delta p - \delta s,o$ vs. flnf/(1 - f) should produce a straight line relationship if the N_2 gas is being evolved from in-situ denitrification in the aquifer. No analyses for NO_3 were taken except at the outcrop site, Ryhall South (LL03), Wilsthorpe (LL04) and Bourne (LL01). However because ε is calculated from a slope, f values and $\delta p - \delta s,o$ values can be obtained for all the sites. This is because a guess at the initial $\delta s,o$ and the initial NO_3 concentration does not significantly affect the calculation of the slope. Taking the initial NO_3 composition to be 50mg/litre, f can be determined by the difference from the observed dissolved N_2 excess. $\delta s,o$ is assumed to be 0.0 °/oo. Ryhall South, Baston Common and Cuckoo Bridge are omitted from this consideration for the reasons mentioned earlier. The data is listed in Table 42 and the corresponding plot shown in Fig. 37.

It is evident that a curved relationship, or alternatively, two straight line relationships are observed in Fig. 37. This in fact suggests that ε may vary as the denitrification (if it is

Table 42. Parameters for the determination of the denitrification enrichment factor in groundwaters from the Lincolnshire Limestone

Site Number	$\Delta^{15}N$	f	$\frac{-f \ln f}{1-f}$
LL01	- 3.4	0.38	0.59
LL02	- 0.7	0.34	0.56
LL04	- 1.7	0.52	0.71
LL06	- 4.0	0.60	0.77
LL07	-23.3	0.84	0.92
LL08	-48.9	0.91	0.95
LL09	-13.5	0.77	0.89

$\Delta^{15}N = \delta^{15}N_D - \delta^{15}N\ (NO_3)$ initial.

f = fraction of nitrate remaining.

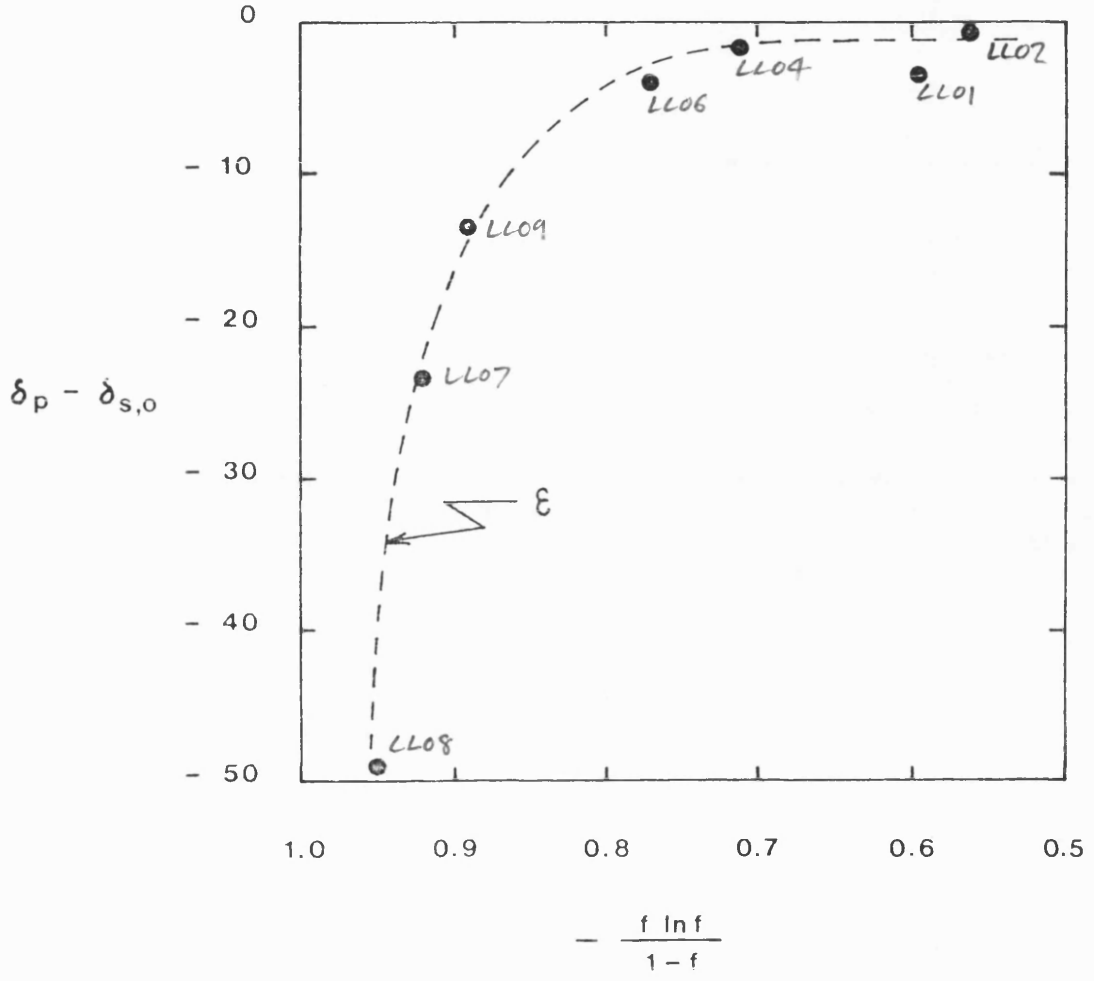

FIG. 37 Enrichment factor estimation from the N_2 gas dissolved in the Lincolnshire limestone groundwaters, using the data listed in Table 42.

δ_p	$\delta^{15}N$ denitrified N_2 gas ($\delta^{15}N_D$)
$\delta_{s,o}$	$\delta^{15}N(NO_3^-)$ original starting composition
f	fraction of nitrate remaining
ε	enrichment factor

N.B. Curve fitted by eye.

denitrification) evolves the N_2. At high NO_3 concentrations, where f is close to 1 and -flnf/(1 - f) is higher ε seems to be greatest in excess of -30 $^{o}/_{oo}$, but at lower NO_3 concentrations where f approaches 0 the ε value is much lower.

There are really two important questions raised by this data. Firstly, if the N_2 is a function of denitrification, why are elevated N_2/Ar ratios not observed throughout the aquifer particularly to the east? In fact with reference to Figs. 35 and 36 the N_2/Ar ratios actually decrease to the east. For some reason the excess N_2 components are concentrated around Northorpe.

One suggestion could be that the excess N_2 is not derived from denitrification at all but is a product of long-term thermal degradation of organic matter located in the interstitial pore spaces of the limestone, and essentially a relic from the time of Jurassic sedimentation. Although pore-fissure mixing certainly does occur with increasing importance to the east of the aquifer, this cannot be occuring around Northorpe because both the chlorinity and conductivity values would show markedly high values reflecting the saline nature of the connate water mixing. Conductivity values are however, quite low (Fig. 32).

Alternatively, denitrification could be occuring at other sites in the aquifer but some process is removing the N_2. Bacterial nitrification or futher bacterial reduction to NH_3 is a possibility but is unlikely because all such reactions whereby reactants go to products should favour the lighter isotope and enrich the residual reactant in ^{15}N. In other words, the $\delta^{15}N_D$ values should become markedly positive in those sites which contain little excess N_2. This is not the case and in fact the opposite is observed, with $\delta^{15}N_D$ very negative.

The reduction of N_2 to NH_4^+ by redox equilibria is a further possibility. Beyond the redox boundary the Eh of the waters is feasibly reducing enough for NH_4^+ to be stable (Edmunds et al., 1985), but the direct inorganic reduction from NO_3^- to NH_4^+ does not seem likely because of thermodynamic constraints as suggested by these authors. Furthermore, there is no evidence of a major dissolved NH_4^+ component in these groundwaters, although NH_4^+ may be present in trace amounts (Towler, 1982).

One possibility is that after the bacterial reduction to N_2 has occured, further inorganic reduction to NH_4^+ occurs followed by ion exchange with Na^+ filled sites on clay minerals within the limestone. This however, also seems unlikely since in dilute aqueous solutions (up to 0.1M) the major cations including Ca^{2+} and Mg^{2+} show much stronger affinities for exchange with Na^+ filled clay exchange sites than does NH_4^+. So although NH_4^+ could exchange with Na^+, it is unlikely to do so because of the overwhelming competition from the Ca^{2+} and Mg^{2+} ions in solution.

The apparent grouping of high N_2/Ar ratios and high excess N_2 is in fact roughly coincident with the redox boundary of the aquifer which is known to inflex eastwards near Bourne (Andrews and Kay, 1982). This suggests that active N_2 production is present in the anaerobic oxidising environment near the redox boundary - and may extend both north and south of the studied area. The evidence for in-situ denitrification in this aquifer seems convincing. What does, however, remain a problem is the ultimate fate of the N_2 gas evolved from the denitrification.

The lower N_2/Ar ratios may simply be a function of mixing between one deeper source of groundwater with a low N_2/Ar ratio (eg 40:1) with a shallower, high N_2/Ar ratio groundwater, the product of denitrification

(eg 50:1). This would produce a groundwater sample with an intermediate and apparently lower N_2/Ar ratio.

The second important observation requiring discussion is the change in the enrichment factor as the nitrate concentration changes (Fig. 37) at high NO_3 concentrations ε is apparently greatest whilst at low concentrations ε approaches 0 implying no fractionation effect at all. Since ε seems to be proportional to f, then this could reflect a change from carbon-limiting conditions to nitrate limiting conditions. The general observations concerning nitrate and carbon limiting systems with respect to denitrification were noted in Chapter 1. A high nitrate (carbon-limiting) system will in general favour a 'short-cut' in denitrification straight down from NO_2^- to NH_3. The production of NH_3 has already been discussed and such accumulations seem unlikely, but the point made here is that the denitrification process may proceed by different metabolic pathways and therefore may involve different respective enrichment factors.

A change from carbon-limiting to nitrate limiting conditions is possible to visualise if one considers that the dissolved NO_3 will be constantly moving down through the aquifer. So, near outcrop, the nitrate could be denitrified to N_2 by the bacteria utilising one particular metabolic pathway (and enrichment factor). The residual nitrate, or indeed excess nitrate as yet unaffected by denitrification, passes down further into the aquifer, where the conditions are now nitrate-limiting. Denitrification still occurs to N_2, but via a different matabolic pathway with an associated lower enrichment factor.

An alternative explanation for the change in ε is that it is a function of the increasing groundwater temperature downgradient. Higher ε values are associated with lower reaction rates and lower

temperatures, so the progression to a lower $\mathcal{C}$ value into the aquifer could simply reflect the increasing reaction rates in response to the increasing groundwater temperature.

CHAPTER V

CONCLUSIONS

5.1 Analytical Techniques

A large part of this work has been concerned with development of techniques as well as obtaining sufficient data for studying aspects of denitrification. Particular attention was devoted to N_2/Ar and nitrogen-isotope analyses, and also data treatment of results derived from noble-gas analyses.

Good reproducibility of N_2/Ar values were obtained for samples collected in duplicate (within 2 %). The extrapolation of ion current m/e ratios from the time of measurement to the time of sample admission to the spectrometer is particularly important. This is because the ion current m/e rates of change may vary markedly, especially according to gas composition.

The nitrogen-isotope preparation gas line was built with the aim of being able to analyse both nitrogen isotopes in nitrates and nitrogen isotopes in groundwater gas samples. Accurate $\delta^{15}N$ data was obtained (within $0{\cdot}2^{o}/oo$) on the basis of comparisons with measurements on the N-1 and N-2 I.A.E.A. Vienna standards obtained by other laboratories.

5.2 Denitrification in the Nottinghamshire Triassic groundwaters

As a generalisation, the small dissolved excess N_2 components of the sampled groundwaters provides the best evidence that in-situ denitrification is not occuring in this aquifer. Sites at outcrop do however, show local excess N_2 enhancements, notably at Everton (NT13) and Rufford (NT19). Denitrification at these two sites could therefore be occuring contrary to the other sites in the Nottinghamshire Trias. It may be that local near surface denitrification has been initiated in response to organic micropollutants and high nitrate contents recently washed into the shallowest parts of the aquifer at these specific sites.

The nitrogen-isotope data on the dissolved nitrates show a scatter with Clipstone (NT18), Rainworth (NT21), and Farnsfield (NT22) exhibiting isotopically heavy $\delta^{15}N(NO_3)$ values of +22.7 to +31.1 °/oo. These outcrop sites have high nitrate concentrations but low N_2 excesses, and so the very positive data values cannot be a function of residual ^{15}N enrichment due to denitrification. The three outcrop sites correlate with the urban areas of New Clipstone, Rainworth and Farnsfield respectively, and probably reflect leakage of waste from urban-sewer systems.

Well sites located on outcrop agricultural land generally have $\delta^{15}N(NO_3)$ values between 0 and +5 °/oo and suggest nitrate inputs from fertiliser applications.

No convincing denitrification trend can be seen from the $\delta^{15}N(NO_3)$ data. Seven sites do in fact correlate with a relationship consistent with denitrification by removal of instantaneous products, but this could be coincidence. If the instantaneous products relationship is real, then it suggests that denitrification occurs in the soil zone and releases small increments of N_2 to the groundwater in excess of that derived from the atmosphere. This would necessitate an initial nitrate concentration of about 44 mg/litre which is isotopically light, about -13 °/oo, and the calculated enrichment factor being -7.8 °/oo. These conditions could reflect recharge from forested land.

The $\delta^{15}N$ data on the dissolved nitrogen gas does not show a consistent relationship with the available comparable $\delta^{15}N$-nitrate data. ε values derived from the isotopic difference between the NO_3 and N_2 give a value of ε = -32.2 °/oo for Markham Clinton and -44.8 °/oo for Burton Joyce. In contrast, inverse isotopic relationships are observed at Rufford (NT19) and Fishpool (NT23). If incremental release of N_2 to

groundwater at recharge is occurring, the ε_r values may be specific to each site and in any case may not be modelled by a unidirectional conversion from nitrate to nitrogen gas by Rayleigh Fractionation. At any event, this data does not support 'in-situ' aquifer denitrification in the groundwaters.

The older confined groundwaters contain very low nitrate concentrations (< 2 mg/l), and very small excess N_2 concentrations equivalent to about 5 mg/l NO_3. This may reflect the natural input level of nitrate to the aquifer in pre-modern times. The nitrate and nitrogen gas $\delta^{15}N$ measurements indicate that both the NO_3 and N_2 are isotopically light, and indicate that the pre-modern input of NO_3 to the aquifer may have been depleted in ^{15}N, perhaps $\delta^{15}N = < -15$ °/oo.

5.3 The evolution of dissolved gases in the Nottinghamshire Triassic groundwaters.

The height of the Devensian Ice Age occurred about 25000 years BP when the ice sheets had advanced southwards to cover most of Wales and Southern England, reaching York and Wolverhapton (Bowen, 1978). Subsequent climatic warming produced a gradual deterioration in the ice front which retreated northwards. At least one interstadial warming is known to have occurred, in particular the late Glacial Interstadial some 13000 years BP. This will have involved at least one glacial readvance after the Interstadial. However the overall climatic warming continued until 10000 years BP which marks the start of the Flandrian Transgression and the present Interglacial.

The oldest carbon-14 date of the Nottinghamshire Triassic groundwaters is about 35000 years BP for Rampton (NT01), whilst outcrop sites essentially contain contemporary recharge waters. The carbon-14

ages are however rather misleading in that all the groundwaters have undergone some degree of mixing with respectively different ages of recharged water. Rampton for example, probably contains a component of groundwater older than its carbon-14 age of 35000 years BP.

During the late Devensian, the ice front will have lain some distance to the north of the outcrop region of the Nottinghamshire Triassic sandstone. The outcrop region must however, have been influenced at times by periglacial conditions.

On the basis of the carbon-14 dates by Bath et al., (1978), the Nottinghamshire Triassic Aquifer was recharged some 35-25000 years BP under average annual air temperatures of 2 - 4^{o}C as determined from the noble gas data. Direct atmospheric equilibration would have fixed the dissolved N_2/Ar ratio to about 37:1. As the water percolated downwards, the viscosity of the cold water was high enough to trap a relatively large proportion of air bubbles, which were subsequently forced into solution. This increased the N_2/Ar ratio to about 41:1. Very small increments of N_2 gas may have been added to the groundwater at this time, perhaps from soil denitrification of some 5 mg/l NO_3. In some cases this increased the N_2/Ar ratio to about 42:1. Of the total dissolved N_2, some 80% was from atmospheric recharge, some 15-20% from extra air entrainment, and some 0-5% from additional N_2 inputs. Natural input levels of NO_3 to the aquifer were very low, usually <2 mg/l and no higher than 5 mg/l.

At this time, the water molecules involved in the recharge would themselves contain isotopes of oxygen and hydrogen fractionated occording to the temperature of cloud condensation. Under these colder conditions, the $\delta^{18}O$ of the water was about -9.0 $^{o}/_{oo}$ and the $\delta^{2}H$ about -62 $^{o}/_{oo}$. Once in the aquifer, the water molecules retained their isotopic recharge

signature during the downgradient flow, although a small amount of mixing may have occurred.

The dissolved gas contents of these waters essentially remained unchanged during the subsequent passage down into the aquifer, except for the removal of dissolved oxygen and the accumulation of radiogenic helium. The oxidation of Fe^{2+} to Fe^{3+} facilitated removal of dissolved O_2 by precipitation of iron minerals. This process nevertheless took thousands of years to complete, on the basis of the persistence of dissolved O_2 into the shallower confined zone of the aquifer.

No carbon-14 ages on groundwaters are available between 25000 years BP and 10000 years BP for the particular sampled sites in question. This suggests that no recharge to the aquifer occurred during this period. The recharge 'gap' is reflected in the bimodal distribution of recharge temperatures, with the younger waters indicating recharge under temperatures of 8 - 10°C. The corresponding isotopic distribution of $\delta\,^{18}O$ and $\delta\,^{2}H$ also reflects a period of no aquifer recharge, with a warming in cloud condensation temperatures of some 2-3°C. A period of extensive permafrost ground can be envisaged essentially sealing the aquifer from outcrop recharge until the permafrost melted. The extent of permafrost may well have persisted for a long time after the maximum advancement of the ice southwards. The present day recharge to the aquifer is much the same as the younger outcrop groundwaters on the basis of their comparable recharge temperatures.

5.4 Denitrification in the Lincolnshire Limestone groundwaters

The Lincolnshire Limestone groundwaters contain notably high N_2/Ar ratios and correspondingly high excess N_2 components particularly at Bourne, Northorpe, Wilsthorpe and Black House Farm. This observation

coupled with the very low nitrate concentrations characteristic of all the sites is good evidence that in-situ denitrification is occuring in this aquifer. The highest nitrogen excess corresponds to the equivalent denitrification of some 33 mg/l NO_3.

The nitrogen isotope data on the dissolved N_2 excess reveals that the enrichment factor may vary according to the quantity of nitrate available for denitrification. This may reflect bacterial denitrification via different metabolic pathways triggered according to the nitrate concentration, or due to an increase in the rate of denitrification.

The occurrence of denitrification in the anaerobic oxidising zone between outcrop and the redox barrier does not explain why the waters to the east of the barrier apparently contain smaller quantities of excess N_2. One explanation could be that the waters are mixing with older freshwater sources from deeper stratified levels in the aquifer which contain no N_2 excess. This would produce a lowering of the N_2/Ar ratio.

Denitrification in the Lincolnshire Limestone groundwaters may not have been an inherent long-term process occuring in the aquifer. It may be that the process has recently developed in response to additional nitrate excesses washed down into the aquifer with the advent of modern farming practices.

5.5 The evolution of dissolved gases in the Lincolnshire Limestone groundwaters.

The Lincolnshire Limestone aquifer contains waters abstracted from recharge which may only be a few years old. However this feature is largely the result of modern pumping regimes in the aquifer. Older groundwaters are present from late Devensian recharge, on the basis of

comparable $\delta^{18}O$ and $\delta^{2}H$ values with the younger waters of the Nottinghamshire Trias ($\delta^{18}O = 8.3$ °/oo; $\delta^{2}H = -55$ °/oo approx.).

In vertical section the aquifer is markedly stratified with respect to age and flow of the waters. This means that deeper level groundwaters contain proportionally more water components from an older source than the near surface groundwaters. In addition to this complication, connate pore waters, a relic from marine sedimentation, are present in the interstitial pores which undergo exchange with the surrounding fissure flow.

The sedimentation and diagenesis of the Lincolnshire Limestone occured some 70 million years ago. Originally seawater may well have been present in fissures in the rock as well as in the interstitial pores. Since earth movements brought the Lincolnshire Limestone to its present geological setting, the saline fissure waters have been flushed out by freshwater recharge at least in the observable upgradient sites.

Freshwater recharge to the aquifer occured at least as far back as 11000 years BP and possibly for much longer. The short residence time of the abstracted waters makes it difficult to determine for how long this freshwater recharge has occured. Atmospheric equilibration fixed the N_2/Ar ratio to about 38:1 under average annual air temperatures of about 9°C, but extra air additions increased this to about 42:1. The oxidation of organic carbon to produce CO_2 rapidly stripped out any dissolved O_2 from the waters when passing into the confined zone. As the waters migrated downgradient a unique environment was present in the shallow confined aquifer which was anaerobic but nevertheless characterised by a high Eh.

The anaerobic, high Eh environment and the availability of organic carbon enabled a colony of denitrifying bacteria to establish themselves,

probably from the flushing through of soil denitrifiers at outcrop.

These waters which do not contain N_2 excesses are characterised by some 80% N_2 from atmospheric equilibration and some 20% from extra air recharge. Those waters containing a nitrogen excess may contribute an excess up to 25% of the total dissolved nitrogen, with N_2/Ar ratios reaching 55:1. Further downgradient, mixing of these waters with older, deeper stratified waters lowered the ratio. Exchange of groundwaters between the fissure waters and the connate waters certainly occurs on the basis of increasing conductivity measurements into the aquifer. This effect is however very small for the sites in question and produces insignificant changes to the dissolved gas concentrations.

5.6 Perspectives and future work

There is no evidence for in-situ denitrification in the Nottinghamshire Trias groundwaters, in view of the very small dissolved nitrogen gas components in excess of that derived from recharge. The nitrogen isotopes from nitrates dissolved in these waters indicates fertiliser inputs are characterised by a $\delta^{15}N$ of 0-5 °/oo, whilst leakages from sewers give $\delta^{15}N$ values of > 20 °/oo. Pre-modern nitrate inputs may be lower than -10 °/oo.

In contrast, the Lincolnshire Limestone groundwaters contain high concentrations of dissolved nitrogen gas that cannot be accounted for by atmospheric inputs. Denitrification would seem to be a likely source. A subsequent lowering of the N_2/Ar ratio to the east of the aquifer may indicate mixing with waters from deeper stratified layers which are older and contain essentially no denitrified nitrogen gas.

It is surprising, considering the wealth of hydrochemical data on major aquifer systems such as the Nottinghamshire Trias and the

Lincolnshire Limestone, just how difficult it can be to categorically state whether or not denitrification is an active process in these aquifers. This ultimately reflects the difficulty of collecting and studying the dissolved gas components of groundwaters, because only identification of the products of denitrification will prove the case unambiguously. This study shows that a very specific type of geochemical data is required before such conclusions can be drawn.

The direction for future work would seem to be a development towards the routine recognition of those dissolved gas components potentially derived from denitrification. It is the recognition of a nitrogen gas excess (or lack of it) that in this study has been most definitive in determining the operation of an in-situ denitrification process. The nitrogen-isotopes on the other hand, although useful in their own right for the potential identification of nitrate sources, did not prove definitive in identifying the absence or presence of denitrification. Only when used in conjunction with the noble gas data could the nitrogen isotope data be more fully evaluated. Since no two aquifers are the same, the use of nitrogen isotopes to identify denitrification may well be applicable to other aquifer systems which have a simpler recharge history.

REFERENCES

Andrews, J.N. and Kay, R.L.F., 1982. U-234/U-238 Activity ratios of dissolved uranium in groundwaters from a Jurassic Limestone aquifer in England. E.P.S.L., 57 139-151.

Andrews, J.N. and Lee, D.J., 1979. Inert gases in groundwater from the Bunter Sandstone of England as indicators of age and palaeoclimatic trends. J. Hydrol., 41 233-252.

Bath, A.H., Edmunds, W.M. and Andrews, J.N., 1978. Palaeoclimatic trends deduced from the hydrochemistry of a Triassic Sandstone aquifer, United Kingdom. Isotope Hydrol., 2 545-566, I.A.E.A., Vienna.

Benson, B.B. and Krause, D., 1976. Empirical laws for dilute aqueous solutions of non-polar gases. J. Chem. Phys., 64 639-

Benson, B.B. and Parker, P.D.M., 1961. N_2/Ar and N-isotope ratios in aerobic seawater. Deep Sea Res., 7 237-253.

Berner, R.A., 1971. Principles of chemical sedimentology. McGraw Hill, New York.

Bremner, J.M. and Keeney, D.R., 1965. Steam distillation methods for determination of ammonium nitrate and nitrite. Anal. Chim. Acta., 32 485-495.

Broecker, W.S., 1974. Chemical oceanography. Harcourt Brace Jovanovich.

Brownlow, A.H., 1979. Geochemistry. Prentice Hall.

Cook, F.D., Wellman, R.P. and Krouse, H.R., 1970. Nitrogen isotope fractionation in the nitrogen cycle. Int. Symp. on Hydrogeochemistry and biochemistry. Tokyo, Sept. 6-12th 1970. Paper B 1/6.

Crovetto, R., Fernandez-Prini, R. and Japas, L.M., 1981. Solubilities of inert gases and methane in H2O and in D2O in the temperature range of 300 K - 600 K. J. Chem. Phys., 76 1077-1086.

Dansgaard, W., 1964. Stable isotopes in precipitation. Tellus, 16 436-468.

Darling, W.G., Bath, A.H. and Brunsdon, A.P., 1982. Revised procedure for the measurement of hydrogen and oxygen isotopes in water samples. Stable Isotope Technical Report No.16, I.G.S. Geophysics and Hydrology Division, Wallingford.

Delwiche, C.C., 1970. The nitrogen cycle. Sci. Am., 223 137-146.

Downing, R.A., Smith, D.B., Pearson, F.J., Monkhouse, R.A. and Otlet, R.L. The age of grouindwater in the Lincolnshire Limestone, England, and its relevance to the flow mechanism. J. Hydrol., 33 201-216.

Downing, R.A. and Williams, B.P.J., 1969. The groundwater hydrology of the Lincolnshire Limestone. Water Resources Board.

Edmunds, W.M., 1973. Trace element variations across an oxidation reduction barrier in a limestone aquifer. Proc. Symp. Hydrochem. Biogeochem. Tokyo (1970) Ingerson (Ed.)

Edmunds, W.M., Bath, A.H. and Miles, D.L., 1982. Hydrochemical evolution of the East Midlands Triassic Sandstone aquifer, England. Geochim. Cosmochim. Acta., 46 2069-2081.

Edmunds, W.M., Burgess, W.G., Kay, R.L.F., and Lee, D.J., 1984. The evolution of saline and thermal groundwaters in the Carnmenellis Granite. Min. Mag., 48 407-424.
Clarke Co., Washington D.C. Vol. 1. 500-520.

Edmunds, W.M., Miles, D.L. and Cook, J.M., 1985. A comparative study of sequential redox processes in three British Aquifers. (In Press).

Edmunds, W.M. and Walton, N.R.G. The Lincolnshire Limestone hydrogeochemical evolution over a ten-year period. Karst Hydrology. Vol. 2. Int. Assoc. of Hydrologists. Bok, W. (Ed).

Evans, G.V., Otlet, R.L., Downing, R.A., Monkhouse, R.A. and Roe, G., 1978. Some problems in the interpretation of isotope measurements in United Kingdom aquifers. Isotope Hydrology., Vol. 2. I.A.E.A., Vienna.

Focht, D.D., 1978. Methods for analysis of denitrification in soils. Nitrogen in the environment. Vol.2. Neilson, D.R. (Ed) Academic Press.

Frick, U. and Pepin, R.O., 1981. Microanalysis of nitrogen isotope abundances: association of nitrogen with noble gas carriers in Allende. E.P.S.L., 56 64-81.

Gonfiantini, R., 1983. Consultants meeting on stable isotope reference samples for geochemical and hydrological investigations. Draft Report, I.A.E.A., Vienna.

Heaton, T.H.E., and Vogel, J.C., 1981. Excess-air in groundwater. J. Hydrol., 50 201-216.

Herbert, R.A., 1982. Nitrate dissimilation in marine and estuarine sediments. Sediment Microbiology. Nedwell, D.B. and Brown, C.M. (Eds.) Academic Press.

Hoefs, J., 1980. Stable isotope geochemistry. 2nd ed. Springer Verlag. New York.

International critical tables of numerical physics, 1928. Vol. 3.

Knowles, R., 1978. Common intermediates of nitrification and denitrification and the metabolism of nitrous oxide. Microbiology - 1978. Washington D.C. American Soc. for Microbiology. 367-371.

Koike, I. and Hattori, A., 1978. Denitrification and ammonia formation in anaerobic coastal sediments. App. Env. Microbiol., 35 378-282.

Konig, H., 1963. Uber die loslichkeit der edolgase in meerwasser. Z. Naturforsch., 18A 363-

Kreitler, C.W., 1975. Nitrogen isotope ratio studies of soils and groundwater nitrate from alluvial fan aquifers in Texas. J. Hydrol., 42 147-170.

Kreitler, C.W. and Browning, L.A., 1983. Nitrogen isotope analysis of groundwater nitrate in carbonate aquifers: natural sources vs human pollution. J. Hydrol., 62 285-301.

Kreitler, C.W., Ragone, S.E. and Katz, B.G., 1978. N-15/N-14 ratios of groundwater nitrate, Long Island, New York. Groundwater. 16. 404-409.

Land, D.H., 1966. Hydrogeology of the Bunter Sandstone in Nottinghamshire Water supply papers of the geological survey of Great Britain. Hydrological Report No. 1. N.E.R.C.

Letolle, R., 1980. Nitrogen-15 in the natural environment. Handbook of environmental isotope geochemistry. Fritz, P. and Fontes, J. Ch. (Eds.) Vol. 1A 407-429.

Macko, S.A., 1981. Stable nitrogen isotope ratios as tracers of organic geochemical processes. Unpublished Ph.D. thesis. University of Texas at Austin.

Macko, S.A., Estep, L.F., Hare, P.E. and Hoering, T.C., 1983. Stable nitrogen and carbon isotopic composition of individual amino acids isolated from cultured microorganisms. Carnegie Inst. Washington Year Book 82. 404-409.

Macko, S.A. and Parker, P.L., 1983. Stable nitrogen and carbon isotope ratios of beach tars on southern Texas barrier islands. Mar. Env. Res. 10 93-103.

Mariotti, A., 1982. Apports de al geochimie isotopique a la connaissance du cycle d'azote. D.Sc. Thesis, Universite P. et M. Curie, Paris.

Mariotti, A., 1983. Atmospheric nitrogen as a reliable standard for natural N-15 abundance measurements. Nature, 303 685-687.

Mariotti, A., 1984. Natural N-15 abundance measurements and atmospheric nitrogen standard calbiration. Nature, 311 251-252.

Mariotti, A., Germon, J.C., Hubert, P., Kaiser, P., Letolle, R., Tardieux, A. and Tardieux, P., 1981. Experimental determination of nitrogen kinetic isotope fractionation: some principles; illustration for the denitrification and nitrification processes. Plant and Soil, 62 413-430.

Mariotti, A., Germon, J.C. and Leclerc, A., 1982. Nitrogen isotope fractionation associated with the NO2-N20 step of denitrification in soils. Can. J. of Soil, 62 227-241.

Mariotti, A., Germon, J.C., Leclerc, A., Catroux, G and Letolle, R., 1982. Experimental determination of kinetic isotope fractionation of nitrogen isotopes during denitrification. Stable Isotopes. Schmidt, H., Forstel, H. and Heinsinger, K. (Eds.) Elsevier.

Mariotti, A. and Letolle, R., 1977. Application de l'edutie isotopique de l'azote en hydrologie et hydrogeologie. Analyse des resultats obtenus sur un example precis: le bassin de Melarchez (Seine et Marne, France). J. Hydrol, 33 157-172.

Matsuo, S., Susuki, M and Mizutani, Y., 1978. Nitrogen to argon ratio in volcanic gases. Terrestrial rare gases. Alexander, E.C. Jnr. and Ozima, M. (Eds.) Center for Academic Publications, Japan.

Morrison, T.J. and Johnstone, N.B., 1954. Solubilities of the inert gases in water. J. of Chem. Soc. 3441-3446.

Openshaw, P., 1983. River pollution. Pt.1 of The School Science Review, 65 243-254.

Ozima, M. and Podosek, F.A., 1984. Noble gas geochemistry.

Rees, C.E., 1973. A steady-state model for sulphur isotope fractionation in bacterial reduction processes. Geochem. Cosmochim. Acta., 37 1141-1162.

Rightmire, C.T., 1979. Changes in formation gas composition and isotope content as indicators of unsaturated zone chemical reactions related to recharge events. I.A.E.A.-S.M./228/35 711-732.

Ross, P.J. and Martin, A.E., 1970. A rapid procedure for preparing gas samples for nitrogen-15 determination. Analyst, 95 817-822.

Schidlovski, M., Hayes, J.M. and Kaplan, I.R., 1983. Isotopic inferences of ancient biochemistries: Carbon, sulphur, hydrogen and nitrogen. Earth's earliest biosphere. Schopf, J.W. (Ed.) Pinceton University Press. 178-185.

Shoor, S.K. and Gubbins, K.E., 1968. Solubility of nonpolar gases in concentrated electolyte solutions. J. Phys. Chem., 73 498-505.

Smejkal, V., Cook, F.D. and Krouse, H.R., 1971. Studies of sulphur and carbon isotope fractionation with microorganisms isolated from springs of Western Canada. Geochim. Cosmochim. Acta.,35 787-800.

Smith, S.P. and Kennedy, B.M., 1982. The solubility of noble gases in water and in NaCl brine. Geochim. Cosmochim. Acta., 47 503-515.

Sorensen, J., 1978. Capacity for denitrification and reduction of intrates to ammonia in a coastal marine sediment. App. Env. Microbiol., 35 301-305.

Stumm, W. and Morgan, J.J., 1970. Aquatic Chemistry. John Wiley and Sons.

Sweeney, R.E., Liu, K.K. and Kaplan, I.R., 1976. Oceanic nitrogen isotopes and their uses in determining the source of sedimentary nitrogen. Int. Symp. Stable Isotopes Geochem. New Zealand, Aug. 4-6, 1976.

Towler, P.A., 1982. Unpublished Ph.D. Thesis, University of Bath, U.K.

Tudge, C., 1984. Whatever happens to nitrogen. New Scientist. 9th Feb., 13-15

Vogel, J.C., Talma, A.S. and Heaton T.H.E., 1981. Gaseous nitrogen as evidence for denitrification in groundwater. J. Hydrol., 50 191-200.

Weiss, R.F., 1970. The solubility of nitrogen, oxygen and argon in water and seawater. Deep-Sea Res., 17 721-735.

Weiss, R.F., 1971. Solubility of helium and neon in water and seawater. J. Chem. Eng. Data, 16 235-241.

Wild, A., 1977. Nitrate in drinking water; health hazard unlikely. Nature, 268 197-

Wolf, I.A. and Wasserman, A.E., 1972. Nitrates, nitrites and nitosamines. Science, 177 15.

Appendix 1.

Preparation of Eh reference solution Zobell 1.

Dissolve the following reagents in distilled water and make up to 1 litre. The solution is stable for several months if stored in a black plastic bottle and kept out of sunlight.

1.4080 g Potassium ferrocynaide GPR (BDH 29611)

$K_4Fe^{II}(CN)_6.3H_2O$

1.0975 g Potassium ferricyanide GPR (BDH 29610)

$K_3Fe^{III}(CN)6$

7.4555 g Potassium chloride GPR (BDH 29594)

KCl

From Wood, Techniques of Water-Resources Investigations of the U.S.G.S., U.S. Government Printing Office, Washington, 1976.

Appendix 2

Derivation of water-gas equilibration correction for N_2/Ar ratios.

Henry's Law of gas solubility states that the gas concentration in solution is directly proportional to its partial pressure in the gas phase, that is:

$$(G) = K_G.P_G$$

In the case of nitrogen at 10^oC, for atmospheric equilibration of the solution:

$$0.0147 = K_N.\ 0.7803$$

and for Argon: $3.98 \times 10^{-4} = K_A.\ 9.56 \times 10^{-3}$

hence $K_N = 1.884 \times 10^{-2}$ cm^3 STP (cm^3 H_2O)$^{-1}$ atm^{-1} and

$K_A = 4.121 \times 10^{-2}$ cm^3 STP (cm^3 H_2O)$^{-1}$ atm^{-1}

Gases may be extracted from solution by reducing their partial pressure in the gas phase in contact with the solution. Thus is a water volume V_W, is opened to an evacuated volume V_B, most of the dissolved gases move into the evacuated space. The extracted gases in V_B, however, exert a small but not negligible partial pressure in the volume V_B. As a result of this, some gases remain dissolved in solution. The fraction of the total dissolved gas extracted by this procedure can be estimated by a successive approximation method. The partial pressure in V_B can first be estimated on the assumption of total gas extraction and then corrected for the gas which returns to solution. As the latter is overestimated because of the initial

overestimation of the partial pressures in V_B, further successive corrections are required.

The volume of gas at STP, V_G, in solution in volume V_W of water, due to equilibration is:

$$V_G = (G).V_W = K_G.P_G.V_W$$

where P_G is the partial pressure of G in the atmosphere. If this gas is totally extracted and expanded into a bulb of volume V_B, its partial pressure in the bulb becomes:

$$P_B = V_G/V_B \text{ atm.}$$
$$= K_G.P_G.V_W/V_B$$

The concentration (G)' and total volume V_G' of gas which would remain in solution in the water volume V_W due to such partial pressure is given by:

$$(G)' = K_G.P_G$$
$$V_G' = K_G.P_G.V_W$$

substituting for P_G:

$$V_G' = K_G^2.P_G.V_W^2/V_B$$

so that, to a first approximation, the fraction of the original gas which remains in solution is:

$$V_G'/V_G = \frac{K_G^2 . P_G . V_W^2}{K_G . P_G . V_W . V_B}$$

$$= K_G . V_W / V_B$$

and the fraction of the original gas in the bulb of volume V_B is:

$$1 - K_G . V_W / V_B$$

so that for a second approximation the partial pressure in bulb V_B by this factor. The second approximation for the fraction of gas remaining in solution is hence:

$$V_G''/V_G = \frac{K_G . V_W}{V_B} \left(1 - \frac{K_G . V_W}{V_B} \right)$$

which on substituting, $X = K_G . V_W / V_B$ becomes:

$$V_G''/V_G = X(1 - X)$$

and the n'th approximation is:

$$V_G^n/V_G = X - X^2 + X^3 - X^4 \ldots . X^n = f(X)$$

$$\simeq X - X^2 + X^3 \text{ for } X \text{ less than } 1$$

so that the fraction of gas extracted into the bulb is:

$$1 - V_G^n/V_G = 1 - X - X^2 + X^3$$
$$= 1 - \lim f(X)$$

If gases in addition to those due to atmospheric equilibration are present in the water sample, the equations need not be altered provided that the gas in volume V_B and the water volume V_W are equilibrated.

The experimentally determined volumetric ratio for gases G1 and G2 must be corrected for the incomplete extraction of the gases, using the above equations.

$$X1 = K_{G1}.V_W/V_B \quad \text{and} \quad X2 = K_{G2}.V_W/V_B$$

and lim f(X1) and lim f(X2) can be calculated.
The measured gas ratio will be:

$$R_{gas} = \frac{V_{G1}\ (1 - V_{G1}^n/V_{G1})}{V_{G2}\ (1 - V_{G2}^n/V_{G2})}$$

Since the original gas ratio is V_{G1}/V_{G2}, the equation can be rearranged so:

$$V_{G1}/V_{G2} = R_{gas} \cdot \frac{(1 - V_{G2}^n/V_{G2})}{(1 - V_{G1}^n/V_{G1})}$$

Small errors in determining V_W, V_B and the temperature of equilibration will have little effect on the correction.

Appendix 3.

The 'AIRCAL - TWO' computer program.

```
100 REM AIRCAL-TWO (EDITED 26-3-86 PROG NO 103A
110 DIM E$(5),E#(5),R(5),M(5),L(5),H(5),V(2,5)
120 REF VOLS A=6.278, B=52.180 C=1.013 KEY$= 0.0080 CM3
130 PRINT "TRACER CALIBRATION WITH AIR SPIKE. ENTER DATE"
140 INPUT D$
150 PRINT "ATMOSPHERIC PRESS.(MB) & TEMPERATURE,C"
160 INPUT P1,T
170 IF T<5 GOTO 220
180 IF T>30 GOTO 220
190 IF P1<700 GOTO 220
200 IF P1>800 GOTO220
210 GOTO 240
220 PRINT"ERROR IN P OR T. REPEAT ENTERIES"
230 GOTO 160
240 PRINT "ENTER THE RELATIVE HUMIDITY AT AIR SPIKE LOADING"
250 INPUT H
260 PRINT "SEQUENTIAL NUMBER OF AIR SPIKE SINCE LOADING ?"
270 INPUT A
280 FOR I=1TO5
290 READ E$(I) :REM ISOTOPE RATIOS DETERMINED
300 DATA "  3HE &   4HE"," 20NE &  22NE"," 36AR &  40AR", " 78KR &  84KR
310 DATA "129XE & 136XE"
320 PRINT "ENTER  ";E$(I);"  ION CURRENTS"
330 INPUT L(I),H(I)
340 IF L(I)=0 GOTO 380
350 IF H(I)=0 GOTO 380
360 R(I) =L(I)/H(I)
370 IF L(I)<>0 GOTO 390
380 R(I)=0
390 NEXT I
400 FOR I= 1TO5
410 READ G$(I)
420 NEXT I
430 DATA "HE","NE","AR","KR","XE"
440 GOSUB 850:REM READ MOL FRACT GAS/ISOTOPES IN ATM. AND TRACER>>>>>>
450 T=T+273.18
460 P2=21.0109-5321.01/T :REM V.P. WATER AT T
470 P2=EXP(P2)
480 P=P1-P2*H/100 :REM CORR. ATM PRESS
490 B=A-1
500 W=2.256115*P/T :REM VOL IN A AT STP
510 W1=0.90904 *W :REM VOL IN B AT STP
520 W2=0.020366*W1*(1-.020366)^B:REM VOL OF AIRSPIKE NO A
530 FOR I=1 TO5
540 IF R(I)=0 GOTO 580
550 V(1,I)=W2*M(I) :REM VOL GAS I IN AIR SPIKE ADMITTED
560 V(2,I)=V(1,I)*(X(4,I)*R(I)-X(3,I))/(X(1,I)-X(2,I)*R(I))
570 REM VOL GAS I IN TRACER =V(2,I)
580 NEXT I
590 Z=Z+1
600 OPEN1,4:CMD 1
```

```
690 PRINT#1
700 PRINT#1, "RUN#";I;"TAPE";TAB(25);"CAL'N NO'S AIRSPIKE."  ;D#
710 PRINT#1
720 FOR I=1TO5
730 IF R(I)=0 GOTO770
740 PRINT#1,G#(I);TAB(7);R(I)
750 NEXT I
760 PRINT#1
770 PRINT#1, "USING DIMS.  I SEQUENTIAL NO.     " ;A
780 PRINT#1
790 PRINT#1, "ATM. PRESS.=" ;P1; "WATER VAP PRESS. AT T=";P2;"MM.HG"
800 PRINT#1, "ROOM TEMP =";T;"K   REL. HUMIDITY=  ";H;"PERCENT"
810 PRINT#1
820 PRINT#1:
830 PRINT#1,  "MOLE FRACTS IN TRACER AND VOL GAS IN AIRSPIKE"
840 PRINT#1, "GAS"; TAB(6);"MF LIGHT";TAB(5);"MF HEAVY      VOL IN AIRSPIKE
850 FOR I=1 TO 5
860 PRINT#1, G#(I);TAB(6);X(1,I);TAB(6);X(2,I);TAB(6);V(1,I)
870 NEXT I
880 PRINT#1
890 PRINT#1,"GAS       I.C LIGHT         I.C HEAVY       IC RATIO"
900 FOR I=1TO5
910 PRINT#1,G#(I),L(I),H(I),R(I)
920 NEXT I
930 PRINT#1:CLOSE1
940 IF Z=2 GOTO 590
950 STOP
960 REM  ********** SUBR ONE **********************************
970 FOR I =1 TO 3 : REM READS MOL FRACTS GAS AND ISOTOPES IN ATM
980 READ M(I),X(3,I),X(4,I)
990 NEXT I
1000 DATA 5.239E-6,1.3E-6,.99999:REM NE
1010 DATA 1.818E-5,.9105,0.0894  :REM NE
1020 DATA 9.34E-3,0.0033,0.996   :REM AR
1030 DATA1.139E-6,0.0035,0.969   :REM KR
1040 DATA 8.60E-8,0.2644,0.3887 :REM XE
1050 REM  **********SUBR ONE CONTD **********************************
1060 FOR I=1 TO5 :REM MOL FRACTS LIGHT AND HEAVY GASES IN TRACER
1070 READX(1,I),X(2,I)
1080 NEXT
1090 DATA .9980,.0100,.9900,.9997,.9702,.0098,.9997,.0003
1100 DATA .0001,.9999
1110 RETURN
1120 END
```

Appendix 4.

The 'GASAN - TWO' computer program.

```
100 REM GASAN -TWO  CODE NO 101 B.EDITED 5-10-82
110 REM TRACER CALIB OF MARCH 82
120 REM V(1,I)=VOL GAS I IN SAMPLE
130 REM V(2,I)=VOL GAS I IN TRACER
140 DIM G$(5),E$(5),R(6),X(6),V(5,6),S(3,6)
150 PRINT"ANALYSIS OF DISSOLVED GASES IN WATER"
160 INPUT"ENTER SAMPLE NAME WITH GRID REFERENCE"
170 INPUT N$
180 PRINT"ENTER COLLECTION DATE AND ANALYSIS DATE"
190 INPUT D1$,D2$
200 PRINT "ENTER COLLECTION TEMPERATURE OF SAMPLE"
210 INPUT T
220 PRINT "SEQUENTIAL NO. OF TRACER SPIKE SINCE CALIB.?"
230 INPUT V1
240 FOR I=1 TO5
250 READ E$(I) :REM ISOTOPE RATIOS DETERMINED
260 DATA "  3HE &  4HE","  20NE &  22NE","  36AR &  40AR","  78KR &  84KR"
270 DATA "129XE & 136XE"
280 NEXT I
290 FOR I=1 TO 5
300 READ G$(I)
310 NEXT I
320 DATA "HE*1E8","NE*1E7","AR*1E4","KR*1E8","XE*1E8"
330 GOSUB 1620  :REM >>>>>>>>>>>>>>>
340 FOR I=1 TO 5 :REM CALC OF GAS CONTENTS
350 PRINT"ENTER     ";E$(I);"  ION CURRENTS"
360 INPUT G(I),H(I)
370 IF G(I)=0 GOTO 520
380 IF H(I)=0 GOTO 520
390 R(I)=G(I)/H(I)
400 V(1,I)=V(2,I)*(X(1,I)-X(2,I)*R(I))/(X(4,I)*R(I)-X(3,I))
410 W=5.8
420 V(1,I)=V(1,I)/W :REM VOL GAS I/CM3 WATER
430 PRINT G$(I)
440 PRINT "I.C. LIGHT =";G(I)
450 PRINT "I.C. HEAVY =";H(I)
460 PRINT "CONC       =";V(1,I)
470 PRINT"IS CONC. WITHIN LIMITS ? YES OR NO?"
480 INPUT O$:IF O$="YES" GOTO 520
490 PRINT "ENTER E$(I) ION CURRENTS"
500 INPUT G(I),H(I):R(I)=G(I)/H(I)
510 GOTO 400
520 NEXTI
530 V(1,1)=V(1,1)*1E8:V(1,2)=V(1,2)*1E7:V(1,3)=V(1,3)*1E4:V(1,4)=V(1,4)*1E8
540 V(1,5)=V(1,5)*1E8:V(1,6)=V(1,6)*1E2
550 V(2,1)=V(2,1)*1E8:V(2,2)=V(2,2)*1E7:V(2,3)=V(2,3)*1E4:V(2,4)=V(2,4)*1E8
560 V(2,5)=V(2,5)*1E8:V(2,6)=V(2,6)*1E2
570 Z=Z+1
580 OPEN1,4:CMD1
590 PRINT#1
600 PRINT#1
610 PRINT#1
620 PRINT#1,CHR$(1)"□□NALYSIS OF □□ISSOLVED □□ASES IN □□ATER"
630 PRINT#1
640 PRINT#1,"SAMPLE NAME:  ";N$
```

```
650 PRINT#1,"SAMPLE COLLECTED ON  ";D$
660 PRINT#1,"VOLUME OF SAMPLE TUBE =  ";V;"  CM3"
670 PRINT#1,"TRACER SEQUENTIAL NUMBER  ";Y1
680 PRINT#1
690 PRINT#1,"***** END OF DATA OF SAMPLE";PRINT#1
700 PRINT#1,"GAS      CONCENTRATION      C.HEAVY          CONC."
710 OPEN2,4,1:OPEN4,4,2
720 PRINT#1,"AAAAAA      9.999      0.000 0.99999,999      0.999999.999"
730 FOR I=1 TO 5
740 IF X(1,I)=0 GOTO 780
750 PRINT#2,G$(I);CHR$(29);G(I);X(1,I);V(1,I)
760 NEXT I
770 PRINT#4:CLOSE4:PRINT#2:CLOSE2
780 IF F<6> =0 GOTO 820
790 PRINT#1
800 PRINT#1
810 PRINT#1,"TRACER CALIB. OF  ";T$;"% SEQUENTIAL FACTOR =  ";S9
820 PRINT#1
830 PRINT#1,"GAS              M.F.LIGHT      M.F.HEAVY          VOLUME CM3"
840 OPEN2,4,1:OPEN4,4,2
850 PRINT#4,"AAAAAA           9.999          9.999           9999.999"
860 FOR I=1 TO 5
870 PRINT#2,G$(I);CHR$(29);X(1,I);X(2,I);V(2,I)
880 NEXTI
890 PRINT#4:CLOSE4:PRINT#2:CLOSE2
900 PRINT#1
910 PRINT#1:CLOSE1
920 IFZ<2 GOTO 570
930 STOP
940 REM ********** SUBR ONE **********
950 FOR I=1 TO5 :REM READS MOL FRACTS GAS AND ISOTOPES IN ATM
960 READ M(I),X(3,I),X(4,I)
970 NEXT I
980 DATA5.239E-6,1.0E-6,0.999999
990 DATA1.818E-5,0.9105,0.0894
1000 DATA 9.34E-3,0.0833,0.996
1010 DATA1.139E-6,0.0035,.569
1020 DATA 8.68E-8,0.2644,.0667
1030 FOR I=1 TO5 :REM READS MOL FRACTS ISOTOPES IN TRACER
1040 READ X(1,I),X(2,I)
1050 NEXT I :REM MOL FRACTS LIGHT AND HEAVY GASES IN TRACER
1060 DATA .9958,.0042,.9812,.9388,.9247,.0053,.9994,.0001
1070 DATA .0001,.9999
1080 Y2=Y1-1
1090 S9=0.9987091^Y2 :REM SPIKE CORR. FACTOR
1100 FOR I=1 TO5
1110 READ V(2,I) :REM READS TRACER CALIB.
1112 V(2,I)=V(2,I)*S9
1120 DATA 6.414 E-6,4.307E-6,1.23  E-3,8.909 E-5,8.859E-7
1130 NEXT I
1140 T$="8 MARCH 83";REM DATE OF TRACER CALIB
1150 RETURN
1160 END
```

Appendix 5

Derivation of successive aliquot extraction equations.

This equation is:

$$Vt = \frac{vV^{n-1}}{(V + v)^n} \cdot z$$

Where z = initial STP vol. of gas in the tracer storage bulb.

V = volume of storage bulb.

v = volume of tracer aliquot.

Vt = STP volume of gas in tracer aliquot.

n = n'th number of aliquot extractions.

1st aliquot

$$Vt = \left(\frac{v}{V + v}\right) \cdot z$$

2nd aliquot

$$Vt = \left(\frac{v}{V + v}\right) \cdot \left(1 - \left(\frac{v}{V + v}\right)\right) \cdot z$$

$$= \frac{vV}{(V + v)^2} \cdot z$$

3rd aliquot

$$Vt = \left(\frac{v}{V + v}\right) \cdot \left(1 - \left(\frac{v}{V + v}\right) - \left(\frac{vV}{(V + v)^2}\right)\right) \cdot z$$

$$= \frac{vV^2}{(V + v)^3} \cdot z$$

and so:
n'th aliquot

$$Vt = \frac{vV^{n-1}}{(V + v)^n} \cdot z$$

Appendix 6.

The 'RCH.BASIC' computer program.

```
00100 'rch.basic edited 26 Jan 83
00110 'Compares experimental IG contents with solubility data and
00120 'estimates saturation temperature.
00130 'Then subtracts 0.0125 E-7 cm.3 from Ne content and amounts
00140 'of He,Ar,Kr,Xe in proportion to their abundance relative
00150 'to Ne in the atmosphere.The saturation temperature is
00160 'then re-estimated.
00170 'The subtraction is  repeated sequentially for up t0 200
00180 'or until t(Ne)>15
00190 'Solubility is matched to temperature to nearest 0.1 deg. above
00200 'Atmospheric partial pressures and relative volumes.
00210 '      Atm.              Relative to Ne        subtracted volumes
00220 '  He 5.239 E-6              0.2882               1.801 E-10
00230 '  Ne 1.818E-5               1.0                0.0625E-8
00240 '  Ar 9.34E-3              513.75                3.211E-7
00250 '  Kr 1.139E-6               0.06265              3.916E-11
00260 '  Xe 8.60E-8                0.004730             2.956E-12
00270 dim g(5,300),t(5,300),h(5),j(5),s(5,300),p(300),f(5,300),c(200),w(200
00280 print "Delete results already on file ? Yes or no."
00290 linput q$
00300 '************************************
00310 gosub 1730'Benson and Krause solubilities
00320 '**************************
00330 print "Benson and krause solubilities routine completed"
00340 file #1: "rch_results"
00350 if len (c$)=2 goto 370
00360 scratch #1
00370 print tab(10);"Recharge temperature estimation "
00380 goto 400
00390 print #1:"
"
00400 print "Sample name ? "
00410 linput n$
00420 print "Sample reference number "
00430 linput n1$
00440 print "Enter He*1E8"  '
00450 input g1
00460 g1=g1*1E-8
00470 print "Enter Ne*1E7 "
00480 input g2
00490 g2=g2*1E-7
00500 print "Enter Ar*1E4"
00510 input g3
00520 g3=g3*1E-4
00530 print "Enter Kr*1E8 "
00540 input g4
00550 g4=g4*1E-8
00560 print "Enter Xe*1E8"
00570 input g5
00580 g5=g5*1E-8
```

```
00590 print #1:
00600 print #1:"     Recharge temperature from Benson and Krause data    ";dat$
00610 print #1:
00620 print #1: "     Sample name: ";n$
00630 print #1:
00640 print #1: "     Reference number : ";n1$
00650 print #1:
00660 print #1:
  "         He          Ne       Ar       Kr       Xe       CI       T       S.D"
00670 g(1,1)=g1
00680 g(2,1)=g2
00690 g(3,1)=g3
00700 g(4,1)=g4
00710 g(5,1)=g5
00720 j=1
00730 '*********************************
00740 gosub 1320'compare g(k,j) with s(k,i) to find t(k,j)
00750 '*********************************
00760 o=1
00770 '*********************************
00780 gosub 1560'print results to file
00790 '*********************************
00800 o=2
00810 'starts sequential subtractions
00820 if g(2,1)<2.3E-7 goto 890
00830 r=g(2,1)-2.30E-7
00840 g(2,1)=g(2,1)-r
00850 g(1,1)=g(1,1)-0.2882*r
00860 g(3,1)=g(3,1)-513.75*r
00870 g(4,1)=g(4,1)-0.06265*r
00880 g(5,1)=g(5,1)-0.004730*r
00890 print "Number or subtraction/recharge temperature subroutines = "
00900 for j=2 to 200
00910 n=j
00920 g(1,j) = g(1,j-1)-1.801E-10
00930 g(2,j) = g(2,j-1)-0.0625E-8
00940 g(3,j)=g(3,j-1)-3.211E-7
00950 g(4,j)=g(4,j-1)-3.916E-11
00960 g(5,j)=g(5,j-1)-2.956E-12
00970 c(j)=g2/g(2,j)'contamination index
00980 '*********************************
00990 gosub 1320'compare g(k) with s(k,i) to find t(k,j)
01000 '*********************************
01010 'evaluates standard deviation; w(j)
01020 s=t(2,j)+t(3,j)+t(4,j)+t(5,j)
01030 s=s/4
01040 for i=2 to 5
01050 d(i)=(t(i,j)-s)^2
01060 next i
01070 d=d(2)+d(3)+d(4)+d(5)
01080 w(j)=sqr(d/4)
01090 print j
01100 if t(2,j)>15 goto 1130
01110 next j
```

```
01120 'identifies minimum standard deviation
01130 for b=2 to n
01140 if b=2 goto 1160
01150 if w(b)>v goto 1180
01160 v=w(b)
01170 z=b
01180 next b
01190 '*********************************
01200 gosub 1430'print results to file
01210 '*********************************
01220 print #1:"     No. subtraction aliquots to minimum S.D. = ";z
01230 print #1:"     Total no. subtractions = ";n
01240 print "Calculation completed"
01250 print "Calculate for another sample?   Yes or no?"
01260 input q$
01270 if len(q$)=3 goto 390
01280 print "Programme completed"
01290 stop
01300 '*********************************
01310 '*********************************
01320 'subroutine to compare g(k,j) with s(k,i) to find t(k,j)
01330 for k =2 to 5
01340 for i=1 to 300
01350 t(k,j)=p(i)-273.18
01360 if g(k,j)<s(k,i) goto 1380
01370 if g(k,j)>s(k,i) goto 1390
01380 next i
01390 next k
01400 return
01410 '*********************************
01420 '*********************************
01430 'subroutine results print to file
01440 if z>9 goto 1490
01450 e=z-1
01460 l=z-e
01470 a=z+e
01480 goto 1510
01490 l=z-9
01500 a=z+9
01510 for j=l to a
01520 if j<>z goto 1540
01530 print #1:
01540 if j<>z+1 goto 1560
01550 print #1:
01560 f(1,j)=g(1,j)*1E8
01570 f(2,j)=g(2,j)*1E7
01580 f(3,j)=g(3,j)*1E4
01590 f(4,j)=g(4,j)*1E8
01600 f(5,j)=g(5,j)*1E8
01610 print #1:using"     -#####.##  -##.##  -##.##  -##.##  -##.## "
      f(1,j),f(2,j),f(3,j),f(4,j),f(5,j)
01620 if o=2 goto 1650
01630 print #1:using"                -##.##  -##.##  -##.##  -##.##",
      t(2,j),t(3,j),t(4,j),t(5,j)
```

```
01640 goto 1690
01650 h=t(2,j)+t(3,j)+t(4,j)+t(5,j)
01660 h=h/4
01670 print #1:using"
       -##.##  -##.##  -##.##  -##.##  -#.## -##.##  -###.##",
      t(2,j),t(3,j),t(4,j),t(5,j),c(j),h,w(j)
01680 next j
01690 print #1:
01700 return
01710 '************************************
01720 '************************************
01730 'subroutine to calculate Ne Ar Kr Xe
       solubilities in 0.1 deg. intervals
01740 'from -10 to 20 deg. cent.   Benson and Krause data
01750 p1=263.08
01760 a2=36.855
01770 for k=2 to 5
01780 read h(k),j(k),n(k)
01790 next k
01800 data 142.50,41.667,1.818E-5
01810 data 168.87,40.404,9.34E-3
01820 data 179.21,39.781,1.139E-6
01830 data 188.78,39.273,8.60E-8
01840 for k=2 to 5
01850 p=p1
01860 for i=1 to 300
01870 p=p+0.1
01880 p(i)=p
01890 t2=h(k)/p(i)-1
01900 s(k,i)=j(k)*t2+a2*t2*t2
01910 s(k,i)=exp(s(k,i))
01920 s(k,i)=s(k,i)*124.4142*1E4*n(k)/1000  'sol/cm3 at temp p(i)
01930 next i
01940 next k
01950 return
01960 '************************************
01970 '************************************
01980 end
```

Appendix 7

Statistical Methods

The mean, range, standard deviation, and standard error on the mean.

where x = individual values

$x2$ = largest value in the distribution

$x1$ = smallest value in the distribution

$\bar{x}$ = mean

n = number of values in the distribution

S = standard deviation

Sm = standard error on the mean

R = range

$$\bar{x} = \Sigma(x)/n$$

$$R = x2 - x1$$

$$S = [\Sigma(x - \bar{x})^2/n]^{1/2}$$

$$Sm = \{[\Sigma(x - \bar{x})^2]/[n(n - 1)]\}^{1/2}$$

Combined standard deviations

Quantity	Standard deviation
R1	S1
R2	S2
R3	S3
R1 + (-) R2	$(S1^2 + S2^2)^{1/2}$
R1 x (/) R2	$R3 \cdot ((S1/R1)^2 + (S2/R2)^2)^{1/2}$

Least squares regression analysis.

For equation $y = mx + c$

where x = X - co-ordinate value

y = Y - co-ordinate value

n = number of co-ordinate X-Y points

$$CSXX = \Sigma x^2 - (\Sigma x)^2/n$$

$$CSYY = \Sigma y^2 - (\Sigma y)^2/n$$

$$CSXY = \Sigma xy - \Sigma x \,.\, \Sigma y/n$$

$$m = CSXY/CSXX$$

$$c = \frac{\Sigma y - (CSXY \,.\, \Sigma x)/CSXX}{n}$$

$$MSEE = \frac{CSYY - CSXY^2/CSXX}{n - 2}$$

Estimated Standard error on c = $(MSEE/CSXX)^{1/2}$

Estimated Standard error on m = $(\Sigma x^2 \,.\, MSEE/(n.CSXX))^{1/2}$

Correlation coefficient = $CSXY/(CSXX \,.\, CSYY)^{1/2}$

Estimation of parameters in curve - fitting polynomial cubic equation.

Data fitted to curve :

$$y = A.x^3 + B.x^2 + C.x + D$$

for n numbers of data pairs, x_i and y_i.

Ten terms are defined, from which twelve constants can be calculated. These constants allow derivation of the parameters A, B, C and D.

$X1 = \Sigma\, x$

$X2 = \Sigma\, x^2$

$X3 = \Sigma\, x^3$

$X4 = \Sigma\, x^4$

$X5 = \Sigma\, x^5$

$X6 = \Sigma\, x^6$

$Y1 = \Sigma\, y$

$P1 = \Sigma\, (x.y)$

$P2 = \Sigma\, (x^2.y)$

$P3 = \Sigma\, (x^3.y)$

$$f1 = \frac{Y1}{n} - \frac{P1}{X1} \qquad f2 = \frac{X3}{n} - \frac{X4}{X1} \qquad f3 = \frac{X2}{n} - \frac{X3}{X1} \qquad f4 = \frac{X1}{n} - \frac{X2}{X1}$$

$$g1 = \frac{P1}{X1} - \frac{P2}{X2} \qquad g2 = \frac{X4}{X1} - \frac{X5}{X2} \qquad g3 = \frac{X3}{X1} - \frac{X4}{X2} \qquad g4 = \frac{X2}{X1} - \frac{X3}{X2}$$

$$h1 = \frac{P2}{X2} - \frac{P3}{X3} \qquad h2 = \frac{X5}{X2} - \frac{X6}{X3} \qquad h3 = \frac{X4}{X2} - \frac{X5}{X3} \qquad h4 = \frac{X3}{X2} - \frac{X4}{X3}$$

Six further constants are now defined :

$$j1 = \frac{f1}{f4} - \frac{g1}{g4} \qquad j2 = \frac{f2}{f4} - \frac{g2}{g4} \qquad j3 = \frac{f3}{f4} - \frac{g3}{g4}$$

$$k1 = \frac{g1}{g4} - \frac{h1}{h4} \qquad k2 = \frac{g2}{g4} - \frac{h2}{h4} \qquad k3 = \frac{g3}{g4} - \frac{h3}{h4}$$

The A, B, C and D parameters can now be obtained :

$$A = \frac{j1.k3 - k1.j3}{j2.k3 - k2.j3}$$

$$B = \frac{k1 - A.k2}{k3}$$

$$C = \frac{h1 - A.h2 - B.h3}{h4}$$

$$D = \frac{Y1 - A.X3 - B.X2 - C.X1}{n}$$

The Root Mean Square Deviation of the Curve (RMSD) is :

$$RMSD = \left(\frac{\Sigma (A.x^3 + B.x^2 + C.x + D - y)^2}{n} \right)^{\frac{1}{2}}$$

Appendix 8

Comparison and manipulation of Delta-values

All ratio comparisons are made by measuring the gases concerned seperately as samples against a common reference gas (MS). The MS may change isotopically over a period of time or run out altogether and be replaced; the isotopic composition of the gas is arbitrary and sample gases may only be codmpared directly if measured over a short period against the same MS. Measurements made against different MS's may only be compared when a standard has been run against each MS.

The convention δ A(B) means that gas B is being compared with reference gas A. Thus, when two gases X and Y respectively are measured against a common MS, the following ratios are measured: δ MS(X) and δ MS(Y). To express X as a change against Y, i.e. δ Y(X), the following expression is used:

$$\delta\, Y(X) = \left[\frac{\delta\, MS(X) - \delta\, MS(Y)}{1000 + \delta\, MS(Y)} \right] . \quad 1000\ ^{o}/_{oo} \qquad (1)$$

If a δ Y(X) value is known, but not the figures from which it was derived, it can be converted to δ X(Y) by:

$$\delta\, X(Y) = \left[\frac{1000}{1000 + \delta\, Y(X)} - 1 \right] . \quad 1000\ ^{o}/_{oo} \qquad (2)$$

Components of any two ratios can be compared providing they share a common gas. If that ratio is on the same side of the ratio then (1) above may be used, but if on opposing sides then the following is used, where Z is the common gas:

$$\delta\, X(Y) = \delta\, X(Z) + \delta Z(Y) + \frac{\delta\, X(Z) \,.\, \delta\, Z(Y)}{1000}\ ^{o}/_{oo} \qquad (3)$$

Appendix 9.

The 'OUTGAS' computer program.

```
100 REM OUTGAS
110 REM CALCS COMPOSITION OF GAS EVOLVED AND GAS REMAINING IN SOLUTION
120 REM FOR VARIOUS RCH. TEMPS (RT) DEGASSING TEMP (DT) AND PRESSURE (P)
130 DIM T(17),KH(17)
140 PRINT "RECHARGE TEMPERATURE :"
150 INPUT RT
160 PRINT "DEGASSING TEMPERATURE :"
170 INPUT DT
180 PRINT "DEGASSING PRESSURE (ATM) :"
190 INPUT P
200 PRINT "CONTAMINATION INDEX (NE) :"
210 INPUT CI
220 PRINT "HCO3 CONTENT (MG/L) :"
230 INPUT BC
240 PRINT" MODEL RADIOGENIC AR ?(Y OR N)"
250 INPUT N$
260 IF N$="N" GOTO 290
270 PRINT" AR-40/AR-36 RATIO : "
280 INPUT AR
290 PRINT" MODEL N2/AR ? (Y OR N)"
300 INPUT Y$
310 IF Y$="N" GOTO 340
320 PRINT" N2/AR RATIO (GAS) :"
330 INPUT NA
340 PRINT" CH4/N2 RATIO (GAS) :"
350 INPUT HN
360 PRINT "RADIOGENIC HE (CM3/CM3 H20 *1E8) :"
370 INPUT EH
380 PRINT "FLUID PH :"
390 INPUT PH
400 PRINT "RECHARGE SALINITY (O/OO) :"
410 INPUT S1
420 M2=S1/64.113
430 PRINT "MEASURED SALINITY (O/OO) :"
440 INPUT S
450 M1=S/64.113
460 REM ESTIMATE VP H2O AT DT
470 PW=((365-DT)*4-265*4)*8.509E-8
480 PH=5.409*(DT-100)-PW
490 PW=2.303*PW/(DT+273.16)
500 PW=EXP(PW)
510 REM PW = VP H2O
520 FOR C=1 TO 5
530 READ U(C),V(C),P(C),G$(C)
540 NEXT C
```

```
550 DATA 131.42,41.824,5.239E-6,HE
560 DATA 142.5,41.067,1.818E-5,NE
570 DATA 168.87,40.404,9.34E-3,AR
580 DATA 179.21,39.781,1.139E-6,KR
590 DATA 128.78,39.273,8.6E-8,XE
600 DATA 162.02,41.712,0.7803,N2
610 FOR I=1 TO 8
620 READ A(I),B(I),C(I),D(I)
630 NEXT I
640 DATA -0.2304,2.2951,-7.7154,9.006
650 DATA -0.3022,3.6278,-13.6641,16.8309
660 DATA -0.405,3.8471,-12.3389,13.6921
670 DATA -0.1124,1.3282,-5.1423,6.8403
680 DATA -0.1611,1.9007,-7.3019,9.5072
690 DATA -0.2427,2.1504,-6.61,7.4294
700 DATA -0.021,0.2089,-0.7894,1.5653
710 DATA -0.0964,1.0183,-3.5065,4.0078
720 G$(7)="CH4":G$(8)="CO2"
730 K$(1)="*1E-8":K$(2)="*1E-7":K$(3)="*1E-4":K$(4)="*1E-8"
740 K$(5)="*1E-8":K$(6)="*1E-2":K$(7)="*1E-2"
750 K$(8)="*1E-2"
760 M=M2
770 T=273.18+RT
780 GOSUB 2850 :REM GET SALTING KS FOR GASES AT RCH
790 GOSUB 2410 :REM GET HLC AT RT
800 FOR I=1 TO 6 :REM IS(I) = INITIAL GAS CONCS. STP AT RECHARGE
810 IS(I)=H(I)*P(I)
820 NEXT I
830 NE=IS(2)
840 IS(2)=NE*CI
850 D=IS(2)-NE :REM D = EXTRA AIR NEON
860 IF EH=0 GOTO 890
870 REM EXTRA AIR ADDITION
880 IS(1)=IS(1)+EH*1E-5
890 IS(1)=IS(1)+D*0.2882
900 IS(3)=IS(3)+D*513.75
910 IF N$="N" GOTO 930
920 IS(3)=IS(3)*AR/295.5
930 IS(4)=IS(4)+D*0.85265
940 IS(5)=IS(5)+D*0.00473
950 IS(6)=IS(6)+D*42923.8
960 T=273.18+DT
970 M=M1
980 GOSUB 2850 :REM GET KS AT DT
990 GOSUB 2410 :REM GET HLC AT DT
1000 GOSUB 2000 :REM GET HLC CORRECTION
1010 GOSUB 2830 :REM GET PP CO2 AT DT
1020 VO=(P-PW)/(UM-1) :REM VO = ESTIMATE PP N2
1030 V1=(IS(6)-VO*H(6))/VL :REM 1ST APPROX VOL GAS PHASE AT DT
1040 IF V1<0.001 GOTO 1650
1050 REM SUCCESSIVELY APPROXES GAS VOL (GP) BY EQUALISING SUM TOTAL (PE)
1060 REM PARTIAL PRESSURES P(I) TO DEGASSING PRESSURE (P)
1070 GV=V1
1080 PE=0
```

```
1090 IF GV<0.0005 GOTO 1650
1100 GV=GV*273.18/T
1110 IF Y$="N" GOTO 1140
1120 FOR I=1 TO 5
1130 GOTO 1150
1140 FOR I=1 TO 6
1150 P(I)=IS(I)/(GV+H(I))
1160 PE=PE+P(I)
1170 NEXT I
1180 IF Y$="N" GOTO 1200
1190 P(6)=P(6)*HW
1200 P(7)=HW*P(6)
1210 IF Y$="N" GOTO 1240
1220 PE=PE+P(7)+P(6)+PW+P(6)
1230 GOTO 1250
1240 PE=PE+P(7)+P(8)+PW
1250 IF PE<P-0.0005 GOTO 1280
1260 IF PE>P+0.0005 GOTO 1280
1270 GOTO 1320
1280 DF=PE/P
1290 GV=GV*DF
1300 GOTO 1080
1310 '**********
1320 V2=GV*273.18*P/T :REM V2=VOL GAS AT STP
1330 V3=(P-PW)*V2/P :REM VOL GAS CORR. FOR VP AT STP
1340 IF Y$="N" GOTO 1380
1350 IS(6)=GV*273/T
1360 IS(6)=IS(6)+H(6)
1370 IS(6)=P(6)*IS(6)
1380 IS(7)=GV*273/T
1390 IS(7)=IS(7)+H(7)
1400 IS(7)=P(7)*IS(7)
1410 V5=0:GS=0
1420 REM V5= INITIAL GAS CONC. EXCL CO2
1430 REM GS= FINAL GAS CONC.
1440 FOR I=1 TO 7
1450 VS(I)=P(I)*H(I)
1460 GS=GS+VS(I)
1470 V5=V5+IS(I)
1480 NEXT I
1490 GS=GS+VS(8)
1500 V4=V3+GS :REM TOTAL INITIAL GAS CONC.
1510 IS(8)=V4-V5 :REM INITIAL CO2 CONC. BY DIFFERENCE.
1520 PG=P*GV*273.18/T :REM PG IS VOL WV AT STP
1530 PS=PG/1245000 :REM PS IS COMPARABLE VOL WATER IN L
1540 M6=M1*64.113/(1+PS):REM SALINITY PRIOR DEGASSING
1550 R(1)=IS(6)/IS(3):R(2)=VS(6)/VS(3):R(3)=P(6)/P(3)
1560 B(1)=IS(1)/IS(2):B(2)=VS(1)/VS(2):B(3)=P(1)/P(2)
1570 O(1)=IS(4)/IS(5):O(2)=VS(4)/VS(5):O(3)=P(4)/P(5)
1580 H(1)=IS(7)/IS(6):H(2)=VS(7)/VS(6):H(3)=P(7)/P(6)
1590 VS(1)=VS(1)*1E5:VS(2)=VS(2)*1E4:VS(3)=VS(3)*10
1600 VS(4)=VS(4)*1E5:VS(5)=VS(5)*1E5:VS(6)=VS(6)*0.1
1610 IS(1)=IS(1)*1E5:IS(2)=IS(2)*1E4:IS(3)=IS(3)*10
1620 IS(4)=IS(4)*1E5:IS(5)=IS(5)*1E5:IS(6)=IS(6)*0.1
1630 IS(7)=IS(7)*0.1:VS(7)=VS(7)*0.1
1640 IS(8)=IS(8)*0.1:VS(8)=VS(8)*0.1
```

```
1650 ZX=0
1660 ZX=ZX+1
1670 OPEN1,4,CH01:PRINT#1
1680 OPEN2,4,2
1690 PRINT#2,"AAA   999.99999999     9999999.9999    9999999.9999   AAAAA"
1700 OPEN3,4,1
1710 PRINT#1,CHR$(1)"      EXSOLUTION OF GASES"
1720 PRINT#1:PRINT#1
1730 PRINT#1," RECHARGE TEMP, DEGREE C      : ";RT
1740 PRINT#1,"DEGASSING TEMP, DEGREE C      : ";DT
1750 PRINT#1,"DEGASSING PRESSURE (ATM)      : ";P
1760 PRINT#1,"EXTRA AIR CONT. INDEX (NE)    : ";C1
1770 PRINT#1,"RADIOGENIC NE (*1E8)          : ";EW
1780 PRINT#1,"HYDROCARBON/NITROGEN RATIO    : ";HN
1790 PRINT#1,"BICARBONATE CONTENT, MG/L     : ";BC
1800 PRINT#1,"FLUID PH                      : ";PH
1810 IF N$="N" GOTO 1840
1820 PRINT#1,"AR-40/AR-36 RATIO = ";AR
1830 GOTO 1850
1840 PRINT#1,"AR-40/AR-36 RATIO = 295.5"
1850 PRINT#1:PRINT#1
1860 IF V1>0.001 GOTO 1890
1870 PRINT#1,"OUTGASSING CANNOT OCCUR AT THIS TEMP. AND PRESS."
1880 GOTO 2340
1890 PRINT#1,"GAS      GAS PHASE        INITIAL SOLN     DEGASSED SOLN"
1900 PRINT#1,"           PP.ATM          CM3 STP/CM3      CM3 STP/CM3"
1910 PRINT#1
1920 FOR I=1 TO 8
1930 PRINT#3,G$(I),CHR$(29),P(I),IS(I),VS(I),K$(I)
1940 NEXT I
1950 H$="H2O"
1960 OPEN4,4,1:OPEN5,4,2
1970 PRINT#5,"AAA    999.99999999"
1980 PRINT#4,H$,CHR$(29),PW
1990 PRINT#2:CLOSE2:PRINT#3:CLOSE3:PRINT#4:CLOSE4:PRINT#5:CLOSE5
2000 PRINT#1
2010 PRINT#1,"1ST. GAS VOL. APPROXIMATION (CM3)          : ";V1
2020 PRINT#1
2030 PRINT#1,"VOL. GAS EVOLVED FROM 1L WATER (CM3)       : ";GV
2040 PRINT#1,"VOL. GAS AT STP (CM3)                      : ";V2
2050 PRINT#1,"VOL. GAS CORRECTED FOR VP (STP CM3)        : ";V3
2060 PRINT#1
2070 PRINT#1,"GAS CONC. PRIOR DEGASSING (STP CM3/L)      : ";V4
2080 PRINT#1,"GAS CONC. AFTER DEGASSING (STP CM3/L)      : ";GS
2090 PRINT#1
2100 PRINT#1,"WATER/GAS VOL. RATIO (DEGASSING T + P)     : ";1000/GV
2110 PRINT#1:PRINT#1
2120 W$(1)="INITIAL SOLN. ":W$(2)="DEGASSED SOLN.":W$(3)="GAS PHASE      "
2130 OPEN2,4,2:OPEN3,4,1
2140 PRINT#2,"AAAAAAAAAAAAAAA     999.999     99999.999    99999.999      9999.99
2150 PRINT#1,"                     N2/AR         HE/NE        KR/XE        CH4/N2
2160 PRINT#1
2170 FOR I=1 TO 3
2180 PRINT#3,W$(I),CHR$(29),R(I),B(I),O(I),H(I)
2190 NEXT I
```

```
2200 PRINT#1:PRINT#1
2210 D$="PCH. SALINITY :"
2220 E$="PRIOR DEGAS   :"
2230 N$="AFTER DEGAS   :"
2240 J$="D/GC"
2250 OPEN4,4,1:OPEN5,4,2
2260 PRINT#5,"SAAAAAAAAAAAAAAA 99999 AAAA"
2270 PRINT#4,D$;CHR$(29);S1;J$
2280 PRINT#1
2290 PRINT#4,E$;CHR$(29);N6;J$
2300 PRINT#4,N$;CHR$(29);S;J$
2310 PRINT#4:CLOSE4:PRINT#5:CLOSE5
2320 PRINT#1
2330 FOR I=1 TO 6:PRINT#1:NEXT I
2340 PRINT#1:CLOSE1:PRINT#2:CLOSE2:PRINT#3:CLOSE3
2350 GOTO 2950
2370 IS(8)=IS(8)*10:VS(8)=VS(8)*10
2380 STOP
2400 '**********************************
2410 REM SUBR CALC HENRYS LAW CONST.
2420 FOR C=1 TO 6
2430 T2=U(C)/T-1
2440 K=V(C)*T2+36.855*T2*T2
2450 K=EXP(K)
2460 B=124.4142*1E4*K
2470 F=M*KS(C)
2480 F=EXP(F)
2490 H(C)=B/F
2500 NEXT C
2510 RETURN
2520 '**********************************
2530 REM SUBR CALC PP CO2
2540 K1=5.01E-7:K2=5.62E-11
2550 H=-PH:H=10↑H
2560 A0=1/(1+K1/H+K1*K2/H↑2)
2570 A1=1/(H/K1+1+K2/H)
2580 A2=1/(H↑2/(K1*K2)+H/K2+1)
2590 BI=BC/(61.005*1000)
2600 P(8)=BI*A0/(KH*A1)
2610 CT=P(8)*KH/A0
2620 CA=A2*KH*P(8)/A0
2630 VS(8)=(CT-BI-CA)*22.414*1000
2640 RETURN
2650 '**********************************
2660 REM SUBR HLC CO2+CH4
2670 Z=T/100
2680 KH=-6.5455*Z↑3
2690 KH=KH+63.6611*Z↑2
2700 KH=KH-207.272*Z+226.3128
2710 REM KH IS L/L/ATM
2720 KH=KH/22.414  :REM MOLES/L/ATM
```

```
 2730 F=M*KS(8)
 2740 F=EXP(F)
 2750 KH=KH/F  :REM COR FOR KS
 2760 XL=-0.1229*Z^3
 2770 XL=XL+1.2416*Z^2
 2780 XL=XL-4.1919*Z+4.7589
 2790 XL=XL*1000  :REM CM3/L/ATM
 2800 F=M*KS(7)
 2810 F=EXP(F)
 2820 H(7)=XL/F  :REM COR FOR KS
 2830 RETURN
 2840 '**********************************
 2850 REM SUBR SALTING KS
 2860 Z=T/100
 2870 FOR I=1 TO 8
 2880 K7=A(I)*Z^3
 2890 K8=B(I)*Z*Z
 2900 K9=C(I)*Z
 2910 KS(I)=K7+K8+K9+D(I)
 2920 NEXT I
 2930 RETURN
 2940 '**********************************
 2950 END
READY.
```

Appendix 10

Example calculation of dissolved N_2 components and the isotopic value of the denitrified component.

Bourne LL01

Noble gas data from the recharge temperature program RCH.BASIC estimates the recharge temperature to be 7.8°C +/- 0.9, with a neon contamination index of 1.36. The measured N_2/Ar ratio is 54.1 +/- 0.2.

From the solubility data, at 7.8°C the atmospherically equilibrated dissolved gas concentrations (WEA) are:

$$N_{2\ WEA} = 1.537 \times 10^{-2}\ cm^3/cm^3\ H_2O\ (STP)$$
$$Ar_{\ WEA} = 4.093 \times 10^{-4}\ cm^3/cm^3\ H_2O\ (STP)$$
$$Ne_{\ WEA} = 2.108 \times 10^{-7}\ cm^3/cm^3\ H_2O\ (STP)$$

The amount of extra air neon, $Ne_{\ EA}$, is based on the contamination index:

$$Ne_{\ EA} = (1.36 \times 2.108 \times 10^{-7}) - 2.108 \times 10^{-7} = 7.5888 \times 10^{-8}$$

In air, the ratio of nitrogen to neon is 42920.8, and the ratio of argon to neon is 513.751; so:

$$N_{2\ EA} = 42920.8 \times 7.5888 \times 10^{-8} = 3.25717 \times 10^{-3}$$
$$Ar_{\ EA} = 513.751 \times 7.5888 \times 10^{-8} = 3.89875 \times 10^{-5}$$

The predicted total concentration of dissolved argon is therefore:

$$Ar_{WEA} + Ar_{EA} = 4.48287 \times 10^{-4}$$

Since the measured N_2/Ar ratio is 54.1, then the dissolved N_2 concentration must be:

$$54.1 \times 4.48287 \times 10^{-4} = 2.42523 \times 10^{-2}$$

This value can be compared with the predicted dissolved N_2 concentration if no denitrification had occurred:

$$N_{2\ WEA} + N_{2\ EA} = 1.86271 \times 10^{-2}$$

The difference suggests an excess potentially due to denitrification, $N_{2\ D}$:

$$N_{2\ D} = N_2 \text{ (measured)} - (N_{2\ WEA} + N_{2\ EA})$$
$$= 5.6252 \times 10^{-3}$$

If no denitrification had occurred, the predicted N_2/Ar ratio would be:

$$\frac{N_{2\ WEA} + N_{2\ EA}}{Ar_{WEA} + Ar_{EA}} = \frac{1.86271 \times 10^{-2}}{4.48287 \times 10^{-4}} = 41.5$$

The difference between the measured 54.1 and the expected N_2/Ar ratio of 41.5 relfects the additional denitrified N_2 component. Since $N_{2\ WEA}$, $N_{2\ EA}$ and $N_{2\ D}$ are all known, each can be expressed as a percentage, which, upon rounding to the nearest percent gives:

$N_{2\ WEA} = 63$

$N_{2\ EA} = 14$

$N_{2\ D} = 23$

Of the total amount of dissolved N_2, $N_T (2.42523 \times 10^{-2})$, the fraction of excess N_2 from denitrification is known, N_{FD}. The nitrate concentration which would correspond to this excess is calculated from the following molar proportions:

$2NO_3^-$	⟶	N_2
2 x 62g	⟶	22.4 l
124g	⟶	22400 cm^3
124 mg/l	⟶	22.4 cm^3/l
124 mg/l	⟶	2.24×10^{-2} cm^3/cm^3 H_2O

(STP)

so:

$$NO_3^- \text{ (mg/l)} = \frac{N_{FD} \times N_T \times 124}{0.0224}$$

which in this case is:

$$\frac{0.23 \times 2.42523 \times 10^{-2} \times 124}{0.0224}$$

$$= 30.9 \text{ mg/l}$$

The data as calculated indicates that the excess N_2 component contributes 23% towards the total dissolved N_2. However there will be an error on this value which is a function of the error on the

recharge temperature and the error on the measured N_2/Ar ratio. If the whole calculation is repeated using the highest recharge temperature and the lowest N_2/Ar ratio (or vice-versa) an extreme result is obtained limited by the extent of the two errors. In this case, using a N_2/Ar ratio of 53.9 and a recharge temperature of $8.7^{o}C$, the following data is obtained:

		$\%N_2$
$N_{2\ WEA}$	$= 1.507 \times 10^{-2}$	63
$N_{2\ EA}$	$= 3.22936 \times 10^{-3}$	14
$N_{2\ D}$	$= 5.38714 \times 10^{-3}$	23
$N_{2\ T}$	$= 2.36865 \times 10^{-3}$	100

The error on the N_2 total is therefore:

$$2.42523 \times 10^{-2} - 2.36865 \times 10^{-2} = 0.0006$$

i.e. error range = +/- 0.0006.

By a similar calculation, the error range on $N_{2\ D}$ expressed as a percentage of the total is +/- 1%.

The $\delta^{15}N_D$ and error value can now be estimated. This is done by calculating the maximum and minimum possible values of $\delta^{15}N_D$ from the error on the measured analysis of $\delta^{15}N$ in the water (+/- 0.1); on the $\delta^{15}N$ value of N_2 equilibrated with water (+ 0.9 +/- 0.1); and on the calculated fraction of denitrified N_2, (f N_D).

Now since air has a $\delta^{15}N_D$ of 0.0 $^{o}/oo$, then

$$\delta^{15}N_T = \delta^{15}N_{WEA}.f_{WEA} + \delta^{15}N_{EA}.f_{EA} + \delta^{15}N_D.f_D$$

becomes:

$$\delta^{15}N_T = \delta^{15}N_{WEA}.f_{WEA} + \delta^{15}N_D.f_D$$

rearranging for $\delta^{15}N_D$:

$$\delta^{15}N_D = \frac{\delta^{15}N_T - \delta^{15}N_{WEA}.f_{WEA}}{f_D} = \frac{x}{f_D}$$

In order to calculate the most positive value, $\delta^{15}N_T$ is set to $\delta^{15}N_T + 0.1$; and $\delta^{15}N_{WEA}$ is set to $\delta^{15}N_{WEA} - 0.1$. If the x term is positive, then in order to calculate the most positive $\delta^{15}N_D$ the smallest f_D value must be used; i.e. $f_D = f_D$- error. In contrast, if the x term is negative, then x must be divided by the largest f_D value.

In order to calculate the most negative value, the opposite approach is used. $\delta^{15}N_T$ is set to the most negative error value ($\delta^{15}N_T - 0.1$); $\delta^{15}N_{WEA}$ is set to 1.0 °/oo, and the x term calculated. If this is negative, then the smallest f_D value is taken and vice-versa.

So, for Bourne:

$$\delta^{15}N = -0.2 +/- 0.1$$

$$f_{WEA} = 0.63$$

$$f_D = 0.23 +/- 0.01$$

To find the most positive $\delta^{15}N_D$ value, x is first calculated:

$$x = -0.2(+0.1) - 0.9(-0.1).0.63 = -0.604$$

In this case x is negative, so f_D becomes 0.23(+0.01) = 0.24 which gives:

$$\delta^{15}N_D = \frac{x}{f_D} = \frac{-0.604}{0.24} = -2.52 \qquad (A)$$

To find the most negative $\delta^{15}N_D$ value, x is again calculated as:

$$x = -0.2(-0.1) - 0.9(+0.1).0.63 = -0.93$$

and f_D becomes $0.23(-0.0.1) = 0.22$

so:

$$\delta^{15}N_D = \frac{x}{f_D} = \frac{-0.93}{0.22} = -4.23 \qquad (B)$$

and $\delta^{15}N_D = \frac{A + B}{2} = -3.4\ ^{o}/_{oo}$

The error range is given by the absolute difference between the mean $\delta^{15}N_D$ and either extreme, in per mille: 3.4 - 2.5 = 0.9.

So for Bourne, $\underline{\delta^{15}N_D = -3.4 +/- 0.9\ ^{o}/_{oo}}$